APR 27 1965

U. S. DEPARTMENT OF COMMERCE

BUREAU OF STANDARDS JOURNAL OF RESEARCH

Vol. 9 DECEMBER, 1932 No. 6

CONTENTS

RP. No.	TITLE AND AUTHOR	Page
501.	Isolation of the three xylenes from an Oklahoma petroleum. Joseph D. White and F. W. Rose, jr.	711
502.	Characteristic equations of vacuum and gas-filled tungsten-filament lamps. L. E. Barbrow and J. Franklin Meyer	721
503.	The calorimetric determination of the intrinsic energy of gases as a function of the pressure. Data on oxygen and its mixtures with carbon dioxide to 40 atmospheres, at 28° C. Frederick D. Rossini and Mikkel Frandsen	733
504.	Shear tests of reinforced brick masonry beams. D. E. Parsons, A. H. Stang, and J. W. McBurney	749
505.	The measurement of low voltage X-ray intensities. Lauriston S. Taylor and C. F. Stoneburner	769
506.	A multi-range potentiometer and its application to the measurement of small temperature differences. H. B. Brooks and A. W. Spinks	781
507.	The density of some soda-lime-silica glasses as a function of the composition. F. W. Glaze, J. C. Young, and A. N. Finn	799
508.	Coiled-filament resistance thermometers. C. H. Meyers	807
509.	Deflection of cosmic rays by a magnetic field. L. F. Curtiss	815
510.	The system: CaO-P_2O_3. Elmer T. Carlson	825
511.	A metal-connected glass electrode. M. R. Thompson	833
	Index	855

BUREAU OF STANDARDS JOURNAL OF RESEARCH

CONTENTS OF RECENT NUMBERS

June, 1932 (Vol. 8, No. 6)

RP446. A method for determining the most favorable design of gas burners. John H. Iseman, Elmer R. Weaver, and Francis A. Smith. Price 10 cents.

RP447. The photographic emulsion: Analysis for nonhalide silver and soluble bromine. Burt H. Carroll and Donald Hubbard. Price 5 cents.

RP448. International comparison of electrical standards. George W. Vinal. Price 5 cents.

RP449. A method for the purification of rubber and properties of the purified rubber. A. T. McPherson. Price 5 cents.

RP450. Tests of a balanced thermocouple and filter radiometer as a standard ultra-violet dosage intensity meter. W. W. Coblentz, R. Stair, and J. M. Hogue. Price 5 cents.

RP451. The isoelectric point of wool. Milton Harris. Price 5 cents.

RP452. An optical method for measuring temperature and convective heat transfer. R. B. Kennard. Price 5 cents.

July, 1932 (Vol. 9, No. 1)

RP453. The use of α-benzoinoxime in the determination of molybdenum. H. B. Knowles. Price 5 cents.

RP454. Effect of zinc coatings on the endurance properties of steel. W. H. Swanger and R. D. France. Price 5 cents.

RP455. Power input and dissipation in the positive column of cæsium discharge. F. L. Mohler. Price 5 cents.

RP456. Thermal expansion of some silicates of elements in Group II of the periodic system. R. F. Geller and Herbert Insley. Price 5 cents.

RP457. An automatic reverberation meter for the measurement of sound absorption. W. F. Snyder. Price 5 cents.

RP458. Note on the probable presence of 2, 2-dimethylpentane in a mid-continent petroleum. Johannes H. Bruun and Mildred M. Hicks-Bruun. Price 5 cents.

RP459. Notes on the orifice meter: The expansion factor for gases. Edgar Buckingham. Price 5 cents.

RP460. Theory of voltage dividers and their use with cathode ray oscillographs. Melville M. Peters, George F. Blackburn, and Paul T. Hannen. Price 10 cents.

August, 1932 (Vol. 9, No. 2)

RP461. A vacuum tube amplifier for feeble pulses. L. F. Curtiss.

RP462. Infra-red spectra of helium. William F. Meggers and G. H. Dieke. Price 5 cents.

RP463. Tests of cellular sheet-steel flooring. J. M. Frankland and H. L. Whittemore. Price 10 cents.

RP464. The influence of temperature on the evolution of hydrogen sulphide from vulcanized rubber. A. D. Cummings. Price 5 cents.

RP465. Some of the factors which affect the measurement of sound absorption. V. L. Chrisler and Catherine E. Miller. Price 5 cents.

RP466. The reciprocal spherical aberration of an optical system including higher orders. Harold F. Bennett. Price 5 cents.

RP467. An attachment for turning approximately spherical surfaces of small curvature on a lathe. L. C. Gardner.

RP468. Wave lengths and Zeeman effects in lanthanum spectra. William F. Meggers. Price 5 cents.

RP469. Note on the freezing point of "iso-octane" 2, 2, 4-trimethylpentane. Johannes H. Bruun and Mildred M. Hicks-Bruun.

RP470. A twin-bomb method for the accurate determination of pressure-volume-temperature data and a simple method for the accurate measurement of high pressure. Edward W. Washburn.

Research papers, where price is given, are already available, and others will be available in the near future as separates for purchase from the Superintendent of Documents, United States Government Printing Office, Washington, D. C.

U. S. DEPARTMENT OF COMMERCE
ROY D. CHAPIN, Secretary
BUREAU OF STANDARDS
LYMAN J. BRIGGS, Acting Director

BUREAU OF STANDARDS JOURNAL OF RESEARCH

December, 1932
Vol. 9, No. 6

UNITED STATES
GOVERNMENT PRINTING OFFICE
WASHINGTON : 1932

For sale by the Superintendent of Documents, Washington, D. C. - - Price 25 cents; $2.50 per year on subscription

For a partial list of previous research papers appearing in BUREAU OF STANDARDS JOURNAL OF RESEARCH see pages 2 and 3 of the cover

ISOLATION OF THE THREE XYLENES FROM AN OKLAHOMA PETROLEUM [1]

By Joseph D. White [2] and F. W. Rose, jr.[2]

ABSTRACT

Each of the three xylenes has been isolated in a high state of purity from an Oklahoma petroleum. The relative amounts present are *o*, 3; *m*, 3; *p*, 1, the total xylene content of the crude oil being about 0.3 per cent. The density, refractive index, boiling point, freezing point, and infra-red absorption spectrum have been determined for each xylene.

CONTENTS

		Page
I.	Introduction	711
II.	Preliminary distillation	712
III.	Extraction with liquid sulphur dioxide	714
IV.	Fractional crystallization of the sulphur dioxide extract	714
V.	Systematic distillation of the crystallization fractions	715
VI.	Isolation of the three xylenes	716
VII.	Properties of the isolated xylenes	717
VIII.	Content of the xylenes in the crude oil	720
IX.	Conclusion	720
X.	Acknowledgment	720

I. INTRODUCTION

The presence of xylene in petroleum was first recognized by de La Rue and Müller.[3] Since then many investigators have reported the presence of *m*-xylene, and two have reported *p*-xylene in European and Asiatic petroleum,[4] but in no case were the hydrocarbons themselves isolated.

In the first allusion to the occurrence of aromatic hydrocarbons in American petroleum,[5] no reference was made to the presence of xylene. Many years later, Mabery [6] established the presence of *m*- and *p*-xylene in the oils of Ohio and Canada and also in those of California [7] by isolating their nitro derivatives from the fraction distilling between 137° and 140° C. Not until recently, however, has *o*-xylene been detected in any petroleum. Tausz,[8] by oxidizing the xylene fraction of a number of oils (including one from Pennsylvania), succeeded in isolating the three phthalic acids. No one, however, has reported heretofore the separation of each of the xylenes from petroleum.

[1] Financial assistance has been received from the research fund of the American Petroleum Institute. This work is part of Project No. 6, The Separation, Identification, and Determination of the Constituents of Petroleum.

[2] Research associate representing the American Petroleum Institute.

[3] Warren de La Rue and Hugo Müller, Proc. Roy. Soc., vol. 8, p. 221, 1856.

[4] Engler-Höfer, Das Erdöl, vol. 1, pp. 361–362, Hirzel, Leipsig, 1913; and the references there cited.

[5] C. Schorlemmer, Chem. News, vol. 7, p. 157, 1863.

[6] C. F. Mabery, Proc. Am. Acad. Arts Sci., vol. 31, p. 35, 1895.

[7] C. F. Mabery and E. J. Hudson, Proc. Am. Acad. Arts Sci., vol. 36, p. 261, 1901.

[8] J. Tausz, Zeit. angew. Chem., vol. 32 (I), p. 361, 1919.

This paper describes the isolation of these three hydrocarbons from an Oklahoma petroleum.[9] Separation of the three isomers from a highly concentrated mixture of the xylenes was accomplished by first extracting with liquid sulphur dioxide the fraction in which the xylenes collected during distillation and then subjecting the extract to systematic crystallization alternated with distillation. *m*-Xylene was also isolated from a eutectic mixture of the *m*- and *p*-isomers by sulphonation and hydrolysis.

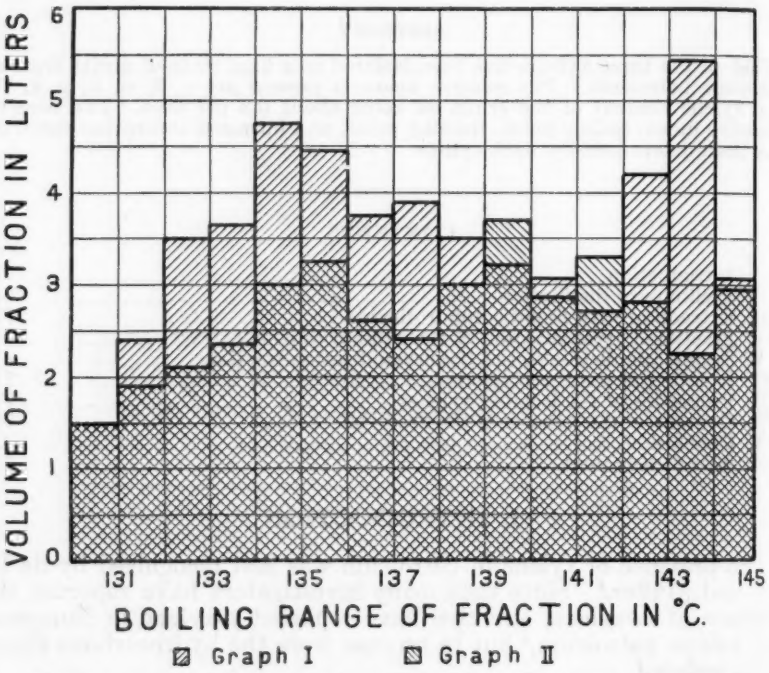

FIGURE 1.—*Distribution of volume of the fractions boiling between 130° and 145° C*

Graph I, before extraction with liquid sulphur dioxide; Graph II, after extraction and subsequent fractional distillation

II. PRELIMINARY DISTILLATION

The petroleum, which had received a preliminary distillation in an oil refinery, was fractionated further with the aid of efficient rectifying columns [10] in the manner described elsewhere.[11] Nearly 45 liters of distillate collected within the temperature range of 127° to 141° C. The distribution by volume of the majority of this fraction with respect to the boiling range is shown by Graph I, in Figure 1. An examination of the 1° cuts of this distillate showed a variation in

[9] For description and properties of the petroleum see E. W. Washburn, J. H. Bruun, and M. M. Hicks, B. S. Jour. Research, vol. 2, p. 469, Table 1, 1929.

[10] (*a*) E. W. Washburn, J. H. Bruun, and M. M. Hicks, B. S. Jour. Research, vol. 2, p. 470, 1929.
(*b*) R. T. Leslie and S. T. Schicktanz, B. S. Jour. Research, vol. 6, p. 378, 1931.
(*c*) J. H. Bruun and S. T. Schicktanz, B. S. Jour. Research, vol. 7, p. 851, 1931.

[11] J. D. White and F. W. Rose, B. S. Jour. Research, vol. 7, p. 907, 1931.

refractive index of $n_D^{20} = 1.420$ to 1.443, with a maximum value for the distillate boiling between 136° and 137° C. The high refractive indices, together with the characteristic odor of the material, strongly suggested the presence of aromatic hydrocarbons. Cooling curves showed that the fraction distilling between 134° and 136° C., which

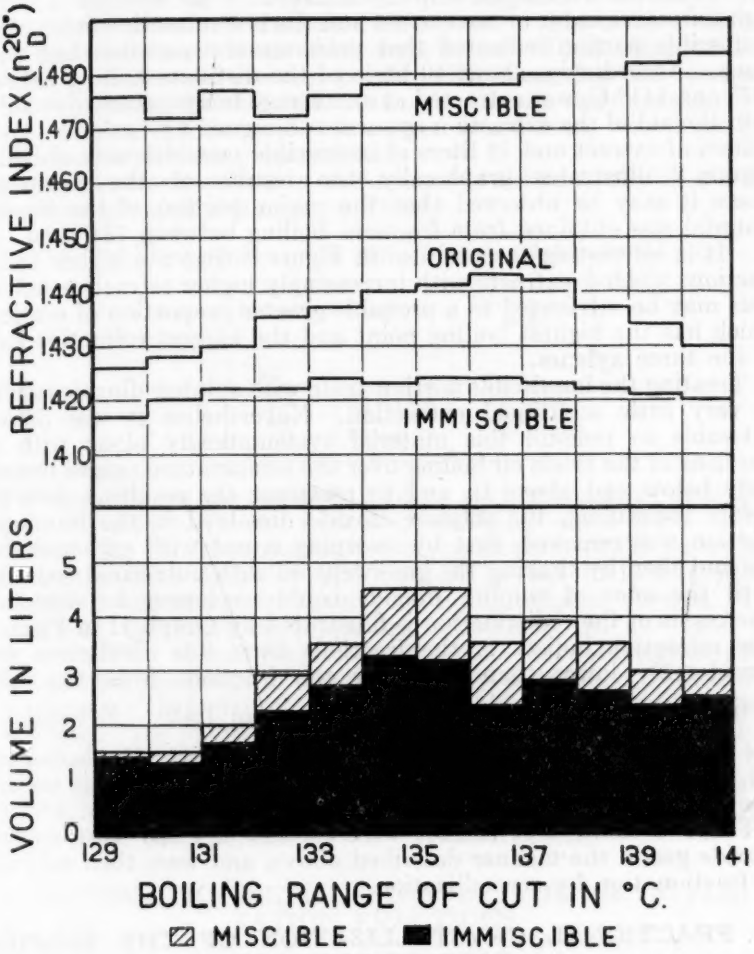

FIGURE 2.—*Change in volume and refractive index of distillation fractions upon extraction with liquid sulphur dioxide*

was the largest, had an initial freezing point of about −80° C. Its behavior on cooling indicated that it might be fractionated further by crystallization. Attempts to fractionate it in this manner resulted in some separation, but not enough to warrant adoption of this method.

III. EXTRACTION WITH LIQUID SULPHUR DIOXIDE

A more promising method for the separation of aromatic hydrocarbons from the distillate was that of extraction with liquid sulphur dioxide.[12] Small samples of a few of the 1° cuts boiling within a range which included the boiling points of ethylbenzene and the xylenes were extracted with liquid sulphur dioxide at −35° to −40° C. The high refractive index of the extract and the low refractive index of the immiscible portion indicated that pronounced separation had taken place. Accordingly, about 40 liters of the distillate boiling between 127° and 141° C. was extracted at an average temperature of −35° C. with the aid of the extraction apparatus designed by Leslie.[13] About 9 liters of extract and 31 liters of immiscible material were obtained. Figure 2 illustrates graphically the results of the extraction. There it may be observed that the major portion of the miscible material was obtained from fractions boiling between 134° and 139° C. It is interesting to note also in Figure 2 that the higher boiling fractions yielded extracts with increasingly higher refractive indices. This may be attributed to a probable greater proportion of *o*-xylene, which has the highest boiling point and the highest refractive index of the three xylenes.

Treating the immiscible portion again with sulphur dioxide resulted in very little additional extraction. Nevertheless it was deemed advisable to redistill this material systematically along with the fractions of the crude oil boiling over the temperature ranges immediately below and above it, and to reextract the resulting distillate. Before redistilling, the sulphur dioxide dissolved in the immiscible fraction was removed, first by sweeping it out with carbon-dioxide gas and then by shaking the gas-swept oil with pulverized soda lime until the odor of sulphur dioxide could no longer be detected.[14] The result of the redistillation is illustrated by Graph II in Figure 1. The refractive indices of the fractions from this distillation were considerably lower than those for the fractions from the initial distillation. In no case was n_D^{20} greater than 1.430. Extraction of the 42-liter portion distilling between 128° and 144° C. yielded only 3.3 liters of extract. As before, the major portion of this material was obtained from the fractions boiling between 134° and 139° C.[15]

The two samples of extract were combined, freed from sulphur-dioxide gas in the manner described above, and were then subjected to fractionation by crystallization.

IV. FRACTIONAL CRYSTALLIZATION OF THE SULPHUR DIOXIDE EXTRACT

A study of the behavior of the extract upon cooling showed that the fractions with the higher refractive indices could be readily

[12] For further study of the merits and technic of extracting petroleum with liquid sulphur dioxide, see
(*a*) L. Edeleanu, Trans. Am. Inst. Min. Eng., vol. 93, p. 2313, 1914.
(*b*) S. E. Bowrey, Pet. Rev., vol. 36, p. 351, 1917.
(*c*) R. L. Brandt, Jour. Ind. Eng. Chem., vol. 22, p. 218, 1918.
(*d*) R. J. Moore, J. C. Morrell, and G. Egloff, Met. Chem. Eng., vol. 18, p. 396, 1918.
(*e*) J. Tausz and A. Stüber, Zeit. angew. Chem., vol. 32 (I), p. 175, 1919.
(*f*) R. T. Leslie, B. S. Jour. Research, vol. 8, p. 591, 1932.

[13] R. T. Leslie, B. S. Jour. Research, vol. 8, p. 591, 1932.

[14] Experience showed that in the presence of even a trace of sulphur dioxide considerable decomposition of the oil took place on heating.

[15] This observation is of interest in view of the fact that o-xylene, which was later found to comprise a fourth of the extract, boils at approximately 144° C.

crystallized in a bath cooled with solid carbon dioxide. The fractions with lower refractive indices yielded no crystals at the sublimation temperature of solid carbon dioxide, but did crystallize when cooled further (to about −90° C.) with liquid air. These promising results made it seem advisable to subject the material to further fractionation by equilibrium melting and accordingly this was done by a method described elsewhere.[16] The melted oil was collected in successive cuts which were preserved according to their refractive indices and melting points. For observing the temperature trend during freezing and melting a toluene thermometer, or a single-junction thermocouple of copper constantan, was kept immersed in the oil during operations.

Systematic fractionation in this manner resulted finally in a series of fractions grouped according to Table 1.

TABLE 1.—*Fractions obtained by crystallizing the sulphur-dioxide extract*

Fraction	Volume	n_D^{20}	Crystallizing range
	ml		°C.
1	5,500	1.495 to 1.500	−50 to −65
2	1,425	1.485 to 1.495	−65 to −80
3	400	1.475 to 1.485	−80 to −90
4	1,750	1.470 to 1.475	−90 to −100

The remainder of the original 12.5-liter portion consisted of mother liquor with $n_D^{20}=1.470$ and with a crystallizing range from −100° to −125° C. Its fractionation by crystallization could be accomplished only with difficulty and resulted in but little separation. Therefore it was extracted again with liquid sulphur dioxide. The extract had the following properties; $n_D^{20}=1.483$, B. P. = 136° C., F. P. = −96° C. These properties, as well as its characteristic odor, indicated that the material was impure ethyl benzene. Work is now in progress on its isolation. The immiscible portion has been preserved also. Its physical properties indicate that it is probably a mixture of naphthenes and iso-nonanes. It should be pointed out that fractional crystallization of the original sulphur dioxide extract served to separate the major portion of these impurities from the xylenes, which concentrated in the "crystal fraction."

V. SYSTEMATIC DISTILLATION OF THE CRYSTALLIZATION FRACTIONS

Oxidation of samples of the crystal fractions, with neutral potassium permanganate, yielded the three phthalic acids. This fact, together with the observed refractive index and the crystallization range, and the further observation that the major portion of the material distilled between 138° and 144° C., indicated that it was a mixture of *p*-, *m*-, and *o*-xylene.

With the aid of the rectifying columns used in the earlier distillations, separate portions of the mixture were fractionally distilled under atmospheric pressure and under a pressure of 215 mm Hg. The distribution of the volumes of the fractions with respect to their

[16] R. T. Leslie and S. T. Schicktanz, B. S. Jour. Research, vol. 6, p. 378, 1931. The apparatus used in this work is illustrated on p. 382 of the reference cited.

boiling range indicated that better fractionation resulted under the reduced pressure. As a consequence the entire mixture of xylenes was subjected to a systematic distillation at a pressure of 215 mm Hg, and was finally separated into two fractions. One of these, consisting of about 2 liters and boiling normally near 144° C., appeared from its behavior on freezing to be impure *o*-xylene. The other portion (a 3-liter fraction) boiling between 138° and 139° C. was found in the same manner to be chiefly a mixture of *p*-, and *m*-xylene.

VI. ISOLATION OF THE THREE XYLENES

The 2-liter fraction of *o*-xylene was further purified by fractional crystallization. With the aid of a centrifuge which could be operated at low temperatures [17] good separation of crystals from mother liquor was attained. As a result of this fractionation a sample of *o*-xylene was isolated, the physical properties of which (see below) indicated it to be of high purity.

Fractional crystallization of the distillate containing the *p*- and *m*-xylene separated it into a *p*-xylene fraction and into a mixture of the two isomers approximating their eutectic in composition. Further fractionation by crystallization of the material rich in *p*-xylene yielded a very pure sample of this hydrocarbon. (See Table 4.)

Systematic crystallization of the impure eutectic mixture resulted in the separation of a crystal fraction which froze at a constant temperature of −55° C. This freezing point agreed well with the value recorded by Nakatsuchi [18] for the freezing point of a synthetic eutectic mixture of *p*- and *m*-xylene. The identity of this material was definitely established by comparing its properties with those of a eutectic mixture of the two isomers, made by mixing them in the proportions prescribed by Nakatsuchi.

By alternating distillation with crystallization as required, a systematic fractionation of the eutectic mixture, in which cuts were made to accord with refractive index and freezing point, resulted in the isolation of a small sample of *m*-xylene. This sample is designated in Table 3 as "best by physical means." [19]

One other sample of *m*-xylene was isolated from the eutectic mixture by sulphonating it at 0° C. Twice the equivalent amount of concentrated sulphuric acid ($d=1.84$) was slowly added to the oil over a period of 6 to 12 hours, during which time the mixture was constantly stirred while surrounded by an ice bath. Reaction was allowed to continue at this temperature for a total of 24 hours, at the end of which time the acid layer was separated, mixed with an equal volume of dilute sulphuric acid (1 : 1 by volume) and steam distilled. Hydrolysis took place most effectively at 130° to 135° C., although to some extent below and above this temperature range.[20] Nearly pure

[17] M. M. Hicks-Bruun and J. H. Bruun, B. S. Jour. Research, vol. 8, p. 528, 1932.

[18] A. Nakatsuchi, J. Soc. Chem. Ind., Japan, vol. 29, p. 29, 1926.

[19] The difficulty of isolating *m*-xylene from its eutectic mixture with *p*-xylene may be appreciated from the fact that the major portion of the mixture distills at substantially a constant temperature, viz, 138.6° to 138.7° C. The residue remaining in the still at the end of the distillation is, however, somewhat richer in *m*-xylene. Moreover, the eutectic mixture contains 85 parts by weight of *m*-xylene and freezes only 7° below the freezing point of that component.

[20] For further study of sulphonation and hydrolysis as a means for separating and analyzing xylene mixtures see: (*a*) O. Jacobsen, Ber., vol. 10, p. 1009, 1877. (*b*) J. M. Crafts, Compt. rend., vol. 114, p. 1110, 1892. (*c*) H. T. Clarke and E. R. Taylor, J. Am. Chem. Soc., vol. 45, p. 830, 1923. (*d*) T. S. Patterson, A. McMillan, and R. Somerville, J. Chem. Soc., vol. 125, p. 2488, 1924. (*e*) N. Kishner and G. Vendelshtein, J. Russ. Phys. Chem. Soc., Chem. Part, vol. 57, p. 1, 1926. (*f*) A. Nakatsuchi, J. Soc. Chem. Ind., Japan, vol. 32, Suppl. Binding, p. 335, 1929.

m-xylene was thus obtained, which upon fractional crystallization yielded a sample of *m*-xylene of very high purity. This sample is designated in Table 3 and Figure 4 as "best by sulphonation."

VII. PROPERTIES OF THE ISOLATED XYLENES

To establish the identity of the isolated xylenes, the purest sample of each was selected on the basis of its behavior on freezing, and the physical properties of each of these were compared with the physical properties of the corresponding synthetic xylene reported in the literature. In addition, a similar comparison was made in the case of *m*-xylene and *p*-xylene, with samples obtained from the Bureau des Étalons Physico-Chimiques in Brussels. These highly pure samples were prepared by J. Timmermans and his coworkers. The results of these comparisons are tabulated in Tables 2, 3, and 4. The density measurements were made by the Division of Weights and Measures of this Bureau. The other properties were determined by the writers. Refractive indices were measured with a calibrated Abbé refractometer (Valentine design) under well-controlled temperature conditions. Readings could be readily made to within two units in the fifth decimal place and the values listed are estimated to be correct to within ± 0.00005. Boiling points were determined in a Cottrell boiling-point apparatus. During the process the entire mercury thread of the thermometer was surrounded by the condensing vapors. Freezing points were determined either with a platinum resistance thermometer or a 5-junction thermocouple calibrated against the thermometer. It is believed that the values reported are correct to within ± 0.02.

TABLE 2.—*Comparison of the physical constants of o-xylene from petroleum with previously reported constants of synthetic o-xylene*

Sample	d_4^{27}	d_4^{20}	n_D^{25}	Boiling point, 760 mm Hg	Freezing point (in dry air)
				°C.	°C.
From petroleum	[1] 0.87445	[2] 0.88040	1.50301	144.4	[3] −25.30
Synthetic (previously reported)	[4] .874	[4] .880	[4] 1.5033	[5] 144	[6] −25.74

[1] ±0.00001. Determined by the section of capacity and density of this bureau.
[2] Calculated from value determined at 27° C., assuming the same temperature coefficient as for *m*-xylene.
[3] Determined with platinum resistance thermometer.
[4] K. Von Auwers, Ann., vol. 419, p. 92, 1919. Calculated from values given for 20° C.
[5] Int. Crit. Tables, vol. 1, p. 219 (McGraw-Hill Book Co., 1926).
[6] A. Nakatsuchi, J. Soc. Chem. Ind., Japan, vol. 32, Suppl. Binding, p. 333; 1929.

TABLE 3.—*Comparison of the physical constants of certain samples of m-xylene with previously reported constants of synthetic m-xylene*

Sample	d_4^{27}	d_4^{20}	n_D^{25}	Boiling point 760 mm Hg	Freezing point (in dry air)
				°C.	°C.
From petroleum:					
Best by sulphonation	[1] 0.85817	[2] 0.86412	1.49467	139.15	[3] −47.89
Best by physical means	[1] .85821	[2] .86416	1.49468	139.15	−49.13
From Bureau des Étalons Physico-Chimiques (Timmermans)	[1] .85821	[2] .86416	1.49467	139.15	[3] −48.05
Synthetic (previously reported)	[4] [5] .85806	[4] [5] .86401	[6] 1.4948	[4] 139.30	[4] [7] −47.55

[1] ±0.00001. Determined by the section of capacity and density of this bureau.
[2] Calculated from values determined at 27° C.
[3] Determined with platinum resistance thermometer.
[4] J. Timmermans, J. chim. phys., vol. 27, p. 402, 1930.
[5] Calculated from value given for 30° C.
[6] Int. Crit. Tables, vol. 1, pp. 219, 277 (McGraw-Hill Book Co.), 1926. Calculated from value given for 20° C.
[7] Recent value given in a private communication from Dr. Timmermans.

TABLE 4.—*Comparison of the physical constonts of certain samples of p-xylene with previously reported constants of synthetic p-xylene*

Sample	d_4^{27}	d_4^{20}	n_D^{25}	Boiling point 760 mm Hg	Freezing point (in dry air)
				°C.	°C.
From petroleum	[1] 0.85498	[2] 0.86107	1.49320	138.4	[3] 13.21
From Bureau des Étalons Physico-Chimiques (Timmermans)	[1] .85509	[2] .86118	1.49320	138.4	[3] 13.21
Synthetic (previously reported)	[4] [5] .85491	[4] [5] .86100	[4] [5] 1.49370	[4] 138.40	[4] 13.35 [6] 13.19

[1] ±0.00001. Determined by the section of capacity and density of this bureau.
[2] Calculated from values determined at 27° C.
[3] Determined in this bureau by B. J. Mair with a platinum resistance thermometer.
[4] J. Timmermans, J. chim. phys., vol. 23, p. 756, 1926.
[5] Calculated from values given for 15° C.
[6] A. Nakatsuchi, J. Soc. Chem. Ind., Japan, vol. 32, Suppl. Binding, p. 333, 1929.

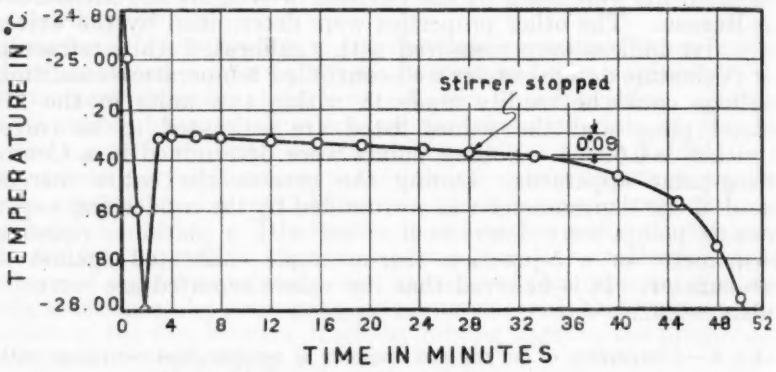

FIGURE 3.—*The time-temperature freezing curve of o-xylene isolated from petroleum*

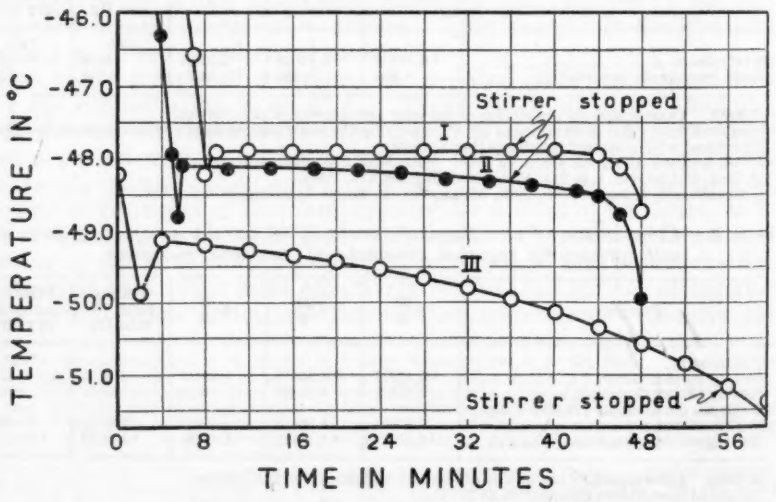

FIGURE 4.—*Freezing curves of m-xylene*

Curve I, from petroleum, best by sulphonation; Curve II, from Bureau des Étalons Physico-Chimiques; and Curve III, from petroleum, best by physical means

As a test of purity of the samples of the isolated hydrocarbons, their behavior during freezing was determined. Figure 3 shows the time-temperature cooling curve of *o*-xylene isolated from petroleum,

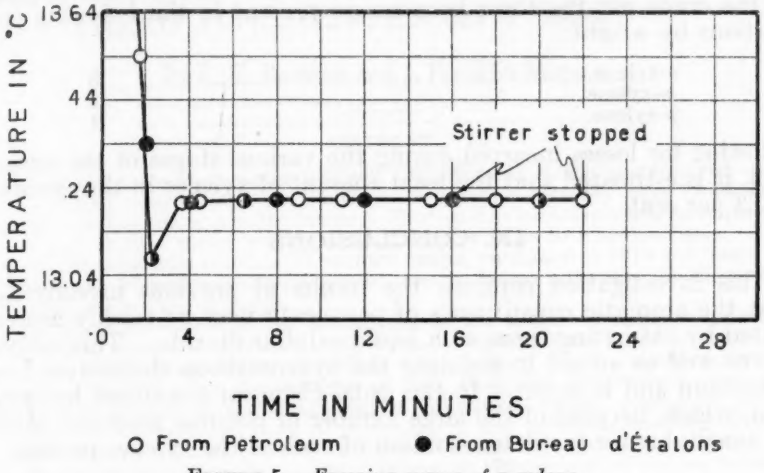

FIGURE 5.—*Freezing curves of p-xylene*

while Figures 4 and 5 show similar curves for the several samples of *m*- and *p*-xylene which include those isolated from petroleum. The very narrow temperature range during the course of freezing (shown by the slope of the flattened portion of the curves) indicates that the

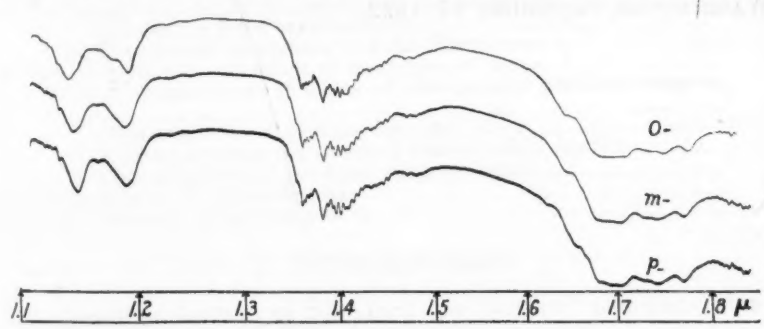

FIGURE 6.—*Infra-red absorption spectra of the xylenes*

Energy transmission curves showing the infra-red absorption spectra of the three isomeric xylenes in 4 mm cell depth from the emission of a tungsten filament lamp. The broad bands from 1.65 μ to 1.76 μ and 1.14 μ to 1.21 μ are the first and second overtones, respectively, of the fundamental hydrocarbon vibration frequency at 3.3 to 3.4 μ. The sharp, peaked absorption bands are due to atmospheric water-vapor in the light-path of the spectrograph. The bands at 1.14 and 1.19 show the clear differentiation in the absorption of the aromatic and aliphatic C ⟷ H vibration; the 1.14 μ band being due to the nuclear C-H absorption, and the 1.19 μ band, the absorption of the side-chain C-H. Slit-width approx. 20 A.

best samples are in a state of high purity. Figure 6 shows the infra-red absorption spectra of the isolated xylenes. The spectra were recorded by U. Liddel, of the Fixed Nitrogen Research Laboratory, Bureau of Chemistry and Soils.

VIII. CONTENT OF THE XYLENES IN THE CRUDE OIL

Analysis of the various xylene fractions by the freezing-point method (thermal analysis) shows that, based upon the total xylene in the crude oil, the three isomers are present in the following proportions by weight:

o-xylene	3
m-xylene	3
p-xylene	1

Allowing for losses incurred during the various stages of the separation, it is estimated that the total amount of xylenes in the crude oil is 0.3 per cent.

IX. CONCLUSIONS

This investigation confirms the results of previous investigators that the aromatic constituents of petroleum may be readily concentrated by extracting them with liquid sylphur dioxide. This method serves well as an aid in isolating the hydrocarbons themselves from petroleum and is superior to the usual chemical treatment by nitration, which, because of the large number of possible products, would be unsuitable for the determination of each of the xylenes present.

X. ACKNOWLEDGMENTS

The writers desire to acknowledge the technical advice of E. W. Washburn, director of American Petroleum Institute Project No. 6, throughout the course of this investigation.

WASHINGTON, September 17, 1932.

CHARACTERISTIC EQUATIONS OF VACUUM AND GAS-FILLED TUNGSTEN-FILAMENT LAMPS

By L. E. Barbrow and J. Franklin Meyer

ABSTRACT

The manufacture of tungsten-filament incandescent lamps has changed very rapidly during recent years, and methods of lamp photometry have necessarily changed with the changes in the lamps. Photometric measurements have passed very largely from a mean horizontal candlepower basis to a lumen basis. The tables of characteristic relations of vacuum lamps, published in 1914 and based on measurements of horizontal candlepower, are no longer adequate for the newer types and larger sizes of lamps.

Logarithmic equations of the second degree are shown to apply to vacuum lamps and to gas-filled lamps in three steps. The equations describe the characteristics of miniature lamps as well as large lamps. Tables of characteristic relations, based on normal efficiencies of 10.0, 12.5, and 16.0 lumens per watt, computed by means of the characteristic equations, furnish means for ready calculation of light output, current, power input, and operating efficiency over a range of voltages from 55 per cent of normal voltage for vacuum lamps, and 80 per cent of normal voltage for gas-filled lamps, to 120 per cent of normal voltage for all types and sizes up to 150 watts, and to 132 per cent of normal voltage for large gas-filled lamps, sizes 200 watts and up.

CONTENTS

	Page
I. Introduction	721
II. The lumen basis of incandescent lamp measurement	722
1. Changes in lamp construction	722
2. Photometry of vacuum and gas-filled lamps	722
III. The characteristic equations of incandescent lamps	723
IV. Tables of characteristic relations of vacuum and gas-filled tungsten lamps	725
1. Characteristics of vacuum tungsten lamps	725
2. Method of using the tables of characteristic relations	726
3. Characteristics of gas-filled tungsten lamps	728
V. Verification of the characteristics	729
VI. Conclusion and acknowledgments	732

I. INTRODUCTION

In a previous Bureau of Standards publication[1] the derivation of characteristic equations of the form

$$y_n = A_n x^2 + B_n x + C \tag{1}$$

from data obtained on vacuum tungsten lamps was fully described and applications of the equations to problems of the lamp standardizing and testing laboratory were illustrated. The equations were shown to express the relations of voltage to candlepower, to current, to watts input, and to the "efficiency," expressed in terms of watts per candle, over the range from 3.3 to 0.7 watts per candle. In these equations the variable x is the logarithm of the ratio of any voltage to that voltage at which a lamp operates when it emits light at an assumed

[1] Middlekauff and Skogland, Characteristic Equations of Tungsten Filament Lamps, B. S. Sci. Paper No. 238. Bull. B. S., vol. 11, p. 483, 1915.

"normal" efficiency. The variable y_n is the logarithm of the ratios of currents, candlepowers, or watts at these voltages, or the logarithm of "efficiency," expressed in watts per candle, at any voltage. A, B, and C are constants. Tables of the characteristic relations were included in the original paper. These have proved very useful in lamp testing and standardization, but need to be revised and extended in order to be applicable to lamps manufactured now. The necessary revisions and extensions are included in this paper.

II. THE LUMEN BASIS OF INCANDESCENT LAMP MEASUREMENT

1. CHANGES IN LAMP CONSTRUCTION

The earlier paper was published before the integrating sphere photometer had come into general use for measuring the total light output of lamps. Practically all lamps then had "squirrel-cage" filaments in clear bulbs and were rated by the manufacturers at so-called efficiencies expressed as watts per mean horizontal candle. Photometric measurements made on a horizontal bar photometer were therefore all that were required for the rating of lamps.

Within the last few years bulb sizes, shapes, and finishes have been changed, as have also the methods of mounting and supporting the filament. Inside-frosted, diffusing bulbs are used now on all sizes of lamps from 15 to 100 watts, and on many of the larger sizes of lamps. The ring-wound, coiled filament has replaced the "squirrel-cage" type of filament mounting. Besides, practically all lamps of 40 watts and above are now gas-filled instead of vacuum. These changes in the construction of lamps have caused changes in their characteristics which have been taken into account in the equations and tables of this paper.

2. PHOTOMETRY OF VACUUM AND GAS-FILLED LAMPS

It has long been known that horizontal candlepower measurements on gas-filled lamps present great difficulties and are generally unreliable.[2] Besides, for most illuminating engineering purposes a knowledge of the total light output of lamps rather than the candlepower in a particular direction is desired. Horizontal candlepower measurements on all types of lamps therefore have been given up almost entirely in commercial and testing-laboratory practice, and measurements of spherical candlepower or total flux have taken their place. In this paper the watts-per-candle basis of the characteristic equations given in Scientific Paper No. 238 has been replaced by a lumen-per-watt basis.

To make the equations of Scientific Paper No. 238 applicable to vacuum lamps when measured in lumens, conversion of mean horizontal candlepower values to lumen values is necessary. The spherical reduction factor, that is, the ratio of mean spherical candlepower to mean horizontal candlepower, for vacuum tungsten lamps, with "squirrel-cage" filament mountings, such as were used in 1914, is approximately 0.78. The normal basis for photometric measurements of vacuum tungsten lamps was formerly generally accepted as 1.20

[2] Middlekauff and Skogland, Photometry of Gas-Filled Lamps, Elec. World, Dec. 26, 1914, p. 1248; and B. S. Sci. Paper No. 264. Bull. B. S., vol. 12, p. 589, 1915–16. C. H. Sharp, Trans. Ill. Eng. Soc., vol. 9, p. 1021, 1914.

watts per mean horizontal candle. This normal value of 1.20 watts per candle becomes 8.17 lumens per watt $\left(\frac{0.78\times 4\pi}{1.20}=8.17\right)$ when the lamps are measured on a lumen basis. This is a much lower efficiency than that at which most vacuum tungsten lamps are now made, and consequently a value of 10.0 lumens per watt has been arbitrarily chosen, on which basis tabular values for vacuum tungsten lamps are calculated in this paper. The characteristics of clear vacuum tungsten lamps as derived in 1914 have been found to apply also to the inside-frosted vacuum lamps as made to-day, so that the equations and tables in this paper for vacuum lamps are fundamentally the same as those contained in Scientific Paper No. 238, but are modified from the candle to the lumen basis and the normal efficiency is increased from 8.17 to 10.0 lumens per watt. The equations for gas-filled lamps have different constants, but are of the same form as the equations for vacuum lamps.

The data from which were derived the equations for gas-filled lamps of sizes ranging from 200 watts up are the result of a very large number of measurements made over a period of 10 years at the Bureau of Standards and at the laboratories of manufacturers of incandescent lamps. The normal efficiency chosen for these equations is 16.0 lumens per watt. It has been found, however, that these equations do not fit the characteristics of the smaller sizes of gas-filled lamps. Two other sets of equations, one for gas-filled lamps of sizes 60 to 150 watts, and the other for gas-filled lamps of 40 and 50 watts have been derived. Both of these sets of equations are on a normal basis of 12.5 lumens per watt. It has been found, also, that the 200 to 500 watt equations and 60 to 150 watt equations describe the characteristics of 32 and 21 candlepower automobile headlamps, respectively, while the 40 to 50 watt equations are suitable for 3 candlepower, 6 to 8 volt lamps.

III. THE CHARACTERISTIC EQUATIONS OF INCANDESCENT LAMPS

The logarithmic form of characteristic equation as applied to vacuum lamps is completely discussed by Middlekauff and Skogland in their original paper,[3] page 494 and following. The form of equation for vacuum lamps:

$$y_n = A_n x^2 + B_n x + C \qquad (n = 1, 2, 3, 4) \qquad (1)$$

is found to apply to gas-filled lamps also. In this equation the independent variable x refers to voltage, and y_n and the corresponding constants A_n, B_n, and C to the efficiency in lumens per watt ($n=1$), light putput ($n=2$), power ($n=3$), and current ($n=4$). There are then four problems to which the general equation is applicable. The variable x is the logarithm of the voltage ratio in each case; that is

$$x = \log \text{ (voltage ratio)}$$

and

$$y_1 = \log \text{ (lumens per watt)}$$
$$y_2 = \log \text{ (light output ratio)}$$
$$y_3 = \log \text{ (power ratio)}$$
$$y_4 = \log \text{ (current ratio)}$$

[3] See footnote 1,

Constants A_n, B_n, and C have been computed on the selected normal bases of 10, 12.5, 12.5, and 16 lumens per watt, respectively, for vacuum lamps and for the three groups of different sizes of gas-filled lamps. These constants for the vacuum-lamp equations were derived from the constants contained in Bureau of Standards Scientific Paper No. 238, as previously indicated. For the various sizes of gas-filled lamps they were determined by setting up logarithmic curves of the relations, voltage ratio to luminous flux ratio, and voltage ratio to efficiency, using data obtained on several sizes of lamps measured over a wide range of voltages. The coefficients B_1 and B_2 were then determined as the slopes of these curves at the normal efficiency. The coefficients A_1 and A_2 were determined from the rates of change of these slopes. Coefficient C is the logarithm of the normal efficiency. Coefficients A_3, A_4, B_3 and B_4 are not independent of the above coefficients, A_3 and A_4 being equal to (A_2-A_1), B_3 being equal to (B_2-B_1), and B_4 being equal to (B_3-1).

TABLE 1.—*Constants in the characteristic equations*

General equation:

$$y_n=A_nx^2+B_nx+C \tag{1}$$

in which x is log (voltage ratio), and y_n is the logarithm of the quantity given in the right-hand column of this table.

CONSTANTS

	Vacuum lamps	Gas-filled lamps			
		Size			
	15–60 w	40–50 w	60–150 w	200–500 w	Used to compute
	Normal lumens per watt				
	10.0	12.5	12.5	16.0	
A_1	−0.918	−1.482	−1.726	−1.690	Lumens per watt.
B_1	1.932	2.162	2.090	1.841	Do.
C[a]	1.00000	1.09691	1.09691	1.20412	Do.
A_2	−.946	−1.425	−1.669	−1.607	Light output (lumens) ratio.
B_2	3.513	3.685	3.613	3.384	Do.
A_3	−.028	.057	.057	.083	Power (watts) ratio.
B_3	1.5805	1.523	1.523	1.543	Do.
A_4	−.028	.057	.057	.083	Current (amperes) ratio.
B_4	.5805	.523	.523	.543	Do.

[a] C=0 for the other relations.

Example.—The lumens-per-watt equation for 500-watt, gas-filled lamps, with normal (100 per cent) value at 16.0 lumens per watt, is

$$y_1=-1.690x^2+1.841x+1.20412$$

where x is the logarithm of the ratio of any desired voltage to the voltage at normal efficiency (16.0 lumens per watt) and y_1 is the logarithm of the efficiency of the lamps at the desired voltage.

It is of interest to note that the coefficient of x (B_1, B_2, B_3, or B_4) in each case in Table 1 is very closely the exponent of the relationship existing between voltage and any one of the dependent variables listed in the last column of the table. For example, the efficiency of 500-watt lamps varies as the 1.84 power of the voltage; the luminous flux varies as the 3.38 power of the voltage; and the current varies as the 0.54 power of the voltage. These exponents are strictly applicable only for small changes of voltage near normal efficiency, but can be used through a wider range of voltages where only fairly close approximations are required.

There are 16 characteristic equations that can be written by using the constants of Table 1 to cover the four groups of lamp sizes, and the

four dependent characteristic variables of each group. It is not convenient, however, to use these equations directly in computations, because one usually does not know the voltage at which a particular lamp is to be operated to give the normal efficiency, and this must be determined before the equations can be used to give the value of any of the dependent variables at any desired voltage. To facilitate computations, Tables 2, 3, 4, and 5, which follow, have been set up by using the 16 characteristic equations, and their use is discussed below.

IV. TABLES OF CHARACTERISTIC RELATIONS OF VACUUM AND GAS-FILLED TUNGSTEN LAMPS

1. CHARACTERISTICS OF VACUUM TUNGSTEN LAMPS

TABLE 2.—*Characteristics of vacuum tungsten lamps, 15 to 60 watts (normal efficiency, 10 lumens per watt)*

$y_1 = -0.918x^2 + 1.932x + 1.000$ (used to obtain column 2)
$y_2 = -0.946x^2 + 3.513x$ (used to obtain column 3)
$y_4 = -0.028x^2 + 0.5805x$ (used to obtain column 4)
$y_5 = -0.028x^2 + 1.5805x$ (used to obtain column 5)

Percentage of normal volts	Lumens per watt	Percentage of normal lumens	Percentage of normal amperes	Percentage of normal watts	Percentage of normal volts	Lumens per watt	Percentage of normal lumens	Percentage of normal amperes	Percentage of normal watts
1	2	3	4	5	1	2	3	4	5
55	2.74	10.6	70.4	38.7	90	8.12	68.7	94.1	84.6
56	2.85	11.4	71.1	39.8	91	8.30	71.5	94.7	86.1
57	2.97	12.2	71.9	41.0	92	8.49	74.4	95.3	87.6
58	3.10	13.1	72.6	42.1	93	8.67	77.3	95.9	89.2
59	3.23	14.0	73.4	43.3	94	8.86	80.3	96.5	90.7
60	3.36	14.9	74.1	44.4	95	9.05	83.4	97.1	92.2
61	3.49	15.9	74.8	45.6	96	9.23	86.6	97.7	93.7
62	3.62	17.0	75.5	46.8	97	9.42	89.8	98.3	95.3
63	3.76	18.1	76.3	48.0	98	9.61	93.1	98.8	96.8
64	3.90	19.2	77.0	49.3	99	9.80	96.5	99.4	98.4
65	4.04	20.4	77.7	50.5	100	10.00	100.0	100.0	100.0
66	4.18	21.6	78.4	51.7	101	10.19	103.5	100.6	101.6
67	4.33	22.9	79.1	53.0	102	10.39	107.2	101.2	103.2
68	4.47	24.3	79.8	54.3	103	10.58	111.0	101.7	104.8
69	4.62	25.7	80.5	55.5	104	10.78	114.8	102.3	106.4
70	4.77	27.1	81.2	56.8	105	10.98	118.6	102.9	108.0
71	4.92	28.6	81.8	58.1	106	11.18	122.5	103.4	109.6
72	5.08	30.2	82.5	59.4	107	11.38	126.5	104.0	111.3
73	5.23	31.8	83.2	60.7	108	11.58	130.6	104.6	112.9
74	5.39	33.5	83.9	62.1	109	11.78	134.8	105.1	114.6
75	5.55	35.2	84.5	63.4	110	11.98	139.2	105.7	116.3
76	5.71	37.0	85.2	64.7	111	12.18	143.6	106.2	117.9
77	5.87	38.8	85.9	66.1	112	12.38	148.1	106.8	119.6
78	6.04	40.7	86.5	67.5					
79	6.20	42.7	87.2	68.8	113	12.59	152.7	107.3	121.3
					114	12.79	157.4	107.9	123.0
80	6.37	44.7	87.8	70.2	115	13.00	162.1	108.4	124.7
81	6.54	46.8	88.4	71.6	116	13.21	166.9	109.0	126.4
82	6.71	49.0	89.1	73.0					
83	6.88	51.2	89.7	74.5	117	13.41	171.8	109.5	128.1
84	7.05	53.5	90.3	75.9	118	13.62	176.8	110.0	129.9
					119	13.83	181.9	110.6	131.6
85	7.23	55.9	91.0	77.3	120	14.04	187.2	111.1	133.3
86	7.40	58.3	91.6	78.8					
87	7.58	60.8	92.2	80.2					
88	7.76	63.4	92.8	81.7					
89	7.94	66.0	93.4	83.1					

2. METHOD OF USING THE TABLES OF CHARACTERISTIC RELATIONS

The method of using these tables is as follows:

1. It is assumed that a lamp has been photometered and that at a given voltage V_0, the current A_0, and lumen output L_0 have been directly measured, and from these values, the watts, W_0, and lumens per watt, l_0 have been computed. It is required to find the current, A_1, lumens L_1, watts W_1, and lumens per watt, l_1, at the required voltage V_1.

2. The tables must be entered at the value of lumens per watt, l_0, or if l_0 is not a tabulated value, then at the value of l_0 interpolated into the table.

3. In the line of the table in which l_0 is found or interpolated (column 2 of each table) read or interpolate V_t, A_t, L_t, and W_t, which are the percentages of normal volts, amperes, lumens, and watts, respectively, for the lamp when operated at l_0 lumens per watt. Thus V_0 is V_t per cent of normal volts, A_0 is A_t per cent of normal amperes, L_0 is L_t per cent of normal lumens and W_0 is W_t per cent of normal watts.

4. The voltage V_1 at which it is required to determine the current, watts, lumens, and lumens per watt of the lamp is then $(V_1/V_0)\times V_t$ per cent of normal volts; that is, letting V'_t be the per cent of normal volts of the lamp at V_1 volts

$$V'_t=(V_1/V_0)\times V_t$$

In the line of the table containing V'_t or in an interpolated line, read or interpolate l'_t, L'_t, A'_t and W'_t, the lumens per watt, per cent of normal lumens, per cent of normal amperes, and per cent of normal watts, respectively, of the lamp when operated at V_1 volts.

Then

$$l_1=l'_t \qquad =\text{lumens per watt at } V_1 \text{ volts}$$

$$L_1=L_0(L'_t/L_t)=\text{lumens at } V_1 \text{ volts}$$

$$A_1=A_0(A'_t/A_t)=\text{amperes at } V_1 \text{ volts}$$

$$W_1=W_0(W'_t/W_t)=\text{watts at } V_1 \text{ volts}$$

also

$$W_1=V_1A_1$$

(a) NUMERICAL EXAMPLES ILLUSTRATING THE USE OF TABLES 2 TO 5

Example 1.—Given a vacuum tungsten lamp, which when burned at 115 volts, emits 243 lumens, and takes a current of 0.220 amperes. This lamp will hereafter in this example be referred to as the test lamp.

To find the lumen output, lumens per watt, current and power input of the test lamp at 124 volts.

Solution.—Find first by direct computation the watts and lumens per watt as follows:

Watts$=115\times0.220=25.3$.

Lumens per watt$=243\div25.3=9.61$.

The known values of the lamp are then:

$V_0=115$ volts.

$A_0=0.220$ amperes.

$W_0=25.3$ watts.

$L_0=243$ lumens.

$l_0=9.61$ lumens per watt.

Enter table 2 (column 2) at 9.61 lumens per watt to determine the per cent of normal voltage at this efficiency. From column 1 of the line containing 9.61 lumens per watt we find that the lamp operates at 98 per cent of normal volts.

Since 115 volts is then 98 per cent of normal volts, 124 volts is $(124/115)\times 98=105.7$ per cent of normal volts. The line of the table, interpolated (column 1) containing 105.7 per cent of normal volts contains also the lumens per watt and percentages of normal lumens, amperes, and watts of the lamp at 124 volts. By multiplying the known values of lumens, amperes, and watts at 115 volts by the ratios of the percentage values read from lines corresponding to 105.7 per cent and 98 per cent of Table 2, values at 124 volts are obtained,

The tabular statement below contains the complete calculations:

	Values read directly from table 2, 9.61 lumens per watt corresponding to 98 per cent volts	Values interpolated into table 2, at 105.7 per cent volts	Computation to 124 volts from columns 2 and 3	Computed values at 124 volts
1	2	3	4	5
Lumens per watt	9.61	11.12		11.12 lumens per watt.
	Per cent	*Per cent*		
Lumens	93.1	121.3	$\frac{243\times 121.3}{93.1}$	317 lumens.
Amperes	98.8	103.25	$\frac{0.220\times 103.25}{98.8}$	0.230 amperes.
Watts	96.8	109.1	$\frac{25.3\times 109.1}{96.8}$	28.5 watts.

NOTE.—Column 5 gives the required values.

Example 2.—A 100-watt, gas-filled tungsten-filament lamp is measured at 125 volts and the following values are obtained:

$V_0=125$ volts.
$A_0=0.912$ amperes.
$W_0=114$ watts.
$L_0=1{,}888$ lumens.
$l_0=16.56$ lumens per watt.

Find amperes, watts, lumens, and lumens per watt at 100 volts. Table 4, page 728 is applicable in this example. Enter Table 4 to find in column 2, 16.56 lumens per watt. It is not found, but by interpolation between 16.49 and 16.76 we have for 16.56 lumens per watt, the following values:

Per cent normal volts $=115.26=V_t$.
Per cent normal lumens $=164.6=L_t$.
Per cent normal amperes $=107.7=A_t$.
Per cent normal watts $=124.2=W_t$.
Lumens per watt $=16.56=l_t$.

Then

$$V'_t=V_t/V_0\times V_t=100/125\times 115.26=92.2$$

Enter table 4 at 92.2 per cent volts, interpolate and compute by using the ratios from lines 115.26 and 92.2 per cent normal volts in the table. We obtain then:

$$\text{Lumens}=1{,}888\times\frac{74.2}{164.6}=851.$$

$$\text{Amperes}=0.912\times\frac{95.9}{107.7}=0.812.$$

$$\text{Watts}=114\times\frac{88.4}{124.2}=81.1.$$

Lumens per watt $=10.49$.

3. CHARACTERISTICS OF GAS-FILLED TUNGSTEN LAMPS

TABLE 3.—*Characteristics of gas-filled lamps, 40 to 50 watts (also 3-candlepower, 6 to 8 volt lamps). Normal efficiency, 12.5 lumens per watt*

$y_1 = 1.482x^2 + 2.162x + 1.09691$ (used to obtain column 2)
$y_2 = 1.425x^2 + 3.685x$ (used to obtain column 3)
$y_3 = 0.057x^2 + 0.523x$ (used to obtain column 4)
$y_5 = 0.057x^2 + 1.523x$ (used to obtain column 5)

Percentage of normal volts	Lumens per watt	Percentage of normal lumens	Percentage of normal amperes	Percentage of normal watts	Percentage of normal volts	Lumens per watt	Percentage of normal lumens	Percentage of normal amperes	Percentage of normal watts
1	2	3	4	5	1	2	3	4	5
80	7.47	42.6	89.1	71.3	100	12.50	100.0	100.0	100.0
81	7.71	44.8	89.7	72.6	101	12.77	103.7	100.5	101.5
82	7.94	47.0	90.2	74.0	102	13.04	107.5	101.0	103.1
83	8.17	49.3	90.8	75.4	103	13.31	111.4	101.6	104.6
84	8.41	51.6	91.4	76.7	104	13.58	115.4	102.1	106.2
85	8.65	54.0	91.9	78.1	105	13.86	119.5	102.6	107.7
86	8.89	56.5	92.5	79.5	106	14.15	123.7	103.1	109.3
87	9.14	59.1	93.0	80.9	107	14.43	128.0	103.6	110.9
88	9.39	61.8	93.6	82.3	108	14.72	132.3	104.1	112.4
89	9.64	64.6	94.1	83.8	109	15.00	136.7	104.6	114.0
					110	15.28	141.3	105.1	115.6
90	9.89	67.4	94.7	85.2	111	15.56	145.9	105.6	117.3
91	10.14	70.3	95.2	86.6	112	15.85	150.7	106.1	118.9
92	10.39	73.3	95.8	88.1	113	16.13	155.5	106.6	120.5
93	10.65	76.3	96.3	89.6	114	16.41	160.4	107.1	122.1
94	10.91	79.4	96.8	91.0	115	16.70	165.4	107.6	123.8
					116	16.99	170.5	108.1	125.4
95	11.16	82.6	97.4	92.5					
96	11.43	86.0	97.9	94.0	117	17.27	175.7	108.6	127.1
97	11.70	89.4	98.4	95.5	118	17.56	180.9	109.1	128.8
98	11.96	92.8	99.0	97.0	119	17.85	186.3	109.6	130.4
99	12.22	96.3	99.5	98.5	120	18.15	191.8	110.0	132.1

TABLE 4.—*Characteristics of gas-filled lamps, 60 to 150 watts, inclusive (also 21-candlepower 6 to 8 volt lamps). Normal efficiency, 12.5 lumens per watt*

$y_1 = -1.726x^2 + 2.090x + 1.09691$ (used to obtain column 2)
$y_2 = -1.669x^2 + 3.613x$ (used to obtain column 3)
$y_4 = 0.057x^2 + 0.523x$ (used to obtain column 4)
$y_5 = 0.057x^2 + 1.523x$ (used to obtain column 5)

Percentage of normal volts	Lumens per watt	Percentage of normal lumens	Percentage of normal amperes	Percentage of normal watts	Percentage of normal volts	Lumens per watt	Percentage of normal lumens	Percentage of normal amperes	Percentage of normal watts
1	2	3	4	5	1	2	3	4	5
80	7.55	43.1	89.1	71.3	100	12.50	100.0	100.0	100.0
81	7.79	45.2	89.7	72.6	101	12.76	103.6	100.5	101.5
82	8.02	47.4	90.2	74.0	102	13.02	107.4	101.0	103.1
83	8.26	49.7	90.8	75.4	103	13.29	111.2	101.6	104.6
84	8.49	52.1	91.4	76.7	104	13.55	115.1	102.1	106.2
85	8.73	54.5	91.9	78.1	105	13.82	119.1	102.6	107.7
86	8.96	57.0	92.5	79.5	106	14.08	123.1	103.1	109.3
87	9.21	59.6	93.0	80.9	107	14.34	127.3	103.6	110.9
88	9.45	62.3	93.6	82.3	108	14.61	131.5	104.1	112.4
89	9.70	65.0	94.1	83.8	109	14.88	135.8	104.6	114.0
90	9.95	67.8	94.7	85.2	110	15.15	140.2	105.1	115.6
91	10.20	70.7	95.2	86.6	111	15.42	144.7	105.6	117.3
92	10.44	73.6	95.8	88.1	112	15.69	149.2	106.1	118.9
93	10.70	76.6	96.3	89.6	113	15.96	153.8	106.6	120.5
94	10.95	79.7	96.8	91.0	114	16.22	158.6	107.1	122.1
95	11.21	82.9	97.4	92.5	115	16.49	163.4	107.6	123.8
96	11.46	86.2	97.9	94.0	116	16.76	168.2	108.1	125.4
97	11.72	89.5	98.4	95.5					
98	11.98	92.9	99.0	97.0	117	17.04	173.2	108.6	127.1
99	12.24	96.4	99.5	98.5	118	17.31	178.3	109.1	128.8
					119	17.58	183.4	109.6	130.4
					120	17.84	188.6	110.1	132.1

TABLE 5.—*Characteristics of gas-filled lamps, 200 to 500 watts (also 32-candle-power, 6 to 8 volt, lamps). Normal efficiency, 16.0 lumens per watt*

$y_1 = -1.690x^2 + 1.841x + 1.20412$ (used to obtain column 2)
$y_2 = -1.607x^2 + 3.384x$ (used to obtain column 3)
$y_4 = 0.083x^2 + 0.543x$ (used to obtain column 4)
$y_5 = 0.083x^2 + 1.543x$ (used to obtain column 5)

Percentage of normal volts	Lumens per watt	Percentage of normal lumens	Percentage of normal amperes	Percentage of normal watts	Percentage of normal volts	Lumens per watt	Percentage of normal lumens	Percentage of normal amperes	Percentage of normal watts
1	2	3	4	5	1	2	3	4	5
80	10.23	45.4	88.7	71.0	105	17.49	117.8	102.7	107.8
81	10.51	47.5	89.3	72.4	106	17.78	121.5	103.2	109.4
82	10.79	49.7	89.9	73.7	107	18.07	125.3	103.8	111.0
83	11.07	52.0	90.5	75.1	108	18.36	129.2	104.3	112.6
84	11.35	54.3	91.0	76.5	109	18.66	133.2	104.8	114.2
85	11.64	56.6	91.6	77.9	110	18.95	137.2	105.4	115.9
86	11.92	59.1	92.2	79.3	111	19.23	141.3	105.9	117.5
87	12.21	61.6	92.8	80.7	112	19.52	145.4	106.4	119.2
88	12.50	64.2	93.3	82.1	113	19.81	149.6	106.9	120.8
89	12.78	66.8	93.9	83.6	114	20.10	153.8	107.4	122.5
90	13.07	69.5	94.5	85.0	115	20.4	158	108.0	124.2
91	13.36	72.2	95.0	86.5	116	20.7	162.5	108.5	125.8
92	13.65	75.1	95.6	88.0	117	21.0	167	109.0	127.5
93	13.94	78.0	96.2	89.4	118	21.2$_8$	172	109.5	129.2
94	14.24	80.9	96.7	90.9	119	21.5$_8$	176.5	110.0	130.9
95	14.53	83.9	97.3	92.4	120	21.8$_8$	181	110.5	132.6
96	14.82	87.0	97.8	93.9	121	22.1$_8$	186	111.0	134.4
97	15.12	90.2	98.4	95.4	122	22.4	190.5	111.5	136.1
98	15.41	93.4	98.9	96.9	123	22.7	195.5	112.0	137.8
99	15.70	96.6	99.5	98.5	124	23.0$_8$	200.5	112.5	139.6
100	16.00	100.0	100.0	100.0	125	23.2$_8$	205.5	113.0	141.3
101	16.30	103.4	100.5	101.5	126	23.5$_8$	210.5	113.5	143.1
102	16.60	106.9	101.1	103.1	127	23.8$_8$	215.5	114.0	144.8
103	16.90	110.5	101.6	104.7	128	24.1	221	114.5	146.6
104	17.20	114.1	102.2	106.2	129	24.4	226	115.0	148.4
					130	24.6$_8$	231.5	115.5	150.2
					131	24.9$_8$	237	116.0	152.0
					132	25.2	242.5	116.5	153.8

V. VERIFICATION OF THE CHARACTERISTICS

The upper range of efficiencies of 500-watt lamps was investigated several years ago in connection with tests made for the optical division of the Bureau of Standards. Starting with a basic value of 17.6 lumens per watt at 105 volts, the following comparison of observed and computed values is an example of the results obtained.

TABLE 6.—*Efficiency of 500-watt lamps*

Volts	Efficiency in lumens per watt	
	Observed	Computed
90	13.2	13.2
100	16.1	16.1
105	17.6	
110	19.1	19.1
120	21.9	22.0
125	23.6	23.4
135	26.3	26.2

Values were recorded for 5-volt steps upward to burn out, which occurred within the step from 195 to 200 volts. Departures from computed values were not very extreme even at the higher points; for example, the observed value at 175 volts was 2.5 per cent below the computed value, and at 185 volts the corresponding difference was 2 per cent. A prohibitive amount of work would be required to assign characteristic values to these extreme points, where the observations have to be taken rapidly against great odds of color difference. Consequently, no attempt has been made to include them in the derivation of equations, and the lumens per watt in Table 5 terminate at 25.2.

Extrapolations have been made to points considerably below the limits of the tables for gas-filled lamps in work done on 500-watt lamps. In this work the voltage and light output at color match with and in terms of vacuum tungsten lamps were determined. At this color the 500-watt lamps operated at about 6.7 lumens per watt. Determinations of light output were then made at voltages corresponding to 16.5 lumens per watt in terms of gas-filled standards. Computed from the voltage and light output for color match with vacuum tungsten standards to these upper voltages, the values of light output checked the values obtained by observation to within 0.3 per cent.

The entire range of all the tables has been explored by means of a physical photometer (phototube photometer). A gas-filled cæsium phototube, corrected for color by means of a suitable filter, and attached to a 60-inch integrating sphere, was used. The phototube circuit is similar to that devised by Sharp and Smith.[4] This phototube photometer has been used at the Bureau of Standards for over a year in the rating of lamps for life test. Every month the characteristics of the photometer are checked by reading on it three of each of seven sizes of standard lamps ranging in size from 15 to 100 watts. The color temperature range of the light from these lamps is approximately 2,400° to 2,800° K. Each time there has been a remarkably close check between the readings thus obtained and the values assigned to the lamps by visual photometry using an 88-inch integrating sphere and Lummer-Brodhun photometer head. There have been other checks on the phototube photometer from time to time and these have shown the photometer to be accurate over a large range of color temperature and flux (lumen output).

All regular sizes of lamps from 15 to 500 watts, and also miniature lamps of 3, 21, and 32 candlepower have been photometered at various voltages to cover the range of the tables of this paper. These lamps were selected at random from the lamps received for life test from five different lamp manufacturers. Typical sets of results are given in Table 7.

[4] Sharp and Smith, Trans. Ill. Eng. Soc., vol. 23, p. 434, 1928.

TABLE 7.—*Observed and computed values of lumens and amperes on lamps of various sizes*

(*a*) AVERAGE OF TWO 15-WATT, VACUUM LAMPS (TABLE 2 USED TO OBTAIN COMPUTED VALUES)

Volts	Lumens		Amperes	
	Photo-tube	Com-puted	Potenti-ometer	Com-puted
80	34.7	34.2	0.106	0.107
90	54	54	.114	.114
100	79	80	.122	.122
115	132		.132	
125	176	176	.139	.139
130	202	204	.142	.142

(*b*) AVERAGE OF TWO 40-WATT GAS-FILLED LAMPS (TABLE 3 USED TO OBTAIN COMPUTED VALUES)

100	252	254	0.332	0.330
110	366	366	.346	.346
120	508	510	.364	.362
125	592		.370	
135	784	784	.384	.385
145	1,005	1,008	.400	.400

(*c*) AVERAGE OF TWO 34-CANDLE-POWER GAS - FILLED LAMPS (TABLE 3 USED TO OBTAIN COMPUTED VALUES)

6.72$_5$	34.2		0.500	
7.50	51.2	51.4	.527	0.528
8.00	64.7	64.8	.544	.547
8.5	79.8	80.6	.560	.564

(*d*) AVERAGE OF TWO 100-WATT, GAS-FILLED LAMPS (TABLE 4 USED TO OBTAIN COMPUTED VALUES)

90	572	570	0.766	0.767
100	852	852	.810	.811
115	1,411		.872	
125	1,888	1,888	.912	.911
130	2,158	2,150	.931	.931

(*e*) AVERAGE OF TWO 21-CANDLE-POWER GAS - FILLED LAMPS (TABLE 4 USED TO OBTAIN COMPUTED VALUES)

5.00	110	109	2.15	2.15
5.50	156	155	2.26	2.26
6.00	211	211	2.36	2.36
6.35	256		2.44	

(*f*) AVERAGE OF TWO 200-WATT, GAS-FILLED LAMPS (TABLE 5 USED TO OBTAIN COMPUTED VALUES)

90	1,208	1,216	1.425	1.424
100	1,778	1,786	1.507	1.507
115	2,912		1.624	
125	3,868	3,847	1.699	1.700
129	4,299	4,285	1.728	1.730

(*g*) AVERAGE OF TWO 32-CANDLE-POWER, GAS-FILLED LAMPS (TABLE 5 USED TO OBTAIN COMPUTED VALUES)

4.00	92	90	2.91	2.89
4.50	142	141	3.08	3.08
5.00	206	206	3.25	3.24
5.50	288	288	3.42	3.42
6.02$_5$	390		3.59	

VI. CONCLUSION AND ACKNOWLEDGMENTS

The equations and tables embodied in this paper have been used for several years at the Bureau of Standards in connection with the routine testing of incandescent lamps. For the various sizes of lamps, slide rules have been devised and these are used to determine the voltages at which lamps are to be burned in order to operate at any desired efficiency, or the operating efficiency of the lamps when burned at any designated voltage. Although this is the general use of the equations and tables here, they have found other occasional uses, such as for determining the voltages at which to calibrate lamps when a designated lumen output or efficiency of the lamps is required. The results obtained by these computations have been checked many times on a visual photometer by groups of experienced observers.

The authors desire to acknowledge the work of the late J. F. Skogland in connection with this paper. He had much of the data here presented nearly ready for publication when he died. It was felt, however, that the equations should be further checked before publication, and this has been done. We wish to state also that the data from which the 200 to 500 watt lamp equations were derived were obtained by cooperative work between the Nela Park laboratories of the General Electric Co. and the Bureau of Standards.

WASHINGTON, August 16, 1932.

THE CALORIMETRIC DETERMINATION OF THE INTRINSIC ENERGY OF GASES AS A FUNCTION OF THE PRESSURE. DATA ON OXYGEN AND ITS MIXTURES WITH CARBON DIOXIDE TO 40 ATMOSPHERES AT 28° C.

By Frederick D. Rossini and Mikkel Frandsen

ABSTRACT

The intrinsic or internal energy, U, of air, oxygen, and mixtures of oxygen and carbon dioxide (to 37 mole per cent), has been determined calorimetrically as a function of the pressure, to 40 atmospheres, at 28° C.

Within the limits of error of the measurements, $(\partial U/\partial p)_T$ is constant over the given range; and its values for the different gases, at 28° C., 0 to 40 atmospheres, in joules per atmosphere per mole, are: Air, −6.08; oxygen, −6.51; 0.075 carbon dioxide and 0.925 oxygen, −7.41; 0.175 carbon dioxide and 0.825 oxygen, −8.74; 0.231 carbon dioxide and 0.769 oxygen, −9.58; 0.366 carbon dioxide and 0.634 oxygen, −12.04. These values are estimated to be accurate within ± 2½ per cent. The data on the mixtures of oxygen and carbon dioxide can be represented by the equation $(\partial U/\partial p)_{301°K.} = -6.51 - 11.0\ x - 11.0\ x^2$, where x is the mole fraction of carbon dioxide. The value of $(\partial U/\partial p)_T$ for air, oxygen, and the mixtures of oxygen and carbon dioxide at other near temperatures can be computed by means of the temperature coefficient of $(\partial U/\partial p)_T$ given by Washburn, namely, −0.4 per cent per degree.

CONTENTS

		Page
I.	Introduction	733
II.	Method	733
III.	Apparatus	736
IV.	Procedure	738
V.	Examination of the gases	739
VI.	Analysis of the measured quantities	739
VII.	Units and auxiliary data	740
VIII.	Experimental data	740
IX.	Results of the present investigation	743
X.	Comparison of the present results with values computed from other data	746
XI.	Acknowledgment	747

I. INTRODUCTION

The theory of determining calorimetrically the intrinsic or internal energy of gases as a function of the pressure has been given in a preceding paper by Washburn.[1] The present paper reports the results of experiments on air, oxygen, and mixtures of oxygen and carbon dioxide (to 36.6 mole per cent), to a pressure of about 40 atmospheres, at 28° C.

II. METHOD

The method employed in these experiments is as follows:

A mass, m, of gas is compressed in a bomb to a pressure of p atmospheres.

[1] Washburn, E. W., B. S. Jour. Research, vol. 9 (RP487), p. 521, 1932.

The bomb with its charge of gas is placed in a calorimeter at the temperature, T.

When the entire system has attained the temperature T, the gas is allowed to escape from the bomb to the atmosphere through a coil of tubing immersed in the calorimeter water. At the same time electrical energy is introduced into the calorimeter at such a rate as to maintain the temperature of the calorimeter sensibly constant at T. The amount of the electrical energy will be equal to the work done by the gas as it pushes back the atmosphere plus the change in internal energy which the gas undergoes as it drops from the pressure p to the atmospheric pressure B.

The work done by the gas as it emerges from the bomb is

$$W = n(Bv)_{1\ \text{atm.}} - Bv_b \tag{1}$$

where n is the number of moles of the gas; $(Bv)_{1\ \text{atm.}}$ is the product of the pressure and volume for 1 mole of the gas at the temperature T and the pressure B (practically 1 atmosphere): v_b is the internal volume of the bomb at the atmospheric pressure B.

The change in internal energy of the gas is, per mole;

$$\Delta U\Big]_p^B = U_B - U_p \tag{2}$$

If the amount of electrical energy, Q, that is added maintains the temperature of the calorimeter constant at T, then

$$Q = n\Delta U\Big]_p^B + n(Bv)_{1\ \text{atm.}} - Bv_b \tag{3}$$

and

$$\Delta U\Big]_p^B + (Bv)_{1\ \text{atm.}} = \frac{Q + Bv_b}{n} \tag{4}$$

When $\Delta U\Big]_p^B + (Bv)_{1\ \text{atm.}}$ is plotted as ordinate against the pressure p as abscissa, the curve, at $p = 1$, will pass through the value of $(Bv)_{1\ \text{atm.}}$, which is constant and known for the given gas. And the slope of the curve will give the value of $-(\partial U/\partial p)_T$ for the gas.

Because of the fact that the steel of the bomb is not an incompressible substance having a zero temperature coefficient of expansion[2] and because the temperature may not remain absolutely constant, several small corrections to equation (4) need be added.

1. The ideal experiment is one in which the temperature of the calorimeter remains absolutely constant at the initial temperature T throughout the experiment. Actually, the temperature changed by a small amount, $\Delta t_{\text{corr.}}$, and the gas left the calorimeter at some average value T_g ($T_g - T$ is about 0.01° C.). The energy required to raise the temperature of the calorimeter from T to $T + \Delta t_{\text{corr.}}$ is equal to the product of $\Delta t_{\text{corr.}}$ and $C_{p(\text{calor.})}$, the heat capacity of the calorimeter. The energy required to raise the temperature of the gas from T to T_g is equal to $C_{p(\text{gas})}(T_g - T)$. The temperature of the issuing gas at any instant was assumed to be that of the calorimeter.

[2] See footnote 1, p. 733.

2. There is a change in the intrinsic energy of the steel bomb itself as the pressure within it changes from p to B atmospheres. This amount of energy is calculable thermodynamically [3] according to the formula

$$\left(\frac{\partial U_b}{\partial p}\right)_T = -T\left(\frac{\partial v}{\partial T}\right)_p - (p-1)\left(\frac{\partial v}{\partial p}\right)_T \tag{5}$$

For the bomb used in the present experiments

$$v = 1.014 \text{ l} \tag{6}$$

$$\frac{1}{v}\left(\frac{\partial v}{\partial T}\right)_p = 33 \times 10^{-6} \qquad °\text{C.}^{-1} \tag{7}$$

$$\left(\frac{\partial v}{\partial p}\right)_T = 39 \times 10^{-6} \text{ l atm.}^{-1} \tag{8}$$

Then, at 28° C., the bomb energy, for a drop in pressure from p to 1 atmosphere, is

$$-\Delta U_b\Big]_p^1 = 1.02\ (p-1) + 0.002\ (p-1)^2 \text{ joules} \tag{9}$$

Equation (9) gives the values shown in Table 1.

At 40 atmospheres, the value of $\Delta U_b\Big]_p^1$ is about 10 per cent of the value of $n\ \Delta U\Big]_p^1$ for air, and about 5 per cent of that for the mixture of 0.634 oxygen and 0.366 carbon dioxide. The uncertainty in the value used for the bomb energy is estimated to be ± 10 per cent of itself, or one-half to 1 per cent of the value of $n\Delta U\Big]_p^1$ for the gases in the experiments at 40 atmospheres.

3. The opening of the valve to let the compressed gas escape from the bomb resulted in the transfer of energy to the calorimeter through friction of the stem on the seat of the valve. This amount of energy was found by measurement to be

$$e = 1.5 \pm 0.5 \text{ -joules} \tag{10}$$

For the present experiments, then

$$\Delta U\Big]_p^B + (Bv)_{1 \text{ atm.}} = \frac{Q + Bv_b - C_{p(\text{calor.})}\,(\Delta t_{\text{corr.}}) - C_{p(\text{gas})}\,(T_g - T) + E}{n} \tag{11}$$

The value of E in equation (11) is given by the sum of equations (9) and (10):

$$E = 1.02\ (p-1) + 0.002\ (p-1)^2 + 1.5 \text{ joules} \tag{12}$$

The temperature of the experiment was taken as T_g.

[3] See footnote 1, p. 733.

TABLE 1

p	$-\Delta U_b\Big]_p^1$
Atmospheres	*Joules*
10	9.3
20	20.1
30	31.3
40	42.8

III. APPARATUS

The calorimeter, thermometric system, energy measuring devices, etc., were the same as those used in previous investigations [4] with the exception that a more sensitive galvanometer was used with the Mueller bridge and platinum resistance thermometer.

The steel bomb used in the present investigation is shown in place in the calorimeter can in Figure 1. Here A is the calorimeter can; B, the steel bomb; C, the copper coil through which the gas passed before leaving the calorimeter; D, the electrical resistance heater; E, the platinum resistance thermometer; F, the glass tube at the exit end of the copper coil; G, the valve; H and I, wrenches for opening the valve; J, the cover of the calorimeter can; K, the current leads.

The heating coil (D, fig. 1) was made by winding enameled constantan wire (No. 30, B. and S. gage) noninductively over mica on a piece of sheet copper made in the form of an inverted trough with open ends. Current leads of enameled copper (No. 24, B. and S. gage) were soldered to the ends of the constantan wire, and the whole was covered with a thin layer of "Pizein" cement. The heater, which had a resistance of about 22 ohms, was placed in position over the fitting which joined the copper coil to the valve of the bomb. Potential leads of enameled copper (No. 28, B. and S. gage) were soldered to the current leads at a point midway between the calorimeter and the jacket, with which all four leads were in good thermal contact.

The bomb, which was tested to 65 atmospheres, had a wall thickness of 1.65 mm; a mass, with valve, of 745 g; a diameter of 10 cm; a height of 16 cm; an internal volume of 1,014 cm^3; and was made of a low carbon (0.12 per cent) steel. The copper coil, whose mass was 1,004 g, was made up of a total length of about 40 feet of ⅛, 3/16, and ¼ inch copper tubing.

The assembly of the apparatus used in filling the bomb and for determining the temperature and pressure of the gas in the charged bomb is shown in Figure 2: A is the storage cylinder; B is a heavy steel purifying tube, which contained "ascarite" (sodium hydroxide-asbestos mixture) and "dehydrite" ($Mg(ClO_4)_2 \cdot 3H_2O$) for the experiments on air and oxygen, and "dehydrite" alone for the experiments on the mixtures of oxygen and carbon dioxide; C is a Bourdon gage for reading the pressure; D is the steel bomb; E is a glass jar containing water; and F is the thermometer for reading the temperature. The connecting tubes were made of ⅛-inch copper tubing.

[4] Rossini, F. D., B. S. Jour. Research, vol. 6 (RP259), p. 1, 1931.

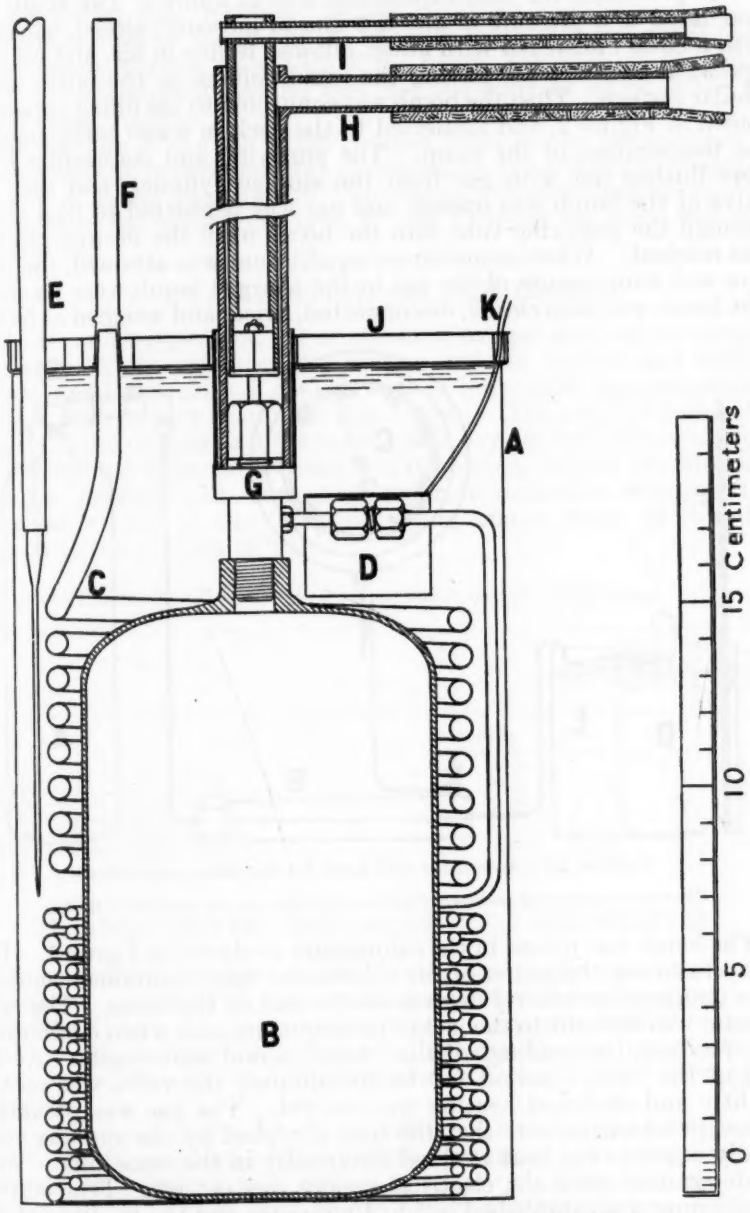

FIGURE 1.—*Assembly of the bomb and the calorimeter can*

The various parts of the assembly, which are drawn to scale, are described in the text

IV. PROCEDURE

The procedure for each experiment was as follows: The bomb was evacuated to a pressure of about 2 mm of mercury, closed, wiped off with a cloth moistened with ether, allowed to dry in air, and weighed against a counterpoise having the same volume as the bomb and a similar surface. Then the bomb was connected to the filling apparatus shown in Figure 2, and immersed to the neck in water maintained at the temperature of the room. The purifying and connecting tubes were flushed out with gas from the storage cylinder, and then the valve of the bomb was opened and gas was permitted to flow slowly through the purifying tube into the bomb until the desired pressure was reached. When temperature equilibrium was attained, the pressure and temperature of the gas in the charged bomb were recorded. The bomb was then closed, disconnected, dried, and weighed as before.

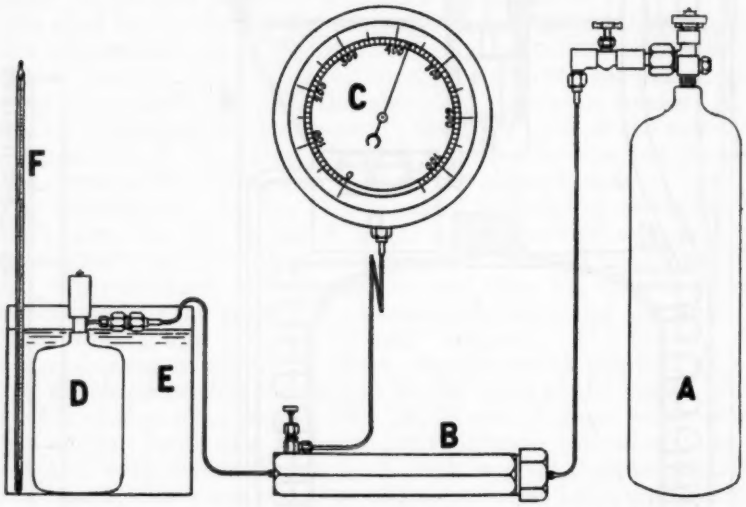

FIGURE 2.—*Apparatus and bomb for the filling operation*

The various parts of the assembly, which are drawn to scale, are described in the text.

The bomb was placed in the calorimeter as shown in Figure 1. The temperature of the jacket of the calorimeter was maintained constant at a temperature several degrees above that of the room. The calorimeter was brought to the jacket temperature, and, when equilibrium was reached, the readings of the "fore" period were begun. At the end of the "fore" period (10 to 20 minutes) the valve was opened slightly and electrical heating was started. The gas was permitted to escape at such a rate that the heat absorbed by the gas was practically equal to the heat evolved electrically in the same time. At a predetermined time the electrical energy was cut off. Temperature equilibrium was established in 5 to 10 minutes and the readings of the "after" period were begun. The lengths of the "fore," "reaction," and "after" periods were usually the same.

After one or two experiments on a given gas it was usually possible to so gage the rate of input of the electrical energy that the net change in the temperature of the calorimeter was not more than 0.01° C.

Readings of the calorimeter temperature, the current, and the voltage were taken every minute and of the jacket temperature every two minutes during the "reaction" period.

The true mass of the gas in the charged bomb was computed from the apparent increase in weight of the bomb, the residual gas in the bomb before charging (several mg) and the buoyant effect of the air on the brass weights.

The pressure of the gas in the charged bomb at the temperature of the calorimetric experiment was computed by correcting the observed pressure p' at the temperature T' to the calorimetric temperature T_g by means of the perfect gas law, T' and T_g being the same within a few degrees.

V. EXAMINATION OF THE GASES

The air and oxygen and the mixtures of oxygen and carbon dioxide were respectively examined for oxygen and for oxygen and carbon dioxide, and the density of the inert gas in the oxygen was determined by the gas chemistry section of this bureau. The average molecular weights of the oxygen and the mixtures of oxygen and carbon dioxide were computed from the percentages of oxygen, carbon dioxide, and inert gas present, and from their separate molecular weights—the molecular weight of the inert gas being known from its density. These results are given in Table 2.

TABLE 2.—*Composition and molecular weights of the gases*

Gas	O_2	CO_2	N_2+rare gases	Molecular weight
	Mole per cent	*Mole per cent*	*Mole per cent*	*g*
Air	20.99	----------	79.01	28.959
"Oxygen"	99.41	----------	.59	32.012
"Oxygen"+carbon dioxide, I	91.66	7.51	.82	32.91
"Oxygen"+carbon dioxide, II	81.71	17.46	.84	34.11
"Oxygen"+carbon dioxide, III	76.18	23.08	.78	34.80
"Oxygen"+carbon dioxide, IV	62.80	36.60	.60	36.40

VI. ANALYSIS OF THE MEASURED QUANTITIES

The quantities involved in the calculation of the results of each experiment, exclusive of the corrections discussed in the latter part of Section II are the mass, pressure, and temperature of the gas in the bomb, the temperature change of the calorimeter, the electrical energy input, the atmospheric pressure, and the internal volume of the bomb.

In Table 3 are given, for the experiments on oxygen at 40 atmospheres, the magnitudes of the various quantities, the sensitivity of the measuring devices with respect to these quantities, and the "allowable error" in each that would contribute an absolute error of 1 joule to the result of each experiment.

TABLE 3.—*Analysis of the measured quantities*

[For an experiment on oxygen at 40 atmospheres]

	Magnitude of the quantity	Sensitivity of the measuring device	"Allowable error" in the quantity	Unit
Mass of gas	55	0.003	0.012	Gram.
Pressure of gas	40	.04	.08	Atmosphere.
Temperature of gas	300	.01	.08	°K.
$\Delta t_{corr.}$	.01	.00002	.0001	°C.
Q	4,700	.2	1	Joule.
B	1	.001	.01	Atmosphere.
v_b	1	.001	.01	Liter.

VII. UNITS AND AUXILIARY DATA

The unit of energy employed in the present work is the international joule.

For computing the value of the product of the pressure and volume for 1 mole of air, oxygen, and carbon dioxide at 28° C. and 1 atmosphere, the following equation was used:

$$(Bv)_{1\ \text{atm.},\ 28\ °\text{C.}} = RT_{0\ °\text{C.}}(1+28\alpha_{28\ °\text{C.}})(1-\lambda_{0\ °\text{C.}}) \qquad (13)$$

R was taken as 8.3115 international joules degree^{-1} mole^{-1}, and $T_{0°C.} = 273.10° K$. The values of the constants [5] for air, oxygen, and carbon dioxide, and the computed values of $(Bv)_{1\ \text{atm.},\ 28°C.}$ are given in Table 4. The values of $(Bv)_{1\ \text{atm.},\ 28°C.}$ for the mixtures of oxygen and carbon dioxide were obtained by interpolation.

TABLE 4.—*Values of* $\alpha_{28°C.}$, $\lambda_{0°C.}$, *and* $(Bv)_{1\ \text{atm.},\ 28°C.}$

Gas	$\alpha_{28°C.}$	$\lambda_{0°C.}$	$(Bv)_{1\ \text{atm.},\ 28°C.}$
			Int. joules mole^{-1}
Air	0.003672	0.00061	2,501.8
Oxygen	.003675	.00094	2,501.1
Carbon dioxide	.003734	.00706	2,489.6
0.075 carbon dioxide+0.925 oxygen			2,500.2
0.175 carbon dioxide+0.825 oxygen			2,499.1
0.231 carbon dioxide+0.769 oxygen			2,498.4
0.366 carbon dioxide+0.634 oxygen			2,496.9

VIII. EXPERIMENTAL DATA

The experimental data obtained in the present experiments are given in Tables 5 and 6. The column headings give the following information: Column 5, the pressure in the bomb $+(1-B)$, giving the initial pressure in the bomb corresponding to a final pressure of exactly 1 atmosphere; 6, T_g the average temperature at which the gas issued from the calorimeter, which is taken as the temperature of the experiment; 13, the value of E, as given by equation (12); 15, a term which corrects the value of $\Delta U\Big]_p^1$ from T_g to 28° C. (computed according to the formula given by Washburn [6]); 17, the value of $(Bv)_{1\ \text{atm.}} + \Delta U\Big]_p^1$ for 28°C.

[5] International Critical Tables, vol. 3, pp. 9, 10, 13. McGraw-Hill Book Co., New York, 1928.

[6] See footnote 1, p. 733. In the last term of that formula $6cT^3$ should read $6c/T^3$.

TABLE 5.—*Experimental data on air and oxygen*

TABLE 5.—*Experimental data on air and oxygen*

Number of experiment	Gas	Mass of gas m	Atmospheric pressure B	Pressure in bomb $+(1-B)$ p	Temperature t_e	Time of electrical energy input Z	Electrical energy input	$\Delta t_{corr.}$	$\Delta t_{corr.} \times C_p$ cal.	De_t	$\frac{C_p(a)}{(T_e-T)}$	E	$n(Be)_{1\text{ atm.}} + n\Delta U]_p^1$ at t_e	Correction of $(Be)_{1\text{ atm.}}$ to 28°C.	Correction of $\Delta U]_p^1$ to 28°C.	$(Be)_{1\text{ atm.}} + \Delta U]_p^1$ at 28°C.
1	2	3	4	5	6	7	8	9	10	11	12	13	14	15	16	17
		g	*Atm.*	*Atm.*	°*C.*	*Seconds*	*Int. joules*	°*C.*	*Joules*	*Joules*	*Joules*	*Joules*	*Int. joules*	*Joules mole*$^{-1}$	*Joules mole*$^{-1}$	*Int. joules mole*$^{-1}$
9	Air (28.956)	49.254	0.990	41.27	28.51	480.00	4,662.5	0.01150	128.0	101.6	0.2	45.8	4,681.7	−4.2	0.4	2,748.8
10		49.340	.996	41.28	28.11	480.00	4,490.0	−.00234	−26.1	102.2	−.5	45.8	4,664.6	−.9	.1	2,737.0
11		48.914	.996	40.86	28.48	480.00	4,457.5	−.00063	−7.0	102.2	−.8	45.3	4,641.2	−4.0	.4	2,744.1
12		47.043	.987	39.20	27.38	480.00	4,472.9	.01640	184.1	101.3	−.3	43.4	4,433.8	5.1	−.5	2,734.0
13		24.420	.987	20.32	26.50	240.00	2,238.0	.01375	155.0	101.3	−.1	21.9	2,206.3	12.5	−.3	2,628.6
14		37.547	.988	31.25	27.03	360.00	3,344.7	−.00218	−24.4	101.4	.1	34.2	3,504.6	8.0	−.6	2,710.4
15		30.306	.998	25.25	27.08	300.00	2,744.7	.00920	103.2	102.4	−.1	27.4	2,771.4	7.6	−.5	2,655.2
16		30.393	.996	25.36	27.50	300.00	2,743.9	.00799	89.6	102.2	−.1	27.5	2,784.1	4.2	−.3	2,656.6
17		36.495	.993	30.39	27.49	360.00	3,284.1	.00691	43.8	101.9	0	33.2	3,373.4	4.2	−.3	2,682.3
18		41.973	.992	35.00	28.02	420.00	3,831.3	.00689	43.7	101.8	0	38.5	3,927.9	−.2	0	2,700.9
48		11.977	.991	10.14	30.97	120.00	1,060.9	.00595	98.4	101.9	0	11.0	1,075.4	−24.5	.6	2,576.3
49		24.107	.988	20.33	31.47	240.00	2,119.4	.00322	35.8	101.4	−.1	22.0	2,207.1	−28.7	1.5	2,624.1
52		24.189	.995	20.39	30.49	240.00	2,119.2	.00343	38.2	102.1	−.2	22.0	2,204.9	−20.6	1.1	2,620.2
19	"Oxygen" (32.012)	26.780	.990	20.20	28.99	240.00	2,185.2	.00600	97.7	100.6	−.1	21.8	2,210.0	−8.2	.5	2,634.1
20		26.759	.980	20.20	28.52	240.00	2,171.4	.00847	93.0	100.6	−.2	21.8	2,200.6	−4.3	.2	2,628.5
21		27.016	.987	20.30	28.53	240.00	2,157.2	.00509	67.3	101.3	−.1	21.9	2,213.2	−.2	−.2	2,618.8
22		55.133	.986	40.84	27.51	480.00	4,305.6	−.02615	−293.1	101.2	−.5	45.3	4,745.7	3.9	−.5	2,759.1
23		55.000	.991	40.71	27.02	480.00	4,605.3	.00249	28.0	101.7	.1	45.2	4,724.1	8.1	−1.5	2,756.7
24		54.725	.991	40.53	27.03	480.00	4,606.5	.00339	40.1	101.7	.6	45.0	4,712.5	8.0	−.9	2,763.7
25		54.950	.998	40.73	27.51	480.00	4,605.3	.00252	28.2	102.4	.1	45.2	4,724.6	4.1	−.5	2,756.0
26		54.225	.993	40.27	27.53	480.00	4,597.0	.00732	81.9	102.1	.4	44.6	4,661.4	3.9	−.5	2,755.3
50		40.327	.995	30.40	30.48	360.00	3,357.3	.00697	77.6	102.1	.2	33.2	3,414.8	−20.5	1.8	2,692.0
51		20.462	.995	15.55	30.48	180.00	1,591.2	.00302	33.7	102.1	−.1	16.7	1,676.4	−20.5	.9	2,693.1

TABLE 6.—*Experimental data on mixtures of oxygen and carbon dioxide*

Number of experiment	Gas	Mass of gas m	Atmospheric pressure B	Pressure in bomb $+(1-B)$ p	Temperature t_e	Time of electrical energy input Z	Electrical energy input	$\Delta t_{corr.}$	$\Delta t_{corr.} \times C_{p\ cal.}$	Bv_b	$C_{p(o)}(T_e - T)$	E	$n(Bv)_{1\ atm} + n\Delta U]_p^1$ at t_e	Correction of $(Bv)_{1\ atm.}$ to 28°C.	Correction of $\Delta U]_p^1$ to 28°C.	$(Bv)_{1\ atm.} + \Delta U]_p^1$ at 28°C.
1	2	3	4	5	6	7	8	9	10	11	12	13	14	15	16	17
		g	*Atm.*	*Atm.*	°*C.*	*Seconds*	*Int. joules*	°*C.*	*Joules*	*Joules*	*Joules*	*Joules*	*Int. joules*	*Joules mole*$^{-1}$	*Joules mole*$^{-1}$	*Int. joules mole*$^{-1}$
27	0.925 "oxygen" +0.075 CO_2 (32.91).	28.212	0.993	20.51	27.55	240.00	2,372.1	0.02396	268.1	101.9	0.4	22.1	2,227.6	3.7	−0.3	2,601.9
28		27.947	.991	20.37	28.11	240.00	2,184.8	−.00151	−16.9	101.7	.1	21.9	2,325.2	−.9	.1	2,737.3
29		56.825	.991	40.84	28.01	480.00	4,341.8	−.03029	−338.0	101.7	−.9	45.3	4,827.7	−.1	0	2,795.8
30		56.615	.993	40.69	27.99	480.00	4,512.5	−.01271	−141.5	101.9	−.7	45.1	4,801.7	.1	−0	2,791.3
31		49.329	.991	35.54	27.99	420.00	4,012.8	−.00252	28.2	101.7	−.4	39.1	4,125.8	−.1	−0	2,752.7
32		27.858	.989	20.53	28.48	240.00	2,286.9	.01503	167.7	101.5	.1	22.1	2,242.7	−4.0	.3	2,645.7
33		27.890	.987	20.50	28.49	240.00	2,203.1	.00676	76.2	101.3	.1	22.1	2,250.2	−4.1	.3	2,651.4
39	0.825 "oxygen" +0.175 CO_2 (34.11).	58.793	.995	40.56	29.48	480.00	4,717.8	−.00435	−49.0	102.1	−.2	45.0	4,914.1	−12.3	2.0	2,840.7
40		60.241	.995	41.55	29.48	480.00	4,708.9	−.01764	−196.9	102.1	−.6	46.1	5,054.6	−12.3	2.1	2,851.8
41		44.094	.993	30.67	29.48	360.00	3,529.1	.00685	76.5	101.9	−.2	33.5	3,588.2	−12.3	1.5	2,764.9
42		29.256	.992	20.53	29.98	240.00	2,197.3	.00097	10.8	101.8	−.4	22.1	2,310.8	−16.4	1.4	2,679.2
34	0.769 "oxygen" +0.231 CO_2 (34.80).	30.562	.986	21.00	28.99	240.00	2,289.4	.00346	38.2	101.2	0	22.6	2,375.0	−8.2	.8	2,696.9
35		61.553	.991	41.15	28.00	480.00	4,898.1	−.00448	−50.2	101.7	.2	45.7	5,095.5	0	0	2,883.8
36		60.746	.990	40.65	28.00	480.00	4,897.5	.00244	27.1	101.6	−.4	45.1	5,017.5	0	0	2,874.4
37		45.246	.996	30.64	28.00	360.00	3,666.2	.01632	182.9	101.2	.4	33.5	3,617.6	0	0	2,782.4
38		30.617	.996	21.00	28.50	240.00	2,290.6	.00363	40.4	101.2	.1	22.6	2,373.9	−4.1	.4	2,694.5
43	0.634 "oxygen" +0.366 CO_2 36.40).	65.394	.993	41.27	29.98	480.00	5,279.8	.00417	46.4	101.9	−.7	45.8	5,381.8	−16.4	4.1	2,983.3
44		64.788	.997	41.03	30.58	480.00	5,274.0	.00887	99.4	102.3	−.2	45.5	5,322.6	−21.3	5.3	2,974.4
45		48.863	.996	31.33	30.97	360.00	3,774.6	.00435	48.2	102.2	−.2	34.3	3,862.7	−24.6	4.7	2,857.6
46		31.089	.995	20.21	30.98	240.00	2,470.5	.02171	242.0	102.1	.1	21.8	2,352.3	−24.6	2.9	2,732.5
47		15.415	.992	10.35	30.98	120.00	1,089.8	.00786	88.2	101.8	0	11.2	1,123.6	−24.6	1.4	2,630.0
53		22.830	1.000	15.10	29.98	180.00	1,778.1	.01871	208.7	102.6	−.1	16.3	1,688.4	−16.4	1.4	2,677.0
54		15.607	1.000	10.39	29.98	120.00	1,179.7	.01424	159.2	102.6	0	11.2	1,134.3	−16.4	1.0	2,630.1

IX. RESULTS OF THE PRESENT INVESTIGATION

The values of $\Delta U\Big]_p^1 + (Bv)_{1\text{ atm.}}$ that are given in Tables 5 and 6 were plotted against the pressure p; and the experimental values

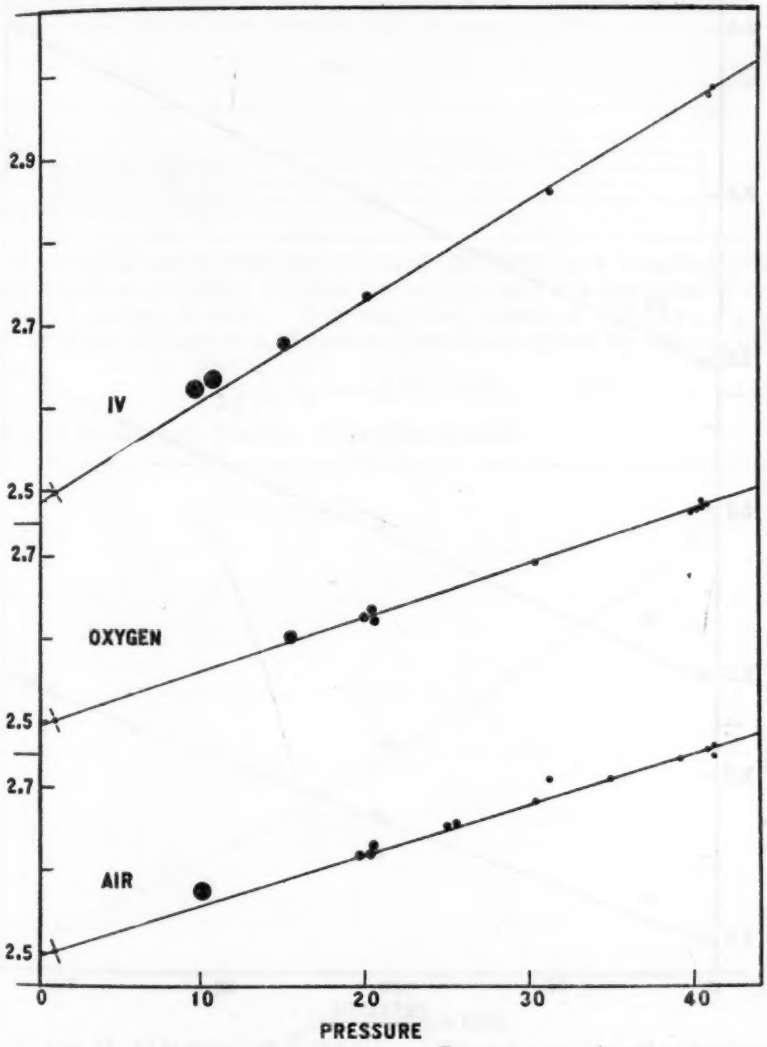

FIGURE 3.—*Plot of the values of* $(Bv)_{1\text{ atm.}} + \Delta U\Big]_p^1$ *for air, oxygen, and mixture IV, at 28° C.*

The scale of ordinates gives the value of $(Bv)_{1\text{ atm.}} + \Delta U\Big]_p^1$ for air, oxygen, and mixture IV (0.366 carbon dioxide and 0.634 oxygen) at 28° C. in international kilojoules mole^{-1}. The scale of abscissas gives the pressure in atmospheres.

and the resulting curves are shown in Figures 3 and 4. The points at $p=1$ are the values of $(Bv)_{1\text{ atm.}}$ computed according to equation (13) and given in Table 4. In each case the experimental points

are drawn with a radius that is equivalent to an error of 4 joules per experiment, which value, for the experiments on oxygen at 40 atmospheres, is 1 per cent of the value of $n\,\Delta U\Big]_p^1$.

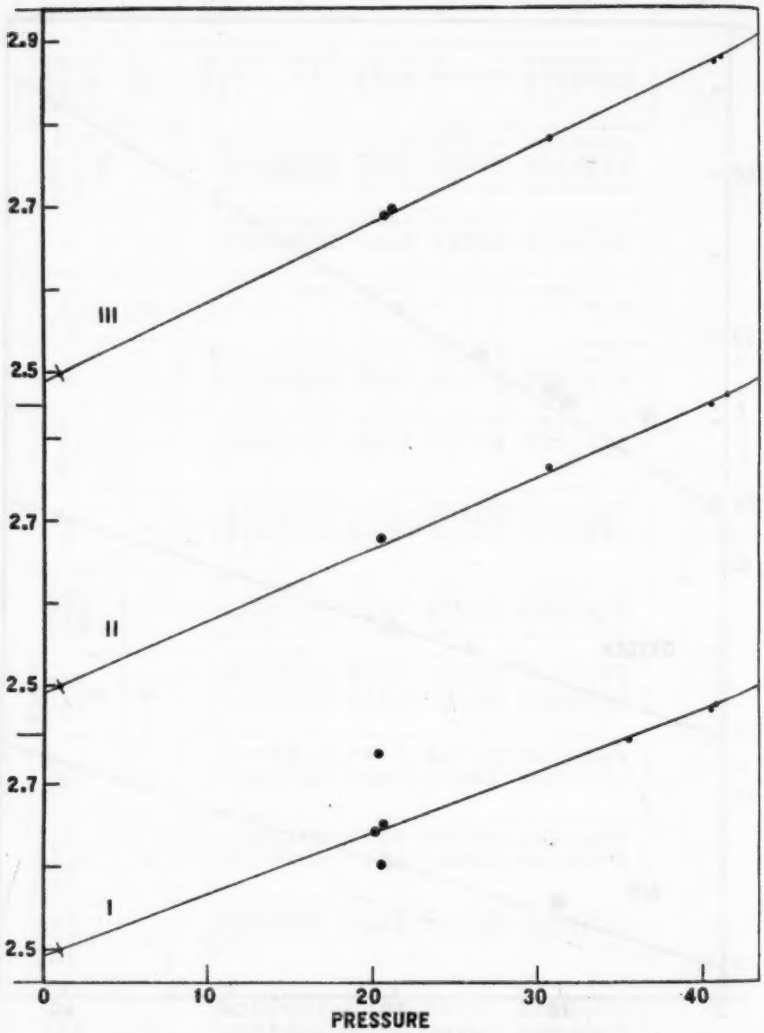

FIGURE 4.—*Plot of the values* $(Bv)_{1\ atm.} + \Delta U\Big]_p^1$ *for mixtures I, II, and III of oxygen and carbon dioxide, at 28° C.*

The scale of ordinates gives the value of $(Bv)_{1\ atm.} + \Delta U\Big]_p^1$ for mixture I (0.075 carbon dioxide and 0.925 oxygen), mixture II (0.175 carbon dioxide and 0.825 oxygen), and mixture III (0.231 carbon dioxide and 0.769 oxygen), at 28° C. in international kilojoules mole^{-1}. The scale of abscissas gives the pressure in atmospheres.

Within the limits of error of the measurements, $\Delta U\Big]_p^1$ is a linear function of the pressure up to 40 atmospheres, and consequently

the value of $(\partial U/\partial p)_T$ is constant. The values of $(\partial U/\partial p)_T$ for the various gases, at 28° C., 0 to 40 atmospheres, in joules per atmosphere per mole, are given in Table 7. These values are estimated to be accurate within ±2½ per cent.

TABLE 7.—*Experimental values of* $(\partial U/\partial p)_T$ *at 28° C., 0 to 40 atmospheres*

Gas	Joules atm^{-1} mole^{-1}
Air	−6.08
Oxygen	−6.51
0.075 carbon dioxide+0.925 oxygen	−7.41
0.175 carbon dioxide+0.825 oxygen	−8.74
0.231 carbon dioxide+0.769 oxygen	−9.58
0.366 carbon dioxide+0.634 oxygen	−12.04

In Figure 5 are plotted the values of $(\partial U/\partial p)_T$, as a function of the mole fraction of carbon dioxide, for oxygen and the mixtures of oxygen and carbon dioxide. The smoothed values of $(\partial U/\partial p)_{301°K.}$ for the mixtures of oxygen and carbon dioxide are given by the equation

$$\left(\frac{\partial U}{\partial p}\right)_{301°K.} = -6.51 - 11.0x - 11.0x^2 \qquad (14)$$

where x is the mole fraction of carbon dioxide.

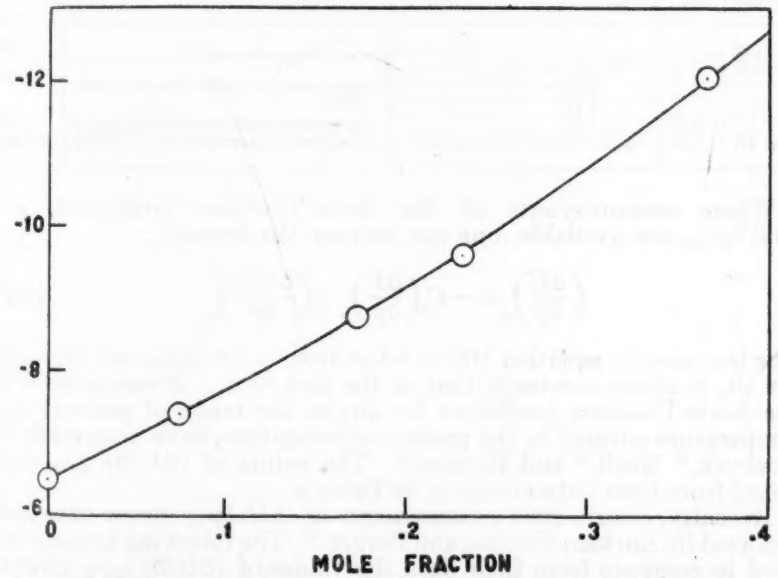

FIGURE 5.—*Plot of the values of* $(\partial U/\partial p)_T$ *against the mole fraction of carbon dioxide, for mixtures of oxygen and carbon dioxide, at 28° C.*

The scale of ordinates gives the value of $(\partial U/\partial p)_T$ at 28° C. in joules atm^{-1} mole^{-1}. The scale of abscissas gives the mole fraction of carbon dioxide. The curve is represented by the equation, $(\partial U/\partial p)_{301°K.} = -6.51 - 11.0x - 11.0x^2$.

The values of $(\partial U/\partial p)_T$ for air, oxygen, and the mixtures of oxygen and carbon dioxide at other near temperatures can be computed by means of the temperature coefficient of $(\partial U/\partial p)_T$ given by Washburn[7], namely, −0.4 per cent per degree.

[7] See footnote 6, p. 740.

X. COMPARISON OF THE PRESENT RESULTS WITH VALUES COMPUTED FROM OTHER DATA

Data similar to that reported in the present paper have not previously been obtained. Nevertheless, values of $(\partial U/\partial p)_T$ for some of the gases pertinent to the present work can be computed by means of the proper thermodynamic formulas from data on appropriate other properties.

Given adequate $p-v-T$ data, one can use the formula

$$\left(\frac{\partial U}{\partial p}\right)_T = -T\left(\frac{\partial v}{\partial T}\right)_p - p\left(\frac{\partial v}{\partial p}\right)_T \tag{15}$$

The $p-v-T$ data for nitrogen have been reviewed by Deming and Shupe,[8] and for nitrogen, air, and oxygen by Beattie and Bridgeman.[9]

From these data the values of $(\partial U/\partial p)_{301°K}$ given in Table 8 have been computed for nitrogen, air, and oxygen.

TABLE 8.—*Values of* $(\partial U/\partial p)_T$ *from various data*

$(\partial U/\partial p)_{301°K}$. 0 to 40 atm. (Joules atm^{-1} mole^{-1})			Reference	Kind of data	Computed by means of formula
Nitrogen	Air	Oxygen			
−5.82			8	$p-v-T$ measurements	(15)
−5.97	−5.82	−6.65	9	$p-v-T$ measurements	(15)
	−5.75		11	Measurements of Joule-Thomson coefficient.	(16)
	−6.17		12	Measurements of Joule-Thomson coefficient.	(16)
	−5.92		13	Measurements of Joule-Thomson coefficient.	(16)
	−6.03		14	Calorimetric measurements of $(\Delta H/\Delta p)_T$.	(17)
(−5.97)	−6.08	−6.51	Present investigation	Calorimetric measurements of $(\Delta U/\Delta p)_T$.	$(\partial U/\partial p)_T$

Where measurements of the Joule-Thomson coefficient, $\mu = (\partial T/\partial p)_H$, are available, one can employ the formula

$$\left(\frac{\partial U}{\partial p}\right)_T = -C_p\left(\frac{\partial T}{\partial p}\right)_H - \left(\frac{\partial (pv)}{\partial p}\right)_T \tag{16}[10]$$

The last term in equation (16) is taken from $p-v$ data, and its value, for air, is about one-tenth that of the first term. Measurements of the Joule-Thomson coefficient for air, in the range of pressure and temperature covered in the present investigation, have been made by Roebuck,[11] Noell,[12] and Hausen.[13] The values of $(\partial U/\partial p)_{301°K}$ computed from their data are given in Table 8.

Recently, calorimetric measurements of $(\Delta H/\Delta p)_T$ for air have been reported by Eucken, Clusius, and Berger.[14] The following formula was used to compute from their data the values of $(\partial U/\partial p)_{301°K}$ given in Table 8:

$$\left(\frac{\partial U}{\partial p}\right)_T = \left(\frac{\partial H}{\partial p}\right)_T - \left(\frac{\partial (pv)}{\partial p}\right)_T \tag{17}$$

[8] Deming, W. E., and Shupe, L. E., Phys. Rev., vol. 37, p. 638, 1931.
[9] Beattie, J. A., and Bridgeman, O. C., J. Am. Chem. Soc., vol. 50, p. 3133, 1928.
[10] $H = U + pv$.
[11] Roebuck, J. R., Proc. Am. Acad. Arts Sci., vol. 60, p. 537, 1925.
[12] Noell, F. Mitteilungen Forschungsarbeiten Gebiete Ingenieurwesens. No. 184, 1916. The data are taken from International Critical Tables, vol. 5, p. 144, McGraw-Hill Book Co., New York, 1929.
[13] Hausen, H., Z. tech. Physik. vol. 7, pp. 371, 444, 1926.
[14] Eucken, A., Clusius, K., and Berger, W., Z. tech. Physik. vol. 13, p. 267, 1932.

In the bottom row of Table 8 are given the values of $(\partial U/\partial p)_{301°K.}$ for air and oxygen as determined from the experiments of the present investigation. The value for nitrogen given in the bottom row was obtained by extrapolation from the values for oxygen and air, assuming the additivity of $(\partial U/p\partial)_T$ for the two components of air.

Inspection of Table 8 shows that, given an estimated error of $\pm 2\frac{1}{2}$ per cent in each of the various values, all are in substantial agreement with the values obtained in the present investigation.

XI. ACKNOWLEDGMENT

The authors acknowledge the technical advice of E. W. Washburn, under whose direction this investigation was carried out.

WASHINGTON, October 1, 1932.

SHEAR TESTS OF REINFORCED BRICK MASONRY BEAMS

By D. E. Parsons, A. H. Stang, and J. W. McBurney

ABSTRACT

Eighteen beams of reinforced brick masonry were tested to determine the resistance of such beams to failure by diagonal tension. The beams were 14 feet long and about 1 foot square in cross section. Beams of three different types of construction were made, an equal number with each of two kinds of brick. A 1:3 Portland cement mortar, with addition of lime equal to 15 per cent of the volume of the cement, was used in all beams. Each beam contained six ½-inch square steel bars as tensile reinforcement. Tensile and shear tests of the bond between mortar and brick and pull-out tests of steel bars embedded in brick masonry were made to supplement the data from the beam tests.

Positions of the neutral axes in the beams varied with kind of brick, arrangement of bricks in the beams, and loads. The ratio of depth to neutral axis to depth of the tensile reinforcement increased with an increase in the number and total thickness of mortar joints in the masonry. The position of the neutral axis corresponded to that calculated by means of the design formulas applying to beams of reinforced concrete, with an assumed modulus of elasticity of the masonry equal to 50 to 70 per cent of that of the masonry piers.

The failures of all beams were accompanied by cracks near the ends of the beams, between a support, and the nearer load. The cracks were evidence of failures by diagonal tension.

Maximum shearing stresses for the different types of beams ranged from 65 to 159 lbs./in.^{2} Resistance to diagonal tension increased with an increase in the proportion of bricks laid with staggered joints. Shearing strengths of the beams were in the same order as shearing and tensile bond strengths of small masonry specimens.

With the relatively absorbent bricks used, tensile and shearing strengths of the masonry were much greater when bricks were wetted before laying than when laid dry.

Bond strengths as determined by pull-out tests of ½-inch square deformed bars embedded about 8 inches in brick masonry ranged from 870 to 950 lbs./in.^{2} Differences in the kinds of brick and curing conditions did not cause significant changes in bond strength.

CONTENTS

	Page
I. Introduction	750
II. Description of specimens and the testing methods	751
1. Bricks	751
2. Mortar	751
3. Reinforcement	751
4. Beams	751
(*a*) Types	751
(*b*) Identification symbols	752
(*c*) Construction	753
(*d*) Aging	754
(*e*) Method of test	754
5. Piers	754
6. Brick-mortar tensile specimens	755
7. Brick-mortar shearing specimens	756
8. Pull-out tests	746

Page

III. Results of the auxiliary tests 757
1. Bricks 757
2. Mortar in the beams 757
3. Reinforcement 758
4. Brick-mortar tensile specimens 758
5. Brick-mortar shearing specimens 759
6. Pull-out tests 759
7. Piers 760
IV. Results of beam tests 761
1. Deformation in the beams 761
2. Positions of the neutral axis 761
3. Types of failures 765
4. Resistance to diagonal tension 765
(*a*) Effect of arrangement and bonding of bricks in beams 765
(*b*) Effect of strength and absorption of the bricks 767
(*c*) Effect of bond strength between mortar and bricks 767
V. Conclusions 768

I. INTRODUCTION

Brick masonry containing steel reinforcement in the form of bars bands or straps, wires or mesh apparently is one of the oldest forms of reinforced masonry construction, and there already exists a fund of information relating to its structural value.[1] Resistance of brickwork to compressive stresses has been extensively investigated, and the information obtained is available in published reports [2] of tests on piers and walls. Data on resistance of brickwork beams to shearing stresses are not as complete as desired and the chief purpose of tests described herein was to obtain information on resistance of reinforced brickwork beams to diagonal tension failures. The compressive strength of masonry having a like arrangement of the bricks, with reference to the direction of stress to that in the beams was also determined, compressive tests being made on piers resembling short lengths of the beams. Tests of the adhesion of mortar to the bricks and to steel were made to supplement the data from the beam tests.

The tests were made by the Bureau of Standards with the cooperation of the Common Brick Manufacturers Association. The association paid for the materials and labor for the construction of all specimens. The beams were built under supervision of and were tested by members of the bureau staff.

The authors are indebted to Robert Hamilton, Judson Vogdes, and Hugo Filippi, representing the association, for their assistance in planning the investigation; to L. R. Sweetman, A. U. Theuer, D. A. Parsons, E. E. W. Bowen, and W. W. Harrison for assisting in making the tests and to S. E. Wade for making the drawings and some of the computations.

[1] Edw. E. Krauss and Judson Vogdes, Reinforced Brick Masonry: History, Summary of Tests. Structures Erected and Bibliography to Date, Report No. 5 of Committee on Reinforced Brick Masonry, National Brick Manufacturers Research Foundation, February, 1932. Reinforced Brickwork: A New Construction Material, Engineering News-Record, vol. 109, p. 71, July 21, 1932.

[2] The Building Code Committee of the Department of Commerce has prepared a mimeographed circular giving test data obtained prior to 1926. B. S. RP108, "Compressive Strength of Clay Brick Walls" describes tests of 297 masonry specimens, completed in 1928.

II. DESCRIPTION OF SPECIMENS AND THE TESTING METHODS

1. BRICKS

Bricks from two localities, Chicago and Philadelphia, were used. Both kinds of bricks were made from surface clays and were formed by the stiff-mud and end-cut process. The Chicago bricks were irregular in shape, contained lime nodules, and were considerably laminated. The Philadelphia bricks were somewhat more regular in shape, quite free from lime nodules, but also laminated. In so far as applicable, methods of specification C67–31 of the American Society for Testing Materials [3] were followed in making the tests.

2. MORTAR

The mortar was proportioned by weight to give a mixture approximately equivalent by volume to 1 part of Portland cement to 3 parts of loose, damp sand, with an addition of hydrated lime equal to 15 per cent of the volume of cement. The weights used were 94 pounds of cement and 6 pounds of hydrated lime to 220 pounds of dry sand, water being added in the amounts desired by the masons.

On each day during construction of the beams a sample of mortar was taken from a mason's board and tested for consistency on the 10-inch flow table,[4] and six 2 by 4 inch cylinders were cast from the same mortar. After remaining in the mold for one day three of each set of cylinders were immersed in water at 70° F. and the other three were stored with the beams. All cylinders were tested for compressive strength at the age of 28 days.

3. REINFORCEMENT

The steel reinforcement consisted of deformed ½-inch square bars. Specimens cut from five bars were subjected to tensile tests following the methods (in so far as applicable) of specification A15–14 of the American Society for Testing Materials.[5]

4. BEAMS

(a) TYPES

Eighteen beams were tested, each being 14 feet long and roughly 1 foot square in cross section. Nine beams were built with common bricks from Chicago and the other nine with common bricks from Philadelphia. The specimens were of three different types of construction, there being three beams of each type with each kind of brick. As illustrated in Figure 1, the bricks in beams of type A were laid in common American bond as for a wall 12½ inches in thickness; in those of type B the bonding was similar to that in a lintel beam with exposed soldier courses. Beams of type C were built on end in which position they resembled portions of a 12½-inch wall with all bricks laid as stretchers and having vertical reinforcement near one face as if designed to resist lateral pressures.

Each beam contained six ½-inch square deformed bars as tensile reinforcement. The ends of all bars were bent into hooks in order

[3] 1931 Supplement to Book of A. S. T. M. Standards, p. 5.
[4] The flow tests were made by the method of Federal specification SS–C–181 for cement; masonry (Jan. 6, 1931).
[5] Book of A. S. T. M. Standards, Pt. I, p. 132, 1930.

to minimize the probability of beam failures resulting from slipping of the bars. The piers contained no reinforcement, but each one was similar otherwise to a short length (about 34 inches) of a beam.

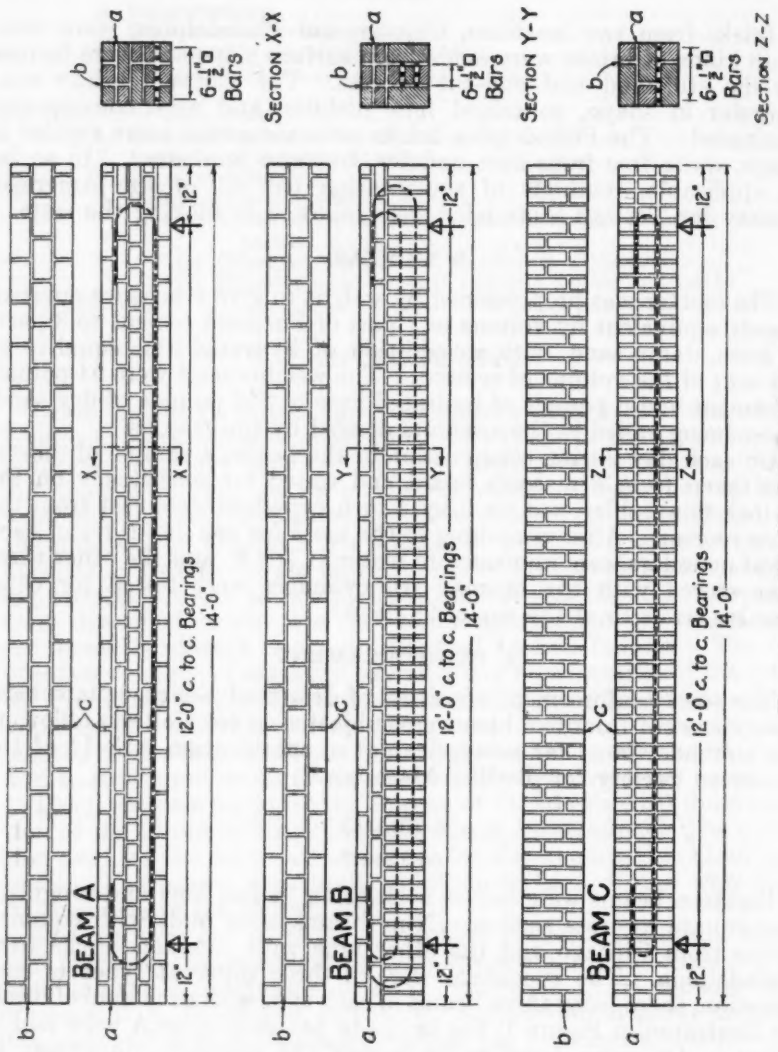

FIGURE 1.—*Details of the test beams*

(b) IDENTIFICATION SYMBOLS

The following symbols, in the order given, are used to identify the beams:

Bricks	C = Chicago. P = Philadelphia.
Type of beam	A as shown in Figure 1. B as shown in Figure 1. C as shown in Figure 1.

Numbers 1, 2, and 3 indicate individual beams.

(c) CONSTRUCTION

The beams were built in the laboratories of the Bureau of Standards by a mason contractor. Bids were obtained from three contractors and the work of constructing the specimens was awarded to the lowest bidder.

The bricks for the beams were dumped from the delivery trucks on an outdoor concrete pavement. On the day before using the bricks they were sprinkled in the pile until the water flowed from every portion. They were again sprinkled in the same manner just before laying.

Beams of types A and B were built on horizontal wooden forms and those of type C were built on end on the laboratory floor. Views of one beam of each type are shown in Figure 2.

The beams were built by two masons working together. The masons were instructed to produce masonry having the spaces between the bricks well filled with mortar, without specifying the method. The method of filling the vertical joints by "slushing" the mortar rather than by "shoving" the bricks was chosen by the masons. During the building of the beams one of the masons was cautioned not to furrow the horizontal beds while the other made smooth spread beds without special effort. Although these masons had no previous experience with reinforced brickwork, the two masons and one helper built the last 12 beams and 12 piers at the rate of one beam and one pier per 3¼ hours.

The average thicknesses of mortar joints as determined from measurements of the beams are given in Table 1.

TABLE 1.—*Thickness of the mortar joints in beams*

Beam No.	Average thickness of mortar joints [1]			Beam No.	Average thickness of mortar joints [1]		
	Horizontal *a*	Vertical in top course			Horizontal *a*	Vertical in top course	
		Longitudinal *b*	Cross *c*			Longitudinal *b*	Cross *c*
	Inches	*Inches*	*Inch*		*Inches*	*Inches*	*Inch*
CA-1	0.66	0.90	0.52	PA-1	0.79	0.85	0.54
CA-2	.66	.90	.69	PA-2	.78	.80	.54
CA-3	.66	.94	.60	PA-3	.59	.70	.54
Average	.66	.91	.60	Average	.72	.78	.54
CB-1	.68	.66	.47	PB-1	.85	.87	.50
CB-2	.70	.68	.53	PB-2	.80	.74	.53
CB-3	.65	.87	.63	PB-3	.80	1.03	.58
Average	.68	.74	.54	Average	.82	.88	.54
CC-1	.99	1.25	.52	PC-1	1.12	1.40	.52
CC-2	1.01	1.25	.44	PC-2	1.02	1.33	.48
CC-3	1.01	1.15	.44	PC-3	1.01	1.13	.48
Average	1.00	1.22	.47	Average	1.08	1.29	.49

[1] With the beam in the same position as during testing. The location of joints *a*, *b*, and *c* are shown in Figure 1.

(d) AGING

The beams of types A and B were lifted from the forms when one week old and were stored, until tested, in stacks which allowed free circulation of air around each specimen. Those of type C were placed in a horizontal position in the same stacks. All beams were tested at ages ranging from 27 to 29 days.

(e) METHOD OF TEST

The beams were tested in a vertical screw-testing machine having a capacity of 600,000 pounds. They were supported over a span of 12 feet and loaded along two lines, each 3 feet from mid span. The type of supports and method of transmitting the loads to the beam are illustrated in Figure 3.

Measurements were made of deflections at mid span of the beams and of deformations in the masonry and steel along longitudinal gage lines near mid span. Deflections were measured by means of micrometer dials which indicated the vertical displacement of the upper surface of the beam at mid span relative to a metal frame supported at each end on steel spheres directly over the beam supports. (Shown in fig. 3.) Compressive longitudinal deformations in the upper surfaces of the beams were measured on 20-inch gage lengths by means of a hand strain gage. Tensile longitudinal deformations in the steel over 8-inch gage lengths were measured in one of the bars near each lateral face of the beams by means of gages clamped to the under sides of the bars. Small strap-iron bars, set in vertical joints, were used to support micrometer dial gages and spacing bars for making measurements over longer gage lengths. With this apparatus the deformations in gage lengths of about 40 inches were measured at each lateral face about 1 inch below the upper surface and about 1 inch above the lower surface of a beam.

In making a test the load was increased by increments until deformations indicated stresses in the steel of about 15,000 lbs./in.^{2}. The total load on the beam was then reduced to 1,000 pounds, and finally the load was increased by increments until failure occurred. Usually the devices for measuring strains were removed before the beams failed.

5. PIERS

Eighteen piers, corresponding to the 18 beams, were also built. The piers contained no reinforcement, but each was similar otherwise to a short length (about 34 inches) of a beam and was built in a manner similar to that of the corresponding beam, identified by the same symbol and aged under the same conditions. A view of an unfinished pier is shown in Figure 2.

The piers were tested in compression under central loading in a 10,000,000-pound-capacity testing machine.[6] The lower bearing surface of the pier was bedded in plaster of Paris (calcined gypsum) on the lower platen of the machine. After tilting this platen until the upper surface of the pier was parallel with the upper platen, the upper surface was capped with plaster of Paris.

Vertical compressometers having gage lengths usually between 20 and 30 inches were attached to two opposite sides of the pier. Read-

[6] Described in Bureau of Standards Research Paper No. 108, p. 526.

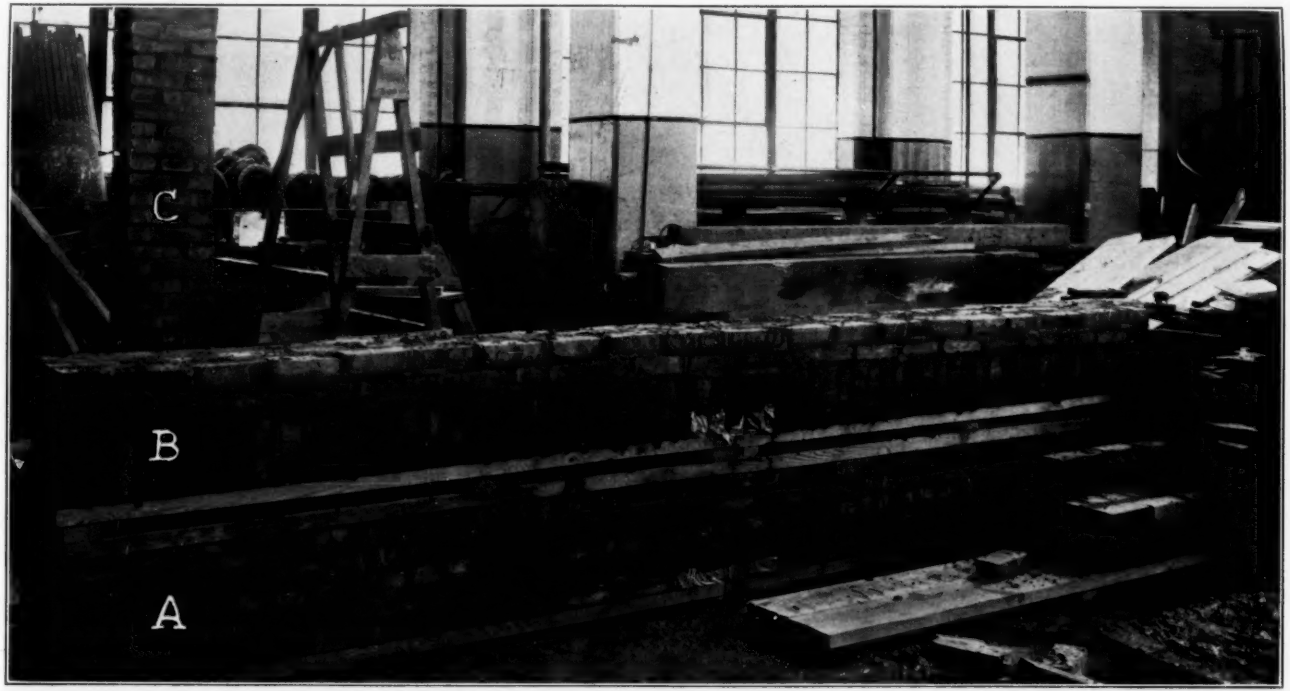

FIGURE 2.—*Test beams under construction*

Note the type C beam on end at the left.

UNIV OF MICH.

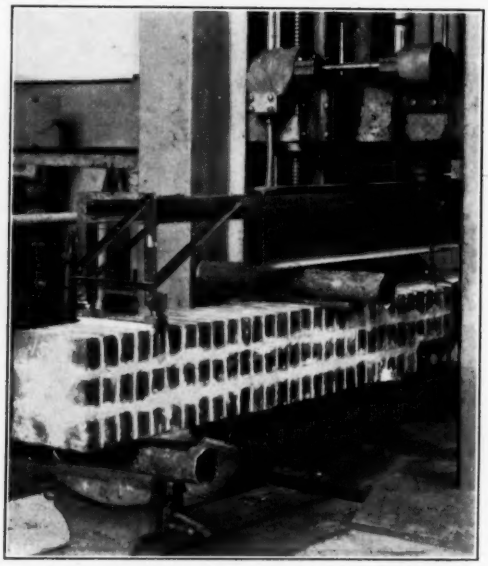

FIGURE 3.—*Beam PC–3 in testing machine*

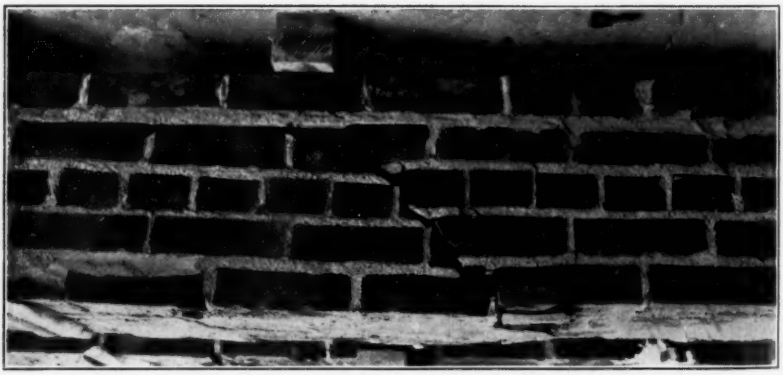

FIGURE 7.—*Beam PA–3 after diagonal tension failure*

ings were taken at equal increments of load usually obtaining about eight readings as the stress increased from 0 to 1,000 lbs./in.^{2}, the load being held constant while each set of readings was made. The compressometers were then removed and the machine run at constant speed until failure occurred.

6. BRICK-MORTAR TENSILE SPECIMENS

As the tensile strength of masonry in beams without web reinforcement is the chief source of resistance to diagonal tension, the factors which affect tensile strengths of brick and mortar specimens probably are the same as those governing web resistance of beams. Failures of specimens of brick and mortar when subjected to tensile stresses might conceivably occur by failures of the bricks, of the mortar, of the adhesion between mortar and brick, or of any combination of these. The purpose of tests described was to compare tensile strengths of specimens made with the same types of bricks and the same mortar as were used in the beams. Variations in moisture content of the bricks when laid and in curing conditions were included in the study in order to obtain an estimate of their influence on the strengths of the masonry.

Tests of strength of bond in tension of brick-mortar joints were made. The specimens consisted of two bricks laid flatwise, separated by mortar, the cross section of the joint being 30 square inches for standard size bricks. Twenty test specimens were made for each of the following conditions: Two makes of bricks (Chicago and Philadelphia), dry bricks and dry cure, dry bricks and damp cure, wet bricks and dry cure, and wet bricks and damp cure.

Bricks were considered as dry after one week's storage in a steam heated room. Some bricks were used after 48 hours in a drying oven at 220° F., followed by 24 hours' cooling in the laboratory.

For wetting bricks, the procedure was to totally immerse previously dried bricks for one hour, stand on end in air for one-half hour, and then make the test specimens within the next half hour.

All construction was done in a room kept at a temperature of 70° ±1° F. and a relative humidity of 40 to 60 per cent. The "dry cure" specimens were left in this room for 48 hours after construction and then removed to a laboratory at "room temperature." The "damp cure" specimens were removed at the end of the half hour construction period to the damp storage room of the concrete laboratory, which is kept at a temperature of 70° ±1° F. and a relative humidity of over 90 per cent.

The mortar used was a cement-lime-sand mixture of the same proportions as that used in constructing the beams. An attempt was made to have the flow immediately after mixing between 110 and 120 per cent. The mortar was proportioned and mixed dry. Time was counted from the moment of adding the water to the mortar mix. A flow test was made before starting construction of the test specimens. Mortar was thrown on the flat of the bottom brick. The top brick was quickly put in place with a shoving motion, using considerable pressure. Excess mortar was cut off with a trowel. Since comparison of the two makes of bricks was considered the main purpose of the investigation, the individual specimens were constructed alternately of Chicago and Philadelphia bricks.

The action of the dry bricks of both makes was to suck water out of the mortar, hence the utmost possible speed was used in getting the bricks in place. At best, a number of joints in the dry brick specimens were imperfectly filled.

Care was taken to avoid jarring specimens after construction. In spite of care used in handling, a considerable number of the dry brick specimens separated before testing.

It was the intention to make all tests at 28 days, hence the specimens were removed from damp storage at the end of 24 days, exposed in the laboratory for two days and then capped. Circumstances required that some of the tests be delayed, but the damp cure was restricted in all cases to 24 days.

The method of determining the tensile strength was essentially that used for testing whole bricks in tension described in another paper.[7] Palmer and Hall [8] further describe the apparatus and method.

7. BRICK-MORTAR SHEARING SPECIMENS

The shearing specimens were equal in number and made with the same mortar mixture and with the same procedure as the brick mortar tensile specimens. The specimens for shear were made by laying three bricks flat, the top and bottom bricks having their ends in line while the center brick was displaced lengthwise from one-half to three-quarters of an inch.

The projecting ends of the two outer bricks of each specimen were capped with plaster of Paris, the surfaces of both caps being in one plane. The projecting end of the center brick was also capped, its surface being as far as possible parallel to the surfaces of the two other caps.

The specimens after capping were loaded in compression, the load being applied to the center brick and the specimen resting on the ends of the two outside brick. This is the method of Douty and Gibson.[9]

8. PULL-OUT TESTS

Specimens for pull-out tests consisted of a ½-inch square deformed steel bar imbedded lengthwise in a mortar joint of a small brick pier. The same variables in brick and curing were used as for the brick-mortar tensile and shearing specimens, but the brick were wetted before laying. A deformed steel bar (one-half inch square) was held vertically by clamps, the lower end resting on oiled paper. Around this bar was built a small brick pier approximately 8 by 8 inches in cross section and three bricks high. The middle course of bricks were laid as headers with respect to the top and bottom courses. Care was taken to secure imbedding of the bar in mortar and to avoid contact of brick with the bar. All joints were filled with mortar. No dry bricks were used in this series, but both kinds of cure were employed. The mortar was the same as that used for the tensile and shearing specimens.

Before testing, the specimens were capped with plaster of Paris on top of the bricks, care being taken to have the capped surface smooth and normal to the projecting steel bar.

---

[7] J. W. McBurney, Strength of Brick in Tension, J. Am. Ceramic Soc., vol. 11 (2), pp. 114–117, 1928.
[8] L. A. Palmer and J. V. Hall, Durability and Strength of Bond Between Mortar and Brick, B. S. Jour. Research vol. 6 (3), pp. 473–492, 1931.
[9] R. F. Douty and H. C. Gibson, Influence of the Absorptive Capacity of Brick Upon the Adhesion of Mortar, Proc. Am. Soc. Testing Materials, vol. 8, pp. 513–530, 1908.

During a test the specimen was inverted, resting on a steel plate supported by the top head of the testing machine. The bar projected downward through a ¾-inch hole in the steel plate and was gripped by wedges in the movable head of the testing machine.

III. RESULTS OF THE AUXILIARY TESTS

1. BRICKS

Results of tests of the bricks are given in Table 2, in which each average value is the mean from 25 tests. As a measure of the dispersion of the results of single tests about their corresponding averages, there are given in Table 2 values for the standard deviations, which were calculated by means of the following formula:

$$\sigma = \sqrt{\frac{\Sigma v^2}{n-2}}$$

where

σ = standard deviation.
n = number of individual values.
Σv^2 = sum of the squares of the deviations of the single values from their mean.

The values of standard deviations given in other tables were calculated by means of the same formula.

2. MORTAR IN THE BEAMS

Results of tests of the specimens representing the mortar in the beams are given in Table 3.

TABLE 2.—*Properties of the bricks*

Each value was derived from results of tests of 25 bricks

Property	Kind of bricks			
	Chicago		Philadelphia	
	Mean value	Standard deviation	Mean value	Standard deviation
Length.....inches..	8.00	0.08	8.15	0.14
Width.....do....	3.64	.06	3.72	.06
Thickness.....do....	2.23	.03	2.29	.02
Compressive strength flatwise.....lbs./in.^{2}..	3,910	860	4,510	840
Compressive strength edgewise.....do....	4,280	950	5,240	950
Compressive strength endwise.....do....	7,030	1,330	4,200	1,750
Modulus of rupture flatwise.....do....	1,530	570	650	340
Absorption by 5 hours immersion.....per cent..	8.8	2.7	11.1	1.6
Absorption by 48 hours immersion.....do....	10.8	2.8	12.7	1.9
Absorption by 5 hours boiling.....do....	14.7	2.6	16.1	1.8

TABLE 3.—*Properties of mortar for the beams*

Each value was derived from results of 21 tests

Property	Mean value	Standard deviation
Flow.....per cent..	108	8.2
Compressive strengths of 2 by 4 inch cylinders, age 28 days:		
Dry storage.....lbs./in.^{2}..	2,340	440
Damp storage.....do....	3,740	530

3. REINFORCEMENT

Tensile properties of the ½-inch square deformed steel bars are given in Table 4.

TABLE 4.—*Properties of reinforcement for the beams*

Each value was derived from the results of five tests

Property	Mean value	Standard deviation
Cross sectional area.....inches²	0.240	0.002
Proportional limit.....lbs./in.²	45,200	6,700
Yield point.....do	51,100	1,600
Tensile strength.....do	81,600	1,400
Modulus of elasticity.....do	29,400,000	1,100,000
Elongation in 8 inches.....per cent	22.4	2.0

4. BRICK-MORTAR TENSILE SPECIMENS

Results of tests of the brick-mortar tensile specimens are given in Table 6.

TABLE 5.—*Properties of mortar for the tensile and shear test specimens*

Each value was derived from results of from 40 to 51 tests. Strength tests at ages ranging from 28 to 60 days

Property	Mean value	Standard deviation
Initial flow.....per cent	116	9.8
Flow one-half hour after mixing.....do	92	14.1
Tensile strengths of briquettes with:		
Dry storage.....lbs./in.²	290	25
Damp storage.....do	470	34
Compressive strengths of 2 by 4 inch cylinders with:		
Dry storage.....lbs./in.²	3,410	400
Damp storage.....do	4,010	250

TABLE 6.—*Results of tensile tests of bond between mortar and brick*

Age at test 28 to 60 days

Brick		Storage	Number of specimens	Average strength	Standard deviation
Kind	Condition when laid				
				Lbs./in.²	*Lbs./in.²*
Chicago	Dry	Dry	16	38	17
		Damp	16	38	13
	Wet	Dry	20	55	17
		Damp	20	61	16
Philadelphia	Dry	Dry	16	18	10
		Damp	17	27	12
	Wet	Dry	20	53	18
		Damp	20	44	13

Mortar used in brick-mortar tensile specimens and in brick-mortar shearing specimens had the same proportions of dry constituents as the mortar in the beams and piers. In the latter, water was added as desired by the masons; while in the brick-mortar specimens, made under more careful laboratory conditions, the amount of water to give

a flow of approximately 110 per cent was used. For this reason, properties of the mortar, given in Table 5, for brick-mortar specimens differ somewhat from values of Table 3 for the mortar of the beams.

Where test specimens represented wetted bricks, the characteristic failure was not at the junction of brick and mortar but was a failure in the brick. Chicago bricks left a "skin" adhering to the mortar, and Philadelphia bricks frequently pulled off or sheared off their flats to a depth of one-eighth of an inch. In other words, when bricks had been wetted, bond between brick and mortar exceeded the strength of the brick. On the other hand, a few of the "dry brick" specimens showed separation in the mortar, mortar adhering to both bricks. The difference between number of tests indicated and the 20 test specimens originally constructed represents failures of bond occurring by handling the specimens. The number of tests is too few and the variation too great to permit much weight to be given either to averages or distributions but several conclusions are evident: First, wetting Chicago and Philadelphia bricks much increased strength of bond; second, the Chicago brick tended to give stronger bonds than the Philadelphia brick.

5. BRICK-MORTAR SHEARING SPECIMENS

Results of tests of brick-mortar shearing specimens are given in Table 7. In general, results of these tests are similar to the results of tests of the brick-mortar tensile specimens.

TABLE 7.—*Results of shear tests of bond between mortar and brick*

Age at test, 28 to 60 days

Brick		Storage	Number of specimens	Average strength	Standard deviation
Kind	Condition when laid				
				Lbs./in.²	*Lbs./in.²*
Chicago	Dry	Dry	16	100	50
		Damp	12	115	47
	Wet	Dry	20	275	59
		Damp	19	245	101
Philadelphia	Dry	Dry	10	91	35
		Damp	11	120	38
	Wet	Dry	19	231	86
		Damp	20	173	70

6. PULL-OUT TESTS

Results of the pull-out tests are given in Table 8. As shown by the data of this table there was not a significant difference in bond strength of specimens made with Chicago or Philadelphia bricks. Furthermore, curing conditions did not affect results significantly. Failure was by splitting of the brickwork usually into halves but in some cases into quarters. Specimens giving highest individual loads had strengths which exceeded the proportional limit of the steel.

TABLE 8.—*Results of pull-out tests*

Specimens were deformed steel bars, one-half inch square, embedded about 8 inches in 8 by 8 inch square brick masonry piers

Brick		Storage	Number of specimens	Age at test	Average bond strength	Standard deviation
Kind	Condition when laid					
				Days	*Lbs./in.²*	*Lbs./in.²*
Chicago	Wet	Dry	5	32–48	880	140
Philadelphia	do	do	4	32–48	950	140
Chicago	do	Damp	5	41–57	870	190
Philadelphia	do	do	5	41–57	920	150

The maximum bond stresses were slightly greater than those reported by Abrams [10] for deformed bars in 1:2:4 concrete two years old. It has been shown that for smooth bars embedded in concrete the bond strength is more dependent on length of embedment than on other size and shape factors.[11] The lengths of embedment in these two series were about the same (8 inches). Hence, if the effects of size and shape of specimens are approximately the same with deformed bars as with smooth bars, it may be concluded that bond strengths in the brick masonry specimens were about the same as in 1:2:4 concrete specimens tested by Abrams.

7. PIERS

Results of tests of the piers are given in Table 9. There was not a marked departure from a linear relation between loads on the piers and their compressive deformations until 25 per cent of the maximum load was reached, after which there was a tendency for the deformations to increase more rapidly than the loads increased.

Table 9 gives values of the secant modulus of elasticity at a stress of 250 lbs./in.², obtained by dividing this stress by the corresponding compressive strain. Values of the secant modulus of elasticity for any stresses less than one-fourth of the maximum did not differ significantly from those given.

TABLE 9.—*Results of pier tests*

Pier	Secant modulus of elasticity to 250 lbs./in.²	Compressive strength	Pier	Secant modulus of elasticity to 250 lbs./in.²	Compressive strength
	Lbs./in.²	*Lbs./in.²*		*Lbs./in.²*	*Lbs./in.²*
CA-1	2,690,000	1,735	PA-1	1,050,000	1,438
CA-2	2,400,000	1,955	PA-2	1,800,000	1,577
CA-3	2,340,000	1,879	PA-3	1,770,000	2,039
Average	2,480,000	1,856	Average	1,540,000	1,688
CB-1	2,120,000	1,956	PB-1	980,000	1,210
CB-2	2,140,000	2,458	PB-2	1,020,000	1,421
CB-3	2,380,000	1,661	PB-3	1,220,000	1,535
Average	2,210,000	2,025	Average	1,070,000	1,389
CC-1	1,570,000	1,235	PC-1	740,000	1,072
CC-2	960,000	810	PC-2	1,070,000	1,423
CC-3	1,020,000	1,019	PC-3	800,000	1,112
Average	1,180,000	1,021	Average	870,000	1,202

[10] Duff A. Abrams, Tests of Bond Between Concrete and Steel, Bul. No. 71, University of Illinois.
[11] W. H. Glanville, Studies in Reinforced Concrete. I. Bond Resistance, Building Research Tech. Paper No. 10, Dept. of Sci. and Ind. Res., London, 1930.

Both the moduli of elasticity and compressive strengths of the piers were greater for piers of types A and B, having some bricks on end, than for those of type C having all bricks flatwise. As indicated by the data of Table 9 on compressive strength of the piers and that of Table 2 on physical properties of the bricks, there were not large differences in strength properties of either bricks or piers.

IV. RESULTS OF BEAM TESTS

1. DEFORMATIONS IN THE BEAMS

Load deformation curves for the brickwork and the steel and load-deflection curves for the beams are shown in Figures 4 and 5. Values shown for the strains in the brickwork and steel are averages calculated from data obtained with the 40-inch gage length extensometer attached to the sides of beams and the readings of the strain gages. The curves are similar in shape to those representing like data from tests of concrete beams containing heavy reinforcement. Disregarding the portion due to the partial release of the load, the curves tend to consist of a short straight portion, corresponding to the first stage of loading, while the brickwork was still effective in resisting tensile stresses; then a curved portion as the failure of the brickwork in tension took place and then a nearly straight portion. Usually this was followed by another curved portion similar to that of a stress strain diagram representing the later stages in a compressive test of brick masonry.

Some bricks under the reinforcement bars at mid span were removed, prior to testing the beams, in order to facilitate attachment of strain gages on the bars. Due partly to their removal and partly to lack of sensitivity of the long and the short gage tensometers, reliable values for extensibility of the brickwork were not obtained.

When loads on the beams were reduced to 1,000 pounds after the first loading, strain and deflection indicators did not return to the positions taken under the first application of a load of 1,000 pounds. The differences, which are measures of sets produced by the loadings, were equal usually to from one-seventh to one-fifth of the deformations under the greatest loading which preceded.

2. POSITIONS OF THE NEUTRAL AXIS

Average positions of the neutral axes for each type of beam at several loads as determined from measured deformations are indicated in Figure 6, k being the ratio of depth of neutral axis to depth of centroid of the steel. Each plotted point represents a value obtained by averaging the data for three like beams. On the same diagram are shown horizontal lines indicating positions of the neutral axes corresponding to several values of n, calculated by means of the following well known formula:

$$k = \sqrt{2pn + (pn)^2} - pn$$

where k = ratio of depth to neutral axis to depth of the centroid of the tensile reinforcement.

p = ratio of area of tensile reinforcement to area of masonry above the centroid of the tensile reinforcement.

$n = \frac{E_s}{E_m}$ = ratio of the modulus of elasticity of steel to that of the masonry.

As loads were increased there was a tendency for the neutral axis to rise in the beams of types A and B, indicating a gradual lessening of tensile resistance of the brickwork. The tendency of the neutral

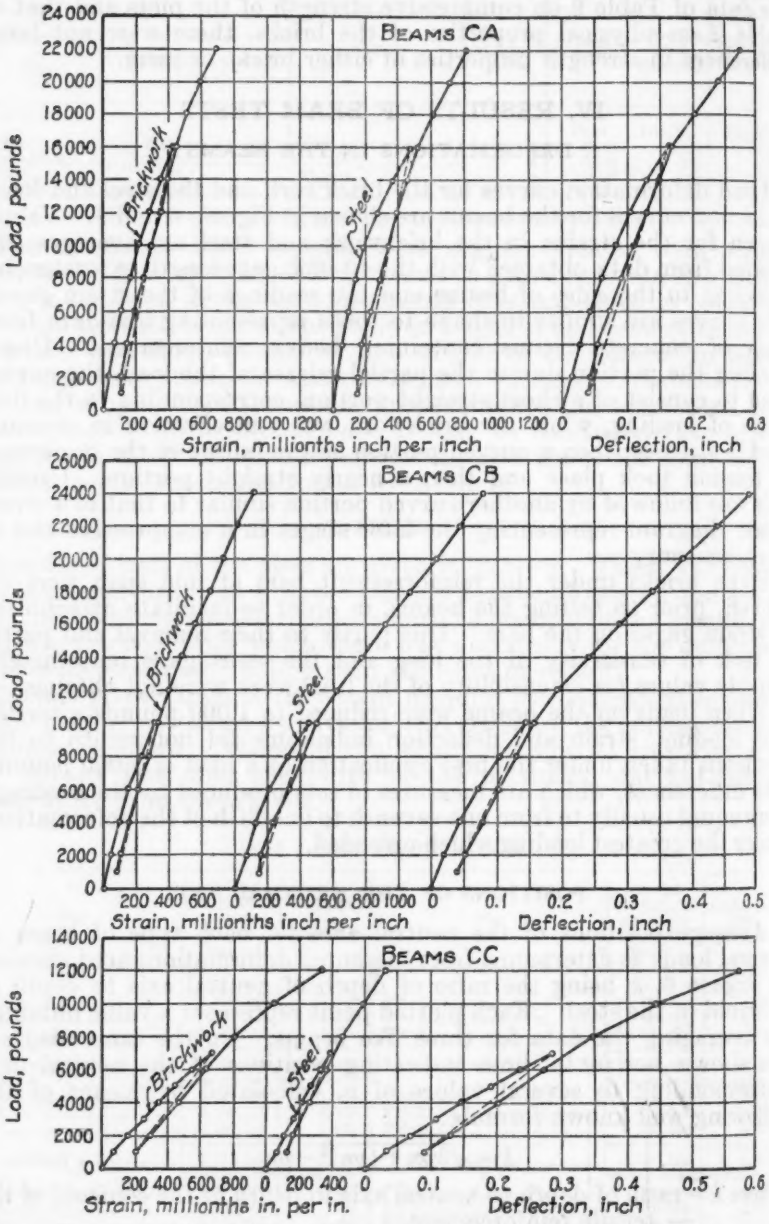

FIGURE 4.—*Load-deformation curves for beams with Chicago brick*

axis to rise continued until the compressive stresses in the brickwork were so great that the rate of change of strain with compressive stress in the brickwork had become great enough to either partially or com-

pletely overcome this tendency. Changes in the depths to the neutral axis with increased loads on these beams resembled those in reinforced concrete beams of similar shape and reinforcement, except that the reduction of tensile resistance of the brickwork in beams of types A and B seemed to take place more gradually than is common in beams of concrete. As the modulus of elasticity of the masonry E_m varies with stress and as the effects of tensile resistance of the

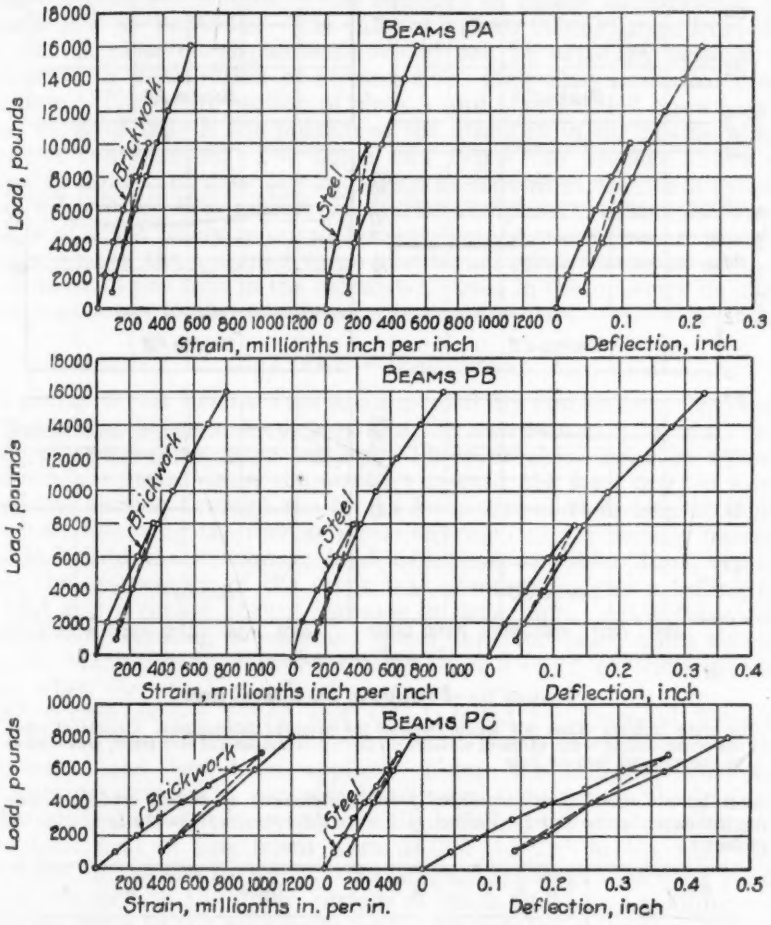

FIGURE 5.—*Load-deformation curves for beams with Philadelphia brick*

masonry are neglected in the derivation of the design formulas, it is desirable to determine what values of n correspond in the formula $k=\sqrt{2pn+(pn)^2}-pn$ to the observed values of k. For this purpose it is best to use data obtained while conditions in the beams most nearly correspond to those assumed in the derivation of the design formulas. The minimum values of the ratio k usually were obtained when loads on the beams were sufficiently large to have caused tensile cracks in the masonry below the neutral axis and yet not large enough to have produced a rapid plastic yielding of the masonry in com-

pression. The minimum values of k observed for two or more loads are given in Table 10, together with values of n calculated by means of the foregoing formula.

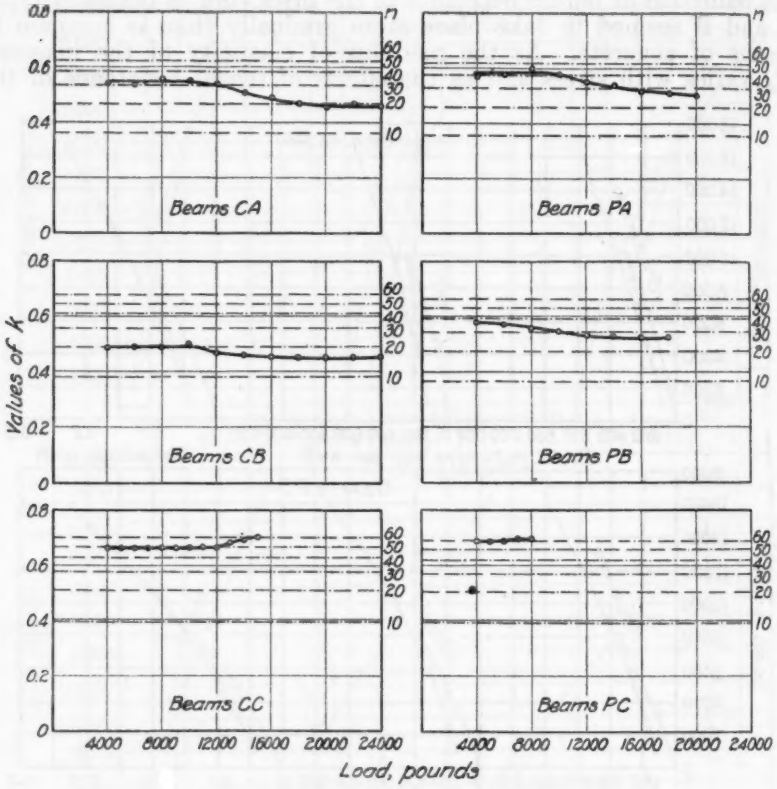

FIGURE 6.—*Position of the neutral axes*

The circles indicate values of k determined from the measured deformations. Calculated values of k corresponding to the values of n, shown on the right-hand scale of each graph, are indicated by the horizonal dash-dot lines

TABLE 10.—*Values of n calculated from dimensions of beams and positions of neutral axes during tests. Values of k were determined from the long gage deformations*

Beam	p	k	n	Beam	p	k	n
	Per cent				*Per cent*		
CA-1	1.03	0.43	16	PA-1	0.97	0.54	33
CA-2	1.01	.44	17	PA-2	.97	.48	23
CA-3	1.00	.45	18	PA-3	1.02	.53	29
CB-1	1.20	.44	15	PB-1	1.07	.48	21
CB-2	1.17	.45	16	PB-2	1.10	.57	34
CB-3	1.16	.45	16	PB-3	1.05	.56	34
CC-1	1.31	.66	50	PC-1	1.24	.70	66
CC-2	1.31	.62	38	PC-2	1.25	.69	62
CC-3	1.30	.68	56	PC-3	1.27	.69	60

These calculated values of n were greater for beams of Philadelphia bricks than with those of Chicago bricks. They were greatest with

beams of type C and least with those of types A and B, the values corresponding in order of magnitude to the average number and total thickness of joints per unit length of beam in the upper two courses of bricks. However, no general relations between dimensions of the mortar joints and values of n exist, probably on account of the laminar structure of the bricks.

Secant moduli of elasticity of the piers were in all cases larger than the effective moduli of the masonry of beams as indicated by values of n in Table 10. The ratios of these values range from 0.5 to 0.9. A close correspondence would not be expected because of difference in distribution of stresses over their unsymmetrical cross sections. The entire section of piers A and C resembled more nearly than those of type B the portion of the masonry in the beams which were in compression. For these two types the average ratios of effective moduli of masonry in beams to moduli of the piers ranged from 0.5 to 0.7. Fortunately, from the standpoint of design, accurate values of n are rarely required for satisfactory results, as an error of 50 per cent in the assumed value of n would rarely cause an error of more than 15 per cent in the calculated stress in the masonry or more than 4 per cent in the calculated stress in the steel.

3. TYPES OF FAILURES

Failures of all beams were accompanied by cracks near the ends of the beams between a support and the nearer load. Figure 7 is a view of two beams after testing. These cracks tended to extend diagonally upward from the support toward the load line, in some instances passing through the bricks for a part of their lengths while in others following the mortar joints entirely. They usually became visible before the maximum load had been applied. In a typical case, the appearance of the crack was accompanied by a falling off of load and a rather abrupt increase in deflection. After this, with the machine running at constant speed, load increased more slowly, but the maximum loads were usually from 5 to 10 per cent greater than when the crack was first observed.

All beams except CA–2 and CC–1 failed by diagonal tension. The tensile reinforcement in beam CA–2 began to yield before the maximum load had been applied. Using the ordinary formulas for working stresses in concrete beams and considering the position of the neutral axis as observed, the calculated maximum stresses under maximum load in this beam were 54,000 lbs./in.^{2} in the steel and 2,400 lbs./in.^{2} in the masonry. Strain-gage readings indicated yielding of masonry in the upper surface of beam CC–1 and spalling was observed prior to the maximum load. Calculated stresses under the maximum load were 34,000 lbs./in.^{2} in the steel and 1,340 lbs./in.^{2} in the masonry. The beams were so conservatively designed against failures by slipping of the bars that the bond stresses developed in the beam tests have no significance.

4. RESISTANCE TO DIAGONAL TENSION

(a) EFFECT OF ARRANGEMENT AND BONDING OF BRICKS IN BEAMS

Resistance of the beams to failures by diagonal tension was affected markedly by the bonding of the bricks as is shown by the data of Table 11. With the Chicago bricks the ratios of the average maxi-

mum shearing stress to that for type C beams were, respectively, 1.69, 1.38, and 1.00 for beams of types A, B, and C; corresponding ratios for beams of Philadelphia bricks were 1.49, 1.42, and 1.00.

TABLE 11.—*Results of beam tests*

Beam No.	Width b	Depth d	j	Maximum load W	Maximum shearing stress $v=\frac{Vr}{bjd}$
	Inches	*Inches*		*Pounds*	*Lbs./in.²*
CA-1	12.73	11.00	0.85	36,700	154
CA-2	12.73	11.25	.85	41,750	171
CA-3	12.80	11.30	.85	37,600	153
Average	12.75	11.18	.85	38,680	159
CB-1	12.23	9.84	.85	28,500	140
CB-2	12.57	9.84	.85	26,000	123
CB-3	12.67	9.84	.85	27,600	130
Average	12.49	9.84	.85	27,370	131
CC-1	12.90	8.50	.78	18,000	105
CC-2	12.90	8.50	.78	14,900	87
CC-3	12.80	8.65	.78	15,900	91
Average	12.87	8.55	.78	16,270	94
PA-1	12.87	11.95	.83	23,450	92
PA-2	12.77	11.65	.83	22,100	89
PA-3	12.57	11.20	.83	26,000	111
Average	12.74	11.60	.83	23,850	97
PB-1	12.90	10.40	.83	20,000	90
PB-2	12.63	10.40	.83	17,400	80
PB-3	13.23	10.40	.83	24,000	105
Average	12.92	10.40	.83	20,470	92
PC-1	13.27	8.75	.77	8,650	48
PC-2	13.20	8.75	.77	14,400	81
PC-3	13.00	8.75	.77	11,700	67
Average	13.16	8.75	.77	11,580	65

NOTE.—$j=1-\frac{k}{3}$, where k is the average of experimentally determined values of ratio of depth of neutral axis to effective depth. The values of k used were taken from Figure 6.

Maximum shearing stresses were in the same order as the proportion of bricks laid with staggered vertical joints. As shown in Figure 1, joints which were vertical in the type C beams during a test were not staggered; they extended over the full width and from the lower to upper surfaces of the beams. In type B beams all vertical joints were staggered, but those between the soldier bricks of the outer wythes had an unbroken vertical length about equal to the height of three courses of bricks laid flatwise. The vertical joints in the A beams were broken at each course. The proportion of the staggered joints in the different beams my be expressed by approximate numerical values as:

15 out of 15 or 100 per cent in the A beams.
9 out of 15 or 60 per cent in the B beams.
0 out of 9 or 0 per cent in the C beams.

(b) EFFECT OF STRENGTH AND ABSORPTION OF THE BRICKS

Resistance of beams to shearing stresses (Table 11) were in reverse order to compressive strengths flatwise and edgewise of the bricks (Table 2), the strengths of Chicago bricks in these tests being less than that of Philadelphia bricks. Chicago bricks were stronger endwise and when laid as in the top course of beams A and B were subjected to compressive stresses in the direction of greatest strength. However, strengths of the C beams were not in the same order as compressive strengths of bricks in the direction of the axis of the beams. It appears, therefore, that there was no consistent relation between compressive strength of bricks and shearing resistance of masonry.

Shearing resistance of the beams was in the same order as moduli of rupture of the bricks. The moduli of the bricks were determined, however, only in the direction of their lengths. Bricks from both sources were laminated and their moduli in other directions may not have been in the same order. Therefore, the data are not conclusive as to the effect of the moduli of rupture of the bricks on shearing strength of the masonry.

Absorption properties of the two kinds of bricks did not differ greatly, and it does not seem likely that the small differences in absorptions had an important effect on the relative strengths of beams made with them.

(c) EFFECT OF BOND STRENGTH BETWEEN MORTAR AND BRICKS

As noted in the description of tensile and shearing tests of brick-mortar specimens, some specimens were made with wet and the rest with dry bricks. Some were aged in damp storage and others in dry storage. Bricks for the beams were wetted before use. Although the beams were aged in the laboratory where some drying would take place, the rate of drying was probably much less than for the smaller bond test specimens stored in air. Hence, it would be expected that the moisture content during fabrication and storage of the beams was not the same as for any of the bond-test specimens but was intermediate between the dry and wet storage bond-test specimens made with wet bricks. Moreover, as conditions during the first few days of storage have a greater effect upon the properties of Portland cement mortars than those during a similar equal period, it seems likely that the properties of the mortars in the beams were more nearly like those of the damp-cured bond specimens.

Table 12 gives ratios of the average maximum shearing stress of beams of Chicago bricks to those of Philadelphia bricks for each type of beam. These were calculated from the data of Table 11. Similar ratios calculated from data of Tables 6 and 7 for bond tests are given also. The close agreement between ratios for the beams and for the damp-cured bond-test specimens indicates, as would be expected,[12] that tensile and shearing strengths of the masonry were closely related to the resistance to diagonal tension of the masonry beams.

[12] Because the appearance of the cracks indicated failures due to diagonal tension.

TABLE 12.—*Effect of tensile and shearing strengths of masonry on shearing resistance of beams*

[Ratio of strength with Chicago bricks to strength with Philadelphia bricks]

Maximum shearing stress beams:	
A	1.64
B	1.43
C	1.45
Bond strength in tension, wet bricks, damp storage	1.39
Bond strength in shear, wet bricks, damp storage	1.41
Bond strength in tension, wet bricks, air storage	1.04
Bond strength in shear, wet bricks, air storage	1.19

V. CONCLUSIONS

1. Maximum shearing stresses for the different types of beams, which are taken as measures of their resistances to diagonal tension, ranged from 65 to 159 lbs./in.^{2}.

2. Resistance to diagonal tension increased with an increase in the proportion of the bricks laid with staggered joints. Maximum shearing stresses in the beams having all bricks laid flatwise with staggered joints were about 60 per cent greater than in beams with continuous (not staggered) joints.

3. Maximum shearing stresses in beams with one kind of brick were from 40 to 60 per cent greater than in beams made with the other kind. These stresses were in the same order as the tensile and shearing strengths of small masonry specimens made with the same kinds of brick and mortar. The shearing strength of the beams appeared to be independent of the compressive strengths of the bricks. The only qualities of the bricks which appeared to have a major influence were those affecting tensile and shearing strength of the masonry.

4. With the rapidly absorbing bricks used in these tests tensile and shearing strengths of the masonry were much greater when the bricks were wetted before laying than when laid dry. Curing conditions had a relatively small effect; specimens made with dry brick were made stronger by damp curing, while those made with wet bricks were stronger when air cured.

5. The neutral axes in the beams rose during the early stages of the loading, but during the later stages usually became lower. The positions as indicated by minimum observed values of k corresponded to values of $n=\frac{E_s}{E_m}$ ranging from 15 to 66. The effective n varied with the kind of bricks in the beam and increased with an increase in the average number and total thickness of mortar joints in the upper course per unit of length of beam. The effective E_m in the beams ranged from 0.5 to 0.7 of the secant modulus of elasticity of the piers, when the bonding of the bricks in the piers was similar to that in the upper half of the beams.

6. The bond strength at an age of from one to two months as determined by pull-out tests of ½-inch-square deformed bars embedded 8 inches in brickwork ranged from 870 to 950 lbs./in.^{2}. Differences in the kinds of bricks and of curing conditions did not cause significant changes in these bond strengths.

WASHINGTON, September 17, 1932.

THE MEASUREMENT OF LOW-VOLTAGE X-RAY INTENSITIES [1]

By Lauriston S. Taylor and C. F. Stoneburner

ABSTRACT

A special type of chamber has been designed to measure the ionization produced by 3 to 12 kv X rays in a known volume of unrestricted air, thus making it possible to express the intensity of the X-ray beam in roentgens per minute. By the use of a very small guarded field ionization chamber (5 by 5 cm), the air-absorption correction is reduced several fold, and hence errors in its determination are not so serious in the final result sought. It is shown that air-absorption corrections must be determined separately for each beam of radiation used, and the chamber is so designed that the necessary corrections may be determined without recourse to other special apparatus. Examples are given showing in detail the methods of making measurements with the chamber described. Compared at higher voltages (40 to 90 kv) with a large primary standard ionization chamber, the small type here described shows a divergence of about ± 0.5 per cent which is believed to be the over-all error present in its use. In order to obtain this close agreement it is necessary to take special precautions in the construction and measurement of the limiting diaphragm and the collector electrode.

CONTENTS

	Page
I. Introduction	769
II. Description of chamber	770
III. Calibration measurements	772
1. Collector electrode	772
2. Chamber-limiting diaphragm	772
3. Saturation voltage	772
4. Effect of scattered radiation	772
5. Field distortion	774
IV. Comparison with standard chamber	774
V. Measurements of "grenz rays"	776

I. INTRODUCTION

With the increasing clinical use of soft X rays, excited by potentials of 3 to 12 kv (peak), arises the necessity for their more accurate measurement such as obtains with the higher voltage radiations. This is particularly important in view of the fact that such radiation may furnish an erythema dose in one or two minutes. In fact errors in measurement assume even greater importance than for high-voltage X rays.

Although several investigators have reported on the measurement of soft X rays (so-called grenz rays), they have given but few essential details of the methods they employed.[2 3 4] This obscurity led us to construct an open-air ionization chamber capable of measuring soft

[1] Presented at annual meeting of Radiological Society of North America, St. Louis, December, 1931.
[2] H. Kustner, Strahlentherapie, vol. 27, p. 124, 1928.
[3] B. Rajewsky and G. Gabriel, Strahlentherapie, vol. 30, p. 20, 1928.
[4] Otto Glasser, Chap. III of Grenz Ray Therapy, by Gustav Bucky, Macmillan, 1929. See also Radiology.

X rays, and to compare it with the standard used for measuring high-voltage X rays.[5] A chamber has, therefore, been designed which measures reliably X rays excited by voltages ranging from 3 to 80 kv (peak), covering not only the "grenz-ray therapy" (3 to 12 kv) but also the lower "diagnostic X-ray range" (60 to 80 kv).

Open-air chambers lacking a guarded field are not readily applicable to the measurement of soft X rays because the large air absorption correction involved can not be determined with desired accuracy. The principle of the guarded-field air-ionization chamber [5] renders it, however, particularly adaptable by permitting the air path between diaphragm and collector plates to be reduced to a minimum. The points essential to its successful application to low-voltage X rays are worked out in the present investigation.

II. DESCRIPTION OF CHAMBER

Described briefly, the guarded-field ionization chamber furnishes adequate field uniformity over the width of the collector electrode of a parallel plate ionization chamber by means of properly charged guard wires stretched across the open faces of chamber, the potentials of the wires being divided in equal successive steps between zero (at collector) and the plate potential. It has been shown that such a system permits the use of grounded metal parts (case, diaphragm, etc.) much closer to the electrodes than would otherwise be possible. In the present case the shielding and the limiting diaphragm may be brought to within 5 cm of the center of the collector plate, and air-absorption correction need be made only for this small distance.

A cross section of this special ionization chamber for soft X rays is shown in Figure 1. The electrode system consists of the high-potential plate, *A*, the two grounded guard plates, *B*, and the collector electrode, *C*, all mounted as a unit, similar to the larger type of guarded field chamber. The 4 rectangular guard wire loops, *a*, *b*, *c*, *d*, made of 10-mil aluminum, are maintained at equal potential steps, respectively, between earth and the potential of *A* by means of 5 half-megohm resistors, *r*, *r*, mounted on a hard rubber supporting frame. The entire electrode system can be slid the length of the box, *D*, on two guide rods, and its position read on the scale, *S*, which also serves as a "handle" with which to move the system from the outside.

The box, *D*, is of ⅛-inch brass, which provides sufficient radiation protection for lower-voltage X rays. For higher-voltage X rays it is further shielded with about 15 mm of lead. The rod, *H*, is connected to a source of sufficiently high potential to produce saturation current in the chamber and makes contact with the plate, *A*, through a sliding spring. Similarly the collector electrode, *C*, is connected by a sliding contact to *E*, which leads to the electrometer system. The rod, *E*, is shielded over its entire length, as shown by the section *X*, for the purpose of preventing any ions not formed within the electrode system from reaching the electrometer system. The adequacy of this shielding was tested experimentally.

The diaphragm, *n*, has an 8-mm orifice with the limiting edges cylindrical and about 1 mm thick. The chamber as a whole is

[5] L. S. Taylor and G. Singer, B. S. Jour. Research, vol. 5 (RP211), p. 507, 1930.

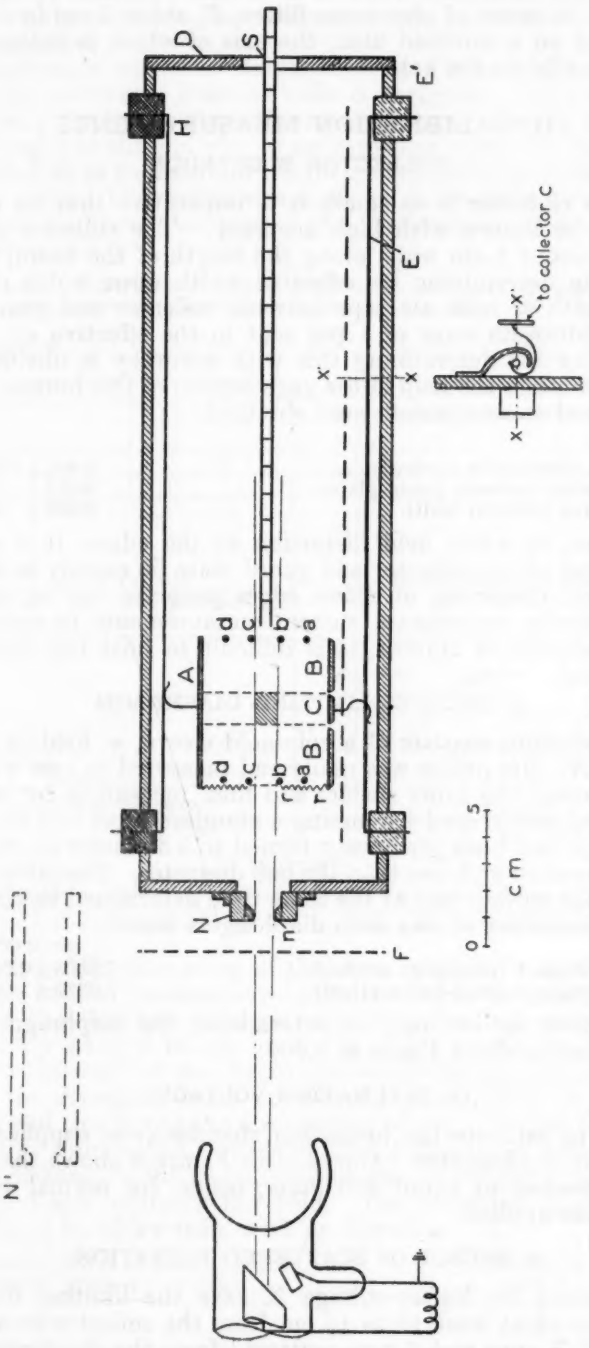

FIGURE 1.—*Cross section of special guarded-field ionization chamber for measuring low-voltage X rays or grenz rays*

mounted on a base that slides in a direction parallel to the X-ray beam axis. A series of aluminum filters, F, about 3 cm in diameter, are mounted on a celluloid disk, the axis of which is independently movable parallel to the axis.

III. CALIBRATION MEASUREMENTS

1. COLLECTOR ELECTRODE

Since the chamber is so small, it is imperative that its essential dimensions be known with high accuracy. The collector electrode being only about 1 cm wide, along the length of the beam, an error of $\frac{1}{10}$ mm in determining its effective width (true width plus one-half the width of both air gaps between collector and guard plate) would introduce an error of 1 per cent in the effective air volume. The necessity for determining this with accuracy is obvious. Accordingly, through the help of the gage section of this bureau, the following typical measurements were obtained:

	mm
Width of collector electrode	9.492±0.005
Separation between guard plates	9.904± .005
Effective collector width	9.698± .005

Furthermore, to avoid field distortion at the edges, it is essential that the faces of the collector and guard plate lie exactly in the same plane. Field distortion at these edges presents one of the most serious obstacles to accurate current measurements in case, during the compensation of current, it is difficult to hold the collector at zero potential.

2. CHAMBER-LIMITING DIAPHRAGM

This diaphragm consists of a coin-gold sleeve, n, held in a Pb-Bi alloy ring, N. Its orifice was made and measured in two ways—the first by lapping the inner surface and then measuring by the plug-gage method; the second by forcing a standard steel ball through an orifice which had been previously turned to a diameter of one or two thousandths of an inch less than the ball diameter. The latter method burnished the surface and at the same time determined its size. The measured diameters of two such diaphragms were:

	mm at 68° F.
Diaphragm 1 (plug-gage method)	7.8608±0.0001
Diaphragm 2 (steel-ball method)	7.9375± .0001

It is seen that the accuracy in determining the diaphragm area by either method is about 1 part in 9,000.

3. SATURATION VOLTAGE

Voltage to saturate the ionization chamber was supplied from a 1,300-volt d. c. generator. Curve A in Figure 2 shows that saturation was reached at about 300 volts; hence, for normal operation, 500 volts was applied.

4. EFFECT OF SCATTERED RADIATION

In chambers for higher-voltage X rays the limiting diaphragm must be placed at least 10 to 15 cm from the collector to avoid the influence of X rays and β rays scattered from the diaphragm edges. Since the radiation from low-voltage X-ray tubes must, in general,

be measured so close to their source that a comparatively divergent beam enters the chamber, the customary type of chamber diaphragm is not satisfactory.

The diaphragm placed as shown in N by Figure 1 is satisfactory, provided the scattering from its walls is negligible. This was tested by measuring the ionization with the diaphragm in place, then again after shifting it to the end of a 10 cm extension tube, N', the chamber being shifted so as to maintain the distance from N to N' to the tube target the same. Correction was made as shown later for absorption in the 10 cm additional air path. Measurements at 40 kv (eff) gave the following results:

Intensity, diaphragm at normal position	0. 964±0. 0033
Intensity, diaphragm shifted to 10 cm	. 970± . 0027
Difference	. 006

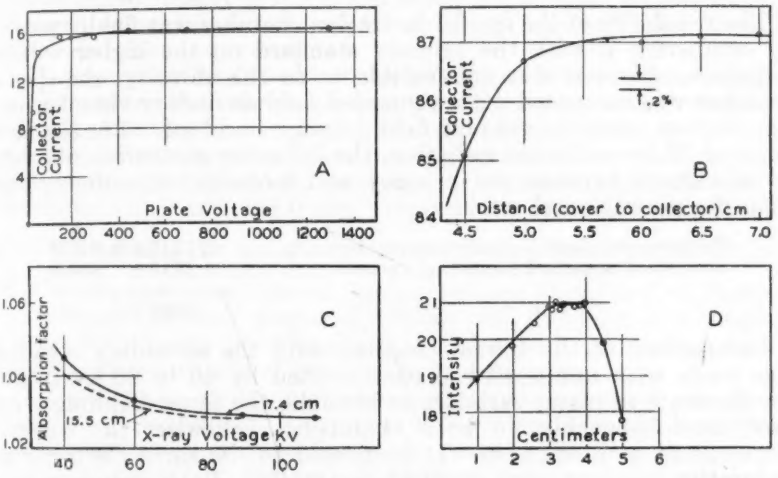

FIGURE 2

a, Saturation curve for special ionization chamber; *b*, variation of measured ionization with distance between diaphragm and ionization chamber; *c*, air absorption factor for calibration of special ionization chamber; *d*, X-ray intensity along cross section of beam used in calibrating ionization chamber.

The observed difference being of the same magnitude as the error of observation but in the direction opposite to that to be expected,[6] it is assumed that the two arrangements give identical results for the comparatively narrow beams used. In other words, the scattering effect from the walls of the diaphragm orifice is negligible.

Use of the divergent beam exposes the guard wires to the direct radiation, and this may have a scattering effect. To test for scattering from this source, two strands of 20-mil aluminum wire were suspended, insulated, in the beam between the 10-mil guard wires *b* and *c*, hence did not influence the field. The following measurements were obtained at 40 kv (eff), with no filtration:

Intensity, wires in beam	0. 295±0. 0016
Intensity, wires out of beam	. 294± . 0008
Difference	. 001

[6] This is probably due to error in the air-absorption correction.

The difference being of the magnitude of the experimental error, no appreciable effect arises from permitting the beam to strike the guard wires.

5. FIELD DISTORTION

To determine how close the electrode system may be brought to the front end of the box without introducing appreciable field distortion, X-ray intensities were measured at each of several successive positions of the electrodes with respect to the box front. Curve *B*, Figure 2, shows the observed increase in ionization as the distance from collector electrode to the diaphragm is increased. Beyond 5 cm, further change is only about 0.2 to 0.3 per cent, a magnitude smaller than the experimental error in these particular measurements.

IV. COMPARISON WITH STANDARD CHAMBER

The reliability of the special ionization chamber was finally proved by comparing it with the primary standard on the higher voltage radiation. Since it was not feasible to do this directly, the special chamber was compared with a guarded field secondary chamber and this, in turn, with the guarded field primary standard. For the same beam of 70 kv unfiltered radiation, the following measurements show an agreement between the primary and secondary chambers closer than the experimental error:

Primary standard ionization current	0.1315±0.00026
Secondary standard ionization current	.1316± .00030
	.0001

Comparison of the special chamber with the secondary standard was made with unfiltered radiation excited by 40 to 90 kv (peak). To eliminate as many variables as possible, the same diaphragm was used interchangeably on both chambers. Likewise, the collector electrode of each chamber was connected to the same electrometer. Saturation voltages were supplied separately. Both chambers were placed in a fixed position and the tube shifted on a track, so that the same beam could enter either chamber as desired. To have this beam moderately well defined, a diaphragm 16 mm in diameter was placed about 2 cm from the wall of the 200 kv thin-walled Coolidge tube used.[7]

Ionization currents were measured by means of a null electrostatic compensator, such as was used in previous work,[8] wherein the ionization charge was compensated over a known interval of time. However, instead of exposing the chamber for a given time by means of an electrically operated shutter in the X-ray beam, the electrometer was connected to the chamber for a definite period by means of an electrically operated switch [9] located at *E'* (fig. 1). The chamber and electrometer were connected by a shielded rubber cable.

The effective length along the beam of the collector of the secondary standard was 4.975 cm, so that, for the same diaphragms, the effective air volumes ionized in the special and secondary chambers were in the ratio 0.9698 to 4.975. All readings with the secondary chamber were

[7] L. S. Taylor, B. S. Jour. Research, vol. 2 (RP56), p. 771, 1929.
[8] L. S. Taylor, B. S. Jour. Research, vol. 6 (RP306), p. 807, 1931.
[9] L. S. Taylor, B. S. Jour. Research, vol. 8 (RP397), p. 9, 1932.

therefore divided by 5.129 to reduce to the same effective air volume as the special chamber.

The distance between the limiting diaphragm and center of the collector electrode on the secondary chamber was 22.5 cm, as compared with 7 cm for the corresponding distance on the special chamber. Absorption in the air-path difference of 15.5 cm will, for the same beam, lower the measured current of the secondary chamber relative to that of the special chamber by a corresponding amount. Since this absorption depends upon such factors as voltage wave form, tube characteristic, and tube wall thickness, it must be determined for each set of conditions employed.

At voltages ranging from 40 to 100 kv, where the X rays pass initially through moderately thick tube walls, the radiation is sufficiently hardened so that its quality undergoes no appreciable further change in passing through 50 cm of air. In such case the air absorption is approximately proportional to the length of the air path.[10] But, as shown later, this is not true for the 4 to 12 kv radiation for which the special chamber is designed.

Air-absorption measurements to be applied in the present comparison were made with the large open air standard ionization chamber,[11] using the limiting diaphragm in a fixed position relative to the target so as to define a narrow beam passing between the chamber plates. X-ray intensities, I_1 and I_2, were then measured with the plates at the distances 110.6 and 128.0 cm, respectively, from the target. The ratio $\frac{I_1}{I_2}$, giving the air absorption correction factor for an air path of 17.4 cm, is plotted against applied voltage in curve *C* of Figure 2. The absorption being practically linear with distance, it is simple to correct it to fit any path length as, for example, 15.5 cm, required in the present set-up and shown by the broken curve.

To insure, in the comparison, proper alignment of the special chamber, measurements were made of the intensity of the X-ray beam over its horizontal cross section in the plane of the diaphragm, *N*. As shown by curve *D* in Figure 2, the area of effective uniformity, about 1 cm wide, indicates the range of proper alignment.[12]

Typical results of the comparison of the special with the secondary chambers, with unfiltered radiation from a thin wall, deep therapy Coolidge tube, are given in Table 1.

TABLE 1.—*Comparisons of special ionization chamber with secondary chamber*

kv	I_s	I_x	Absorption factor $(I_1/I_2)_{15.5}$	$\frac{I_s}{I_x}\left(\frac{I_2}{I_1}\right)_{15.5}$
40	4.63	4.46	1.040	0.998
50	2.30	2.205	1.033	1.008
70	2.88	2.79	1.028	1.003
90	6.08	6.08	1.027	.968

Column 2 gives the intensities I_s in Röntgens per minute as measured with the special chamber; column 3, the intensities, I_x, at the

[10] L. S. Taylor and G. Singer, B. S. Jour. Research, vol. 6 (RP271), p. 219, 1931.
[11] L. S. Taylor, B. S. Jour. Research, vol. 2 (RP56), p. 771, 1929.
[12] L. S. Taylor, B. S. Jour. Research, vol. 3 (RP119), p. 807, 1929.

middle of the collector, as determined with the secondary standard but uncorrected for air absorption in the extra 15.5 cm of path; column 4, the corresponding air-absorption factor as obtained from the broken curve of Figure 3 (*C*), and by which I_x is multiplied in order to obtain the intensity 15.5 cm nearer the diaphragm, at which point the special chamber is used; and the last column gives the ratio of the intensities furnished by the two chambers.

At 90 kv (peak) the small chamber indicates definitely too little ionization. This is attributed to the close spacing (5 cm) of the collector, *C*, and high-potential plate, *A*, which does not permit full utilization of the range of the photoelectrons emitted along the path of the X-ray beam. This sets a definite X-ray voltage limit above which the small chamber should not be used. The safe working range for the present chamber includes, however, the lower part of the diagnostic X-ray region and may be used where, due to "wall effect," measurements with most thimble ionization chambers become inaccurate.

V. MEASUREMENTS OF "GRENZ RAYS"

Having found agreement between the indications of the special and the standard chambers at voltages ranging from 40 to 80 kv (peak), the use of the special chamber may be extended down to any X-ray voltage for which adequate air absorption correction can be made.

For measuring so-called "grenz rays," 4 to 12 kv (peak), the necessary corrections will be indicated and the necessity for accurately measuring the air absorption for each set of experimental conditions under which the radiation is used will be brought out.

Very soft X rays (4 to 12 kv) are absorbed by air to such a degree that the radiation quality changes rapidly even in a distance of only 5 cm. The beam intensity should, therefore, be measured at the exact position, with respect to both tube and filter, where the radiation is to be applied, because it is unsafe to apply the inverse square law for computing intensitites at points other than where measured. Furthermore, it is essential to determine the air absorption between diaphragm and collector, *C*, for an air column having exactly the same position with respect to the target as the column between diaphragm and collector when the chamber is in its working position, if the point of application is taken at the position of the limiting diaphragm.

The requirements are illustrated in Figure 3, which gives a plot of the intensity of an X-ray beam as a function of the distance, *e*, from the target, *T*. At the lower part are indicated several possible positions of an ionization chamber with respect to the tube. Suppose, for example, the intensity, I_b, at the position, *b*, is to be measured. The chamber diaphragm would be placed at position, $n_1 = b$, and the middle of the collector electrode at e_1, a distance, *d*, from n_1, where *d* is the minimum working distance between collector and diaphragm. Owing to air absorption over the path, $b - c$, the intensity measured at e_1 must be corrected to give the value as if at the position, n_1. This correction can not be obtained by simply keeping n_1 fixed, and moving e_1 away an equal distance, *d*, to the position e_1' because, due to the filtering action of the air, the radiation quality at *g* is different from that at *c*.

To obtain the air absorption factor to be applied in the chamber working position, it is necessary to move the chamber, including diaphragm, toward the tube a distance, d, to the position, n_2, and then measure the intensities, I_b and I_c, obtained, respectively, at the two

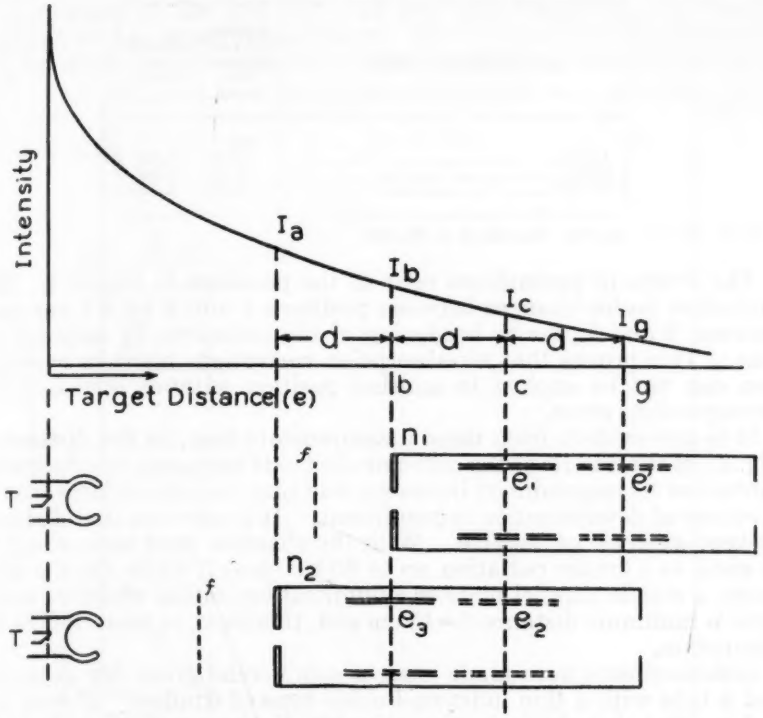

FIGURE 3.—*Diagram of working positions of special ionization chamber in determining air absorption factors*

positions of the collector plate, $e_3 = n_1$, and $e_2 = e_1$. The ratio $\frac{I_b}{I_c}$ gives the air absorption factor to be applied to the readings made with the chamber at the position n_1. Corrections made in this manner are

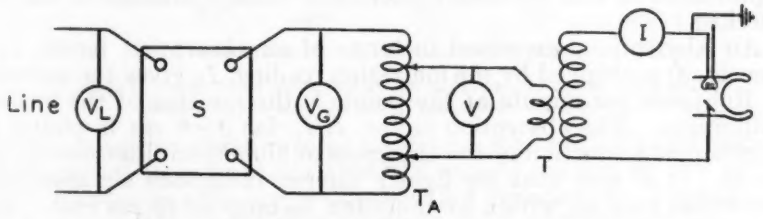

FIGURE 4.—*Power circuit for grenz-ray generator*

limited to distances, d, or greater, from the X-ray tube. The special chamber described, owing to its small size, is particularly well adapted to the problem; an unguarded field type can not be made sufficiently small without introducing too great field distortion.

The observed change in the air absorption factor, as the distance from the tube is changed, is given in Table 2.

TABLE 2.—*Air absorption factors 8 kv (peak) (Slack window, Grenz ray tube)*[1]

Diaphragm position	Absorption path distance from target	Absorption factor
	cm	
1 (*a*–*b*)	12–18	1.635
2 (*b*–*c*)	18–24	1.593
3 (*c*–*d*)	24–30	1.576

[1] C. M. Slack, J. Opt. Soc. Am., vol. 18, p. 123, 1929.

The letters in parentheses refer to the positions in Figure 4. The correction factor changes between positions 1 and 2 by 4.2 per cent; between 2 and 3, due to hardening of the radiation, by only 1.7 per cent. This proves that air-absorption corrections made in one position can not be applied to another position without introducing a corresponding error.

It is also evident from these measurements that, as the distance, d (fig. 3), of the middle of the collector electrode increases, the absorption correction correspondingly increases, and may become so large that its accuracy of determination is insufficient. It is obvious that d should be kept as small as possible. With the chamber used here, d may be as small as 5 cm for radiation up to 80 kv (peak); while, for the same range, a simple parallel plate or cylindrical ionization chamber would have a minimum distance $d=13$ cm and, therefore, at least double the absorption.

Measurements were made using a commercial grenz ray generator and a tube with a thin indrawn-bubble type of window[13] of such size and position that the ionization chamber diaphragm could be brought to about 5 cm of the target. The filament side of the tube was grounded (fig. 4) and the voltage regulated by means of a slide wire auto transformer T_A in the primary circuit of the high-voltage transformer. Peak voltage was determined from the manufacturer's calibration in terms of the voltage, V, on the primary of the transformer. (Since accurate values of the tube voltage were of no great significance in this particular work, the voltage calibration was not checked.)

Air absorption, expressed in terms of an absorption factor, I_b/I_c (see fig. 3) multiplied by the ionization reading, I_c, gives the intensity in Röntgens per minute at the point, b, the position of the limiting diaphragm. The absorption factor, I_b/I_c, for $d=6$ cm is plotted in Figure 5 as a function of the thickness of aluminum filter used in the beam. It is seen that for lightly filtered radiations air absorption correction may be, with 6 kv radiation, as large as 40 per cent. The need for accuracy of this correction is obvious.

Figure 6 gives a series of curves showing the intensity, I_b, in Röntgens per minute at the position $b=12$ cm as a function of the aluminum filtration. The lower curve of each pair gives the measured

[13] See footnote to Table 2.

intensity while the upper curve gives the corresponding calculated value at the diaphragm—obtained by multiplying by the appropriate absorption factor from Figure 6. It is interesting to note in this connection that a lateral shift, corresponding to 0.0055 mm thickness of aluminum, of the first curve of any pair brings the two curves together, within experimental error. This means that the absorption of 6 cm of air is equivalent to 0.00055 cm of aluminum for the range

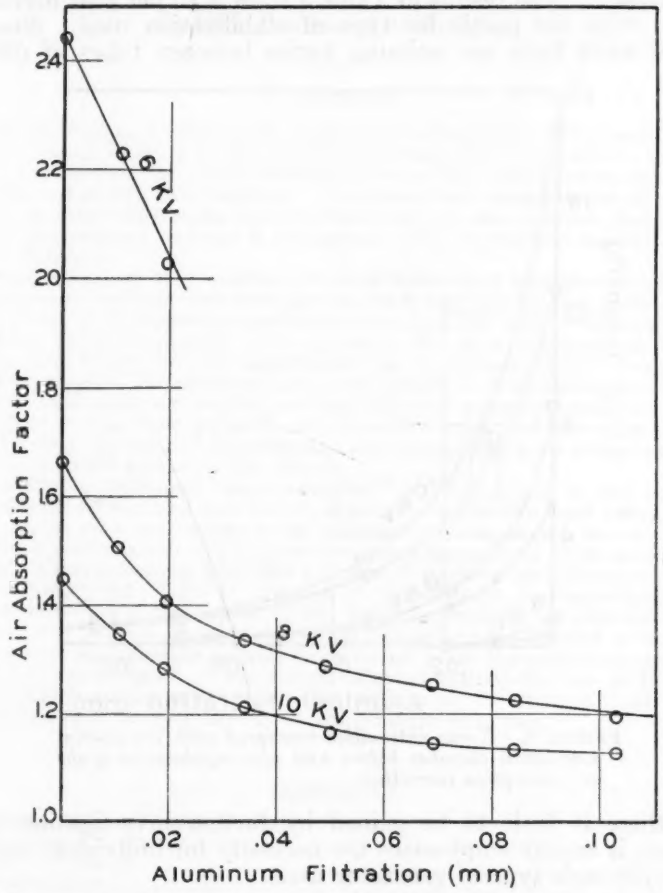

FIGURE 5.—*Air absorption factor for different voltage X rays necessary in the use of special ionization chamber*

of voltages and qualities covered in Figures 5 and 6. The aluminum equivalence of air is from this 9.2×10^{-5} mm Al per mm of air; which agrees favorably with the value 9×10^{-5} reported by Siegbahm.[14] but is appreciably higher than Glasser's value of 7.9×10^{-5} mm.

The logarithm of the intensity plotted against thickness of filter shows a distinct curvature up to 0.1 mm/Al filtration and indicates that there is no "homogeneity filter" [15] beyond which the quality does not change. Typical examples of intensity and absorption

[14] M. Siegbahm, The Spectroscopy of X Rays (Oxford), 1925.
[15] H. Behnken, Zeit. fur. Tech. Phys., vol. 2, p. 153, 1921.

curves for grenz rays have been given by Jacobson [16] and others. Such curves have value only for a particular tube and should be determined separately for each type of generator, as brought out by using the system indicated in Figure 4. Here tube emission was measured for a constant voltage, V, applied to the transformer, T, and constant current, I, through the tube, the input voltage V_G, to the control autotransformer being stabilized in one case and unstabilized in the other.[17] The results in Table 3 show a 50 per cent decrease in emission with the particular type of stabilization used. Since the effect of wave form on emission varies between tubes of different

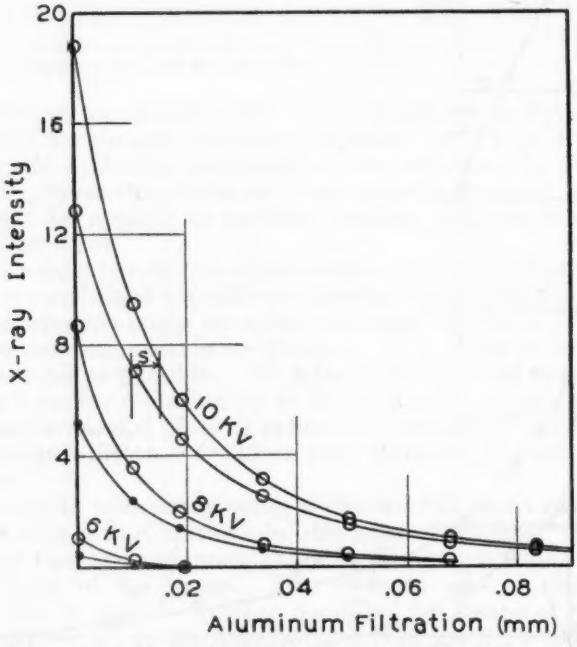

FIGURE 6.—*X-ray intensities measured with the special ionization chamber before and after application of the air absorption correction*

types, there is little to be gained by further investigation of the variation; it simply emphasizes the necessity for individual measurements with each type of generator used.

TABLE 3.—*Grenz-ray emissions for different voltage wave forms*

Line voltage V_L	Stabilizer	Input voltage V_G	Emission
109	Out	109	16.07
104	do	104	16.24
109	In	106.5	8.83
104	do	106.5	8.52

WASHINGTON, August 1, 1932.

[16] L. Jacobson, Am. J. Roent., vol. 22, p. 547, 1929.
[17] All stabilizers of the general type here used produce a distorted wave form depending on the load power factor. This does not affect the usefulness of the instrument for its intended purpose.

A MULTIRANGE POTENTIOMETER AND ITS APPLICATION TO THE MEASUREMENT OF SMALL TEMPERATURE DIFFERENCES

By H. B. Brooks and A. W. Spinks

ABSTRACT

In determining, as a criterion of purity, the boiling range or the freezing range of a liquid which is being purified by fractionation, it is convenient to be able to determine accurately the small difference between the boiling points or the freezing points of the two end fractions. The occasional measurement of relatively large temperature differences between two fractions also requires that the total range of measurement be large in comparison with the smallest measurable temperature difference.

Thermocouples are very suitable for measurements of temperature difference. To increase the electromotive force per degree it was decided in a particular case to use a group of 10 copper-constantan thermocouples in series. Even with these 10 couples, the electromotive force corresponding to a difference of 0.001° C. would be only 0.4 μv, and its measurement to the nearest 0.0001° would require the measurement of the electromotive force to 0.04 μv. Measurements accurate to such a small quantity require not only that the potentiometer used shall be extraordinarily free from parasitic electromotive force, but also that provision should be made for readily detecting and eliminating any such intruding electromotive force in the galvanometer circuit.

The relatively little-used "second method" of Poggendorff, as first realized in practical form by Lindeck and Rothe, appeared to offer the most desirable basis for the design of a multirange potentiometer suitable for the above purposes. The potentiometer which will be described has 6 ranges, and when used with the group of 10 thermocouples provides 6 ranges of temperature difference; namely, from 0° to 0.1°, 0.2°, 0.5°, 1°, 2°, and 5°, respectively, corresponding in each case to a deflection of the pointer of 100 divisions, readable by estimation to 0.1 division. The potentiometer is readily adaptable to read directly in microvolts or in temperature difference, as may be preferred. For the particular application for which it was designed, it was desired to avoid entirely the use of the curves or tables which are necessary when the readings are in microvolts, and it was therefore arranged to read directly in temperature difference.

CONTENTS

		Page
I.	Introduction	782
II.	Principle of operation	782
III.	Basis for design	783
IV.	Construction	784
	1. Plan of circuits	784
	2. Main resistor	786
	3. Milliammeter	787
	4. Bath-temperature scale	787
	5. Galvanometer keys	790
	6. Parasitic emf compensator	792
	7. Miscellaneous details	793
V.	Tests	794
	1. Parasitic emf in component parts	794
	2. Main resistor	795
	3. Bath-temperature scale	795
	4. Over-all accuracy	795
	5. Parasitic emf in complete potentioneter	795
VI.	Procedure in use	796

I. INTRODUCTION

In the work of isolating particular hydrocarbons from petroleum by fractionation it became necessary to measure the difference between the boiling points or the freezing points of two nearly identical liquids with a precision which could be very moderate when the boiling points differed by several degrees, but which had to be much greater as the two boiling points approached equality. For example, if the difference in boiling points was only 0.001° C., it was desired to determine it within, say, 0.0001° C. If the boiling points differed by 0.1° C., a measurement of the difference to about 0.001° C. would suffice, and so on for still larger differences. The requirements were such that some form of electric thermometer was evidently needed, and the thermocouple was chosen as being well suited to the purpose. To obtain an adequate value of thermal emf with the very small temperature differences to be measured a group of 10 copper-constantan couples in series was used. It was decided to cover a range of temperature differences up to 5° C., and to be able to detect a change of 0.0001° C. when measuring temperature differences of 0.1° C. or lower. This required that the parasitic emf in the potentiometer to be used should be well below 0.04 μv, even under relatively severe thermal conditions. It was felt that no potentiometer was commercially available in which the extreme precautions necessary to secure this result had been taken; furthermore, it was desired that the potentiometer should be capable of ready adaptation to make it read directly in temperature difference rather than in a unit of electromotive force. For these reasons the design of a special potentiometer was undertaken.

II. PRINCIPLE OF OPERATION

In announcing his development of the "compensation" process which forms the basis of the art of potentiometry, Poggendorff [1] described what he called the "first method" and the "second method." The first method was taken up with great interest by other workers, and has resulted in a long line of potentiometers, embodying many ingenious ideas to extend the range and increase the precision of measurements. The underlying idea of the first method is the balancing of the unknown emf by an equal potential difference which is adjusted by changing the value of resistance between two tap-off points on a circuit in which a current is maintained constant at a preassigned standard value.

During all of this active development of the first method, Poggendorff's second method was almost forgotten. It was used in 1896 by Holman,[2] who merely assembled stock pieces of apparatus for the purpose. The first recorded development of Poggendorff's second method into a definite instrument for specific applications appears to have been made by Lindeck and Rothe [3] at the Reichsanstalt in 1899. The instrument was developed with the cooperation of Siemens and Halske,[4] who placed it on the market.

---

[1] J. C. Poggendorff, Ann. der Physik und Chemie, vol. 54, p. 161, 1841.

[2] Holman, Lawrence, and Barr, Proc. Am. Acad. Arts and Sci. vol. 31, pp. 218–233, 1895–96.

[3] Lindeck and Rothe, Zeitschrift für Instrumentenkunde, vol. 20, pp. 293–299, 1900; foreshadowed in the annual report of the Reichsanstalt, ibid., vol. 19, p. 249, 1899. Hoffmann and Rothe, ibid., vol. 25, pp. 273–275, 1905, described a recording potentiometer developed from the Lindeck-Rothe potentiometer, using the deflection-potentiometer principle.

[4] Keinath, Elektrische Temperaturmessgeräte, 1923 edition, pp. 30–31.

In Poggendorff's second method the adjustment of the controllable potential difference was effected by changing the value of the current through a circuit while the resistance between the two tap-off points remained constant. This method requires the use of an instrument which will measure a direct current of any value between zero and a given maximum value; that is, ordinarily, an ammeter. Herein lies the chief limitation of the method, for an ordinary ammeter can be read to a precision of only about 0.001 of the full-scale value, and the total error resulting from inaccuracy of marking of the scale, imperfect elasticity of the springs, etc., in a good instrument may be assumed to be several times this value. At the start, therefore, one must reckon with this limitation, and apply the second method only where its limited absolute accuracy is sufficient. When this is the case the second method offers the following noteworthy advantages: (*a*) With a given ammeter, any number of ranges in any desired relation to each other may be readily obtained by providing a corresponding number of tap-off points; (*b*) sliding contacts being absent from the measurement circuit, parasitic emf can be excluded to almost any desired degree; and (*c*) since one has liberty of choice of both the I and the R which by their product give the desired potential difference the "internal resistance" of the potentiometer may in principle be made as low or as high as desired by choosing an ammeter of corresponding range.

Two possible misconceptions regarding potentiometers of the Lindeck-Rothe type should be avoided. The first is that they are "deflection potentiometers." This is not correct because in the deflection potentiometer, properly so called, an unbalanced part of the unknown emf occasions the observed deflection of the indicating instrument, which is directly in the measurement circuit. In the Lindeck-Rothe potentiometer the deflection is all occasioned by a current from an auxiliary source, and all of the unknown emf is balanced by the IR drop in the potentiometer, hence no current flows through the source of the unknown emf. The other possible erroneous idea is that the apparatus is not a potentiometer, because the entire result of the measurement depends on a deflection, and no standard cell is used. A potentiometer may be broadly defined as an instrument for measuring an unknown potential difference by balancing it, in whole or in part, against a known potential difference produced by the passage of known currents through a network of known electrical constants. Where the usual types of potentiometer produce this adjustable potential difference by means of an adjustable value of resistance and a current of fixed value which is frequently checked by reference to a standard cell, the Lindeck-Rothe potentiometer utilizes a fixed resistance and an adjustable current which is checked less exactly and much less frequently, namely, when the accuracy of the milliammeter is checked by reference to a resistance standard and a standard cell.

III. BASIS FOR DESIGN

In practice the auxiliary current for a Lindeck-Rothe potentiometer will be supplied by some form of battery, and should therefore be kept down to moderate values. While storage cells are much used with potentiometers, they have some objectionable features which

make the use of dry cells attractive. This suggests the use of currents not exceeding a few hundredths of an ampere, a suggestion which is fortified by the fact that the accuracy of direct-current milliammeters in which the entire current to be measured flows through the moving coil is almost independent of changes of the instrument temperature.[5]

In the present case the current to give full-scale deflection of the milliammeter could be conveniently given the value 10 milliamperes. To produce a potential difference of 2,000 μv,[6] this current must flow through a resistance of 0.2 ohm, a value which is negligible in comparison with the resistance of the group of thermocouples, namely, about 50 ohms. Considerations of speed of working required that the galvanometer to be used should be critically (or slightly under) damped with this latter resistance across its terminals.[7]

The galvanometer selected has a nominal coil resistance of 12 ohms, is critically damped with an external resistance of 40 ohms, has a sensitivity of 5 mm (at 1 m) per microvolt with this external resistance and a complete period of five seconds. It is constructed in such a way as to be relatively free from parasitic emf, but because of the very stringent requirements of the problem, the potentiometer was provided with means for readily detecting any parasitic emf in the galvanometer and for neutralizing its effect. Although the parasitic emf compensator can also be used to neutralize the effect of parasitic emf within the potentiometer, it was considered much better to simplify the manipulation by keeping such internal parasitic emf below the limit of detection, even at the expense of extraordinary precautions in design, materials, and construction.

IV. CONSTRUCTION

1. PLAN OF CIRCUITS

Figure 1 illustrates the principle of operation of the potentiometer and Figure 2 shows the plan of circuits used. In Figure 2, a resistor R_{13} of manganin strip [8] is provided with nine taps, of which the two outside ones are used as potential leads. A current from the dry cell B_2, controlled by the coarse rheostat R_5 and the fine rheostat R_4, flows through the slide rheostat R_{11}, the shunted milliammeter MA, the current-limiting resistor R_6, the reversing switch S_1, then through the manganin resistor R_{13}, entering at the common point C and leaving at one of the six taps connected to the studs of the range-changing switch S_2. The values of the 4-terminal resistance of R_{13} for the six positions of this switch are (from left to right) 0.004, 0.008, 0.02, 0.04, 0.08, and 0.2 ohm.

---

[5] This independence of temperature changes depends on the facts (1) that no change in distribution of the measured current between the moving coil and a shunt circuit can occur as a result of temperature change; (2) that the small temperature coefficient of magnetic flux density in the air gap (about 0.01 to 0.03 per cent per degree C.) tends to offset a temperature coefficient of rigidity of the springs, which is about 0.04 per cent per degree C.

Although the requirements of the present case made it necessary to use a shunt around the moving coil, it was possible to give the shunt a value of temperature coefficient which reduced the temperature coefficient of the instrument (as a milliammeter) to zero.

[6] These nominal values of current and potential difference would correspond to the use of the actual group of thermocouples in baths at a mean temperature of about 22° C. As explained further on, the milliammeter was provided with a continuously adjustable Ayrton-Mather shunt which increased the total current for full-scale deflection to values between the limits 10.57 and 14.76 milliamperes, corresponding to the rate of change of thermal emf with temperature at mean bath temperatures of 50° and 300° C., respectively.

[7] This criterion is the one to be used in selecting a moving-coil galvanometer for a specific application, rather than the old rule, still quoted occasionally, that the galvanometer resistance and the resistance of the circuit to which it is connected should be as nearly equal as practicable.

[8] This strip was three-sixteenths inch wide, 25 mils thick, and was about 6 feet long.

The potential difference between the ends of the resistor R_{13} is opposed, through a galvanometer, to the emf of the thermocouples, the terminals of which are brought to the binding posts A and B. In the lead from the left-hand end of the resistor R_{13} to the binding post A are included three keys, two having the protective resistors R_1 and R_2. The lead from the right-hand end of the manganin resistor to one of the galvanometer binding posts includes the copper rheostat

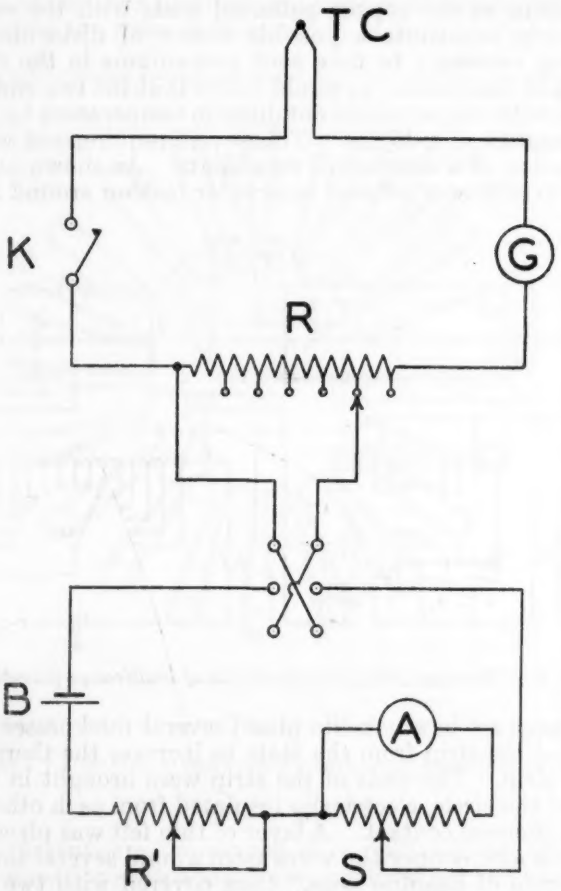

FIGURE 1.—*Diagram illustrating the principle of operation of the multirange potentiometer*

The emf developed in the thermocouple *TC* is balanced by the drop of potential produced in the resistor *R* by the current from a battery *B*. This current is adjusted by the rheostat *R'* and measured by the shunted milliammeter *A*.

R_3 forming part of the parasitic emf compensator. A very small current from a flashlight cell B_1 may be made to flow in either direction through any part of R_3 from zero up to one-half of R_3. Depression of the key marked "Shunt off" opens a shunt circuit across the galvanometer, namely, a copper resistor, R_{12} with taps at 30, 40, 60, and 80 ohms. As much of this coil is used as will make the motion of the galvanometer coil critically damped when the keys R_1, R_2, 0 are open.

The function of the reversing switch S_1 is to change the sign of the potential difference between the ends of the resistor R_{13} to take care of the fact that either of the two baths of liquid may on occasion be the hotter. The fixed resistance R_7 and the slide rheostat R_8 constitute the continuously adjustable Ayrton-Mather shunt to the milliammeter.

2. MAIN RESISTOR

The junctions of the copper potential leads with the ends of the manganin strip constitute a possible source of disturbing thermal emf.[9] It was necessary to take such precautions in the design and construction of this resistor as would insure that the two end junctions of manganin with copper would not differ in temperature by more than a few thousandths of a degree. This severe requirement was met by the combination of a number of expedients. As shown in Figure 3, the manganin strip was reflexed in circular fashion around two circles

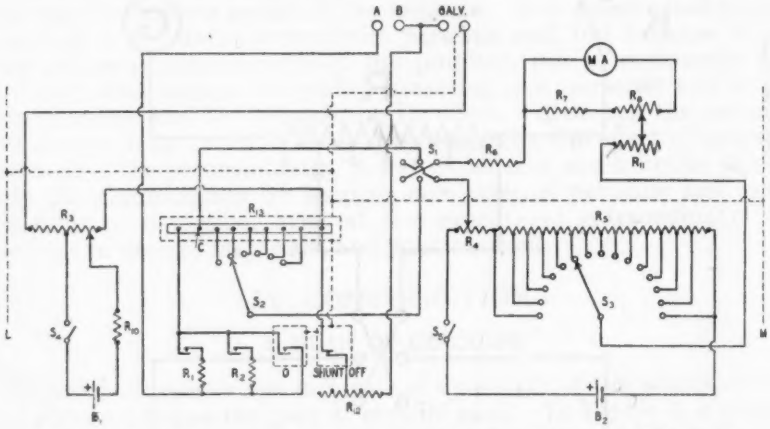

FIGURE 2.—*Diagrammatic plan of circuits of multirange potentiometer*

of bakelite pegs set in a bakelite plate; several thicknesses of 1/16-inch felt separated the strip from the plate to increase the thermal insulation of the strip. The ends of the strip were brought in radially to the center of the circle, electrically insulated from each other by mica, but in good thermal contact. A layer of thin felt was placed over the strip, and the nine copper tap wires were wound several times around the outer circle of bakelite pegs,[10] then covered with two additional layers of felt and a second bakelite plate which was then secured by screws through the corners to the first plate. The space between the two bakelite plates was then filled in by winding a narrow strip of felt over the outer circle of bakelite pegs.

Before the main resistor was mounted in the structure just described, a similar resistor of constantan, made and mounted in this manner, was used as a check. Tests, such as placing a can of water

[9] For a copper-manganin junction at ordinary room temperature, the thermal emf changes at the rate of about 1 to 2 μv per °C.

[10] The object of this procedure was to increase the length of path along which heat from other parts of the potentiometer must travel in order to reach the main resistor, and at the same time to permit heat exchange between these wires. The flow of heat uniformly to (or from) all parts of the main resistor would have no bad effect because it would not cause a difference of temperature between the end junctions.

at 40° C. on the upper bakelite plate, produced a thermal emf of the order of a microvolt. This showed that only a few hundredths of a microvolt would be developed with a manganin resistor similarly treated. To be on the safe side, however, the complete structure, with the manganin resistor in it, was mounted below the bakelite top of the potentiometer, midway between the bakelite and the bottom of the box, on four bakelite posts symmetrically placed, and was covered with a box of sheet aluminum 0.03 inch thick. In Figure 4 the bottom of this box has been removed to show the bakelite structure containing the main resistor.

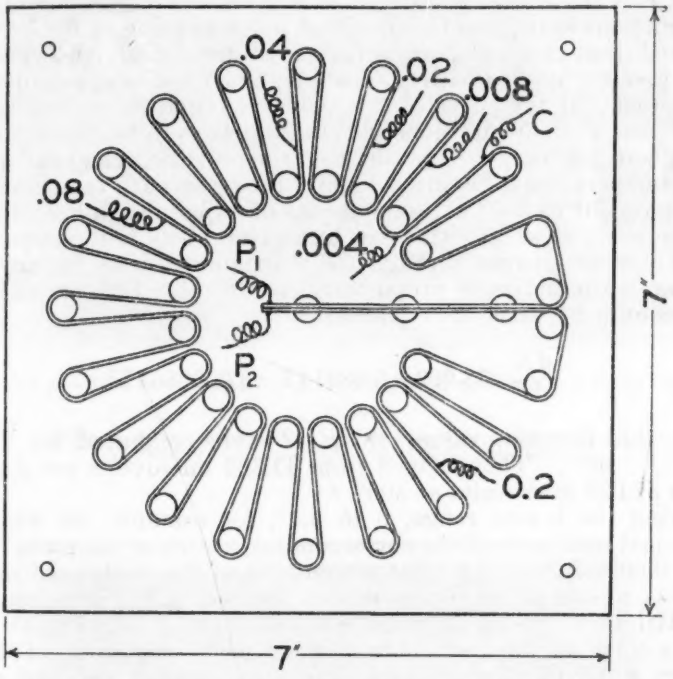

FIGURE 3.—*Plan view of main resistor with upper bakelite plate removed*

3. MILLIAMMETER

This instrument is a fan-shaped d. c. milliammeter of a type primarily intended for switchboard use, modified by the use of a knife-edge pointer, a parallax mirror, and a fine-line 100-division scale of the quality used in standard portable instruments. The resistance of the instrument was about 5 ohms and the current for full-scale deflection (before applying the shunt) was 10 milliamperes.

4. BATH-TEMPERATURE SCALE

In the ordinary procedure for measuring temperatures or temperature differences by means of thermocouples and a potentiometer, the latter is usually graduated to read in terms of a unit of emf (millivolt or microvolt) and its readings are subsequently translated into tem-

peratures (or temperature differences) with the help of curves or tables for the particular couples used. In the present case, it was desired to be able to adapt the potentiometer to read directly in temperature difference for a given group of couples. To determine the electrical conditions which must be satisfied to obtain this result, one must start with the temperature-emf relation of the couples used. A sample couple made of the same wires as the 10 couples to be used was certified as having the following relation:

$$E=38.062T+0.04457T^2-0.0000288T^3$$

where E is the emf in microvolts and T is the temperature of one of the junctions in degrees C., the other junction being at 0° C. It was assumed that a similar equation, with numerical coefficients ten times greater, applied with sufficient accuracy to the group of couples to be used. If the curve of the above equation be plotted between $T=0°$ and $T=300°$, its slope, dE/dT, will be seen to increase with T throughout this range. In order that the potentiometer shall indicate small temperature differences directly for mean bath temperatures in the region 50° to 300° C., some means of adjustment must obviously be incorporated which, when set to a given mean bath temperature, will make the current through the manganin resistor for any given reading of the indicator proportional to dE/dT. Differentiating the expression for E gives the equation

$$\frac{dE}{dT}=38.062+0.08914T-0.0000864T^2$$

Using this formula, values of dE/dT were computed for $T=50°$, 60°, . . . 300°. They ranged from 42.303 microvolts per degree at 50° to 57.028 microvolts at 300°.

Taking the lowest range, 0 to 0.1°, for example, for which the 4-terminal resistance of the corresponding section of the main resistor R_{13} is 0.004 ohm; if the full-scale current of the unshunted milliammeter is passed through this section the potential difference at the potential terminals of R_{13} will be $0.004\times0.01=0.00004$ volt $=40$ μv. This is equal to the thermal emf of the particular group of thermocouples when the temperature difference between the two sets of junctions is 0.1° C. and their mean temperature is 22.2° C., and consequently for these conditions the full-scale deflection of the milliammeter corresponds to 0.1° C. temperature difference. As the mean bath temperature increases from 22.2° to 300° C. the value of dE/dT increases continuously from 40 μv per degree to 57.028 μv per degree. Therefore, the current which must be passed through any section of the main resistor R_{13} to give a difference of potential equal to the thermal emf of the couples, for a given temperature difference, must be greater than 10 milliamperes by a factor which is equal to dE/dT for the given temperature divided by that for 22.2° C., namely 40 μv per degree. Thus for a mean bath temperature of 50° a shunt must be connected across the milliammeter to increase the full-scale current of the shunted instrument by the factor 42.303/40; that is, to 10.576 milliamperes; for a mean bath temperature of 300° the current for full-scale deflection must be 10 milliamperes multiplied by the factor 57.028/40; that is, 14.257 milliamperes; and similarly for intermediate values of mean bath temperature. This object was

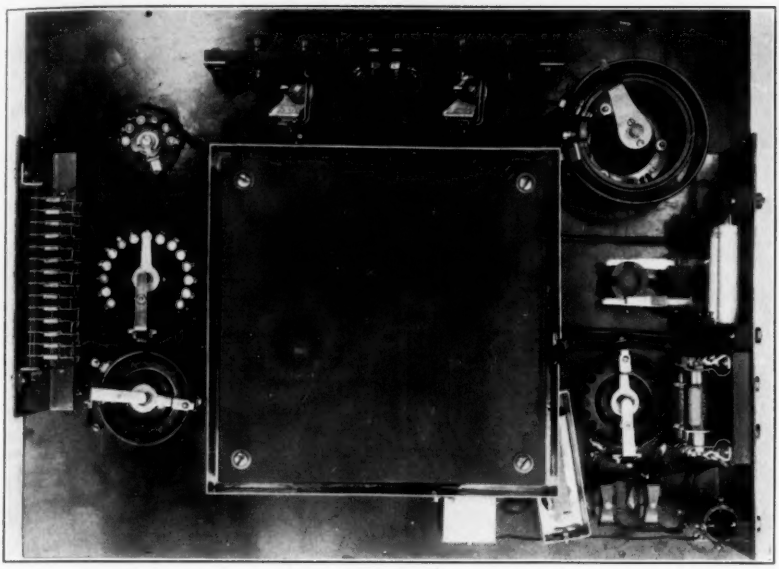

FIGURE 4.—*Structure of multirange potentiometer as seen from below the bakelite top*

Part of the aluminum thermal shield has been removed from the main resistor (center) and from the key marked 0 (near lower right-hand corner of main resistor).

FIGURE 5.—*Plan view of multirange potentiometer*

UNIV. OF MICH.

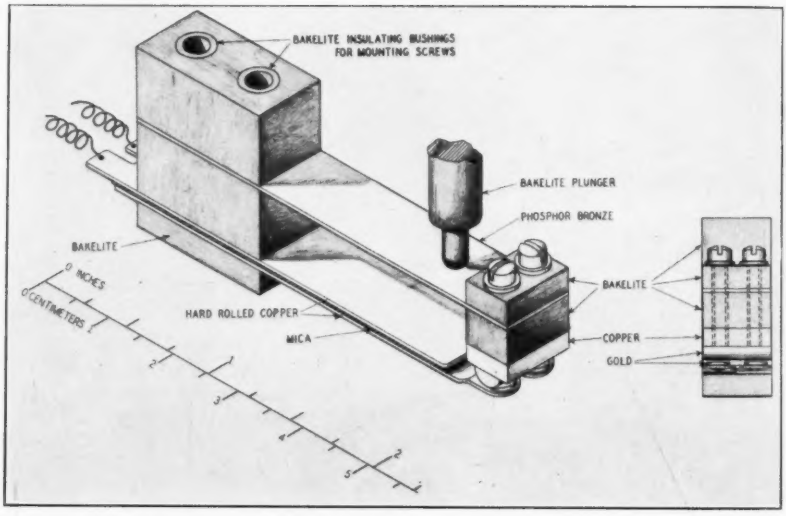

FIGURE 6.—*Galvanometer key embodying refinements to minimize thermal emf*

readily attained by a continuously adjustable shunt of the Ayrton-Mather type [11] connected to the terminals of the milliammeter. This shunt is shown diagrammatically in Figure 2 as consisting of a fixed resistor R_7 in series with the winding of a circular slide rheostat R_8, the two being connected to the terminals of the milliammeter. The current enters by the slider of R_8 and divides between the two parallel paths. As the slider is moved toward the left, the total current for full-scale deflection of the milliammeter increases. A pointer attached to the slider may therefore indicate on a fixed scale either the corresponding value of dE/dT in microvolts per degree or the mean bath temperature. The former would be preferable in general because it would facilitate the use of the potentiometer with any thermocouple for which the value of dE/dT under the conditions of use fell within the range of the scale. In the present instrument, however, it was desired to avoid entirely the use of tables and curves, and the scale was accordingly marked in terms of mean bath temperature for the particular set of copper-constantan thermocouples which had already been made. Attention is called to the fact that the scale divisions were engraved on a disk which is an integral part of the knob of the circular slide rheostat which performs the function of R_8 in Figure 2, and only a fiducial mark was engraved in the bakelite top. (See figure 5.) If for any reason the original set of couples is to be replaced by another, a new scale may be engraved on the disk, which may be readily removed for the purpose. If desired, the scale of bath temperature could be replaced by another scale reading values of dE/dT in microvolts per degree.

If the circular slide rheostat R_8 were of the ordinary type in which the rate of change of resistance with respect to rotation is approximately constant, the bath-temperature scale would be open at one end and crowded at the other because of the quadratic form of the relation between dE/dT and T. It was possible to obtain a nearly linear scale by using a circular slide rheostat in which the resistance wire is wound on a tapered strip of sheet insulating material, giving a quadratic relation between the resistance and the angle of rotation. The close approach to a linear bath-temperature scale which was obtained may be seen from Figure 5, in which the dial at the upper left-hand corner of the potentiometer is the one to be set to the mean bath temperature. The scale was laid out by adjusting the current through the shunted milliammeter successively to the computed values of current for full-scale deflection for bath temperatures of 50°, 60°, . . . 300°, and turning the knob of the bath-temperature rheostat until the pointer of the milliammeter came to the full-scale mark. For each such adjustment a mark was drawn, opposite the fiducial mark, on the scale disk which moves with this knob. The 10° lines were then engraved, with 5° lines spaced midway between them. The results of a test to check the correctness of the resulting scale are given in a later section of this paper.

The current-regulating rheostats R_4 and R_5 operate properly only if the resistance of the circuit beyond them (that is, connected between the slider of R_4 and that of R_5) is substantially constant. The effect of moving the slider of R_8 to the left is to increase the resultant resistance of the milliammeter and its shunt, and the tapered slide

[11] Ayrton and Mather, J. Inst. Elecl. Engrs. (London), vol. 23, p. 314, 1894.

rheostat R_{11}, connected as shown, compensates for this change and maintains a substantially constant resistance in the circuit beyond the sliders of R_4 and R_5.

5. GALVANOMETER KEYS

In the effort to reduce parasitic emf in the "measurement circuit" to a value below the limit of detection, particular attention was given to some of the keys which had to be used. These keys must be operated frequently; they must contain contact points of metals or alloys nobler than copper because the latter is subject to corrosion; heat from the observer's hand will flow to the contact points through the key spindle; and heat is developed at the contact points by their mutual friction. In many ways the problem of avoiding parasitic emf in the keys is much more difficult than in the main resistor, which has no moving parts and can be thermally shielded to any desired degree.

Referring to Figure 2, it will be seen that there are four keys in the galvanometer circuit. Of these, the ones marked R_1 and R_2 may be of ordinary construction because they are used only in obtaining an approximate balance between the emf to be measured and the adjustable potential difference developed within the potentiometer. The "working microvolt sensitivity"[12] with either R_1 or R_2 in circuit is too low to permit the effect of parasitic emf to be detected. The keys marked "0" and "Shunt off," on the contrary, are in circuit with the galvanometer when measurements are being made; the total resistance in the galvanometer circuit is then low and the working sensitivity correspondingly high; consequently any appreciable parasitic emf in these keys will cause an error in the measurement. The conditions in these two keys are somewhat different. The key marked "0," normally open, is closed just before a reading is taken; that marked "Shunt off" is closed until just after the key marked "0" is closed. Any parasitic emf in the "Shunt-off" key would cause an error in the zero reading of the galvanometer while any such emf in the "0" key would cause an error in the deflection. It was obviously necessary to make these keys so nearly "thermofree"[13] that no perceptible error could be introduced by them. Their design, materials, and construction are based upon the results of a series of experiments which will not be detailed here. If a galvanometer key be constructed of random materials, with consideration given only to its mechanical functioning, it is liable to be the source of objectionable thermal emf under many conditions encountered in practice. The production of a good thermofree key[14] requires that attention be given to three important matters, each of which acts in its own way to minimize the thermal emf. These three matters are:

---

[12] This term, ordinarily to be abbreviated to "working sensitivity," has been proposed by one of the authors (B. S. Jour. Research, vol. 4, p. 299, 1930) to denote a constant of importance to the galvanometer user, defined as follows: "The working sensitivity applies only to the user's particular problem at the moment, and may be defined as the response of the galvanometer for unit electromotive force in a circuit which includes the galvanometer and a particular external circuit."

[13] This term is offered as an arbitrary short equivalent of complete but unwieldy expressions, such as "free from thermoelectric forces," "thermal emf free," "thermoelectrically neutral," etc. While it was suggested by the well-known German adjective "thermokraftfrei," it was felt unnecessary to include the English equivalent of the syllable "kraft."

[14] Some makers of potentiometers have been using keys intended primarily for telephone purposes. Some telephone keys contain pairs of springs of very dissimilar alloys (evidently phosphor bronze and nickel silver) and in consequence should not be used in the construction of potentiometers. There should be no difficulty in having telephone keys assembled for the purpose with none but bronze springs.

1. The choice of materials for the key springs and the contact points which are very close to copper in their thermoelectric properties.

2. The design of the key to be "thermoelectrically astatic" with respect to heat flow; that is, so that all junctions of dissimilar metals occur in adjacent pairs so arranged that a flow of heat in any direction will set up nearly equal thermal emf's of opposite sign in the circuit containing the key.

3. The inclosure of the key within a shield which tends to maintain uniformity of temperature of all parts of the key in spite of heat radiation and conduction to or from the shield.

Such a shield may be a jacket of heat-insulating material, or a metal shield of high thermal conductivity, or a multi-layer thermal shield embodying both these features repeated as often as necessary. It is clearly useless to incur expense in reducing the parasitic emf much below a value which will produce a barely perceptible deflection (for example, 0.1 mm) of the galvanometer to be used.

The plunger for operating the key provides a path along which heat may travel into the key structure. The plunger should therefore be preferably of material of low thermal conductivity and be rounded or pointed where it bears on the part of the key to be depressed; furthermore, special care should be taken to make this part of the key "astatic." If the use of metal for the plunger is considered essential, it may be noted that either manganin or constantan is preferable to brass because of their very much lower heat conductivity.

Keys meeting the exacting needs of the present case have been made by caring for the three principal matters as follows: (*a*) The use of hard-rolled copper for the key springs and United States coin gold [15] for the contact points, (*b*) using an astatic arrangement which will be described below, and (*c*) inclosing the key in a box of sheet aluminum 0.03 inch thick.

These two keys, one with part of the aluminum shield removed to show the interior, are shown in Figure 4 near the lower edge of the bakelite top, to the right of the center. To the right of them are the two ordinary keys, R_1 and R_2.

Figure 6 shows the construction of the key marked 0. Two springs of hard-rolled copper, separated by a sheet of mica, are clamped at one end between bakelite blocks and carry gold contact disks at their free ends. Above these contacts is a transverse half-cylindrical gold contact piece soldered to the lower surface of a block of copper which is secured to a flat phosphor-bronze spring by blocks of bakelite used for thermal rather than electrical insulation. The plunger through which the bronze spring is depressed is of bakelite to retard the flow of heat from the observer's hand. However, even if an appreciable amount of heat did flow through the plunger, the construction of the key is thermally astatic to such a high degree that the development of an appreciable thermal emf would be almost impossible. Heat entering the bronze spring by way of the plunger will flow in part to the left, where a thick block of bakelite impedes its flow to the upper copper strap. Although the temperature of this strap will be slightly raised above that of the lower strap, the adjacent junctions to connecting wires are of hard-rolled copper to soft copper,

[15] This alloy is composed of gold 90 parts, copper 10 parts, and has a thermal emf against copper, at room temperature, of 2.2 μv per ° C.

for which combination the thermal emf is very small, namely, about 0.25 μv per °C.

Heat flowing to the right through the bronze spring is retarded by the block of bakelite between the spring and the massive copper block. Because of the symmetrical construction there will be no tendency for unequal heating of the copper block; and even if heat did enter the upper surface of the copper block in a nonuniform manner, the high thermal conductivity of the copper and the small rate of heat transfer would maintain a very high degree of temperature uniformity in the copper and therefore in the transverse gold contact piece soldered to it. Heat will flow from this contact piece to the gold contact disks in the free ends of the hard-rolled copper springs. However, this part of the key is astatic to heat flow in the vertical direction because a current in the circuit which is closed by the key flows up to the transverse gold contact piece on one side and down on the other. Any thermal emf in one of the copper-gold junctions will thus be balanced by an equal and opposing emf in the other junction.

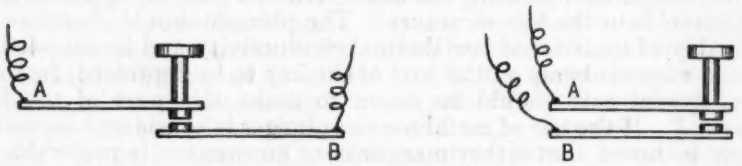

FIGURE 7.—*Keys illustrating poor design (left) and mediocre design (right) as regards the liability to thermal emf*

In contrast to this key, Figure 7 shows diagrammatically two constructions which are not thermally astatic. The key at the left has the junctions A and B as far apart as possible, and is consequently not astatic as to lateral heat flow. The key at the right is free from this objection, but neither key is astatic as to vertical heat flow.

6. PARASITIC EMF COMPENSATOR

The parasitic emf compensator, shown diagrammatically as R_3 in Figure 2, is shown in Figure 4 just above the two ordinary keys. It is merely a circular slide rheostat as used in radio apparatus but with the resistance-alloy winding replaced by one of copper wire. The material [16] of which the sliding contact lever is made is of no consequence thermoelectrically.

The manner of using the parasitic emf compensator may be understood by reference to Figure 2, which shows that when none of the four keys is depressed the tapped copper coil R_{12} is across the terminals of the galvanometer. Assuming that the slider of R_{12} is at the central point of its winding (or that the switch in series with the cell B_1 is open), any parasitic emf in the galvanometer will maintain a deflection. When the "Shunt off" key is depressed, the galvanometer coil will come to its true zero position, revealing by its motion the fact that an unwanted emf exists in the galvanometer circuit. With the switch S_4 closed, the slider of R_3 may be moved until a position is

[16] An interesting experience illustrates the necessity for great caution in the construction of highly thermo-free apparatus. The complete potentiometer, exposed to heat radiation from a slide rheostat 10 inches away, dissipating 300 watts, showed a parasitic emf of 0.2 μv. Careful search revealed that a strip of metal, forming a lug to which one end of the copper winding of the compensator had been soldered, was of bronze instead of copper as had been assumed. After this strip had been replaced with one of copper, the parasitic emf with the radiation test above described dropped to about one-tenth of its previous value.

found for which the galvanometer coil does not move when the "Shunt off" key is opened or closed. In this condition the parasitic emf in the galvanometer is just annulled by an equal and opposite potential difference in the copper winding of the compensator.

The resistor R_{10} in series with the cell B_1 has a resistance of 50,000 ohms. It is of the "wire-wound" type developed in recent years for radio purposes, and may be easily removed from holding clips if a change in the value of this resistance is desired. The greater the parasitic emf found in the galvanometer by actual use, the lower this resistance must be, but it is desirable not to make it much lower than necessary. The current taken from the flashlight cell is so small as to have no appreciable effect on the life of the cell, and the only reason for providing the switch S_4 for opening the circuit of this cell is to provide a ready means of annulling the small compensating emf set up by the parasitic emf compensator, without altering the position of the slider.

7. MISCELLANEOUS DETAILS

When the temperature difference between the baths A and B changes sign the direction of the thermal emf to be measured reverses. One way to meet this situation would be to provide a reversing switch between the leads from the couples and the potential taps from the ends of the manganin resistor R_{13}. (See fig. 2.) This would require that the reversing switch be highly thermofree. A better method was used, which is shown in Figure 2, namely, the reversing switch S_1 is placed in the wires which carry the adjusted current from R_4 and R_6 to the main resistor. Parasitic emf in the switch can do no harm whatever with this arrangement. Above the bakelite top the two positions of this switch are marked "A higher" and "B higher," respectively, A and B being the designations of the two baths of liquids.

The dry cells B_1 and B_2 are contained in metal receptacles within the potentiometer. There is a door in the back of the potentiometer box which does not appear in Figure 5 and which gives access to the cells and to four copper binding posts. These posts are supported on a small bakelite panel attached to the bakelite top, as shown near the top of Figure 4. As a precaution against possible differences of temperature among the four wires which come from the couples and the galvanometer to these binding posts, the two insulated wires from the couples, twisted together, enter the rear wall of the box and pass through a copper tube which extends to a point near two of the binding posts; and the pair of wires from the galvanometer pass through a similar tube. Any difference of temperature between the two wires of either pair will be equalized by their thermal contact with each other and with the tube.

Near the middle of the small bakelite panel are mounted two pairs of jacks for disconnecting the dry-cell leads when the bakelite top is to be removed from the box. Below the binding-post panel (fig. 4) are the two single-pole switches S_4 and S_5 of Figure 2, for opening the circuits of the two dry cells.

When the potentiometer was under test for freedom from thermal emf during the winter some difficulty was experienced because of electrostatic effects. For example, the galvanometer was found to deflect when the observer rubbed his shoes on the dry floor while his hands

were on the galvanometer keys. These difficulties were overcome by shielding as indicated in Figure 2, in which the dotted lines L and M denote two brass angle plates for supporting some of the resistors at the sides of the potentiometer (see fig. 4) and the dotted outlines around R_{13} and the keys marked 0 and "Shunt off" denote the aluminum thermal shields. These five metal structures were connected together and to the right-hand galvanometer binding post as shown by the dotted lines. It was also necessary to shield the leads from the potentiometer to the galvanometer by inclosing them in a metal tube which was electrically connected to the same binding post.

V. TESTS

1. PARASITIC EMF IN COMPONENT PARTS

In testing experimental keys and other parts to determine their thermoelectric behavior under thermal exposure, a sensitive reflecting galvanometer was used in series with a parasitic emf compensator [17] and a device (a small Lindeck-Rothe potentiometer) by means of which a measured emf from 0 to 10 μv could be injected into the galvanometer circuit. To prepare for the measurement of parasitic emf in a key, for example, the galvanometer circuit as above described was first closed by directly joining two copper wires. No current flowed in the compensator circuit and no emf was injected into the galvanometer circuit by the Lindeck-Rothe potentiometer. The resulting deflection, if any, was caused by parasitic emf in the galvanometer, and was then reduced to zero by using the compensator. Then a small emf, say 1 μv, was injected, and the resulting deflection noted as the basis for reducing to microvolts the subsequent observations with the key in ciruit and the injected emf removed.

While ordinary keys, not designed to be specially thermofree, showed appreciable values of parasitic emf, the combination of good materials and thermally astatic design reduced the thermal emf to values so small as to be almost inappreciable. Two expedients assisted in the measurements of emf of only a few hundredths of a microvolt. The first was to replace a part made of good material (for example, the hard-rolled copper spring of a key, or the manganin main resistor) by a similar part made of a very unsuitable material. Constantan was used for the latter. Since its thermal emf per degree with respect to copper is about 20 times the thermal emf per degree for the combination manganin-copper, the values of parasitic emf observed with constantan, divided by 20, gave the values of thermal emf which would have been obtained for the same structure made of good materials; that is, with copper for the key springs and manganin for the main resistor.

The other expedient, used in final tests of parts (and later of the complete potentiometer) which had been made of very suitable materials, was to increase very greatly the sensitivity of reading the galvanometer deflection. A special optical arrangement was devised, usable only for very small (but nevertheless adequate) angular deflections of the galvanometer coil, which gave a sensitivity equal to that which would have been obtained if the galvanometer had been

[17] This compensator was similar to the one in the potentiometer. It was a small, self-contained device, complete with dry cell, and has been very convenient for purposes other than the present development.

used in the ordinary way, but with the scale 13 m from the galvanometer mirror.

2. MAIN RESISTOR

The 4-terminal resistances of the six sections of the main resistor were determined after final adjustment and found to have the desired values within 0.06 per cent. The manganin strip composing this resistor had been formed on an iron plate with two circles of iron pegs, which was a replica of the bakelite housing in which the strip was finally mounted. The manganin was annealed while on the iron plate at about 550° C. to relieve internal stresses. It is believed that this treatment insures the permanency of the resistance values to a degree much higher than the needs of the case require.

3. BATH-TEMPERATURE SCALE

The second of the two factors which jointly determine the accuracy of measurements with the potentiometer is the accuracy with which the current for full-scale deflection of the milliammeter approaches the ideal values, calculated from the emf-temperature relation of the couples, as the bath-temperature dial is turned to various readings over its range of 50° to 300° C. This matter was checked by measuring the full-scale current, using a resistance standard and Wolff potentiometer, at each of the 10° divisions over the entire range. The relative differences between these measured currents and the currents calculated from the emf-temperature relation for the thermocouples averaged 3 parts, maximum 8 parts, in 10,000. The errors in temperature-difference measurements from this cause will therefore be below the usual limit of reading of the scale.

4. OVER-ALL ACCURACY

The final test of the potentiometer was a direct check of the accuracy of the potential difference which it develops at the terminals marked A and B (fig. 2) for full-scale deflection of the milliammeter and various settings of the bath-temperature scale. This potential difference was measured with a Wolff potentiometer, with the bath-temperature dial set in succession at each 10° point over its whole range. The check was made with the range-changing switch S_2 set at the extreme position on the right, corresponding to a difference of 5° C. between the temperatures of the two baths for full-scale deflection of the milliammeter. The average relative difference between observed and computed values of potential difference in microvolts was 0.1 per cent, the differences ranging from 0 to 0.2 per cent at various points on the bath-temperature scale.

5. PARASITIC EMF IN COMPLETE POTENTIOMETER

In addition to the heat-radiation tests of separate portions of the potentiometer, main resistor, keys, etc., as constructed, to determine how much parasitic emf would be set up in them, a similar test was made on the complete potentiometer. The source of heat was a small tubular slide rheostat dissipating 300 watts. It was placed on the table 10 inches from the front of the potentiometer; that is, in about the usual position of the observer when measurements are in progress. With the heat source in this position, the heat passing

through the wooden box would be communicated to the keys and the main resistor. (See fig. 4.) That these parts were properly designed and well protected by their aluminum shields was shown by the fact that even after prolonged exposure the thermal emf in the potentiometer was so minute that it would have produced an error corresponding to about 0.1 division on the indicator scale with the lowest range (0 to 0.1° C.); that is, corresponding to an error of 0.0001° C. in the result. Although, it would doubtless be possible to reduce parasitic emf in potentiometers to a lower amount, by more refined methods of shielding the "thermoelectrically vulnerable" parts, the refinement would not usually be worth the extra cost because even high-grade moving-coil galvanometers would not be capable of showing the difference in performance.

VI. PROCEDURE IN USE

The complete procedure to be followed in measuring the temperature difference of the two baths is as follows:

1. With both battery switches open, depression of the "Shunt off" key will show whether any appreciable deflection of the galvanometer has been existing because of parasitic emf. If the spot of light moves when this key is depressed, the left-hand battery switch is to be closed and the knob of the parasitic emf compensator is to be turned by trial to a position such that the spot of light does not move when the "Shunt off" key is depressed.

2. The bath-temperature dial is to be set to the mean temperature of the two baths, as determined by independent means. This temperature does not need to be known very accurately because an error of 5° to 10° C. in T will produce an error of only 1 per cent in the value of dE/dT.

3. The right-hand battery switch is to be closed, the range-selecting switch set to a value of full-scale temperature difference which includes the estimated or expected value, and the reversing switch set to "A higher" or "B higher" as may be thought necessary; then by means of the coarse rheostat and the fine rheostat at the right of the "indicator" (milliammeter) the pointer is brought to a reading corresponding to the estimated temperature difference. Key R_1 is now closed, the direction of the galvanometer deflection noted, and the reading of the indicator changed by using the coarse rheostat until the direction of the galvanometer deflection becomes reversed. With the aid of the fine rheostat the deflection is to be reduced to zero; the key R_2 is then closed, increasing the working sensitivity; the resulting deflection is again reduced to zero; and similarly with both the keys 0 and "Shunt off" depressed. The difference between the temperatures of the baths is then indicated by the pointer, the reading in divisions being interpreted in degrees C. by noting the setting of the range-selecting switch. If the actual temperature difference is greater than the anticipated value, it may be impossible to reduce the galvanometer deflection to zero until the range-selecting switch has been advanced to a higher setting. If the temperature of bath B is actually higher than that of bath A, and the knob has been set to "A higher," the fact will be shown by the impossibility of reducing the galvanometer deflection to zero, this deflection increasing con-

tinually as the reading of the indicator increases and as the range-selecting switch is advanced to higher settings.

The check for parasitic emf in the galvanometer, made as the first step in the procedure, should be repeated occasionally, the intervals depending on the degree of freedom of the galvanometer from such emf, its environment as regards temperature uniformity, air currents, etc., and the magnitude of the temperature difference under measurement. The smaller this difference the more carefully must parasitic emf be detected and compensated.

By setting the bath-temperature scale at 158°, at which temperature dE/dT is 50 μv per degree, the potentiometer may be made to indicate the potential difference between the terminals A and B (fig. 2) in microvolts, the full-scale deflection of 100 divisions then corresponding to 50, 100, 250, 500, 1,000, and 2,500 μv when the range switch is set at 0.1°, 0.2°, 0.5°, 1°, 2°, and 5°, respectively. This procedure adapts the potentiometer to the measurement of very small values of emf for any purpose where the limitations on the relative accuracy of Poggendorff's second method do not interfere. A good illustration is the determination of the emf of a standard cell in terms of the emf of another cell taken as a reference cell, the two emfs being opposed and their difference being measured by the potentiometer. Even if the two cells differed in emf by as much as 1,000 μv and the relative error of measuring this quantity were 0.5 per cent, the value of the unknown cell in terms of the reference cell would be obtained with an error of only 5 parts in 1,000,000. Reading directly in microvolts, the potentiometer may be used with thermocouples of characteristics different from those for which it was designed, and might also be used, with the couples for which it was designed, for temperatures lower than 50° or higher than 300°. However, since this procedure would involve inconvenient calculations or reference to curves to obtain values of temperature difference, a more convenient method would be as follows:

For any given mean bath temperature, set the bath-temperature dial to a corresponding value, taken from a curve or table, such that all observed values of temperature difference need only multiplication by a convenient factor to give actual temperature difference. For example, in the present case, the range +50° C. down to −40° C. can be covered by setting the bath-temperature dial at 208° for actual bath temperature of 50°; at 57° for actual bath temperature of −40°, and multiplying observed temperature differences by 1.25. The use of the factor 1.5 makes it possible to cover the range −40° to −100° C., and the factor 2 continues this down to −160°. These factors, increasing as the bath temperature decreases, represent the fact that dE/dT decreases with the temperature.

It would be possible to design the rheostat R_8 (see fig. 2) to provide a scale of dE/dT (or of mean bath temperature) covering a very much wider range of bath temperature, but this might make the scale more crowded than is desirable. It is probably preferable, as a rule, to provide an open scale covering the temperature range for which the greater part of the work is to be done, and to use expedients, such as those of the preceding paragraph, for the very occasional work outside this range.

Although particular attention has been given in this paper to the specific application which occasioned the design and construction of this potentiometer, it is obvious that it, or others of similar design, may readily be adapted to many other purposes involving the rapid measurement of small electromotive forces, particularly in the lower ranges where it is necessary to avoid errors arising from parasitic electromotive forces in the measurement circuit.

WASHINGTON, August 16, 1932.

THE DENSITY OF SOME SODA-LIME-SILICA GLASSES AS A FUNCTION OF THE COMPOSITION

By F. W. Glaze, J. C. Young, and A. N. Finn

ABSTRACT

Thirty-seven soda-silica and 22 soda-lime-silica glasses were made in platinum crucibles and the density and chemical composition of each glass were determined. From the data obtained equations were derived and a diagram was prepared showing the relations between density and composition of these glasses. Within the range of compositions considered, the diagram makes it possible to predict with considerable accuracy (1) the density of any glass from the composition and (2) the compositions of the various glasses having equal densities. Some evidence is presented indicating that the density of the soda-silica glasses is a simple function of certain soda-silica compounds which may be present in the glass.

CONTENTS

		Page
I.	Introduction	799
II.	The measurement of density	799
III.	Data obtained and results	801
IV.	Conclusions	805

I. INTRODUCTION

Studies of the relations between chemical composition and certain physical properties of glasses have received considerable attention in the past and a report on The Index of Refraction of Some Soda-Lime-Silica Glasses as a Function of the Composition, by C. A. Faick and A. N. Finn, was recently published.[1] In that report the purpose of this general study was given, the method of making the glasses was detailed, essential parts of the methods of chemical analysis were outlined, and the condition of annealing was described.

Since that report was published some additional glasses were made, and the present paper gives the results obtained with respect to density.

II. THE MEASUREMENT OF DENSITY

The samples prepared for the work on index of refraction were also used for density determinations and weighed approximately 20 g each. Since no samples were used that contained gaseous inclusions of sufficient magnitude to affect results, no corrections for "seeds" were necessary.

Density was determined by weighing the samples in air and then weighing them suspended in kerosene by means of a platinum wire basket which was connected with the balance beam by means of a single platinum wire. The suspending wire was covered with unbur-

[1] B. S. Jour. Research, vol. 6 (RP320), p. 993, June, 1931; also J. Am. Cer. Soc., vol. 14 (7), p. 518, 1931.

nished electroplated gold. The density of the kerosene was determined at first by means of a 25 ml pycnometer; later it was determined by means of a plummet whose volume was 35.0300 ml at 20° C. and whose weight (corrected for buoyancy of air) was 43.7584 g.

The density of the kerosene (average of 24 determinations) was 0.80870; the maximum change in density of the kerosene, based on observations extending over a period of 14 months, was 0.00028. Measured densities of kerosene were computed to the density at 20° C., using the coefficient 0.0007 per degree, which is sufficiently accurate if the temperature of observation does not differ from 20° C. by more than 5°. When the densities of a large number of glasses were determined during the same day, the density of the kerosene was determined before and after the other determinations; the maximum observed change in any one day, probably resulting largely from unavoidable temperature variations, was 0.00014; the average change was 0.00005.

The average variation in density observations, as determined from the results on six stable glasses, was 0.0003, but since some of the other glasses were decidedly hygroscopic, the reported values for the latter may be in error by as much as 0.001.

All weights were corrected for the buoyancy of air and results were computed to the density of water at 4° C. The data obtained are given in Table 1, as are also values computed by equation (3), differences between computed and observed values and temperatures at which the various glasses were annealed.

TABLE 1.—*Composition, observed and computed densities, and annealing temperatures used for 59 soda-lime-silica glasses*

Glass No.[1]	Composition			Density			Annealing temperature used
	SiO_2	Na_2O	CaO	Observed	Computed	Difference $\times 10^4$	
	Per cent	*Per cent*	*Per cent*				°C.
1	50.22	49.78		2.5656	2.5666	−10	430
2	50.51	49.49		2.5640	2.5654	−14	450
3	51.61	48.39		2.5607	2.5602	+5	440
4	52.60	47.40		2.5537	2.5555	−18	460
5	53.62	46.38		2.5515	2.5508	+7	450
6 (4)	54.14	45.86		2.5475	2.5484	−9	420
7	56.56	43.44		2.5383	2.5372	+11	450
8 (5)	57.45	42.55		2.5318	2.5330	−12	430
9	58.98	41.02		2.5266	2.5261	+5	460
10	59.69	40.31		2.5240	2.5226	+14	450
11	59.71	40.29		2.5228	2.5224	+4	470
12 (6)	59.97	40.03		2.5208	2.5210	−2	430
13	62.77	37.23		2.5071	2.5062	+9	470
14 (7)	62.86	37.14		2.5044	2.5058	−14	440
15 (8)	63.06	36.94		2.5038	2.5047	−9	440
16 (9)	65.30	34.70		2.4890	2.4930	−40	450
17 (10)	65.32	34.68		2.4924	2.4928	−4	480
18	66.52	33.48		2.4865	2.4862	+3	480
19 (11)	67.14	32.86		2.4807	2.4819	−12	500
20 (12)	69.65	30.35		2.4644	2.4650	−6	515
21 (13)	70.21	29.79		2.4612	2.4612	0	525
22 (14)	70.44	29.56		2.4603	2.4597	+6	525
23 (15)	72.15	27.85		2.4488	2.4483	+5	525
24	72.33	27.67		2.4479	2.4472	+7	500
25	74.16	25.84		2.4343	2.4351	−8	505

[1] Figures in parentheses are the numbers of the same glasses in the refractivity paper.

TABLE 1.—*Composition, observed and computed densities, and annealing temperatures used for 59 soda-lime-silica glasses*—Continued

Glass No.[1]	Composition			Density			Annealing temperature used
	SiO_2	Na_2O	CaO	Observed	Computed	Difference $\times 10^4$	
	Per cent	*Per cent*	*Per cent*				°C.
26	74.69	25.31		2.4305	2.4323	−18	505
27 (16)	75.29	24.71		2.4260	2.4264	−4	560
28	76.60	23.40		2.4140	2.4133	+7	510
29	76.65	23.35		2.4133	2.4128	+5	510
30	76.70	23.30		2.4126	2.4124	+2	550
31 (17)	77.85	22.15		2.4007	2.4011	−4	575
32 (18)	78.61	21.39		2.3938	2.3936	+2	575
33 (19)	79.73	20.27		2.3813	2.3829	−16	575
34	82.76	17.24		2.3545	2.3541	+4	550
35[2] (20)	82.86	17.14		2.3536	2.3531	+5	600
36	85.15	14.85		2.3307	2.3319	−12	540
37 (21)	86.41	13.59		2.3204	2.3203	+1	600
38[2]	100			2.2033	2.2026	+7	
39	50.18	37.80	12.02	2.6413	2.6400	+13	460
40	50.30	43.04	6.66	2.6076	2.6082	−6	450
41 (23)	54.37	32.85	12.78	2.6236	2.6232	+4	530
42 (24)	56.20	34.00	9.80	2.5976	2.5978	−2	480
43 (25)	56.76	34.48	5.76	2.5719	2.5718	+1	470
44 (26)	58.41	38.54	3.05	2.5474	2.5476	−2	480
45 (27)	60.32	24.50	15.18	2.6074	2.6068	+6	530
46 (28)	63.34	24.39	12.27	2.5757	2.5755	+2	525
47 (29)	64.14	21.22	14.64	2.5851	2.5845	+6	565
48 (30)	64.70	26.84	8.46	2.5460	2.5460	0	525
49 (31)	65.71	28.79	5.50	2.5229	2.5234	−5	520
50 (32)	66.47	21.74	11.79	2.5564	2.5555	+9	565
51 (33)	67.30	29.43	3.27	2.4998	2.5009	−11	520
52 (34)	67.98	22.50	9.52	2.5331	2.5333	−2	565
53 (35)	70.50	23.00	6.50	2.4980	2.4980	0	530
54 (36)	72.08	14.21	13.71	2.5276	2.5269	+7	580
55 (37)	72.61	24.24	3.15	2.4641	2.4640	+1	525
56 (38)	74.09	15.23	10.68	2.4935	2.4932	+3	545
57[2] (39)	74.69	12.28	13.03	2.4961	2.4964	−3	590
58 (40)	75.48	15.26	9.26	2.4734	2.4724	+10	590
59 (41)	78.77	16.33	4.90	2.4190	2.4184	+6	545
60 (42)	80.59	16.17	3.24	2.3886	2.3921	−35	565

[1] New analysis made since report on refractivity.
[2] This sample was not made at the Bureau of Standards, nor was it analyzed.

III. DATA OBTAINED AND RESULTS

If the densities of the soda-silica glasses are plotted against the silica or soda content of the glasses, an approximately smooth curve will be obtained for those glasses containing less than 80 per cent silica; the best equation derived to represent that portion of the curve was

$$D = 2.4756 + 0.00301B - \frac{2.988}{B-1} \qquad (1)$$

in which D is the density and B is the percentage of soda. This equation is not very satisfactory because of its limited range and also because it could not easily be adapted to glasses containing lime.

Since, in the paper on index of refraction, it was pointed out that more satisfactory results could be obtained by drawing straight lines between certain points on a composition-refractivity diagram for the soda-silica glasses, the same procedure was applied to the density

data. In this case the need for straight lines rather than a continuous curve again became evident, but the changes in slope of the straight lines drawn through the plotted data were not decidedly pronounced.

When, however, specific volumes (reciprocal of density) were plotted against silica, a very satisfactory series of straight lines could be drawn through the plotted data. (Fig. 1.) The intersections of these lines occurred at approximately 59.4, 66.3, and 74.9 per cent silica. These values correspond closely to three simple molecular ratios of soda to silica, namely, 4:6, 3:6, and 2:6. Of these the only

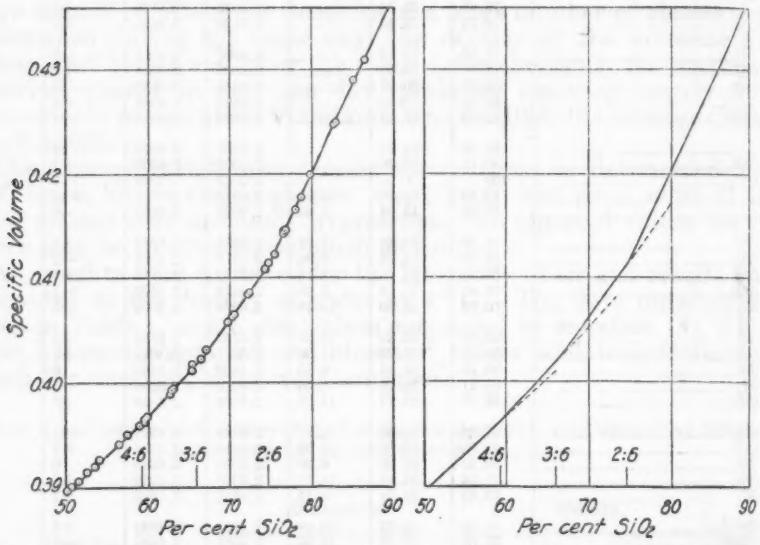

FIGURE 1.—*Diagram showing relation between composition and specific volume of some soda-silica glasses; three molecular ratios of soda to silica are also indicated*

All reported observations are plotted in the graph at the left and are omitted in the graph at the right; the lines in both these graphs are identical and the dotted extensions are added, in the right-hand graph, to emphasize the change in slope of the various sections

one obtained in a crystalline state is the 3:6 compound [2] (ordinarily written 1:2).

Equations of the form $\frac{1}{D}=a+bA$, in which A is the percentage of silica, can be used to express the four straight lines in Figure 1. Since such equations involve only one constituent of the binary glasses they could not be readily applied to more complex glasses; consequently the initial equations were converted, through the relation $A+B=100$, to the form

$$\frac{1}{D}=\alpha A+\beta B \qquad (2)$$

in which α and β are empirical constants having different values for the different ranges of composition, as shown in Table 2. A simul-

[2] Morey, G. W., and Bowen, N. L., The Binary System Sodium Metasilicate-silica, J. Phys. Chem., vol. 28, No. 11, pp. 1167–1179, 1924.

taneous solution of each adjacent pair of equations gives the indicated silica limits.

In general the data on the soda-lime glasses were treated as if the combined amount of soda and lime were all soda, and a value for $\frac{1}{D}$ for each glass was computed from equation (2), using appropriate constants. The differences between these computed values and the observed specific volumes were plotted as functions of the percentage of lime, C, and four equations of the form

$$f(C) = kC + \gamma' C^2$$

were obtained, k and γ' being empirical constants. Each of these equations, when added to its corresponding soda-silica equation, gives the completed form

$$\frac{1}{D} = \alpha A + \beta(B + C) + kC + \gamma C^2$$

or

$$\frac{1}{D} = \alpha A + \beta B + \gamma C + \gamma' C^2 \qquad (3)$$

in which A, B, and C represent the percentages of silica, soda and lime, respectively, and α, β, γ, and γ' are empirical constants having the values indicated in Table 2.

It is evident that this procedure assumes initially that the lines of demarcation (aa', bb', and cc', in fig 2) will lie along constant silica lines, but a simultaneous solution of each adjacent pair of equations (3) gives the following values of the silica limits for the glasses containing lime:

$$A_a = 59.4 - 0.23C + 0.032C^2 \text{ (indicated by } aa' \text{ in fig. 2)}$$

$$A_b = 66.3 + .15C - .004C^2 \text{ (indicated by } bb' \text{ in fig. 2)}$$

$$A_c = 74.9 - .017C^2 \text{ (indicated by } cc' \text{ in fig. 2)}$$

in which A_a, A_b, and A_c represent, respectively, the percentages of silica for the lines aa', bb', and cc'.

In arriving at the best values for γ and γ', therefore, it was necessary with some glasses near the limiting silica values to depart from the general procedure outlined by using an adjacent set of values of α and β in anticipation of the final positions of the lines of demarcation. The proper selection of the values of α and β could only be determined by trial. These curved lines are preferred to the straight lines indicated in the refractivity paper because density changes with composition are approximately seven times greater than corresponding refractivity changes, and, hence, give a better criterion of the location of these lines. Equation (3) and the constants in Table 2 were used in computing data to draw the lines of equal density shown in Figure 2 in which all the experimental glasses are indicated. As additional data are obtained, however, it may be necessary to make other changes in the location of these lines of demarcation.

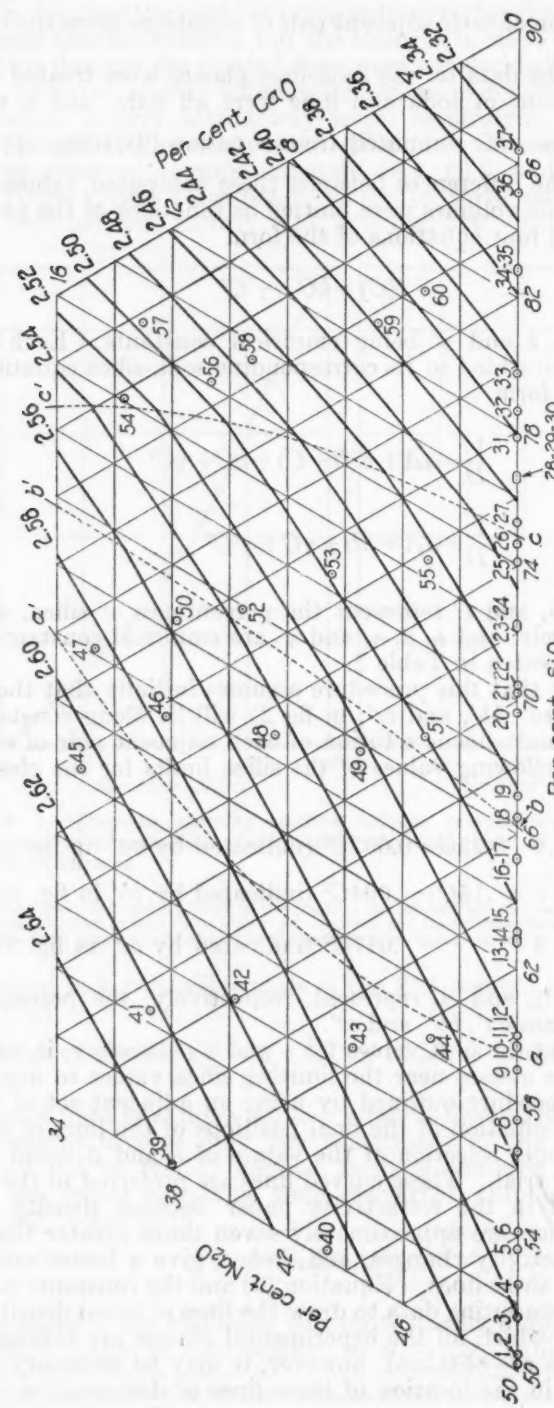

FIGURE 2.—*Diagram showing the relation between composition and density of some soda-lime-silica glasses*

TABLE 2.—*Silica limits and values of corresponding constants for equations (2) and (3)*

Silica limits, per cent silica	α	β	γ	γ'
50 (?) to A_a	0.0042520	0.0035370	0.002545	0.0000080
A_a to A_b	.0043028	.0034628	.002500	.0000040
A_b to A_c	.0043922	.0032872	.002285	.0000050
A_c to 100.0	.0045400	.0028460	.001844	.0000148

IV. CONCLUSION

Considering the data on the soda-silica glasses only (and disregarding the trend of specific volume changes in the soda-lime glasses), it is difficult to avoid the conclusion that the increment in specific volume of any of these glasses between the end members of the group (indicated in Table 2) in which that particular glass lies, is directly proportional to the increment in silica. In other words, the data suggest that the soda-silica glasses, in the range studied, should be regarded either as simple compounds or as simple mixtures of two adjacent compounds.

WASHINGTON, August 3, 1932.

145879—32——7

COILED FILAMENT RESISTANCE THERMOMETERS

By C. H. Meyers

ABSTRACT

Platinum resistance thermometers with strain free windings which are smaller than those previously used are described, and the method of construction is given. By double helical winding the coil of a 25 ohm thermometer is reduced to about 5 mm diameter and 2 cm length, and the outside diameter of the thermometer is about the same as that of the ordinary mercury-in-glass thermometer. These thermometers are hermetically sealed, and thermometric lag is reduced by filling them with helium.

CONTENTS

	Page
I. Introduction	807
II. Thermometer coil	807
III. Leads and thermometer head	810
IV. Characteristic properties of the thermometers	812
V. Acknowledgments	813

I. INTRODUCTION

In a previous paper, T. S. Sligh [1] has discussed the properties of platinum resistance thermometers in general, explained the method used for calculating temperatures, and described the construction of resistance thermometers ordinarily used at this bureau.

Strain-free thermometers with smaller dimensions have sometimes been found desirable for use in special apparatus, and to fill this need several such thermometers have been constructed. When these thermometers are mounted in a glass tube the over-all diameter is about 7 mm, or about the size of an ordinary mercury-in-glass thermometer. Since the length of the coil is only about 2 cm this design of resistance thermometer is suitable for any location where a mercury thermometer may be used.

A detailed description of this special design of thermometer coil and its construction will be given as well as a description of modifications in the design of leads and thermometer head.

II. THERMOMETER COIL

The design of the thermometer coil is illustrated in Figure 1, which is a photograph of a model built for illustrative purposes. In Figure 1, (*A*) shows this model mounted on the quartered mandrel upon which it was wound, and (*B*) shows the coil removed from the mandrel. The size of the actual thermometer coil is illustrated by the scale drawn in (*A*).

In the construction of the thermometer coil, the platinum winding was mounted upon a mica cross of the type mentioned in Sligh's

[1] B. S. Sci. Papers, vol. 17 (S407), p. 49, 1922.

paper. The various steps in the construction of this cross and the coil are given in Figure 2. The dimensions given are those actually used and are given in millimeters unless otherwise stated in the figure.

Mica was cut into strips by clamping the part to be used under a bar of the proper width and trimming away the portions extending on each side by a repeated back and forth motion of a sharp-edged steel tool. As mentioned in the paper already referred to, a thin safety-razor blade forms a convenient source of material for such a

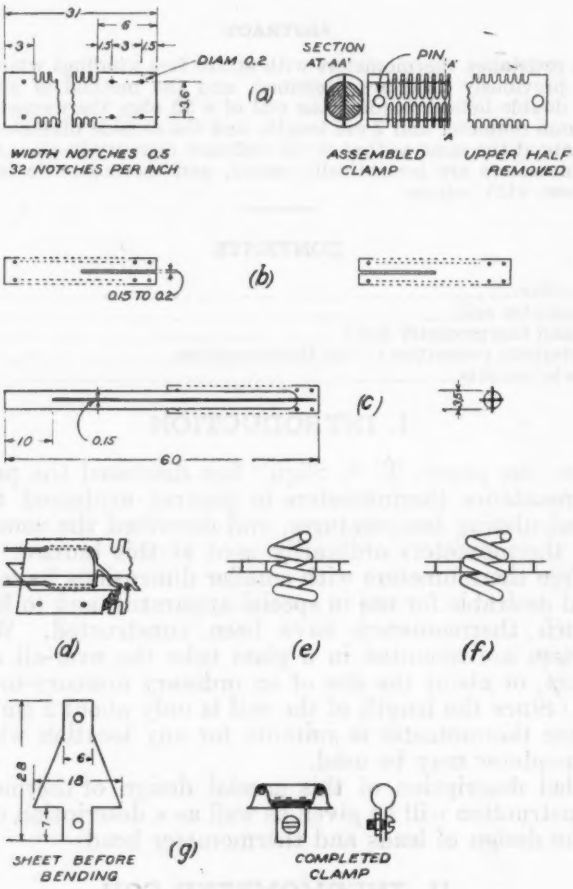

FIGURE 2.—*Construction of thermometer coil*

tool. The mica strip may be split to the desired thickness (about 0.1 mm), or teeth may cut in the strip before splitting. For cutting the teeth the mica was placed in a toothed clamp, such as shown to the right in Figure 2 (*a*), the halves of which were kept in alignment by pins. This clamp was gripped between vise jaws. Teeth were cut in the mica with a special saw consisting of 0.5 mm steel wire mounted upon a light jeweler's hack-saw frame. The saw cut equally well when the wire was charged with carborundum by rolling between two plates of glass or when the wire was merely roughened by rub-

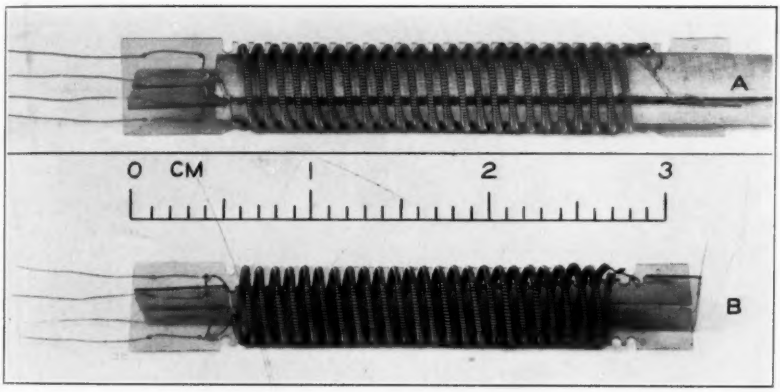

FIGURE 1.—*Large model of thermometer coil*

A, Mounted upon mandrel; B, removed from mandrel.

UNIV. OF MICH.

bing transversely with a carborundum stone. This saw produced a smooth-edged notch with parallel sides and a rounded bottom. Both steel piano wire and nickel wire have been used successfully in cutting notches from 0.1 to 0.5 mm wide. Copper wire was not found as satisfactory on account of excessive stretching of the wire. After the mica had been notched it was removed from the clamp, and the six holes shown in Figure 2 (*b*) were drilled. Piano wire was ground to form a flat drill for this purpose. The slots shown were cut and the slotted pieces of mica were pushed together to form a cross in which the teeth were arranged to accommodate a bifilar winding of uniform pitch. This cross was inserted in the quartered steel mandrel illustrated in Figure 2 (*c*).

Platinum wire nominally 0.1 mm in diameter was used in these thermometers, and the length of wire required was 1.8 to 2.4 m, depending upon the actual diameter of the lot of wire used. The requisite amount of wire was cut into two pieces, each of which was wound into a helix with an outer diameter of about 0.45 mm. For this purpose a steel wire (0.23 mm diameter) was used as a mandrel, one end being mounted in a lathe and the other end attached to a ball bearing, an arrangement which permitted fairly uniform rotation of the taut steel wire. When hard-drawn platinum wire was available the following procedure was successful: One end of the wire was attached to the mandrel and the other end to a thread which led over a pulley to a weight of about 30 g. The pulley was placed in such position relative to the lathe that the consecutive turns of the helix were wound in contact; it was far enough from the lathe (about 3 m) so that the angle of winding remained substantially constant. When the winding was completed both ends of the helix were released and one end was kept from rotating while the lathe was rotated in such direction as would tend to unwind the helix until the other end began to slip on the mandrel. The mandrel was then removed from the lathe, its end freed from any roughness which might scratch the platinum wire and the helix pushed off. The helix was then stretched until its length under no tension was approximately doubled, the result being an almost uniform spacing of the wire.

The method just described was not successful for annealed platinum wire. When the use of such wire was necessary, it was either wound along with a spacing wire so that the turns were in contact and the spacing wire later unwound, or the platinum wire was fed from the moving tool carriage of a thread-cutting lathe. For the latter method a lathe with two heads geared together is desirable since the irregularities in the motion of the ball bearing cause irreugular spacing of the wire. After winding, the mandrel was dissolved in hot hydrochloric acid.

Short leads of platinum were welded to form a T on one end of each of the two helices. A small oxy-gas flame was used in the present work, although the arc method described by Sligh might have been used with due precaution to arrange the work so that the electric current would not anneal the helix. It was found that the helices stretched less during winding and that the coil suffered less from accidental distortions if the wire was not annealed until the winding upon the mica cross was completed. Both pairs of leads were then threaded into the mica cross as shown for one pair in Figure 2 (*d*).

The choice of the direction of winding upon the cross was determined by the direction of winding of the helices which had been wound with a left-hand pitch. Figure 2 (*e*) and (*f*) show a magnified view of the edge of the mica with such a helix crossing it. The direction of winding upon the cross corresponding to that at (*e*); that is, a winding with a right-hand pitch was chosen as the one in which two consecutive turns of the helix would be less likely to straddle the mica. The helices were wound upon the cross under the tension caused by a weight of 2 or 3 g attached to each of their free ends. The clamp of thin sheet copper designed as shown in Figure 2 (*g*) for both right and left hand windings, was slipped over the coil to hold the winding in place while the ends of the helices were joined to the platinum tie wire visible in Figure 1, and tied to the mica. After removing the clamp and the quartered mandrel from the coil, the latter was annealed in an electric furnace for two or three hours at 600° to 650° C.

During this annealing the resistance of the 25 ohm thermometers decreased about 0.5 ohm, an amount which had to be allowed for in choosing the initial length of wire.

After the preliminary annealing the resistance of the coil was adjusted by cutting out the proper amount of wire and rewelding, the mandrel and clamp being replaced during the operation. The coil was then again annealed at the same temperature for about five hours.

III. LEADS AND THERMOMETER HEAD

As in the thermometers described by Sligh, mica disks served the double purpose of separating the internal leads and breaking up convection currents in the stem of the thermometer. The mica disks were cut with a punch and die of the type ordinarily used for blanking and perforating sheet metal. An attempt to use Sligh's method of keeping the mica disks normal to the axis of the thermometer by staggering the holes through which the leads were threaded was unsuccessful for the small size of washers used.

Better results were obtained by tapering the wire so that disks with holes which fitted the wire snugly could be used. Although tapering the full length of the leads gave the best appearing result, it was found that with care the mica disks could be slid along the uniform wires without serious enlargement of the holes, and that part or all of the tapered portion could be discarded. Gold wire 0.2 mm diameter was tapered in hot acqua regia by moving the wire up and down thus varying the time of immersion along the length of the wire. The holes in the disks used with these leads were made with drills formed from 0.16-mm steel wire. A pile of the disks was placed in the jig illustrated in Figure 3 (*a*) and four equally spaced holes were drilled. The insertion of a piece of the wire used for drills in one hole before removal of the disks from the jig made it possible to thread the whole pile of disks onto the ends of the leads as a unit. After the requisite number of disks had been threaded on, the leads were put under tension and each disk slid singly into the desired position, the spacing used being about 5 to 10 mm. A short copper wire was silver soldered or welded to one end of each of the gold leads for convenience in later sealing the thermometer head with soft solder, and one of the short platinum leads on the thermometer coils was welded to the other end.

Since some of these thermometers were to be used in an inverted position and would probably come in contact with oil, it was desirable to avoid the use of cement or wax for sealing. The method of bringing the internal leads out through the Pyrex tube is shown in Figure 3 (*b*). Four platinum disks 0.02 or 0.03 mm thick were beveled at the edge

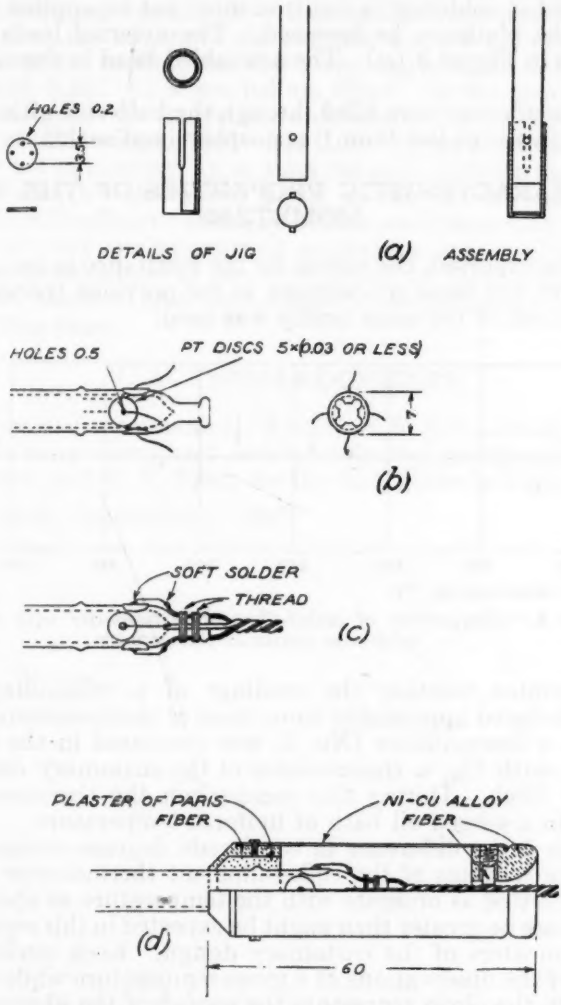

FIGURE 3.—*Construction of leads and head*

by running through rolls and curled to fit the glass tube. These were temporarily held in place by a clamp of nichrome wire and fused to the glass as described by Housekeeper.[2] It was found that the formation of bubbles under the platinum could be minimized by keeping the work far out in the flame. The addition of some oxygen to the air supplied to the torch was also found advantageous for Pyrex. Holes

[2] J. Am. Inst. Elect. Eng., vol. 42, p. 954, 1923.

through the platinum and glass were made at the centers of the disks with a hot tungsten wire. Benton [3] used a hot platinum wire for perforating glass, but tungsten has the advantage of being stiffer and forming an oxide which does not readily stick to the glass.

The short copper wires at the end of the gold leads were threaded through the holes, which were then closed with soft solder. Caution must be used in soldering; a hot iron must not be applied to the cold glass lest the platinum be loosened. The external leads were then attached as in Figure 3 (*c*). The assembled head is shown in Figure 3 (*d*).

The thermometers were filled through the bulb end with dry helium at various pressures less than 1 atmosphere and sealed.

IV. CHARACTERISTIC PROPERTIES OF THE THERMOMETERS

As is to be expected, the values for the resistance in ice, steam, and sulphur have the same proportions as for previous thermometers in which platinum of the same purity was used.

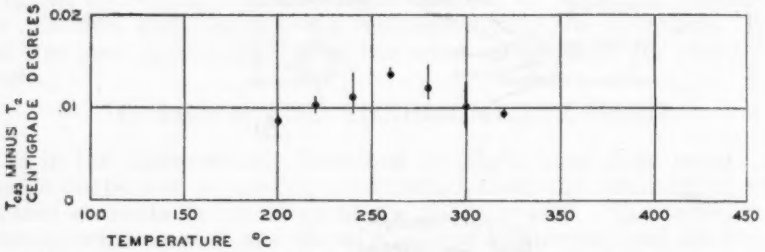

FIGURE 4.—*Comparison of coiled-filament thermometer with ordinary platinum resistance thermometer*

To determine whether the readings of a coiled-filament thermometer deviated appreciably from those of thermometers previously used, such a thermometer (No. 2) was compared in the range 200° to 320° C. with C_{23}, a thermometer of the customary design as described by Sligh. During this comparison the thermometers were immersed in a stirred oil bath of uniform temperature.

In Figure 4 the difference in centigrade degrees obtained by subtracting the readings of the coiled-filament thermometer from those of C_{23} are plotted as ordinate with the temperature as abscissa. The differences are no greater than might be expected in this region between two thermometers of the customary design. Each circle represents the mean of the observations at a given temperature while the vertical line through the circle represents the spread of the observations. A curve of differences should by definition pass through zero at 100° and at 444° C., but experimental errors in calibration, especially at the latter point, probably introduce considerable differences on the scale chosen in Figure 4, hence no attempt has been made to draw such a curve. It may be concluded that the coiled-filament winding introduces no appreciable peculiarity in the readings of the thermometer.

Since winding the wire in a helix reduces the effective area for heat

[3] J. Ind. Eng. Chem., vol. 11, p. 623, 1919

transfer between the thermometer and its surroundings, it is to be expected that the thermometric lag will be thereby increased, as well as the temperature difference between the thermometer coil and its surroundings necessary to dissipate the heat generated by the measuring electric current.

Measurements of the apparent resistance in an ice bath for several values of measuring current show that this temperature difference is proportional to the square of the current, and for 1.5 ma through a 25 ohm coil 5 mm in diameter and 2 cm long is about 0.004°C. when air filled and 0.001° C. when helium filled. In the paper by Sligh already mentioned the temperature difference for the larger type of thermometer filled with air is given as 0.001° C. for a current of 1.5 ma.

With the use of currents up to 5 ma the ratio between this temperature difference and the power input in the thermometer may be determined with sufficient accuracy so that variations with time in this ratio may be used as a measure of air leakage into the thermometer tube. One thermometer of the type described filled with helium at about 40 mm absolute pressure has shown no appreciable leakage over a period of two years.

V. ACKNOWLEDGMENTS

The author wishes to thank H. F. Stimson, F. R. Caldwell, and others for valuable suggestions and assistance in the construction of these thermometers, and E. F. Fiock for the data given in Figure 4.

WASHINGTON, September 1, 1932.

RP509

DEFLECTION OF COSMIC RAYS BY A MAGNETIC FIELD

By L. F. Curtiss

ABSTRACT

A continuation of earlier experiments on this subject (Phys. Rev., vol. 34, p. 1931, 1929; vol. 35, p, 1433, 1930), gives decisive evidence that a considerable fraction of an unfiltered cosmic-ray beam can be deviated by a magnetic field of 7,000 gauss. Using four Geiger-Müller tube counters, coincidences were observed with and without a magnetic field. The arrangement was such that electrons in the beam, possessing energies corresponding to 10^9 volts or less, could be prevented from producing coincidences. Observations were made for a total of 615 hours without the field and 508 hours with the field, in alternating periods of about 48 hours. The average number of coincidences without the magnetic field was found to be 1.31 ± 0.09 per hour and with the magnetic field 0.88 ± 0.14 per hour. This indicates that, for approximately 70 per cent of the cosmic-ray particles, the deviation is less than that for 10^9 volt electrons. This harder portion of the beam may contain, in addition to electrons of higher energy than 10^9 electron volts, protons of 5×10^8 electron volts and neutrons. These data indicate that the results obtained by Rossi (Nature, vol. 128, p. 300; 1931) and of Motth-Smith (Phys. Rev., vol. 37, p. 1001; 1931), showing no effect of the magnetic field, were affected by scattering or absorption in the iron core in which the magnetic field was produced.

CONTENTS

		Page
I.	Introduction	815
II.	Experimental arrangement	816
III.	Observations	819
IV.	Discussion	821
V.	Acknowledgments	823

I. INTRODUCTION

In a letter[1] to the Physical Review for November, 1929, a report was made of experiments with Geiger-Müller tube counters which seemed to show that cosmic rays consisted, in part at least, of electrically charged particles which could be deflected by a magnetic field. These observations were made with a pair of tube counters, the coincidences between which were observed by making simultaneous records on a paper tape with dotting pens actuated by the counters through amplifiers. Although qualitatively there was indication of a decrease on applying a magnetic field between the counters, the method was too crude to serve as a basis for a definite decision of the point in question.

The experiments were, therefore, repeated, using the vacuum tube circuit developed by Bothe[2] for resolving coincidences electrically and following the suggestion by Tuve[3] of using more than two counters so that a more sharply defined beam of cosmic rays may be studied.

[1] Phys. Rev., vol. 34, p. 1391, 1929.
[2] W. Bothe, ZS. f. Phys., vol. 59, p. 1, 1929.
[3] M. Tuve, Phys. Rev., vol. 35, p. 651, 1930.

These experiments were made with three counters, the results of which were reported to the Physical Society [4] in April, 1930. These data also pointed to a magnetic deviation of a part of the cosmic-ray beam. A decrease of the order of 25 per cent in coincidence was observed on applying a magnetic field of 7,000 gauss to the path of the rays between two of the counters. These observations were made with considerable difficulty. The counters were necessarily of a small size, since they could be no longer than the air gap of the electromagnet (5 cm). This reduced the sensitivity of the arrangement, requiring, therefore, long periods of observation. Much trouble was also encountered with the Bothe screen grid vacuum tube circuit as modified for use with three counters. An even more serious source of trouble and possible error was discovered when it was noticed that the counters themselves are very considerably affected by changes of temperature. Sealed counters, described elsewhere,[5] were used for these experiments. The rate of counting at a given voltage falls off rapidly as the temperature is increased. Some counters have been found to cease counting entirely when their temperature is raised 10° or 15°. This effect has not been investigated, but it is presumably caused by the increase of vapor pressure of nonpermanent gases and more volatile substances present in the partially exhausted counters. It could easily falsify observations made with the magnetic field, since the temperature of the windings of the electromagnet rises considerably during the prolonged periods of observations, causing the temperature of some of the counters to rise also.

Another disturbing condition in the former experiments was the presence in the building of several grams of radium which, although stored at some distance in a safe with lead walls 6 inches thick, nevertheless increased the rate of counting. This penetrating radiation could not be screened off readily and was responsible for a large number of accidental coincidences, these being proportional to the rate of counting of each counter.

Interest in the question of the magnetic deviation of cosmic rays was increased by the reports made by Rossi [6] and by Mott-Smith [7] that no deflection was observed when cosmic ray beams pass through magnetized iron. It is of importance to make certain of the earlier results. Therefore the investigation has been continued under improved conditions designed to eliminate as far as possible difficulties and sources of error encountered in the earlier experiments. This paper gives an account of the results which have been obtained.

II. EXPERIMENTAL ARRANGEMENT

The most annoying difficulties encountered in the previous experiments arose from the presence of a relatively large number of accidental coincidences and from changes in counting rate due to temperature changes. Particular attention was given to the elimination of these disturbances.

Considerable reduction in the number of accidental coincidences was effected by the removal of the apparatus from the building in which

[4] Phys. Rev., vol. 35, p. 1433, 1930.
[5] B. S. Jour. Research, vol. 4 (RP 165), p. 593, 1930.
[6] B. Rossi, Nature, vol. 128, p. 300, 1931.
[7] L. M. Mott-Smith, Phys. Rev., vol. 37, p. 1001, 1931.

radium is stored. Since the accidentals are proportional to the product of the rate of the individual counters, the importance of this change, which reduces simultaneously the rate of all counters, is obvious. It seemed desirable, however, to reduce these accidentals even further, in view of the long periods covered by the observations. At most, only a few genuine coincidences per hour could be expected so that it was desirable to reduce as far as possible the probability of any accidental coincidences.

The most effective method of reducing accidentals is to increase the number of counters. Accordingly a fourth counter, added to the previous arrangement, had the desired effect of reducing the accidental coincidences practically to zero. The advanatge of additional counters can best be shown by computing the accidentals for the case of two and four counters under otherwise similar conditions. For two counters the expected number, E, of accidentals is given by

$$E = 2\ N_1\ N_2\ \tau$$

where N_1 is the average rate of counting of the first counter, N_2 the rate for the second, and τ is the "resolving power" of the apparatus used to detect coincidences. Putting $N_1 = N_2 = 30$ per minute and $\tau = 10^{-3}$ sec., E becomes 1.7 per hour. For the case of four counters

$$E = 2^3\ N_1\ N_2\ N_2\ N_4\ \tau^3$$

Putting $N_1 = N_2 = N_3 = N_4 = 30$ per minute and $\tau = 10^{-3}$ sec., E drops in this case to 1 coincidence in about 70 years. Consequently it is safe to assume in general that a circuit using four counters only responds to the passage of an ionizing particle through all four counters. A possible exception will be mentioned in the discussion of the results.

The vacuum tube circuit devised by Rossi [8] was adopted, since it is simpler and easier to operate when extended to four counters than any other arrangement which has been tried. The details of the circuit are shown in Figure 1. The output was connected to a telegraph relay which actuated electrically a dial counter. Switches were arranged to shunt out any three counters by applying a negative voltage to the grids of the three vacuum tubes connected with these counters. In this way the rate of counting of the fourth alone could be observed directly, making possible a frequent check of the rate and sensitivity of each counter.

To eliminate errors arising from changes in temperature each counter was inclosed in a thermally insulated box containing a heating coil and thermostat capable of maintaining the temperature constant to within a few tenths of a degree. The electromagnet and counters were also inclosed so that their temperature could be kept uniform by rapid circulation of the air by means of an electric fan. A small radium preparation inclosed in lead was used to test the sensitivity to penetrating γ-rays.

The geometrical arrangement of the counters with respect to the poles of the electromagnet is shown in Figure 2, which is drawn to scale. The air gap between the poles, 5 cm long, determined the useful length of the counters. Observations were made with a magnetic

[8] B. Rossi, Nature, vol. 125, p. 136, 1930.

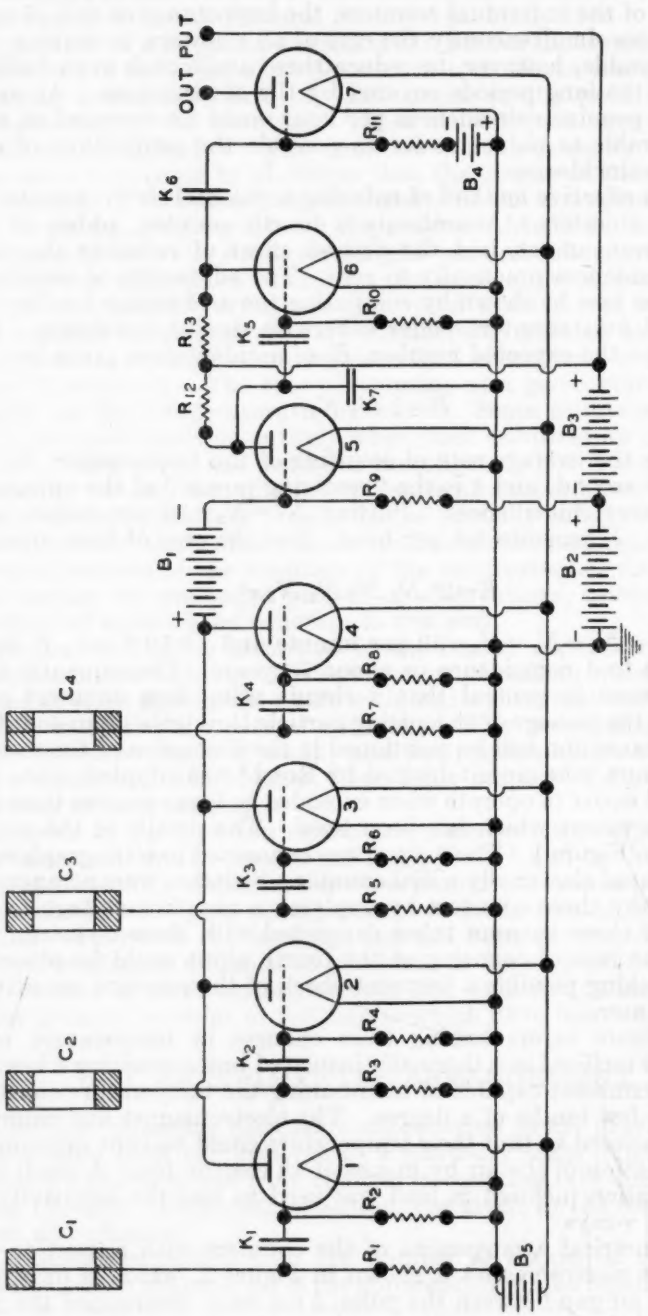

FIGURE 1.—*Wiring diagram of Rossi coincidence circuit for four counters*

C_1, C_2, C_3, C_4=Geiger-Müller tube counters. K_1, K_2, K_3, K_4=0.00005 μf condensers. K_5, K_6=0.1 μf condenser. K_7=0.5 μf condenser. R_1, R_2, R_3, R_4=10^8 ohms. R_5, R_6, R_7, R_8=5×10^8 ohms. R_9, R_{10}, R_{11}=10^9 ohms. R_{12}, R_{13}=0.25×10^9 ohms. B_1=16 volts, B_2=6 volts, B_3=90 volts.

field in the air gap of 7,000 gauss, determined from a calibration curve. As indicated by the dotted lines across the end view of the pole face, a beam of 10^9 volt electrons would, with this arrangement, be deviated just sufficiently to miss the lower counter.

The experiments were carried out under a thin wooden roof with no other filtering, so that the softer components of the cosmic radiation are included in the observations. Since the walls of the counters were of steel, approximately 1 mm thick, and a particle to produce one coincidence would have to traverse 7 mm of steel, beta-radiation of radioactive origin could produce very few systematic coincidences.

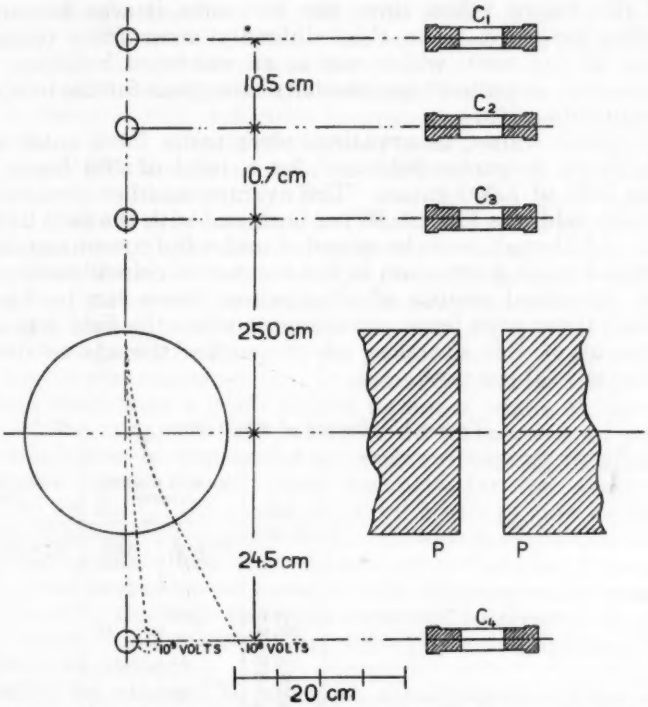

FIGURE 2.—*Plan of arrangement of counters with respect to poles of electromagnet*

C_1, C_2, C_3, C_4=Geiger-Müller tube counters. PP=poles of electromagnet.

Actual observations were preceded by a careful study of the operating characteristics of each counter, making it possible to select for each an operating temperature such that all four could be run at the same voltage. A small 110-volt alternating-current generator driven by a synchronous motor, having its output stepped up by a transformer to about 1,100 volts, supplied this voltage. All parts of this circuit were inclosed and kept at a constant temperature.

III. OBSERVATIONS

The experiments were undertaken primarily to determine whether or not cosmic-ray particles could be deflected by a magnetic field. Accordingly, the procedure adopted in taking observations was to

record the number of coincidences for several hours in the absence of the magnetic field and then to take a similar record with the field applied. This method does not permit a study of the direction of deflections to determine the sign of the charge carried by the particles. The small size of the counters made long periods of observation necessary so that it was decided to settle first, if possible, the question of the existence of a deflection.

A summary of observations is given in the following table. Although in some cases uninterrupted series of observations of a week or more were possible, interruptions frequently occurred. A failure of any part of the complicated arrangements was cause for the rejection of the record taken since the last time it was known to be functioning properly. The chief difficulty arose from temperature variations of the room which was in an unheated building. These variations were sometimes too sudden or too great for the temperature controls to cope with.

As the table shows, observations were made for a total of 636.5 hours with no magnetic field and for a total of 508 hours with a magnetic field of 7,000 gauss. The average number of coincidences without the field was 1.31 ± 0.09 per hour and with the field 0.88 ± 0.14 per hour. Although, as to be expected under the circumstances, there was a considerable fluctuation in the number of coincidences per hour between individual periods of observation, there can be very little doubt that there were fewer coincidences when the field was applied. The amount of this decrease, as shown by the above data, was approximately 30 per cent.

TABLE 1.—*Record of observations*

Dates	Duration (hours)	Number of coincidences—		Coincidences per hour—	
		Without field	With field	Without field	With field
June 23–25	48.75	107		2.19	
June 25–29	100.00		141		1.41
July 5–6	20.00	14		.70	
July 7–8	23.75		7		.30
July 15–16	24.00	45		1.87	
July 16–18	45.25		37		.82
July 18–21	71.25	71		1.00	
July 21–23	45.50		104		2.29
July 23–25	50.25	79		1.57	
July 26–28	41.75		24		.56
July 28–Aug. 1	95.25	117		1.23	
Aug. 1–4	70.50		62		.88
Aug. 5–8	72.00	105		1.46	
Aug. 9–11	41.50		32		.77
Aug. 12–13	27.50	36		1.31	
Aug. 13–17	92.50		48		.52
Aug. 17–20	72.75	64		.88	
Aug. 20–22	47.25		19		.40
Aug. 25–26	23.75	15		.63	
Aug. 26–27	25.25	42		1.66	
Sept. 2–6	95.75	113		1.18	
Average number of coincidences per hour				1.31 ± 0.09	0.88 ± 0.14

IV. DISCUSSION

Although the figures given represent only a preliminary approach to the study of the magnetic deviation of cosmic-ray particles, certain conclusions concerning the energy and character of the cosmic-ray particles can be drawn from them. Referring to Figure 2, it is seen that a beam of electrified particles consisting of electrons of energy greater than 10^9 electron volts or protons of energy greater than 5×10^8 electron volts will be detected in the undeflected beam when the magnetic field is applied. This represents 70 per cent of the cosmic rays according to the figures given above. If these undeflected particles have no charge, these experiments reveal nothing concerning their energy. The results could then be explained quite simply by assuming that the primary cosmic-ray beam consists of neutrons. One of the characteristics of the neutron, known at present, is its ability to transmit high velocities to protons and, to a lesser extent, to electrons. Thus, a beam of neutrons penetrating our atmosphere should be accompanied by protons and electrons with high velocities. From the results obtained by Dee [9] and by Feather,[10] one would expect the protons to predominate. Thus, if it could be shown that, of the 30 per cent of the beam that shows a deflection, the protons greatly exceed the electrons in number, it could be taken as an indication of the existence of neutrons in the cosmic-ray beam. A more direct attack would be to determine the loss of particles for various strengths of magnetic fields up to the values greatly in excess of that used in the present experiments. It seems reasonable to suppose that under such conditions a point should be found where an increase of strength of the magnetic field produced no further loss of particles. The deviability to be expected for a neutron moving in a magnetic field depends upon the structure assumed for the neutron. As pointed out by Huff,[11] the model proposed by Pauli may be deflected in a nonhomogeneous magnetic field. However, this deflection is of observable magnitude only when the neutron is traveling at low speeds when it would probably not ionize at all. Consequently, a beam of neutrons, having the high velocities necessary to account for cosmic-ray phenomena, could not be distinguished by a magnetic experiment from a beam of photons.

In making an attempt to interpret the apparent existence of an undeflected beam of cosmic rays amounting to approximately 70 per cent of the total radiation, the possibility of psuedo coincidences must be considered. Such coincidences are caused by the simultaneous ejection of several secondary particles by a single cosmic ray in such a way that separate secondary particles traverse different counters at the same time. Such an effect has been demonstrated experimentally by Rossi [12] and by Johnson and Street.[13] If an appreciable number of the coincidences observed in the present experiments were produced in this way, it would be difficult to arrive at any satisfactory interpretation of the results obtained. It is easy to see in a general way that this could not be true, since the effect is only readily detectable when masses of absorbing material of high atomic number (that is,

[9] P. I. Dee, Proc. Roy. Soc., vol. 136, p. 727, 1932.
[10] N. Feather, Proc. Roy. Soc., vol. 136, p. 709, 1932.
[11] Huff, L. D., Phys. Rev., vol. 38, p. 2292, 1932.
[12] Rossi, B., Phys. ZS, vol. 33, p. 304, 1932.
[13] Johnson, T. H., and Street, J. C., Phys. Rev., vol. 40, p. 638, 1932.

lead) are placed slightly above and in the immediate neighborhood of the counters. The secondary particles which cause the pseudo coincidences are projected mainly in the direction of the primary radiation which has its maximum of intensity in the vertical direction. In the present experiments the only large mass of heavy material, the iron of the electromagnet, was below all except one of the counters. There was no absorbing material of high atomic number above the counters. Nevertheless it is important to make certain of this by an experimental determination of the probable number of coincidences which might be caused by this effect. Observations extending over several weeks were made in which one of the counters was placed entirely out of line from the others but near to its original position. The average number of coincidences under these conditions was found to be 0.15 per hour. Although representing about 10 per cent of the total number of coincidences observed with no magnetic field, this figure is but slightly greater than the experimental error. Thus it seems that the effect under discussion presumably did not contribute appreciably to the coincidences observed when all four counters were in line.

The fact that a large proportion of the cosmic rays appear to be less deviable than 10^9-volt electrons seems to offer, when considered in connection with the suggestion made by Johnson,[14] and explanation for the failure of Rossi,[15] and of Mott-Smith [16] to obtain evidence of a deflection when allowing the cosmic rays to pass through magnetized iron. The results given above show that only the softer 30 per cent of the cosmic rays could be expected to show an effect. This is the portion of the beam most easily absorbed or scattered. The scattering of particles in this portion of the beam may be sufficient, when passing through several centimeters of iron, to prevent any of these particles from producing a systematic coincidence.

It is of interest to compare the results obtained here with some of the more recent investigations which offer a basis of comparsion. The remarkable photographs obtained by Anderson [17] of cosmic ray particles in a Wilson chamber, in the presence of a magnetic field, exhibit particles showing a wide range of magnetic deviations. From the analysis of these photographs which he gives it is seen that of a total of 64 observed particles, 58 have energies over 10×10^6 electron volts and could be expected to produce coincidences through 7 mm of steel. Only 13 of these 58 particles have energies greater than 400×10^6 electron volts and might, therefore, be considered to form a part of the undeflected beam in the present experiments. These particles are of the energy range where accurate measurements of the Wilson photographs are difficult and, therefore, there may be considerable error in this estimate. On this basis only about 25 per cent of the cosmic-ray beam should have been undeflected in the present experiments as opposed to about 70 per cent observed. Even allowing for the low precision of the observations of coincidences, this discrepancy appears to be genuine, and points to the existence of high-energy cosmic-ray particles of an ionizing power sufficient to actuate a tube counter but difficult to distinguish in a Wilson photograph. This assumption is also supported to some extent by the experiments of

[14] Johnson, T. H., Phys. Rev., vol. 40, p. 468, 1932.
[15] See footnote 6, p. 816.
[16] See footnote 7, p. 816.
[17] Anderson, C. D., Phys. Rev., vol. 41, p. 405, 1932.

Johnson, Fleisher, and Street,[18] in which Wilson photographs were taken only when coincidences occurred between the two tube counters. Although, in the absence of exact information regarding geometrical arrangements and number of possible accidental coincidences, no definite conclusion can be drawn, it is significant that a considerable number of photographs showed no tracks.

V. ACKNOWLEDGMENTS

The writer wishes to thank B. W. Brown and L. L. Stockman for help in constructing the apparatus and recording the observations. He is also indebted to Dr. A. V. Astin for helpful discussions of various phases of the experiment.

WASHINGTON, October 12, 1932.

[18] Johnson, T. H., Fleisher, W., and Street, J. C., Phys. Rev. vol. 40, p. 1048, 1932.

RP510

THE SYSTEM: CaO–B_2O_3

By Elmer T. Carlson

ABSTRACT

The phase equilibrium diagram for the system CaO-B_2O_3 has been partially worked out by means of heating curves. Completion of the diagram was impossible because the melting point of B_2O_3 could not be determined, while that of CaO was beyond the range of the apparatus. The following compounds were identified and their optical properties determined with the petrographic microscope: $CaO \cdot 2B_2O_3$, melting at $986° \pm 5°$ C.; $CaO \cdot B_2O_3$, melting at $1{,}154° \pm 5°$ C.; $2CaO \cdot B_2O_3$, melting at $1{,}298° \pm 5°$ C.; and $3CaO \cdot B_2O_3$, melting at $1{,}479° \pm 5°$ C. Mixtures containing less than 23 per cent CaO were found to separate, on fusion, into two liquid layers, one of which contained 23 per cent CaO, while the other was nearly pure B_2O_3. This immiscibility region extended above 1,500° C.

CONTENTS

	Page
I. Introduction	825
II. Experimental work	826
1. Preparation of mixtures	826
2. Analysis of mixtures	827
3. Experimental procedure	827
4. Interpretation of heating curves	828
III. Results	829
1. Binary compounds	829
2. The phase-equilibrium diagram	829
IV. Summary	832

I. INTRODUCTION

The study of this system was undertaken as a preliminary to a study of part of the ternary system, CaO-B_2O_3-SiO_2, the purpose of the latter being to determine the effect of the addition of small amounts of B_2O_3 to the calcium silicates found in Portland cement. It is hoped, however, that the results of the investigation of the binary system, CaO-B_2O_3, may also prove of interest in connection with the production of glazes and other ceramic materials.

Very little work has been done on the anhydrous calcium borates in recent years, and much of the earlier data is conflicting or inconclusive. The first comprehensive study of the system CaO-B_2O_3 was made by W. Guertler,[1] who constructed the liquidus diagram through the use of cooling curves. He found maxima at 1,030°,[2] 1,095°, and 1,225°, corresponding to the compounds $CaO \cdot 2B_2O_3$, $CaO \cdot B_2O_3$, and $2CaO \cdot B_2O_3$, respectively. Due to the limitations of his apparatus, he was unable to go much beyond the last of these, although he argued from analogy with the system BaO-B_2O_3 that the compound $3CaO \cdot B_2O_3$ should exist. Due to the excessive super-

[1] Guertler, On the Melting Points of Mixtures of the Alkaline Earths with Boric Anhydride, Z. anorg. Chem., vol. 40, pp. 337–354, 1904.

[2] All temperatures given in °C. unless otherwise stated.

cooling which occurs in this system, the accuracy of his results is somewhat doubtful.

The four borates mentioned have since been prepared by R. Griveau,[3] who also studied their heats of formation. He gives the values 1,025°, 1,100°, and 1,215° as the approximate melting points of the compounds $CaO \cdot 2B_2O_3$, $CaO \cdot B_2O_3$, and $2CaO \cdot B_2O_3$, respectively. Roberts [4] reported a melting point of 1,304° for $2CaO \cdot B_2O_3$. Optical properties for the metaborate, $CaO \cdot B_2O_3$, are given by A. N. Winchell.[5]

Burgess and Holt [6] reported that CaO is insoluble in B_2O_3 in small quantities, but if present in larger amounts the mixture fuses to a clear glass. Guertler [7] found that a fused mixture of B_2O_3 and a small amount of CaO separated into two liquid layers which were immiscible even at 1,400°.

The melting point of pure CaO was placed at 2,572° by Kanolt,[8] and at 2,849° K. (2,576° C.) by Schumacher.[9] The melting point of boric oxide is unknown, as this compound has never been obtained in crystalline form.

Because of the absence of optical data for most of the calcium borates, as well as the conflicting nature of the melting-point data, it seemed desirable to make a study of the system CaO-B_2O_3, tracing the liquidus as far as possible and determining the optical properties of the various phases appearing in the system.

The general plan followed was to prepare mixtures of CaO and B_2O_3 in varying proportions and to determine their melting points by means of heating curves. The phases existing in equilibrium with the melt at the liquidus were identified by petrographic examination of samples quenched from various temperatures near the liquidus.

II. EXPERIMENTAL WORK

1. PREPARATION OF MIXTURES

Calcium carbonate ($CaCO_3$) and boric acid (H_3BO_3) were used in the preparation of the mixtures. The percentage composition of the calcium carbonate was as follows: Ignition loss, 43.65; SiO_2, 0.07; R_2O_3, 0.04; MgO, 0.04; CaO (by difference), 56.20. The boric acid was analyzed only for impurities (analysis by chemistry division of this bureau), which were reported as follows: Fe, <0.001 per cent; SO_3, <0.01 per cent; Cl, <0.001 per cent. This material was recrystallized in order to render it finer, as it was difficult to pulverize the flakes by grinding.

For each mixture the calculated amount of calcium carbonate was first calcined and then thoroughly mixed with the required quantity of boric acid and heated over a burner (Meker type). The materials combined readily to form a mixture sufficiently homogeneous for the

[3] Griveau, Heats of Formation of the Anhydrous Calcium Borates, Compt. rend., vol. 166, pp. 993–995 1918.

[4] Roberts, Some New Standard Melting Points at High Temperatures, Phys. Rev., vol. 23, pp. 386–393, 1924.

[5] A. N. Winchell, The Optic and Microscopi Characters of Artificial Minerals. Univ. of Wisconsin Studies in Science, 1924.

[6] Burgess and Holt, The Behavior of Metallic Oxides Toward Fused Boric Anhydride, Proc. Chem. Soc., vol. 19, pp. 221–222, 1903.

[7] Guertler, On the Limits of Miscibility of Boric Anhydride and Borates in the Fused State, Z. anorg. Chem., vol. 40, pp. 225–53, 1904.

[8] Kanolt, Melting Points of Some Refractory Oxides, B. S. Bull., vol. 10, pp. 295–313, 1914.

[9] Schumacher, Melting Points of Barium, Strontium, and Calcium Oxides, J. Am. Chem. Soc., vol. 48, pp. 396–405, 1926.

purpose for which it was intended. The product varied in appearance from a glass to a soft clinker, depending on the compostion. In some instances a test for free lime was made by the ammonium acetate titration method,[10] but no free lime was found except in one mixture containing CaO in excess of $3CaO \cdot B_2O_3$.

2. ANALYSIS OF MIXTURES

Due to the loss of boric acid by volatilization during the preparation of the mixtures, it was necessary to analyze the product in each case.

CaO was determined by titration with half-normal hydrochloric acid, using methyl red as indicator. The acid also served as a solvent for the sample, as the calcium borates are only slightly soluble in water. The B_2O_3 was then determined on the same sample by adding mannite and titrating with half-normal sodium hydroxide to the end point indicated by phenolphthalein.

In general, it was found that mixtures containing an excess of either uncombined lime or boric oxide were hygroscopic, while the others showed low ignition losses. The moisture present was of no significance, since it was expelled when the samples were heated in the furnace. Consequently the percentages of CaO and B_2O_3 were in all cases adjusted so as to total 100 per cent on a nonvolatile basis.

Although free boric oxide is somewhat volatile at high temperatures, it was found by analysis that no appreciable loss of B_2O_3 occurred when the mixtures, prepared as described above, were subsequently used in obtaining heating curves.

3. EXPERIMENTAL PROCEDURE

The melting points of the various mixtures were determined by means of heating curves. For this purpose a platinum-wound, vertical-tube furnace, equipped with automatic temperature control,[11] was used. Temperatures were measured by means of platinum: platinum-rhodium thermocouples.

In obtaining a heating curve the sample was placed in one compartment of a small platinum thimble which was divided vertically by a platinum septum welded in place. The other half of the thimble was filled with artificial corundum as a reference medium. The two hot junctions of a differential thermocouple were imbedded in the two materials and the thimble suspended in the furnace. The temperature was raised at a rate of 5° per minute, and readings of the actual and differential temperatures were taken every minute, or, when necessary, every half minute.

Due to pronounced supercooling, no satisfactory cooling curves could be obtained.

In order to determine the solid phase present at the liquidus, a small sample of each mixture was wrapped in platinum foil, suspended in the furnace, and held at a constant temperature near the melting point for 15 minutes to allow it to come to equilibrium. It was then quenched by dropping it into water or mercury, and the phases present identified with the aid of the microscope. This process was then repeated at a temperature 2° or 3° higher or lower until a point was found, above which the primary solid phase did not appear.

[10] Lerch and Bogue, Revised Procedure for the Determination of Uncombined Lime in Portland Cement, Ind. Eng. Chem., Anal. ed., vol. 2, pp. 296–298, 1930.
[11] Adams, J. Opt. Soc. Am., vol. 9, p. 599, 1924.

Unfortunately, mixtures containing more than about 45 per cent CaO were found to crystallize during quenching, thus limiting the use of this method.

4. INTERPRETATION OF HEATING CURVES

A few words regarding the interpretation of the heating curves may be helpful.

The curves fall into two general classes. In the first class are those which resemble the typical heating curve for a pure compound or a

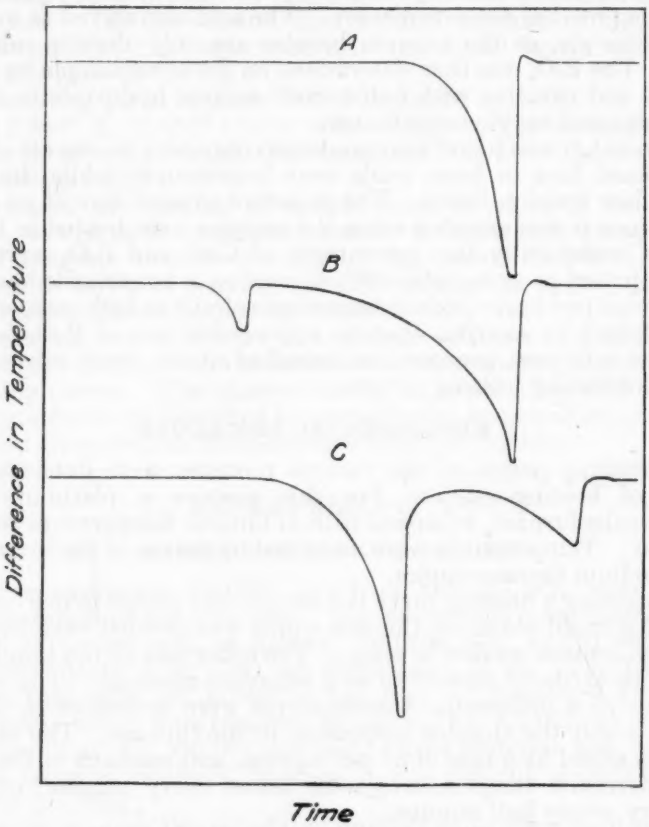

FIGURE 1.—*Types of differential heating curves*

eutectic mixture (curve *A*, fig. 1). Due to the temperature gradient in the sample, the outer edges fuse first, gradually reducing the amount of heat conducted to the thermocouple, which causes the curve of the differential temperature to dip downward. As the melting proceeds toward the center, the curve drops more and more sharply, reaching a minimum at the instant at which fusion is complete. Recovery is then very rapid, resulting in an almost vertical rise in the curve. The point at which the curve reaches the minimum was taken as the melting point of the sample. Heating curves for a pure reference material, potassium sulphate (m. p. = 1,069° [12]), confirmed this interpretation.

[11] See footnote 4, p. 826.

Mixtures lying between a eutectic and a compound give curves of the second type, represented by *B* (fig. 1). The first break represents the melting point of the eutectic; that is, the last portion of the mixture to solidify on cooling. Continued heating causes a gradual fusion (or solution) of the solid phase until it has completely disappeared. This is illustrated by the gradual drop in the curve, culminating as before in a sudden turn upward.

Curve *C* is of the same type as curve *B*, but in this case the composition is closer to that of the eutectic, causing the first break to be very pronounced, whereas the upper break, representing the true melting point, is relatively faint. For several of the mixtures whose compositions were close to those of the various eutectics the upper break was obscured entirely, making an absolute determination of the composition of the eutectic by this method impossible.

III. RESULTS

1. BINARY COMPOUNDS

Four binary compounds were found in the system: $CaO{\cdot}2B_2O_3$, $CaO{\cdot}B_2O_3$, $2CaO{\cdot}B_2O_3$, and $3CaO{\cdot}B_2O_3$.

Calcium diborate, or calcium tetraborate, $CaO{\cdot}2B_2O_3$.—This compound occurred as the primary phase in all the mixtures containing up to about 28 per cent CaO. As ordinarily prepared it remained in the form of a glass; but by heating for a few minutes at a temperature slightly below the melting point, this could be devitrified readily. It appears as irregular grains, highly birefringent, uniaxial, negative; $\omega = 1.638$, $\epsilon = 1.568$. Whether or not it melts congruently could not be determined with certainty, as its composition apparently lies at the break in the liquidus. The melting point is $986° \pm 5°$.

Monocalcium borate or calcium metaborate, $CaO{\cdot}B_2O_3$.—This compound occurs as the primary phase in mixtures containing approximately 29 to 51 per cent CaO. It appears as long, flat plates, highly birefringent, biaxial, negative, with a large optic axial angle; $\alpha = 1.550$, $\beta = 1.660$, $\gamma = 1.680$. It melts congruently at $1{,}154° \pm 5°$.

Dicalcium borate or calcium pyroborate, $2CaO{\cdot}B_2O_3$.—This compound occurs as the primary phase in mixtures containing approximately 51 to 64 per cent CaO. It appears as irregular grains, highly birefringent, biaxial, negative, with small optic axial angle; $\alpha = 1.585$, $\beta = 1.662$, $\gamma = 1.667$. It melts at $1{,}298° \pm 5°$.

Tricalcium borate or calcium orthoborate, $3CaO{\cdot}B_2O_3$.—This compound occurs as the primary phase in mixtures containing from 64 to at least 71 per cent CaO, and probably somewhat higher. It appears as irregular grains, highly birefringent, uniaxial, negative; $\omega = 1.728$, $\epsilon = 1.630$. It melts at $1{,}479° \pm 5°$.

2. THE PHASE EQUILIBRIUM DIAGRAM

The phase equilibrium diagram is shown in Figure 2.

Mixtures containing less than 24 per cent CaO were found to separate into two immiscible liquids (which for convenience may be designated as *A* and *B*) on fusion. The heavier of the two liquids (*A*) on cooling formed a clear glass with a refractive index of about 1.56. It was nearly insoluble in water but soluble in hydrochloric acid. The other liquid (*B*) formed a cloudy glass, which was seen

under the microscope to be full of minute globules, presumably of the other glass. These appeared to separate during cooling, since in quenched samples both glasses were clear. The index of the lighter glass was about 1.45. It was soluble in water, thus affording a simple method of separating it from the other glass for analysis. The water-soluble glass was found to be practically pure B_2O_3, while the other contained about 23 per cent CaO.

An attempt was made to determine the temperature above which the components would be completely miscible, but little evidence of a change in composition was found up to 1500°. For this experiment a small amount of one of the mixtures was placed in a platinum thimble and held at a definite temperature long enough to permit

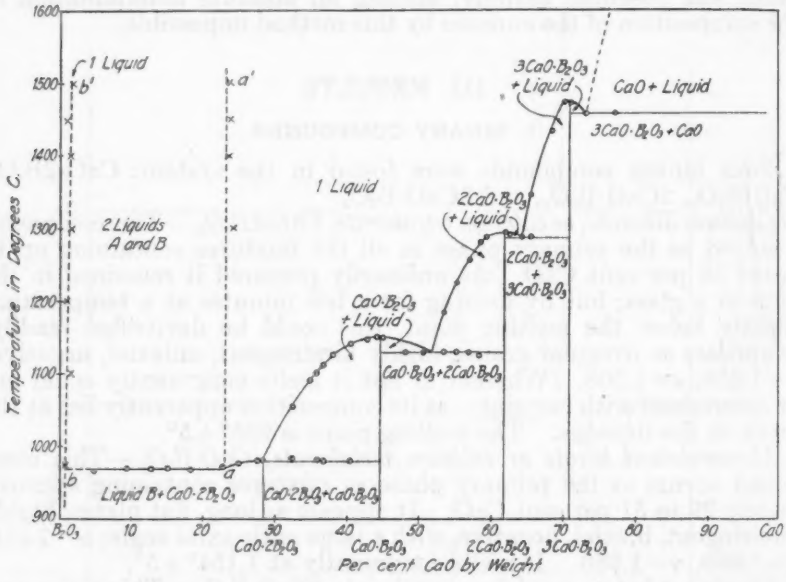

FIGURE 2.—*Phase equilibrium diagram for the system $CaO–B_2O_3$*

the liquids to separate into two layers. The charge was then cooled quickly, the two glasses separated by solution of the upper one in water, and the ratio of CaO to B_2O_3, determined in each. The results are given in Table 1.

TABLE 1.—*Composition of the immiscible liquids in the system $CaO–B_2O_3$, at various temperatures*

Temperature in °C.	Composition of glass A		Composition of glass B		Temperature in °C.	Composition of glass A		Composition of glass B	
	CaO	B_2O_3	CaO	B_2O_3		CaO	B_2O_3	CaO	B_2O_3
	Per cent	*Per cent*	*Per cent*	*Per cent*		*Per cent*	*Per cent*	*Per cent*	*Per cent*
900–950	23.0	77.0	0.6	99.4	1,200			.9	99.1
	23.1	76.9	.6	99.4	1,300	24.2	75.8	1.5	98.5
	24.9	75.1	.2	99.8	1,400	23.5	76.5	1.4	98.6
975			.7	99.3	1,450	23.9	76.1	.9	99.1
1,100			1.5	98.5	1,500	23.7	76.3	1.7	98.3

It will be seen that the data are not entirely consistent, but this is not surprising considering the slowness of attainment of equilibrium, the possibility of particles of one glass remaining dispersed throughout the other, and the rather inexact method of separation. In considering the values for the composition of glass *A* it should be borne in mind that this glass represents the lower CaO limit of stable liquid mixtures in this system. Hence it seems reasonable to take the minimum value obtained, 23.0 per cent CaO and 77.0 per cent B_2O_3, as the most reliable figure for the composition of this glass.

The data seem to indicate a slight increase in the CaO content of glass *B* with increasing temperature, but this is not definitely proved. The low CaO values are more reliable because of the probability that glass *B* was contaminated with glass *A*. This supposition is supported by the observation that glass *B* was always cloudy, due to the suspension in it of minute droplets of the other phase.

It is probable that the compositions of these two liquids approach each other, and that there is some temperature above which only one liquid phase can exist. Data obtained at 1,600° showed a marked tendency in this direction, but they can not be considered reliable, as the problem is complicated by the high volatility of B_2O_3 at this temperature, as well as by the failure of the two glasses to separate completely.

The region of liquid immiscibility up to 1,500° is represented approximately by the area between the dotted lines *a a'* and *b b'* in Figure 2. Any mixture in this area must exist as two liquid phases. On cooling, it will solidify to a mixture of two glasses; but if held for a few minutes at a temperature slightly below 970°, the compound $CaO{\cdot}2B_2O_3$ starts to crystallize out from liquid *A*. As this will tend to increase the proportion of B_2O_3 remaining in *A*, it is evident that a small amount of liquid *B* must also separate out, and this will continue until the mixture consists entirely of the compound and liquid *B*, the latter solidifying to a glass on cooling. A heating curve of the partially crystallized mixture will show a break at about 971° corresponding to the melting of $CaO{\cdot}2B_2O_3$ in the presence of B_2O_3 glass. The melting point for any mixture in this region is represented by the horizontal line in Figure 2, extending from 0.2 to 23 per cent CaO.

From *a* the liquidus rises gradually to 986°, the melting point of the diborate, $CaO{\cdot}2B_2O_3$ (composition, CaO, 28.71 per cent; B_2O_3, 71.29 per cent). The curve near this point is nearly horizontal, and it could not be determined with certainty whether the compound melts congruently or not. A mixture consisting of 28.6 per cent CaO and 71.4 per cent B_2O_3 showed a trace of monocalcium borate as the primary phase. This would indicate that calcium diborate is unstable at the melting point. However, the composition of the mixture in question was so close to that of $CaO{\cdot}2B_2O_3$ that if allowance is made for a slight error in chemical analysis the above conclusion is unwarranted.

From the melting point of $CaO{\cdot}2B_2O_3$, the liquidus rises sharply, reaches a maximum of 1,154° at the composition $CaO{\cdot}B_2O_3$ (CaO, 44.61 per cent; B_2O_3, 55.39 per cent), and descends to 1,132°, the melting point of a eutectic containing approximately 51.5 per cent CaO and 48.5 per cent B_2O_3. As previously mentioned, the true melting points near the eutectic could not be determined from the heating curves. The two points to the left of the eutectic in the diagram,

therefore, represent the melting point of the eutectic itself, rather than those of the two mixtures.

The curve then rises to another maximum of 1,298°, corresponding to the melting point of $2CaO \cdot B_2O_3$ (CaO, 61.70 per cent; B_2O_3, 38.30 per cent), and drops to 1,291°, the melting point of a second eutectic containing approximately 64 per cent CaO. A maximum of 1,479° corresponds to the melting point of $3CaO \cdot B_2O_3$ (CaO, 70.73 per cent; B_2O_3, 29.27 per cent), which is followed by a drop in the curve to another eutectic melting at 1,460° and consisting of about 73 per cent CaO and 27 per cent B_2O_3. Heating curves on two mixtures still higher in lime indicated the melting of this eutectic, but showed no further breaks up to 1,600°, the maximum temperature attained. Petrographic examination of these samples after fusion showed that they consisted of two phases, $3CaO \cdot B_2O_3$ and CaO. Hence it is assumed that no compounds are formed containing more CaO than the orthoborate, $3CaO \cdot B_2O_3$, and that the liquidus rises continuously to the melting point of CaO at 2,572°.

IV. SUMMARY

The phase equilibrium diagram for the system $CaO \cdot B_2O_3$ has been partially worked out. A region of liquid immiscibility was found, extending from 0.2 to 23 per cent CaO, and from 971° to above 1,500° C. The optical properties of the four compounds in this system were determined. The melting points of these compounds are given in Table 2, together with the melting points determined by previous investigators.

TABLE 2.—*Melting points of the calcium borates*

Compound	Melting point, determined by—			
	Guertler (1904)	Griveau (1918)	Roberts (1924)	Carlson
	°C.	°C.	°C.	°C.
$CaO \cdot 2B_2O_3$	1,030	ca. 1,025		986±5
$CaO \cdot 2B_2O_3$	1,095	ca. 1,100		1,154±5
$2CaO \cdot B_2O_3$	1,225	ca. 1,215	1,304±5	1,293±5
$3CaO \cdot B_2O_3$				1,479±5

WASHINGTON, October 10, 1932.

A METAL-CONNECTED GLASS ELECTRODE

By M. R. Thompson

ABSTRACT

Glass electrodes have come into extensive use for the measurement of hydrogen-ion activity in special cases in which other kinds of electrodes are unsuitable. Previous methods of construction have produced glass electrodes which were fragile, had an uncertain length of life, and required connecting in circuit with two standard electrodes.

In the work reported in this paper a glass electrode was developed which has a comparatively thick wall and a direct metallic connection to the glass. This makes a very durable apparatus and eliminates one standard electrode from the circuit. It is shown that the accuracy of such a metal-connected glass electrode is comparable with that of other electrodes used in pH measurement.

CONTENTS

	Page
I. Introduction	833
II. Historical	834
III. The metal-connected glass electrode	835
1. Principle	835
2. Construction	836
IV. Experimental work and conclusions	839
1. Apparatus and general methods	839
2. Useful pH range	845
3. Effect of age	845
4. Effect of alkali salts (salt error)	846
5. Effect of heavy metal salts	848
6. Effect of protein	850
7. Effect of oxidants and reductants	850
8. Applications	851
V. Summary	852
VI. Acknowledgments	852
VII. Bibliography	852

I. INTRODUCTION

The glass "electrode," or, more strictly speaking, the glass half-cell, has come into extensive use recently to measure hydrogen-ion concentration in certain kinds of solutions for which other types of electrodes are unsuitable. Its advantages include freedom from disturbance by oxidation-reduction potentials and obviation of added reagents, such as gaseous hydrogen or solid quinhydrone. Its disadvantages are the inherent high resistance (at present greater than 1 megohm), requiring the use of delicate or special apparatus for detecting potential changes; and the fragility, which makes the useful life short or uncertain. The purpose of this investigation was to remove or reduce these disadvantages.

II. HISTORICAL

The discovery of a reaction between glass and hydrogen ions goes back at least to Cremer (1).[1] Haber and Klemensiewicz (5), who acknowledged Cremer's work, appear to have been the first to actually apply the principle to laboratory measurements. Their systematic and extensive treatise is so well known that they are usually credited with the development of the glass electrode in something like its present form. As often happens, over a decade elapsed before further notice appeared, and about 20 years passed before general interest in the subject was aroused.

Numerous theories have been proposed to account for this peculiar action of glass. These theories may be roughly classified into three groups, based on phase boundary, ion adsorption (or exchange), and liquid junction (or diffusion) potentials. All of these seem to imply that the glass contains or attracts water and hydrogen ions (protons), and some of them imply that only hydrogen ions can penetrate into or through the glass. The situation is complicated by the fact that glass is not unique in this respect. Thus, similar effects have been detected at interfaces of water with quartz (41), paraffin, zeolite minerals (19, p. 252), and benzene (5). Borelius (8, p. 447) summarize concisely three possible conditions for electrode action. Much information on the theoretical aspects will be found in recent papers by MacInnes and Belcher (34), and by Dole (35) (44).

The composition of the glass used is important and has been studied by Hughes (23), MacInnes and Dole (27) (31), Elder (29), and others. Most investigators agree that a soft glass containing about 22 per cent of Na_2O, 6 per cent of CaO, and 72 per cent of SiO_2 [2] gives the best results. Means to effect further improvement in the electrode action of glass are not now apparent, but it is conceivable that the abnormalities shown in very acid and alkaline solutions might be decreased by the addition of other substances to the glass.

Small bulbs with thin walls have been used by most investigators, including Haber and Klemensiewicz (5), Hughes (9) (23), Elder and Wright (25), Voegtlin, De Eds and Kahler (32), Robertson (36), and others. Kerridge (20) modified this construction by blowing a local reentrant thin area (0.025 to 0.030 mm thick) in the bulb wall to serve as the active surface. Horovitz (15, p. 345) sealed a relatively thick (0.05 to 0.1 mm) plate of glass on the end of a glass tube. MacInnes and Dole (27) used an electrode of similar shape, but with an extremely thin (0.001 mm) active surface, about 4 mm in diameter, obtained from the wall of a glass bubble. This might be called a "membrane" electrode. The forms described may be conveniently classified into the two general types of bulb and membrane, although there appears to be no essential difference in their action. Figure 1 shows several types of electrodes and methods of connection.

The characteristic arrangement for these active glass surfaces has been with a solution on each side of the bulb or membrane wall. One solution is of known or fixed hydrogen ion activity, while the other is of unknown or variable activity. This in effect makes a hydrogen

[1] Figures in parenthesis here and throughout the text refer to the numbers used in the bibliography at the end of this paper.

[2] Commercial glass of this composition is obtainable, for instance, No. 015 glass of the Corning Glass Co., Corning, N. Y. Tubing with an outside diameter of 7 mm, and 1 mm wall is convenient for blowing membrane electrodes.

electrode on each side of the glass. A standard electrode of some sort is immersed in each solution to complete the circuit. These standard electrodes need not be identical but, if so, their potentials are opposed and cancel each other in the measurement. It is important to note that in this arrangement only electrolytic contact is made with the glass.

Maximum sensitivity is associated with minimum resistance, and consequently the tendency has been to make the glass as thin as possible. For small electrodes, the practical lower limit of resistance thus reached lies between 2 and 50 megohms (27) (34) (36), as determined by direct-current measurement (27) (34). The best electrodes thus become rather difficult to construct, excessively fragile, and of uncertain life even with careful handling.

Where extreme compactness is not required, more durable, although not necessarily as sensitive, electrodes of the same resistance could obviously be prepared by using a thicker wall with a larger area. The bulb type is better suited to this modification than the membrane type, as it is difficult to properly seal a large area of membrane. Hazel and Sorum (39), however, have recently increased the membrane diameter to about 10 mm. On the other hand, the results obtained by Robertson (36) indicate that it is possible to form a comparatively small bulb having a resistance as low as that of a membrane.

The situation described limits the widespread use of glass electrodes, especially in industrial work, where rugged and permanent apparatus is desirable.

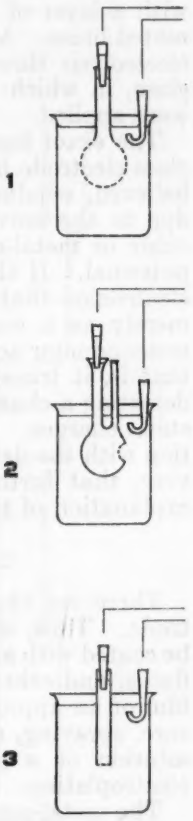

FIGURE 1.—*Forms of the ordinary glass electrode*

(The active surface portion is shown in dotted line. Each glass electrode is connected to two calomel electrodes, of which only the tips are shown.) 1, plain bulb; 2, reentrant bulb; 3, membrane

III. THE METAL-CONNECTED GLASS ELECTRODE

1. PRINCIPLE

In connection with the mechanical advantages of thick-walled electrodes, it appeared possible to greatly simplify the mounting and eliminate the extra (inside) standard electrode by substituting a direct metallic connection to the glass wall. With glass of sufficient thickness to withstand ordinary handling, for instance, 0.1 to 0.5 mm, such a metallic connection could be easily applied and would furnish additional protection to the glass. This was tried (March 25, 1930) by wrapping tinfoil around a soft-glass tube, and the results were promising enough to warrant further trial and development, as reported in this paper.

No publication has been noted which describes the use of a metal to glass connection for the systematic accurate measurement of hydrogen-ion concentration. Previous investigators have doubtless made incidental trials of a simple metallic connection, such as mercury within a glass bulb, analogous to the mercury cups so often used in

making electrical contact with sealed-in wires on glass apparatus. B. von Lengyel (41, pp. 426 and 431) tried a mercury to quartz connection, but found it to be unsatisfactory. He also used a Wood's metal to quartz connection for checking an electrode chain. Haber and Klemensiewicz (5, p. 424) used a connection, not with glass, but with a layer of benzene, by means of an immersed disk of amalgamated brass. Many experiments have also been published describing electrolysis through glass, or determinations of the conductivity of glass, in which electrodes of metal, amalgam, or powdered graphite were applied.

The exact function of the metal coating on a "metal-connected" glass electrode has not yet been determined. If, as is very generally believed, conduction through glass is entirely electrolytic; that is, due to the movement of ions, there may be set up a metal-metal oxide or metal-metal silicate electrode with a comparatively steady potential. If the passage of current through the glass results from electronic—that is, solid conduction—the metal serves, of course, merely as a convenient terminal. Besides being a conductor (or nonconductor according to the point of view) glass is also a dielectric; that is, it transfers charges by induction. The apparatus used for detecting a change of potential in the circuit is capable of measuring static charges. This point will be mentioned subsequently in connection with the details of construction. It should be emphasized, however, that further work will be required to furnish a satisfactory explanation of the complicated phenomena involved.

2. CONSTRUCTION

There are obviously many ways of arranging a metal-glass electrode. Thus, wires, rods, sheets, and tubes of suitable metals might be coated with a film of the proper glass; or, conversely, tubes, beakers, flasks, and other vessels of the proper glass might be coated with a film of an appropriate metal. The latter might be applied by pressure, spraying, casting, sputtering, or chemical precipitation from a solution or a gas, and subsequently thickened and protected by electroplating. Various possible arrangements are shown in Figure 2.

The metal-connected glass electrodes first employed in this investigation were constructed from various stocks of laboratory tubing, using tinfoil on those containing the solution to be tested, and mercury or coiled wire inside those dipping into the solution. Subsequent work showed that glass having the composition ordinarily used for membranes also gave the best results for metal-connected electrodes, and that silvering followed by copper plating gave a more durable and satisfactory coating than tinfoil. Electrodes of the dipping type were found to be less accurate than those of the containing type. Further investigation is needed, but this difference may be the result of greater dehydration of the outer surface during the working of the hot glass.

For the final exploratory work, three containing and three dipping type electrodes were prepared from Corning No. 015 glass tubing by blowing it into the shape of test tubes with walls about 0.5 mm thick. These tubes had an outside diameter of 1.2 cm and a length of 12 cm, and contained (or displaced) about 10 ml of solution. Silvering was applied on either the inside or outside surface by the Rochelle salts

process (37), and copper [3] was then deposited to a thickness of about 0.008 mm. The glass tubes were coated with paraffin for about 1 cm on the outside at the open end to diminish surface leakage. A copper

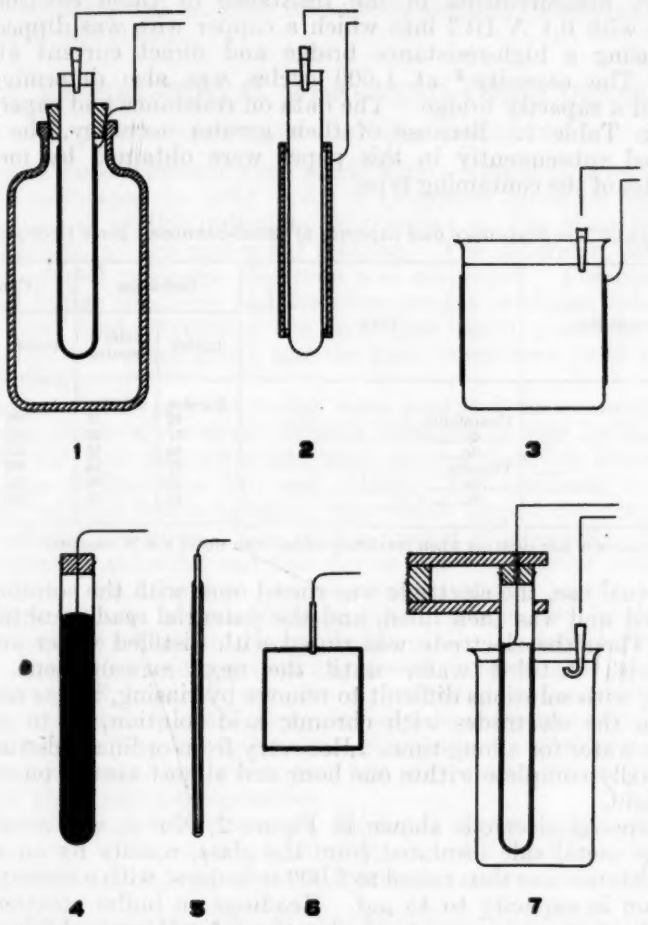

FIGURE 2.—*Arrangements of the metal-connected glass electrode*

(Only the tips of calomel electrodes are shown.) 1, Containing type; tube form, metal coated; 2, containing type; tube form, with metal portion insulated from the glass by means of mica wedges at top and bottom, and an air gap. For special study; 3, containing type; beaker form, metal coated; 4, dipping type; tube form, mercury filled; 5, dipping type; metal rod or wire form, coated with glass; 6, dipping type; metal sheet form, coated with glass; 7, dipping type; tube form, metal coated and supported by bakelite clamp.

wire was wrapped or pressed against the metal coating and the completed electrode was mounted in a suitable support. This consisted

[3] Plating on the outside was done with a solution containing 100 g/l of $CuSO_4.5H_2O$. The coating was applied by "flashing" at a current density of about 5.5 amp/dm² for a few minutes, after which plating was continued at 0.6 amp/dm² for one-half hour. Plating on the inside was found difficult on account of the small bore and consequent poor circulation. Satisfactory results were finally obtained by using a more concentrated solution containing 250 g/l of $CuSO_4.5H_2O$, and an accurately centered copper wire as anode. Because of the necessarily excessive anode current density, the 110-volt circuit with a rheostat in series was required to overcome anode polarization. A flash of copper was applied at about 5 amp/dm² for one minute, after which plating was continued for one and one-half hours at 0.36 amp/dm². All plating was done at room temperature. The copper coating was lacquered, except at the pressure contact with the connecting wire.

of a rubber-stoppered glass bottle for a containing electrode and a bakelite clamp on a stand for a dipping electrode. (See fig. 2, Nos. 1 and 7.)

Rough measurements of the resistance of these electrodes, in contact with 0.1 *N* HCl into which a copper wire was dipped, were made using a high-resistance bridge and direct current at 1,000 volts.[4] The capacity [5] at 1,000 cycles was also determined, by means of a capacity bridge. The data on resistance and capacity are given in Table 1. Because of their greater accuracy, the results presented subsequently in this paper were obtained by means of electrodes of the containing type.

TABLE 1.—*Resistance and capacity of metal-connected glass electrodes*

Electrode No.	Type	Resistance		Capacity	
		Initial	After 8 months	Initial	After 8 months
		megohm	*megohm*	*μμf*	*μμf*
1 [1]	Containing	43	53	590	625
2	do	37	39	660	695
3	do	48	55	535	555
4	Dipping	57	58	460	505
5	do	53	48	530	525
6	do	53	60	510	495

[1] The resistance of this electrode when previously coated with tinfoil was 70 megohms.

In actual use, the electrode was rinsed once with the solution to be measured and was then filled, and the potential reading obtained at once. Then the electrode was rinsed with distilled water and kept filled with distilled water until the next measurement. When working with solutions difficult to remove by rinsing, it was necessary to clean the electrodes with chromic acid solution, or to immerse them in water for a long time. Recovery from ordinary disturbances was usually complete within one hour and almost always on standing over night.

The special electrode shown in Figure 2, No. 2, was constructed with the metal side insulated from the glass, mainly by an air gap. The resistance was thus raised to 5,000 megohms, with a corresponding reduction in capacity to 45 *μμf*. Readings on buffer solutions were unsteady, but an accuracy of about ±0.5 pH was obtained even under these very unpromising conditions. This experiment indicated that electrode action does not require actual contact between

[4] This scheme was used merely for convenience and is not suggested for general use. The application of a high voltage tends to cause the passage of appreciable current, with the possibility of polarization and disturbance to readings. These electrodes were affected temporarily, as shown at *A* in Figure 7; but after standing in contact with water for a few weeks, they returned to the original condition.

It has been pointed out by MacInnes and Belcher (34) that resistance measurements on glass electrodes made with direct current are conventional and that alternating current gives much lower and more accurate results. They concluded, however, that: "It does not appear desirable to change the current practice of reporting the apparent direct-current resistances of electrodes in megohms."

In measurements using direct current, MacInnes and Dole (27), (31) applied much lower voltages, either 3.7 or 1.2 volts; MacInnes and Belcher (34) applied less than 1 volt. It may be pointed out that the surface ratio of a metal-connected electrode to a membrane electrode, each of the usual size, is about 3,300 to 12 mm². The application of 1,000 volts on the former produces the same current density as does 3.6 volts on the latter, if both have the same total resistance. As a matter of fact, the direct-current resistances obtained for the metal-connected glass electrodes are of the expected order of magnitude, when compared with the direct-current resistances of membrane electrodes as measured by the author, using the method of MacInnes and Dole (27) (31).

[5] Residual noise in the telephones indicated a wide phase angle. This is characteristic of low dielectric resistance, or of a "leaky" condenser.

metal and glass. Completion of the circuit may have been effected through surface leakage, or possibly by induction. In this connection, Borelius (6) (7) (8) has published many measurements including electrolytic potentials at glass or paraffin surfaces, where an air gap was used in the circuit.

IV. EXPERIMENTAL WORK AND CONCLUSIONS

1. APPARATUS AND GENERAL METHODS

Potential measurements were made with a "student type" potentiometer calibrated to ±0.5 mv. A Compton quadrant electrometer[6] was used as the indicating instrument in the glass electrode measurements, by the null-point method. The saturated potassium chloride-calomel reference electrode was employed. For standardization of buffer solutions and for comparative readings, other electrodes were used, including the hydrogen (with platinum black), the quinhydrone (with gold), and the glass membrane (with Corning No. 015 glass).

The glass-membrane electrodes were mounted or connected, not through an inside silver-silver chloride electrode as used by MacInnes and Dole (27) but through a saturated calomel electrode according to the system of Kerridge (20) and others. The electrode was filled with any suitable buffer solution, into which dipped the plugged tip of the calomel electrode. The plug consisted of agar jelly saturated with potassium chloride, and this device was used for its mechanical convenience. Such devices are, of course, possible sources of error by the introduction of an additional potential into the circuit. The error in this case appeared to be negligible within the limits of accuracy sought. An alternative procedure would involve the use of an extremely small bent tip, or else a ground-glass seal (20). The second or reference calomel electrode had a bent tip, according to the usual scheme. (See fig. 1, No. 3.) Silver-silver chloride electrodes are more compact, but somewhat less convenient to prepare and maintain than calomel electrodes.

A saturated calomel electrode, having a tip plugged with agar jelly saturated with potassium chloride, was also used for connection with the containing type of metal-connected glass electrodes. (See fig. 2, No. 1.)

Potential readings were made at room temperature, usually about 25° C. As the saturated calomel electrode was used for reference and most of the solutions were buffered, the accuracy of the measurements was about ±0.1 pH (±6 mv). This was sufficient for the exploratory purposes of this investigation. The readings, including those with the metal-connected glass electrode, were made, however, to the nearest 0.02 pH (±1 mv) and occasionally to 0.01 pH (±0.5 mv). The observations indicated that with closer control of temperature and a decreased wall thickness the accuracy with this electrode could probably be made equal to the above precision.

Switches in the circuit of the electrometer and glass electrode were made of paraffin blocks with mercury-filled copper cups as terminals.

[6] Where portability is required, the Lindemann electrometer may be substituted. Numerous circuits have been published in which the delicate and relatively expensive electrometer was replaced by vacuum tubes. A recent paper by Compton and Haring (47) described a compensated thermionic electrometer which is stated to have possibilities for use with thick glass electrodes. Robertson (36) reported the use of a galvanometer of high sensitivity with electrodes of very low resistance.

Fused sulphur would probably have been better than paraffin, but it is less easy to handle. The electrometer leads were insulated with mica and were run in grounded brass pipes, although bakelite insulation was used in a few places for convenience. The electrometer switches were placed in a grounded copper gauze cabinet, one compartment of which also served to hold and partially shield the glass-calomel

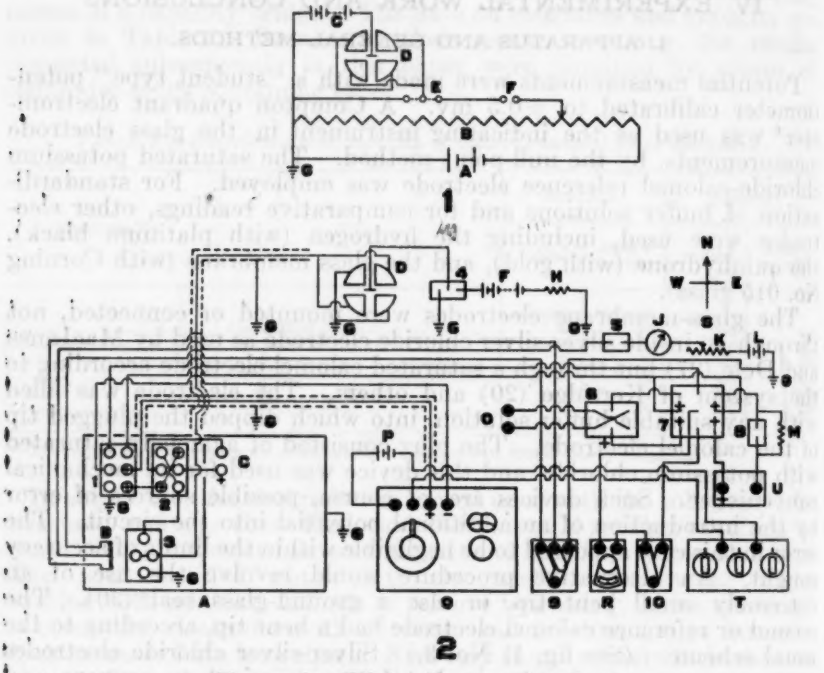

FIGURE 3.—*Wiring diagram of apparatus*

1. Simplified diagram for the potentiometer using an electrometer by the null-point method. *A*, Battery for potentiometer; *B*, potentiometer; *C*, battery for electrometer needle; *D*, electrometer; *E*, single pole double throw switch; *F*, binding posts for connecting glass electrode-standard electrode cell; *G*, ground. 2., Complete diagram (student type potentiometer). *A*, shielded cabinet holding special paraffin base switches and the glass electrode-standard electrode cell; *B*, electromagnets (1 ohm each) for tripping electrometer switch; *C*, terminals for connecting glass electrode-standard electrode cell; *D*, electrometer; *F*, battery for electrometer needle (it makes no difference which pole is connected to the needle); *G*, ground; *H*, protective resistance (0.1 megohm) for *F*; *J*, ammeter (1 ampere scale) for reading the electromagnet current; *K*, variable resistance (3 ohms) for controlling the electromagnet current; *L*, battery (3 volts) for supplying the electromagnet current; *M*, protective resistance (20,000 ohms) for standard cell; *O*, terminals for connecting hydrogen or quinhydrone electrodes; *P*, battery for potentiometer; *Q*, potentiometer (student type); *R*, galvanometer (desk type); *T*, variable resistance (1,000 ohms) for adjusting potentiometer; *U*, standard cell; *1*, paraffin base main D. P. D. T. switch; *2*, paraffin base reversing D. P. D. T. switch; *3*, paraffin base electrometer S. P. D. T. switch; *4*, porcelain base electrometer needle S. P. D. T. switch; *5*, porcelain base S. P. S. T. switch for *B* circuit; *6*, porcelain base D. P. D. T. reversing switch; *7*, porcelain base T. P. D. T. switch; *8*, porcelain base S. P. S. T. shorting switch; *9*, hard rubber base three point key; *10*, hard rubber base two point key. Switching directions, adjusting potentiometer, (*1*) north and (*7*) east. Set potentiometer by means of *U*, *R*, and (*10*). Using hydrogen or quinhydrone electrode, (*1*) north and (*7*) west. Hydrogen or quinhydrone electrode connected to *O* at north reads on potentiometer, using *R* and (*10*). (*6*) west for hydrogen electrode. (*6*) east for quinhydrone electrode and pH below 7.67. (*6*) west for quinhydrone electrode and pH above 7.67 (using saturated calomel electrode). Using glass electrode, (*1*) south, glass electrode reads on potentiometer, using the electrometer, close (*5*) to operate (*3*), use (*9*) for remote control of (*3*), set (*2*) as may be necessary.

cell. The main switch connecting the electrometer was tripped by an electromagnet operated by remote control from a key placed outside the cabinet. This device proved very convenient and eliminated any disturbance due to body capacity. The other paraffin switches needed only occasional shifting, which could be done manually without difficulty.

Electrometer disturbances could usually be traced to either too much or too little mercury, or to dirty mercury, in the switch cups. A quick, positive make or break is necessary and contact electromotive forces must be prevented. In view of occasional difficulties, however, the elimination of mercury is being considered, by means of a switch with solid contacts of the brush or spring type. It was preferable not to operate the electrometer at maximum sensitivity, on account of its instability. Best results were obtained with the particular instrument used by keeping the needle voltage as low as possible, about 70 volts usually being satisfactory. A scale deflection of 3 mm/mv at 1 m scale distance was then obtained by lift and tilt adjustment of the quadrants. This sensitivity was adequate for the present work, although a much higher sensitivity is possible and has been used at times by others (34).

It is occasionally stated that an electrometer can not be used in very humid weather. In these experiments, suitable measurements could be obtained up to 80 per cent humidity of the room atmosphere. This favorable result may have been due to special care in insulating and shielding the circuit. It was sometimes found advantageous to ground the glass electrode just before connecting it to the electrometer for a reading. This removed stray charges from the system.

The potentiometer circuit was so wired that either hydrogen, quinhydrone, or glass electrodes could be connected in the appropriate position and all necessary measurements could be obtained by means of permanently connected switches and keys. The wiring diagram is shown in Figure 3. When using a more accurate potentiometer, such as the "type K" which has more of the accessory apparatus located internally, certain changes would be required in the wiring (34, p. 3316). The equations applying to the respective electrodes when used at 25° C. in combination with a saturated calomel reference electrode are given in Table 2, in both an extended and a somewhat simplified form. The extended form shows the factors which control the first term on the right-hand side of the simplified equation used in the actual measurements. E is the measured cell potential, expressed in volts, from which the desired pH value is computed.

TABLE 2.—*Electrode equations at 25° C.*

Electrode	Extended equation	Simplified equation
Hydrogen (24, p. 672)	$pH=\frac{-E-0.2458}{0.05912}$	$pH=-4.16-\frac{E}{0.05912}$
Quinhydrone (24, p. 672)	$pH=\frac{0.6992-E-0.2458}{0.5912}$	$pH=7.67-\frac{E}{0.05912}$
Glass (*a*), mounted with silver-silver chloride electrode and 0.1 *N* HCl (28).	$pH=\frac{0.3524-E-0.2458}{0.05912}$	$pH=1.80-\frac{E}{0.05912}$
Glass (*b*), mounted with saturated calomel electrode and 0.1 *N* HCl (24, p. 672).	$pH=\frac{-E+0.0636}{0.05912}$	$pH=1.08-\frac{E}{0.05912}$
Glass (*c*), mounted with saturated calomel electrode and 0.05 *M* acid potassium phthalate (20).	$pH=\frac{-E+0.2349}{0.05912}$	$pH=3.97-\frac{E}{0.05912}$
Glass (*d*), mounted with saturated calomel electrode and any buffer solution of pH=*K*.	$pH=\frac{-E-E_X}{0.05912}$	$pH=K-\frac{E}{0.05912}$
Glass (*e*), metal-connected; *X* (determined by calibration) is the pH of the solution for which *E*=0.		$pH=X-\frac{E}{0.05912}$

In the equations of Table 2, liquid junction potentials and uncertainties in pH values have been disregarded, but in most cases these are too small to need consideration for the present purposes. Any appreciable potential due to the glass itself, variously known as the self, strain, or asymmetry potential, must be determined, however, and a corresponding correction applied to the over-all potential. The asymmetry potential is readily measured with the ordinary glass electrode by having the same kind of solution and auxiliary electrode on each side. (With the metal-connected glass electrode it is not possible to determine the asymmetry potential, which is included in the calibration.) With good electrodes, this potential is seldom more than a few millivolts at the start and tends to decrease to zero in a short time. It is less confusing to omit such a term from the above equations, with the understanding that it must be subtracted (algebraically) from E when necessary, as will be illustrated below.

The equations are given in algebraic form, and potential values must be inserted with proper signs. In general, the sign of any electrode is defined as that of the charge on the outside metal terminal. As the saturated calomel electrode is used here as the standard half cell for reference, the sign of the measured cell potential (E) is that of the other electrode with respect to the calomel, or the same as that on the outside terminal of the other electrode. A little consideration of the circuit conditions also shows that the sign of a glass bulb or membrane electrode is that of the inside connecting electrode (whether silver-silver chloride, calomel, etc.) in the solution the pH of which is kept constant. This is brought out in Figure 4, in which the relative number of + or − signs indicates conventionally the tendency for current to flow to the external circuit in the ordinary sense. With the metal-connected glass electrode, the sign is that of the terminal of the metal coating, wherever this is located; that is, whether or not the electrode contains, or is immersed in, the solution to be tested.

The following calculations are typical for a glass bulb or membrane electrode filled with 0.05 M acid potassium phthalate and mounted between two saturated calomel electrodes.

With 0.05 M acid potassium phthalate also placed on the outside—

$E_1 = -0.002$ volt = asymmetry potential (measured).
(Inner calomel negative to outer calomel. In other instances the sign might be opposite.)

With solution of unknown pH placed on the outside:

$E_2 = -0.126$ volt (measured).
(Inner calomel negative to outer calomel.)

$E = E_2 - E_1 = -0.126 - (-0.002) = -0.124$ volt.

$$\text{pH} = 3.97 - \frac{-0.124}{0.0591} = 3.97 + 2.10 = 6.07$$

As most publications on this subject omit any explanation of the signs, it is believed that the above brief treatment may be helpful.

The conventional straight line graphs for the various equations listed in Table 2 are shown for illustrative purposes in Figure 5. Such a diagram is useful for bringing out the relations involved and for quickly plotting the position of an ordinary glass electrode when the conditions are changed. The following relations should be noted:

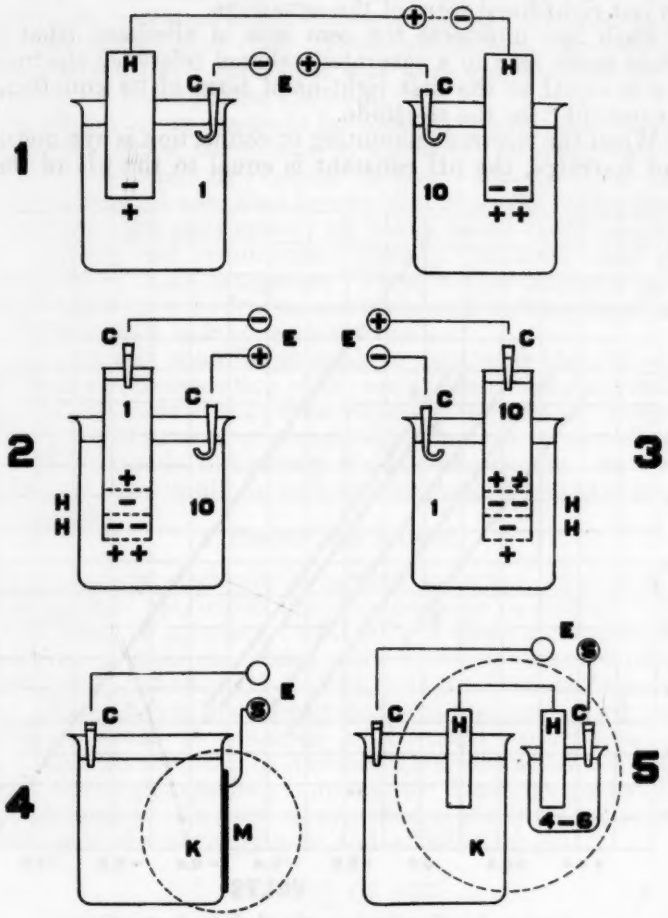

FIGURE 4.—*Sign of electrodes*

(Only the tips of calomel electrodes are shown). *1*, example of two hydrogen electrodes connected with two calomel electrodes. *H*=hydrogen electrode. *C*=calomel electrode. pH of left solution=1. pH of right solution=10. *E*=measured potential. The hydrogen electrode in the solution of lower pH is + to the other hydrogen electrode. The calomel electrode in the solution of higher pH is + to the other calomel electrode. Taking one calomel electrode as the standard of reference, in a solution of fixed pH, the sign of *E* is that of this electrode; *2*, example of a membrane glass electrode filled with a solution of relatively low and constant pH. The membrane is imagined to be divided into two hydrogen electrodes connected in series as in (*1*). *H*, *C*, and *E* as before. pH of solution within membrane electrode=1. pH of solution in beaker=10. The calomel electrode within the glass electrode is the standard of reference and is negative, which is taken as the sign of *E*. This results from the lower hydrogen electrode being negative to the upper hydrogen electrode, just as in (*1*) the right hydrogen electrode is negative to the left hydrogen electrode. The relation is similar if a silver-silver chloride electrode is substituted for the inside calomel electrode; *3*, this is like (*2*), with all conditions reversed. As before, the sign of *E* is that on the inside calomel electrode, or + in this case; *4*, example of a containing type metal-connected glass electrode. pH of the solution to be measured=*K*. The sign of *E* is that on the terminal *S*, which is connected to the metal, as is explained in (*5*); *5*, the area within the dotted circle represents in more detail the supposed conditions within the dotted circle of (*4*). The glass-metal section can be substituted by two hydrogen electrodes in series, as in (*1*). One hydrogen electrode is immersed in the solution of pH=*K* and the other hydrogen electrode is immersed in a solution of constant pH, in these experiments somewhere between 4 and 6. The circuit is completed by another calomel electrode in the latter solution. This electrode becomes the standard of reference, as in (*1*). The sign of *E* is that on terminal *S* as in (*4*)

(*a*) All lines are parallel and have the same (negative) slope of 0.05912 volt per unit pH at 25° C., corresponding to the denominator of the last right-hand term of the equations.

(*b*) Each line intersects the zero axis of abscissae (that is, each electrode reads zero to a saturated calomel reference electrode) at a pH value equal to the first right-hand term of its equation, or the "pH constant" for the electrode.

(*c*) When the electrode mounting or connection is symmetrical like that of Kerridge, the pH constant is equal to the pH of the inside

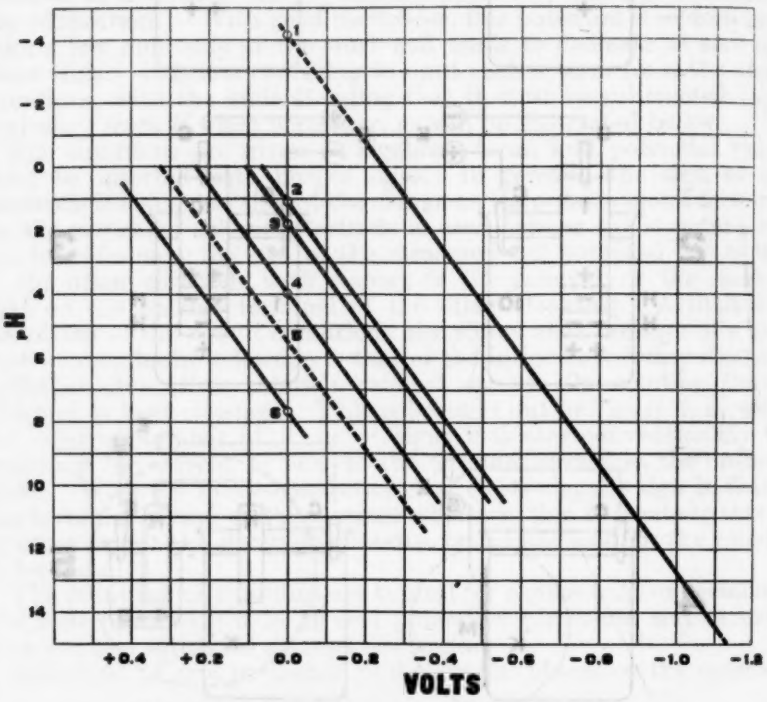

FIGURE 5.—*Standard graphs of electrode equations*

pH and potential in volts v. saturated calomel electrode at 25° C. (See Table 2.) *1*, Hydrogen electrode; *2*, glass electrode filled with 0.1 *N* HCl and connected with an inside saturated calomel electrode; *3*, glass electrode filled with 0.1 *N* HCl and connected with an inside silver-silver chloride electrode; *4*, glass electrode filled with 0.05 *M* acid potassium phthalate and connected with an inside saturated calomel electrode; *5*, metal-connected glass electrode. This line is shown dotted to indicate that the position is only approximate and must be determined by calibration; *6*, quinhydrone electrode

solution. Hence, a line can be immediately drawn in for a given value of pH for the inside buffer solution.

(*d*) The sign of the electrode reverses when the pH of the solution being measured passes the electrode constant, being positive for lower pH values and vice versa.

(*e*) An electrode (glass or other) will be positive to any other electrode placed in the same solution, if the first electrode line lies to the left, and vice versa.

(*f*) The approximate useful pH range for each electrode is indicated by the positions of the ends of its line.

The various kinds of standard and glass electrodes used in this investigation were calibrated or checked by means of a series of buffer solutions that were either 0.05 or 0.1 *M* and prepared according to the directions of Clark (24). These solutions included phthalate, phosphate, borate, and carbonate and were standardized by either the hydrogen or quinhydrone electrode.

The suitability of an electrode for measuring hydrogen ion concentration depends upon the extent to which the accuracy and reproducibility are affected by various factors. Among these are: (*a*) Useful pH range; (*b*) age; that is, any change in the calibration with time; (*c*) alkali salts (salt error); (*d*) heavy metal salts; (*e*) proteins; and (*f*) oxidants and reductants. Certain "poisons" may also be found in some of these categories. Thus, copper sulphate (a heavy metal salt) poisons a hydrogen electrode and sodium bisulphite (a reductant) poisons a quinhydrone electrode.

A brief study was accordingly made to determine the effects of the above factors on the operation of the metal-connected glass electrode. It should be emphasized that these experiments were not designed to redetermine the constants of certain solutions, nor to establish exact limits for the electrode, but merely to determine trends. In this way, the general behavior could be defined and possible means of improvement indicated.

2. USEFUL pH RANGE

Every secondary electrode is subject to errors outside of some favorable range of pH, which therefore needs to be defined. Briefly, within the limits of accuracy (± 0.1 pH) of these measurements the metal-connected glass electrodes were found to function linearly [7] and reproducibly between pH–1 and pH–11, in dilute buffer solutions. Down to pH–0; that is in concentrated acid solutions, fairly satisfactory readings could be obtained by frequent calibration. Above pH–11, hydroxide solutions of increasing concentration must be used and attack of the glass surface is probable. Readings above pH–11.5 were unsatisfactory. In general, any kind of electrode tends to show discrepancies in the strongly acid and alkaline ranges.

3. EFFECT OF AGE

The metal-connected electrodes were calibrated occasionally by means of buffer solutions, using the technique previously described. Typical calibrations are shown for illustrative purposes in Figure 6 [7]. The approximate variation in the constant thus determined for the same electrodes over a period of about eight months [8] is shown in Figure 7.

The change in the constant is evidently due to a change in the initial potential of (or in) the glass. This is usually accompanied by a slight increase in resistance (Table 1), but without any apparent decrease in accuracy. The change can not, therefore, be definitely ascribed either to increased surface leakage or to deterioration of the

[7] MacInnes and Dole (31) and MacInnes and Belcher (34) showed by very accurate measurements that glass of the type used for electrodes did not function linearly in very alkaline (31) (34) or very acid (34) solutions, especially when these were concentrated. In dilute solutions, however, the deviation was less than ± 0.1 pH for the pH range used in the present work. This point should be kept in mind, however, whenever work of higher accuracy is attempted with metal-connected glass electrodes.

[8] A recent examination of one of these electrodes (No. 2) showed it to be in useful condition at the end of one year. The constant was then about 5.83, which indicated practically no change in the last four months.

glass. Except in rare cases, the normal drift or rate of change was probably less than 0.01 pH per day. In two cases the constant decreased, and at an increasing rate (fig. 7, Nos. 1 and 3), while in the third case (fig. 7, No. 2) it is remarkable that very little change occurred, although this electrode was most frequently used in the experiments.

The electrodes were actually used to a much greater extent than is indicated in Figure 7, but were not always calibrated for other than a required short range of pH, which did not necessarily include the pH constant. Figure 7 merely records observed limits and was not used for purposes of measurement. Like other types of electrodes,

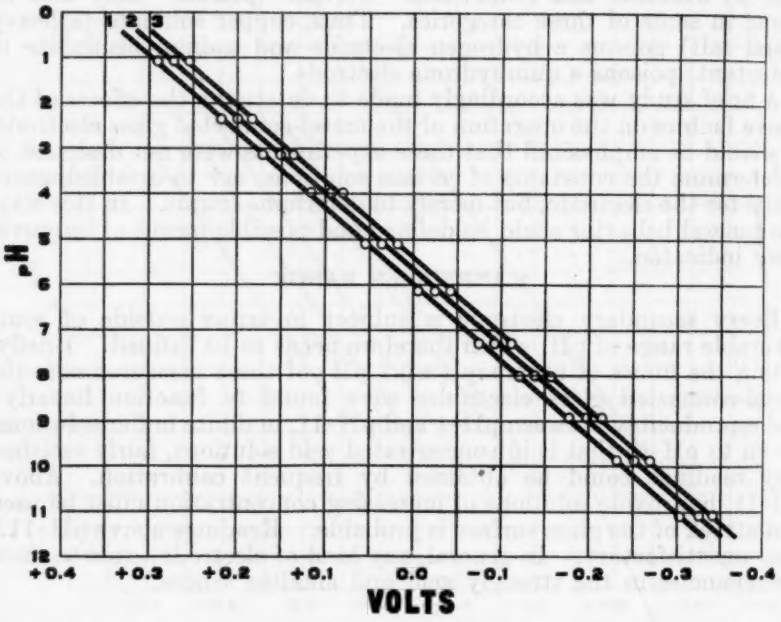

FIGURE 6.—*Actual calibrations of three metal-connected glass electrodes of the containing type*

pH and potential in volts versus saturated calomel electrode at 25° C.

the metal-connected glass electrode required frequent checking, depending on the accuracy desired and the kind of solution under study. It was found advantageous to check an electrode in use several times daily.

4. EFFECT OF ALKALI SALTS (SALT ERROR)

At a given pH, the total concentration and kind of neutral salt present affect the potential of an electrode, causing what is known as the salt error. For the hydrogen electrode this error is zero by definition and for the quinhydrone electrode it is relatively small. To determine the approximate salt error for the metal-connected glass electrode, buffer solutions were prepared containing a large amount of potassium chloride or sodium chloride. The apparent change in pH was then determined.

The results obtained are shown in Tables 3 and 4.

TABLE 3.—*Effect of addition of normal potassium chloride to buffer solutions*

Buffer solution		Change in pH after addition			Salt error	
Composition	pH without addition	Hydrogen electrode	Quinhydrone electrode	Metal-connected glass electrode	Quinhydrone electrode	Metal-connected glass electrode
0.1 *N* HCl	1.10	−0.20	−0.18	−0.24	+0.02	−0.04
0.05 *M* KH_2PO_4+K_2HPO_4	7.00	−.41	−.37	−.44	+.04	−.03
0.1 *N* K_2CO_3	11.20	−.28	.....	−.32	.....	−.04

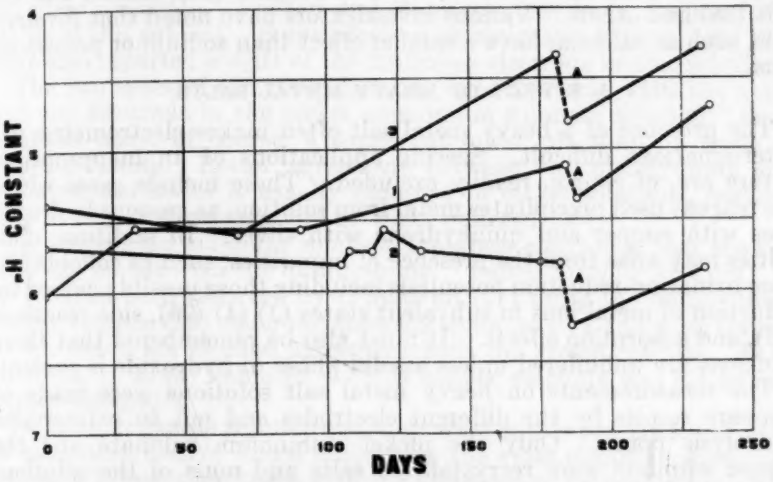

FIGURE 7.—*Variation of pH constant with time for three metal-connected glass electrodes of the containing type*

pH and potential in volts versus saturated calomel electrode at 25° C. *A*, Effect of applying 1,000 volts d. c. for a measurement of resistance

TABLE 4.—*Effect of addition of sodium chloride to buffer solutions*

Buffer solution composition.	NaCl added *N*	Change in pH after addition			Salt error	
		Hydrogen electrode	Quinhydrone electrode	Metal-connected glass electrode	Quinhydrone electrode	Metal-connected glass electrode
0.1 *N* HCl	1	−0.26	−0.28	−0.24	−0.02	+0.02
	2	−.50	−.43	−.41	+.07	+.09
	4	−.90	−.79	−.66	+.11	+.24
0.05 *M* KH_2PO_4+K_2HPO_4	1	−.71	−.62	−.70	+.09	+.01
0.1 *N* K_2CO_3	1	−.46	.....	−.76	.....	−.30
	2	−.66	.....	−1.03	.....	−.34
	4	−.81	.....	−1.39	.....	−.58

The addition of salts caused a decrease in pH (an increase in hydrogen ion activity) in every case. As mentioned above, the change for the hydrogen electrode is attributed to an actual change in the solution and the differential change between the hydrogen and any other electrode then becomes the salt error for that electrode.

Table 3 shows that the salt error caused by potassium chloride up to 1 *N* is only a few hundredths pH throughout the useful range of the

metal-connected glass electrode, or about the same as for the quinhydrone electrode. The salt error caused by sodium chloride (Table 4) is also low in the acid and neutral ranges, but is quite appreciable in the alkaline range.

While these data are not complete, it seems safe to conclude that for best results the total salt concentration should be kept below 1 *N* if possible, and that potassium salts are preferable in alkaline solutions. When high salt concentrations are unavoidable it may be possible to secure more accurate measurements by calibrating the electrode in concentrated buffer solutions.

Similar results have been reported by Hughes (23), Kahler and De Eds (38) and others. Various investigators have noted that divalent ions, such as calcium, have a smaller effect than sodium or potassium ions.

5. EFFECT OF HEAVY METAL SALTS

The presence of a heavy metal salt often makes electrometric pH determinations difficult. Specific applications of an inappropriate nature are, of course, readily excluded. These include cases where the reagent used precipitates metal from solution, as gaseous hydrogen does with copper and quinhydrone with silver. In addition, difficulties may arise from the presence of impurities, such as colloids (2), from oxidation-reduction potentials including those possibly caused by reduction of metal ions to subvalent states (3) (4) (26), side reactions (18), and adsorption effects. It must also be remembered that these solutions are unbuffered unless a solid phase of hydroxide is present.

The measurements on heavy metal salt solutions were made to compare results by the different electrodes and not to redetermine hydrolysis points. Only the nickel ammonium sulphate and the copper sulphate were recrystallized salts and none of the solutions was treated with the corresponding metal hydroxide. The salts used were, however, all of high quality and there is reason to believe that the values obtained are typical, except possibly for manganese.

Colorimetric measurements of pH (uncorrected) could be obtained conveniently with these solutions and were therefore made by the Gillespie drop ratio method (24).

The results obtained with a few typical heavy metal solutions are given in Table 5.

TABLE 5.—*Effect of heavy metal salts on electrodes*

Solution 0.05 *M*	pH of solutions: Hydrogen electrode	Quinhydrone electrode	Membrane glass electrode	Metal-connected glass electrode	Colorimetric (uncorrected)[1]
$ZnSO_4$	5.2–5.6	5.1–5.8	6.15	5.80	6.55 B. c. p. 6.55 B. t. b.
$MnCl_2$	5.5–5.6	4.8–5.2	6.05	5.95	6.80 B. c. p. 7.00 B. t. b.
$NiSO_4$[2]	5.20	5.40	5.45	5.40	5.70 M. r. 5.80 B. c. p.
$CuSO_4$		4.20	4.40	4.30	4.75 B. p. b. 4.50 M. r.
$HgCl_2$			3.60	3.50	3.80 B. p. b.
$AgNO_3$[3]				5.07	6.65 B. c. p. 6.80 B. t. b.

[1] B. p. b., brom phenol blue; M. r., methyl red; B. c. p., brom cresol purple; B. t. b., brom thymol blue.
[2] As $NiSO_4 \cdot (NH_4)_2SO_4 \cdot 6H_2O$.
[3] 0.1 *M*.

The two types of the glass electrode showed good agreement in all the solutions except that of zinc sulphate. In this case the metal-connected electrode gave a value that was nearer than that of the membrane electrode to the hydrogen and quinhydrone values, although these were unsteady. Britton's (14, p. 2120) result for a more dilute (0.025 *M*) solution was 5.2 by the hydrogen electrode. Kolthoff and Kameda (42) found for 0.1 *M* solution a value of 5.67 by means of a specially prepared hydrogen electrode (with a bright platinum deposit) and colorimetrically by methyl red a value of 5.66, practically the same. Britton and Dodd (45) have recently found about 6.3 (interpolated from their fig. 1, p. 1943) for a 0.01 *M* solution, by the glass electrode. Britton and Robinson (46) have discussed the status of this subject. Some previous investigators (2) (21) (22) (26) have also reported a drift of the hydrogen electrode in zinc solutions.

The two types of the glass electrode agreed closely with the quinhydrone electrode in the nickel ammonium sulphate solution. Such solutions have, of course, a somewhat lower pH than do those of nickel sulphate. Better agreement between the quinhydrone and hydrogen electrodes is usually obtained in nickel solutions, particularly at higher concentrations or when buffered (30).

In the copper sulphate solution the glass electrodes also showed good agreement with the quinhydrone. Values for 0.05 *M* $CuSO_4$ at 18° C have been reported by O'Sullivan (17) using the quinhydrone and by Hughes (23) using the glass electrode, as 4.14 and 4.24, respectively, which are in good agreement with the present results. Britton's (14, p. 2148) value for 0.02 *M* copper sulphate was 5.4 by the oxygen electrode.

In the manganese solution readings were somewhat unsteady with all electrodes used. Those made with the glass electrode were considerably higher than those with the hydrogen or quinhydrone. The latter both showed drifts and did not agree closely. Rideal (18) has pointed out that manganese salts tend to catalyze the auto-oxidation of quinhydrone, so that the result by the quinhydrone electrode is doubtful. The accepted value for manganese solutions in the literature is 8.5 to 8.8 (11) (14, p. 2110) by the hydrogen electrode, indicating that these solutions at equilibrium conditions are slightly alkaline, a conclusion that seems anomalous in view of the weakly basic character of divalent manganese. Possibly an oxidation-reduction potential interferes.

The value obtained for the mercuric chloride solution is close to that of Britton and Dodd (45), who found about 3.7 (interpolated from their fig. 1, p. 1943) for a 0.01 *M* solution, by the glass electrode. This replaces an earlier and much higher value of 7.3, by the oxygen electrode, reported by Britton (14, p. 2148).

The value for the silver nitrate solution agrees with that of about 5.0 (interpolated from their fig. 1, p. 1943) found for a more dilute (0.01 *M*) solution by Britton and Dodd (45), by the glass electrode. Britton (14, p. 2148) previously found 5.7 for 0.02 *M* silver nitrate, by the oxygen electrode. He then adopted "pH 9 (?)" tentatively, however, basing this figure on calculations of the solubility product of silver hydroxide. Evidently, this value was too high and the experimental one was nearer correct. Further data and discussion have been given by Britton and Robinson (46). Horovitz (10, p. 389) thought that he detected a silver electrode function of glass in silver

solutions, but this was not confirmed by Hughes (23). Any direct effect of the silver (or copper) coating of the metal-connected electrode is unlikely, as the glass used contained no heavy metals and was comparatively thick.

In general, the results by the colorimetric method (uncorrected) show somewhat higher salt errors for the indicators than would be expected for such dilute solutions. Combination between metal ion and indicator may have occurred in some cases.

6. EFFECT OF PROTEIN

It is well known that proteins are likely to disturb electrode readings. Gelatin was selected for trial, as it is a substance of special interest in electrochemical work, and a few experiments were made on solutions containing various amounts at low, intermediate and high pH values. The data obtained are presented in Table 6.

TABLE 6.—*Effect of gelatin*

Buffer solution	Gelatin g/l	pH		
		Hydrogen electrode	Quinhydrone electrode	Metal-connected glass electrode
0.1 *N* HCl	0	----------	1.13	1.19
	1	----------	1.19	1.17
	5	----------	1.19	1.17
	10	----------	1.17	1.14
0.05 *M* KH_2PO_4+K_2HPO_4	0	----------	6.98	7.01
	1	----------	6.99	7.01
	5	----------	6.98	7.02
	10	----------	6.96	6.98
0.1 *N* K_2CO_3	0	11.00	----------	11.03
	1	10.94	----------	10.98
	5	10.77	----------	10.88
	10	10.59	----------	10.73

Large amounts of gelatin did not appreciably affect the readings of the metal-connected glass electrode at low and intermediate pH values, as compared with the quinhydrone electrode. It is well known that the quinhydrone electrode is itself affected by some proteins. The metal-connected electrode agreed closely with the hydrogen electrode at the high pH when only small amounts of gelatin were present. The pH of the carbonate solution actually decreased when gelatin was dissolved in it. This was accompanied by a slight precipitation.

7. EFFECT OF OXIDANTS AND REDUCTANTS

Strongly oxidizing or reducing compounds cause a potential separate from that of hydrogen ions and usually great enough to prevent the use of the hydrogen or quinhydrone electrode. The latter can be used occasionally, for instance, in dilute nitric acid. Sometimes a metal-metal oxide electrode can be substituted, as that of mercury, manganese, or antimony, which may be convenient even if empirical. Indicators are usually unsatisfactory.

Previous types of the glass electrode have been shown by Hughes (9) MacInnes and Dole (27) and others to be quite unaffected by oxidation-reduction potentials. To determine if this relation holds also for the metal-connected electrode, comparative measurements with this and the membrane glass electrode were made on a few typical solutions. The results are presented in Table 7.

TABLE 7.—*Effect of oxidants and reductants*

Solution	pH		Solution	pH	
	Membrane electrode	Metal-connected electrode		Membrane electrode	Metal-connected electrode
0.1 *M* HNO_3[1]	1.10	1.20	0.1 *M* $K_2Cr_2O_7$	3.75	3.85
1 *M* CrO_3	.45	.65	0.2 *M* K_2CrO_4	9.25	9.30
0.45 *M* $K_2Cr_2O_7$[2]	3.60	3.80	0.05 *M* As_2O_3	5.60	5.55
1 *M* K_2CrO_4	9.45	9.55	0.25 *M* $Na_2S_2O_3$	4.90	4.80
0.2 *M* CrO_3	.90	1.05	0.1 *M* NaCN[3]		11.0

[1] 1.14 by quinhydrone electrode.
[2] Saturated solution.
[3] 11.5 (maximum) by hydrogen electrode.

The two types of glass electrodes gave about the same results. The lower values by the membrane electrode, particularly in the more concentrated oxidizing solutions, are probably more accurate, as this type seems less subject to disturbances, possibly of the nature of adsorption effects.

The results for the chromic acid and chromate solutions agree roughly with the end points of the titration curves published by Hughes (9) and by Britton (12) (13) (43, p. 73, p. 162). Hughes used a glass electrode of the bulb type and 0.1 *M* chromic acid, while Britton used both oxygen and hydrogen electrodes in very dilute (about 0.025 *M*) chromic acid.

It is of interest to note the great difference in strength between dichromic and chromic acid, on account of which chromate solutions are distinctly alkaline because of hydrolysis. (The acidity of the dichromate solutions may be attributed to secondary dissociation of the dichromate ion.)

Readings in the bisulphite solution were often unsteady, probably because of absorption of oxygen from the air and a resulting change in acidity. The hydrogen (43, p. 73), quinhydrone and oxygen (43, p. 73) electrodes all fail in bisulphite or sulphite solutions.

The value for sodium cyanide is consistent with the hydrolysis measurements of Harman and Worley (16) and with a measurement by Britton and Robinson (40) on dilute potassium cyanide solution (0.04 *M*), with the antimony electrode. Britton and Dodd (45) later found the glass electrode to be more accurate than the antimony electrode, in cyanide solutions. The hydrolysis of alkali cyanide is evidently about the same as that of alkali carbonate.

8. APPLICATIONS

Applications of the metal-connected glass electrode in research have been made by the author in connection with pH measurements

on chromic acid and chromium chromate solutions, cyanide silver-plating solutions (preferably diluted), and ammoniacal silver bromide-gelatin photographic emulsions. In general, consistent and useful results were obtained. These will be published in separate papers by other investigators.

V. SUMMARY

1. Glass electrodes with a direct metallic connection may be constructed having comparatively good accuracy and sensitivity.

2. This shows that an equilibrium between hydrogen ions on opposite sides of a glass wall is not essential to the functioning of glass as an electrode, and suggests that deep penetration of hydrogen ions into the glass may not occur.

3. The metal-connected electrodes may be constructed with walls thick enough to make breakage unlikely with ordinary care in handling.

4. Their useful life is indefinite and measured by months or years.

5. Only small errors are caused by alkali salts in moderate concentration, by heavy metal salts in low concentration and by gelatin.

6. Oxidation-reduction potentials have little, if any, effect with this or other types of glass electrodes.

VI. ACKNOWLEDGMENTS

The writer acquired his first experience with the technique of glass electrodes during March and April, 1929, as a guest at the Rockefeller Institute for Medical Research in New York City. Grateful acknowledgment is herewith made to Dr. D. A. MacInnes of that institution and to Dr. M. Dole, formerly there but now at Northwestern University, Evanston, Ill.

Acknowledgment is also made to Dr. W. Blum, who directed this research and whose advice has been most helpful.

VII. BIBLIOGRAPHY

1. Cremer, M., Zeits. Biologie, vol. 47, p. 562. 1906.
2. Denham, H. G., J. Chem. Soc., vol. 93, p. 41. 1908.
3. Denham, H. G. and Allmand, A. J., J. Chem. Soc., vol. 93, p. 424. 1908.
4. Denham, H. G., J. Chem. Soc., vol. 93, p. 833. 1908.
5. Haber, F. and Klemensiewicz, Z., Zeits. Phys. Chemie, vol. 67, p. 385. 1909.
6. Borelius, G., Ann. Physik (4), vol. 42, p. 1129. 1913.
7. Borelius, G., Ann. Physik. (4), vol. 45, p. 929. 1914.
8. Borelius, G., Ann. Physik (4), vol. 50, p. 447. 1916.
9. Hughes, W. S., J. Am. Chem. Soc., vol. 44, p. 2860. 1922.
10. Horovitz, K., Zeits Physik., vol. 15, p. 369. 1923.
11. Allmand, A. J. and Campbell, A. N., Trans. Faraday Soc., vol. 20, p. 379. 1924.
12. Britton, H. T. S., J. Chem. Soc., vol. 125, p. 1572. 1924.
13. Britton, H. T. S., J. Chem. Soc., vol. 127, p. 1896. 1925.
14. Britton, H. T. S., J. Chem. Soc., vol. 127, pp. 2110, 2120, 2142, and 2148. 1925.
15. Horovitz, K., Sitz. Akad. Wiss. Wien, Abt. IIa, vol. 134, p. 335. 1925.
16. Harman, R. W., and Worley, F. P., Trans. Faraday Soc., vol. 20, p. 502. 1925.
17. O'Sullivan, J. B., Trans. Faraday Soc., vol. 21, p. 319. 1925.
18. Rideal, E. K., Trans. Faraday Soc., vol. 21, p. 325. 1925.
19. Rideal, E. K., an introduction to Surface Chemistry, Cambridge University Press. London, 1926.
20. Kerridge, P. M. T., J. Sci. Instruments, vol. 3, p. 404, 1926.

21. Frölich, Per K., Trans. Am. Electrochem. Soc., vol. 49, p. 395. 1926.
22. Thompson, M. R., Trans. Am. Electrochem. Soc., vol. 50, p. 193. 1926.
23. Hughes, W. S., J. Chem. Soc., p. 491. 1928.
24. Clark, W. M., The Determination of Hydrogen Ions, 3d ed. 1928. Williams & Wilkins Co., Baltimore, Md.
25. Elder, L. W., jr., and Wright, W. H., Proc. Nat. Acad. Sci., vol. 14, p. 936. 1928.
26. Denham, H. G., and Marris, N. A., Trans. Faraday Soc., vol. 24, p. 510. 1928.
27. MacInnes, D. A., and Dole, M., Ind. & Eng. Chem., Anal. ed., vol. 1, p 57. 1929.
28. MacInnes, D. A., and Dole, M., J. Gen. Physiol., vol. 12, p. 805. 1929.
29. Elder, L. W., jr., J. Am. Chem. Soc., vol. 51, p. 3266. 1929.
30. Blum, W., and Bekkedahl, N., Trans. Am. Electrochem. Soc., vol. 56, p. 291. 1929.
31. MacInnes, D. A., and Dole, M., J. Am. Chem. Soc., vol. 52, p. 29. 1930.
32. Voegtlin, C., De Eds, F., and Kahler, H., Reprint No. 1413, Public Health Reports, vol. 45, p. 2223. 1930.
33. Elder, L. W., jr., Trans. Am. Electrochem. Soc., vol. 57, p. 383. 1930.
34. MacInnes, D. A., and Belcher, D., J. Am. Chem. Soc., vol. 53, p. 3315. 1931.
35. Dole, M., J. Am. Chem. Soc., vol. 53, p. 4260. 1931.
36. Robertson, G. R., Ind. & Eng. Chem., Anal. ed., vol. 3, p. 5. 1931.
37. The Making of Mirrors by the Deposition of Metal on Glass, circular of the Bureau of Standards, No. 389. 1931.
38. Kahler, H., and De Eds, F., J. Am. Chem. Soc., vol. 53, p. 2998. 1931.
39. Hazel, F., and Sorum, C. H., J. Am. Chem. Soc., vol. 53, p. 49. 1931.
40. Britton, H. T. S., and Robinson, R. A., J. Chem. Soc., 458. 1931.
41. Lengyel, B. v., Zeits. Physik. Chem., Abt. A, vol. 153, p. 425. 1931.
42. Kolthoff, I. M., and Kameda, T., J. Am. Chem. Soc., vol. 53, p. 832. 1931.
43. Britton, H. T. S., Hydrogen Ions, 2d ed., D. Van Nostrand Co., New York City. 1932.
44. Dole, M., J. Am. Chem. Soc., vol. 54, p. 3095. 1932.
45. Britton, H. T. S., and Dodd, E. N., J. Chem. Soc., p. 1940. 1932.
46. Britton, H. T. S., and Robinson, R. A., Trans. Faraday Soc., vol. 28, p. 531. 1932.
47. Compton, K. G., and Haring, H. E., Trans. Electrochem. Soc., vol. 62. 1932 (preprint).

WASHINGTON October 11, 1932.

145879—32——10

INDEX TO VOLUME 9

A

Page

Aberrations of lenses, RP466 187
Absorption of sound by air, RP465 175
Absorption spectra, chromium dichromate, RP476 353
Acken, J. S., J. G. Thompson and, Determination of alumina and silica in steel by the hydrochloric acid residue method, RP496 615
Adhesion of mortar to brick and steel, RP504 749
Air, sound absorption of, RP465 175
variation with pressure, of intrinsic energy, RP503 733
Alloy steels, creep in, at elevated temperatures, RP481 441
Alloys, nickel-chromium-iron, tensile properties of, at elevated temperatures, RP474 327
Alumina, determination of, in steel, RP496 615
Aluminum nitride, effect of, in residue analysis, RP496 615
Ammonium bromoosmate, density of, RP471 297
preparation of, RP471 279
Ammonium chloroosmate, density of, RP471 279
preparation of, RP471 279
Amplifier for feeble pulses, RP461 115
Amyl bromide, normal, physical constants of, RP482 457
purification of, RP482 457
synthesis of, RP482 457
Analysis of lanthanum spectra, RP497 625
Analysis of solutions containing rhodium and iridium, RP489 547
Analysis of weighted silk, RP498 669
Analysis, residue methods of, in steel, RP496 615
Angle variation, RP493 583
Arc spectra, infra-red, photographed with xenocyanine, RP473 309
Areas of reinforcement bars, RP486 509
Artichokes, hydrolysis of, RP495 597
Atomic weight of osmium, RP271 279
Audio-frequency amplifier, RP461 115
Axial loading of fatigue tests of steel, RP454 9

B

Barbrow, L. E., and J. Franklin Meyer, Characteristic equations of vacuum and gas-filled tungsten-filament lamps, RP502 721
Barometric pressure, effect on sound absorption of air, RP465 175
Basic chromium chromate, RP476 353
Beams, brickwork, reinforced, shear tests of, RP504 749
Bennett, Harold F., The reciprocal spherical aberration of an optical system including higher orders, RP466 187
Benzoinoxime, use of, RP453 1
Blackburn, George F., Paul T. Hannen, Melville F. Peters and, Theory of voltage dividers and their use with cathode ray oscillographs, RP460 81
Boeckner, C., Radiation from cæsium and other metals bombarded by slow electrons, RP478 413
——, Variation with angle of emission of radiation from metals by slow electrons, RP493 583
Bond for reinforced brickwork, RP504 749
Bond strength of brick masonry to steel, RP504 749
Bond strength of mortar to brick, RP504 825
Boric oxide, binary system with lime, RP510 733
Brick, bond of mortar to, RP504 749
Brick masonry, reinforced, RP504 749

Page

Brooks, H. B., and A. W. Spinks, A multirange potentiometer and its application to the measurement of small temperature differences, RP506 781
Bruun, Johannes H., and Mildred M. Hicks-Bruun, Note on the freezing point of "iso-octane" (2, 2, 4-trimethylpentane), RP469 269
——, ——, Note on the probable presence of 2, 2-dimethylpentane in a midcontinent petroleum, RP458 53
Buckingham, Edgar, Notes on the orifice meter: The expansion factor for gasses, RP459 61

C

Cæsium discharge, collisions of the first and second kind in the positive column of, RP485 493
power input and dissipation in the positive column of a, RP455 25
Calcium borates, optical properties and melting points of, RP510 825
Calcium oxide, binary system with boric oxide, RP510 733
Carbon dioxide and oxygen mixtures, variation, with pressure, RP503 733
Carlson, Elmer T., The system: CaO–B_2O_3, RP510 825
Carroll, Burt H., and Donald Hubbard, The photographic emulsion; variables in sensitization by dyes, RP488 529
Ceramic bodies of low absorption maturing at temperatures below 1,000° C., a study of, RP483 473
Ceramic ware, expansion of, RP472 291
Characteristic equations of lamps, RP502 721
Chase, W. D., J. A. Mathews, R. F. Jackson and, Analytical methods for the determination of levulose in crude products, RP495 597
Chrisler, V. L., and Catherine E. Miller, Some of the factors which affect the measurement of sound absorption, RP465 175
Chromic acid, structure, RP476 353
Chromium deposition, theory, RP476 353
Chromium dichromate, structure, RP476 353
Chromium sulphate, state in chromic acid, RP476 353
Cobalt, infra-red arc spectrum, RP473 309
Coff, R. M., C. G. Weber and, Register studies in offset lithography, RP480 427
Collisions of the first and second kind in the positive column of cæsium discharge, RP485 493
Column curves and stress-strain diagrams, RP492 571
Color sensitization, RP488 529
Columns, strength of, RP492 571
Composition and density of glass, RP507 799
Conductivity of chromium dichromate solutions, RP476 353
Considère-Engesser theory of column failure, RP492 571
Cosmic rays, deflection of, by a magnetic field, RP509 815
Constructing platinum resistance thermometers, TP508 807
Counters, Geiger-Müller, RP509 815
Creamer, A. S., R. F. Geller and, "Moisture expansion" of ceramic whiteware, RP472 291
Creep in alloy steels, RP481 441

Page

Cummings, A. D., The influence of temperature on the evolution of hydrogen sulphide from vulcanized rubber, RP464 ... 163
Curtiss, L. F., A vacuum tube amplifier for feeble pulses, RP461 ... 115
Curtiss, L. F., Deflection of cosmic rays by a magnetic field, RP509 ... 815

D

Decane, normal, physical constants of, RP482 ... 457
purification of, RP482 ... 457
synthesis of, RP482 ... 457
Deformation of chromate ion, dichromate ion, RP476 ... 353
Density and composition of glass, RP507 ... 799
Density of lime glasses, RP507 ... 799
Dimethylpentane in petroleum, RP458 ... 53
Dimethylpentane, infra-red absorption spectrum, RP458 ... 53
Dividers, voltage, for cathode ray oscillographs, RP460 ... 81
theory of, and their use with cathode ray oscillographs, RP460 ... 81
Dodecane, normal, physical constants of, RP482 ... 457
purification of, RP482 ... 457
synthesis of, RP482 ... 457
Dyes, photographic sensitizing, RP488 ... 529

E

Earthenware, expansion of, RP472 ... 291
Efficiency of tungsten lamps, RP502 ... 721
Electrode, metal connected glass, RP511 ... 833
Electrometric titration of chromic acid, RP476 ... 353
Electron radiation {RP478 ... 413 / RP493 ... 583}
Electrophoresis, basic chromium chromate, RP476 ... 353
Elevated temperatures, creep of steels at, RP481 ... 441
Empirical column formulas compared with Considère-Engesser theory, RP492 ... 571
Emulsions, photographic, RP488 ... 529
Endurance properties of steel, RP454 ... 9
Energy, intrinsic, of gases, measurement of, RP487 ... 521
Equations of tungsten lamps, RP502 ... 721
Evans, D. N., R. F. Geller and, A study of some ceramic bodies of low absorption maturing at temperatures below 1,000° C., RP483 ... 473
Expansion factor for gasses, RP459 ... 61
Expansion, moisture, of ceramic whiteware, RP472 ... 291
Expansion of ceramic ware, RP472 ... 291
Expansion of earthenware, RP472 ... 291
Expansion, thermal, of lead, RP500 ... 703
of some silicates of elements in Group II of the periodic system, RP456 ... 35
Expansion of whiteware, RP472 ... 291

F

Factor, expansion, for gasses, RP459 ... 61
Fatigue limits of coated steels, RP454 ... 9
Fatigue testing, notch effect in, RP454 ... 9
Fatigue testing of steels, RP454 ... 9
Finn, A. N., J. C. Young, F. W. Glaze and, The density of some soda-lime-silica glasses as a function of the composition, RP507 ... 799
Floors, light-weight steel, RP463 ... 131
France, R. D., W. H. Swanger and, Effect of zinc coatings on the endurance properties of steel, RP454 ... 9
Frandsen, Mikkel, Frederick D. Rossini and, The calorimetric determination of the intrinsic energy of gases as a function of the pressure. Data on oxygen and its mixtures with carbon dioxide to 40 atmospheres at 28° C., RP503 ... 733
Frankland, J. M., and H. L. Whittemore, Tests of cellular sheet steel flooring, RP463 ... 131

Page

Freezing point lowering, of chromium solutions, RP476 ... 333
Freezing point of iso-octane, RP469 ... 269
Freezing point of octane, RP469 ... 269
Fruits, analyses of, RP495 ... 507

G

Gage, Whittemore, attachment of, to specimen, RP463 ... 131
Gages, strain, Whittemore, RP463 ... 131
Gardner, I. C., An attachment for turning approximately spherical surfaces of small curvature on a lathe, RP467 ... 227
Gas-filled tungsten lamps, equations of, RP502 ... 721
Gases, expansion factor for, RP459 ... 61
intrinsic energy, measurement of, as function of pressure, RP487 ... 521
P—V—T data for, RP470 ... 271
variation, with pressure, of intrinsic energy of, RP503 ... 733
Guarded field ionization chamber, RP505 ... 769
Geiger-Müller counters, RP509 ... 815
Geller, R. F., and A. S. Creamer, "Moisture expansion" of ceramic whiteware, RP472 ... 291
—— *and D. N. Evans*, A study of some ceramic bodies of low absorption maturing at temperatures below 1,000° C., RP483 ... 473
—— *and Herbert Insley*, Thermal expansion of some silicates of elements in Group II of the periodic system, RP456 ... 35
Generators, high voltage, RP491 ... 661
Gilchrist, Raleigh, A method for the separation of rhodium from iridium and the galvimetric determination of these metals, RP489 ... 547
——, A new determination of the atomic weight of osmium, RP471 ... 279
Glass, composition and density of, RP507 ... 799
Glass electrode, application in chromic acid, RP476 ... 353
metal-connected, RP511 ... 833
Glasses, density of lime glasses, RP507 ... 799
Glaze, F. W., J. C. Young, and A. N. Finn, The density of some soda-lime-silica glasses as a function of the composition, RP507 ... 799
Gough, C., L. R. Sweetman, A. H. Stang and, The areas and tensile properties of deformed concrete-reinforcement bars, RP486 ... 809
Green chromic dichromate, nonexistence, RP476 ... 353
Green chromium sulphate, in chromic acid solution, RP476 ... 353
Green ray measurements, RP505 ... 769

H

Half value layer, X rays, RP475 ... 333
Hamilton, E. H., J. G. Thompson and, Nitrogen content of some standard-sample steels, RP494 ... 503
Hannen, Paul T., George F. Blackburn, Melville F. Peters and, Theory of voltage dividers and their use with cathode ray oscillographs, RP460 ... 81
Harris, Milton, The isoelectric point of silk, RP490 ... 657
Heat of formation of hydrogen chloride, RP499 ... 679
Helium, infra-red spectrum of, RP462 ... 121
Helix, inductance of, RP479 ... 419
Heptane, normal, physical constants of, RP482 ... 457
Hexane, normal, physical constants of, RP482 ... 457
purification of, RP482 ... 457
synthesis of, RP482 ... 457
Hicks-Bruun, Mildred M., Johannes H. Bruun and, Note on the freezing point of "iso-octane" (2, 2, 4-trimethylpentane), RP469 ... 269
——, ——, Note on the probable presence of 2, 2-dimethylpentane in a midcontinent petroleum, RP458 ... 53

Page

Hidnert, Peter, and W. T. Sweeny, Thermal expansion of lead, RP500 703
High pressures, accurate method for measurement of, RP470 271
High temperatures, tensile properties of cast nickel-chromium-iron alloys and alloy steels at, RP474 327
High voltage generators {RP475 ..... 333 / RP491 561
High voltage measurements {RP475 ..... 333 / RP491 561
Hoffman, James I., The determination of magnesia in phosphate rock, RP484 487
Honey, analyses of, RP495 597
Hubbard, Donald, Burt H. Carroll and, The photographic emulsion; variables in sensation by dyes, RP488 529
Humidity, effect of, on sound absorption of air, RP465 175
Hydrocarbons, normal, physical constants of, RP482 457
purification of, RP482 457
syntheses of, RP482 457
petroleum extraction of, with liquid sulphur dioxide, RP501 711
xylene, in petroleum, RP501 711
xylene isolation of, from petroleum, RP501 711
Hydrochloric-acid residue method for steel, RP496 615
Hydrogen chloride, calculation of some thermodynamic data for, RP499 679
Hydrogen chloride, heat of formation, RP499 679
Hydrogen ion concentration, effect on chromium deposition, RP476 353
Hydrogen ion concentration of chromium chromate solutions, RP476 353
Hydrogen sulphide, rate of evolution from vulcanized rubber, RP464 163

I

Inductance of helix, RP479 419
Infra-red arc spectra photographed with xenocyanine, RP473 309
Infra-red spectra of helium, RP462 121
Insley, Herbert, R. F. Geller and, Thermal expansion of some silicates of elements in Group II of the periodic system, RP456 35
Intrinsic energy of gases, variation of, with pressure, RP503 783
Ionization chambers, RP505 769
Iridium, determination of RP489 547
Iridium dioxide, hydrolytic precipitation of, RP489 547
Iridium, separation of rhodium from, RP489 547
Iridium sulphate, preparation of solutions containing, RP489 547
Iron, determination of molybdenum in, RP453 1
infra-red arc spectrum of, RP473 309
Isoelectric point, basic chromium chromate, RP476 353
Isoelectric point of silk, RP490 557
Iso-octane, freezing point of, RP469 269

J

Jackson, R. F., J. A. Mathews, and W. D. Chase, Analytical methods for the determination of levulose in crude products, RP495 597
Jordan, Louis, William Kahlbaum and, Creep at elevated temperatures in chromium-vanadium steels containing tungsten or molybdenum, RP481 441
——, ——, Tensile properties of cast nickel-chromium-iron alloys and some alloy steels at elevated temperatures, RP474 327
Joule-Thompson coefficient, calorimetric measurement of, RP487 521

K

Kahlbaum, William, and Louis Jordan, Creep at elevated temperatures in chromium-vanadium steels containing tungsten or molybdenum, RP481 441

Page

Kahlbaum, William, and Louis Jordan, Tensile properties of cast nickel-chromium-iron alloys and some alloy steels at elevated temperatures, RP474 327
Kasper, Charles, The structure of chromic acid plating bath; the theory of chromium deposition, RP476 353
Kessler, D. W., and W. H. Sligh, Physical properties and weathering characteristics of slate, RP477 377
Kiess, C. C., William F. Meggers and, Infra-red arc spectra photographed with xenocyanine, RP473 309
Knowles, H. B., The use of α-benzoinoxime for the determination of molybdenum, RP453 1

L

Lamps, characteristic equations of, RP502 721
tungsten, gas-filled, RP502 721
tungsten vacuum, RP502 721
Lane and Eynon method, modification of, RP495 597
Lanthanum, an analysis of spectra, RP497 625
Lanthanum spectra, RP468 239
Lathe, attachment for turning spherical surfaces on, RP467 227
Lead, detection of, in weighted silk, RP498 669
thermal expansion of, RP500 703
Lens grinding tools, attachment for turning on lathe, RP467 227
Lenses, aberrations of, RP466 187
Levulose, determination of, RP495 597
Light, infra-red, absorption by xylenes of, RP501 711
Lime, binary system with boric oxide, RP510 825
Lithographic papers, RP480 427
Lithography, factors affecting register, RP480 427
register of prints, RP480 427
Low voltage X rays, RP505 769
Lugs, effect of, on tensile properties of bars, RP486 509

M

McBurney, J. W., A. H. Stang, D. E. Parsons and, Shear tests of reinforced brick masonry beams, RP504 749
Machined reinforcement bars, tests of, RP486 509
Magnesia in phosphate rock, RP484 487
Magnetic deflection, RP509 815
Mair, B. J., The synthesis, purification, and certain physical constants of the normal hydrocarbons from pentane to dodecane, of *n*-amyl bromide and *n*-monyl bromide, RP482 457
Manganese silicates, recovery of, by residue analysis, RP496 615
Manganous oxide, recovery of, by residue analysis, RP496 615
Masonry, brick, reinforced, RP504 749
Mathews formula, RP495 597
Mathews, J. A., W. D. Chase, R. F. Jackson and, Analytical methods for the determination of levulose in crude products, RP495 597
Mease, Ralph T., Analysis of weighted silk, RP498 669
Measurements, high voltage, RP491 561
Measurement of high pressures, RP470 271
Meggers, William F., Wave lengths and zeeman effects in lanthanum spectra, RP468 239
——, *Henry Norris Russell and*, An analysis of lanthanum spectra (La I, La II, La III), RP497 625
——, *and C. C. Kiess*, Infra-red arc spectra photographed with xenocyanine, RP473 309
——, *and G. H. Dieke*, Infra-red spectra of helium, RP462 121
Metal-connected glass electrode, RP511 833
Metal radiation {RP478 ..... 413 / RP493 583
Meter, an automatic reverberation, for the measurement of sound absorption, RP457 47

Page

Meter, notes on the orifice, RP459 61
Meyer, J. Franklin, L. E. Barbrow and, Characteristic equations of vacuum and gas-filled tungsten-filament lamps, RP502 721
Meyers, C. H., Coiled-filament resistance thermometers, RP508 807
Miller, Catherine E., V. L. Chrisler and, Some of the factors which affect the measurement of sound absorption, RP465 175
Misregister in offset lithography, RP480 427
Mohler, F. L., Collisions of the first and second kind in the positive column of cæsium discharge, RP485 493
——, Power input and dissipation in the positive column of cæsium discharge, RP455 25
Moisture expansion of ceramic whiteware, RP472 291
Molybdenum, determination of, RP453 1
in iron, RP453 1
in ores, RP453 1
in steel, RP453 1
Mortar, adhesion to brick and steel, RP504 749
Multi-range potentiometer, RP506 781

N

Nickel, infra-red arc spectrum of, RP473 309
Nitrogen in standard-sample steels, RP494 593
Nonane, normal, physical constants of, RP482 457
purification of, RP482 457
synthesis of, RP482 457
Nonyl bromide, normal, crystalline modifications of, RP482 457
physical constants of, RP482 457
purification of, RP482 457
synthesis of, RP482 457
Notch effect in fatigue testing, RP454 9
Nuclear sensitization, RP488 529

O

Octane, normal, synthesis of, RP482 457
physical constants of, RP482 457
purification of, RP482 457
Octane (2, 2, 4-trimethylpentane), freezing point of, RP469 269
Offset lithography, misregister, RP480 427
paper and register, RP480 427
register of prints, RP480 427
Optical systems, aberrations of, RP466 187
Optics, lens aberrations of, RP466 187
Ores, determination of molybdenum in, RP453 1
Orifice meter, notes on the, RP459 61
Osgood, William R., Column curves and stress-strain diagrams, RP492 571
Osmium, determination of the atomic weight of, RP271 279
preparation of pure, RP271 279
Oxygen, variation, with pressure, of intrinsic energy of, RP503 733

P

Parsons, D. E., A. H. Stang, and J. W. McBurney, Shear tests of reinforced brick masonry beams, RP504 749
Pentane, normal, physical constants of, RP482 457
purification of, RP482 457
synthesis of, RP482 457
Peters, Melville F., George F. Blackburn, and Paul T. Hanne, Theory of voltage dividers and their use with cathode ray oscillographs, RP460 81
Petroleum, extraction of xylenes from, with liquid sulphur dioxide, RP501 711
Petroleum, occurrence of dimethylpentane in, RP458 53
Petroleum, xylenes in, RP501 711
Phase equilibrium diagram for system: CaO-B_2O_3, RP510 825
Phosphate, detection of, in weighted silk, RP498 669
Phosphate rock, magnesia in, RP484 487

Page

Photographic emulsions, RP488 529
Photographic sensitizing dyes, RP488 529
Physical properties of slate, RP477 377
Physical tests on slate, RP477 377
Planimeter method of area determination, RP486 509
Platinum resistance thermometers, RP508 807
Polarization in chromic acid solutions, RP476 393
Positive column of cæsium discharge, collision of the first and second kind in the, RP485 493
Positive column of cæsium discharge, power input and dissipation in the, RP455 25
Potentiometer, a multi-range, RP506 781
Lindeck-Rothe type, RP506 781
Power input and dissipation in the positive column of cæsium discharge, RP455 25
Pressure coefficient of intrinsic energy of gases, RP503 733
Pressure-volume-temperature data, twin bomb method for, RP470 271
Pressures, high, accurate method for measurement of, RP470 271
Properties of steel, RP454 9
Pulse, a vacuum tube amplifier for feeble, RP461 113

R

Radiation, electron {RP478 413 / RP493 593
metal {RP478 413 / RP493 593
Reciprocal spherical aberration, RP466 187
Reduction of chromic acid, mechanism, RP476 393
Reinforcement bars, areas and tensile properties of, RP486 509
Reinforced brickwork beams, RP504 749
Residue methods of analysis for steel, RP496 615
Resistance thermometers, coiled-filament resistance, RP508 807
Reverberation meter, an automatic, for the measurement of sound absorption, RP457 47
Reverberation time, measurement of, RP465 175
Rhodium, determination of, RP489 547
Rhodium dioxide, hydrolytic precipitation of, RP489 547
Rhodium, separation of iridium from, RP489 547
solution in sulphuric acid of, RP489 547
sulphate, incomplete precipitation of rhodium by hydrogen sulphide from, RP489 547
preparation of solutions containing, RP489 547
Rock, phosphate, magnesia in, RP484 487
Roofing slate, RP477 377
Rose, Jr., F. W., Joseph D. White and, Isolation of the three xylenes from an Oklahoma petroleum, RP501 711
Rossini, Frederick D., The heat of formation of hydrogen chloride and some related thermodynamic data, RP490 679
——, *and Mikkel Frandsen,* The calorimetric determination of the intrinsic energy of gases as a function of the pressure. Data on oxygen and its mixtures with carbon dioxide to 40 atmospheres, at 20° C., RP503 733
Rotating beam fatigue tests, RP454 9
Rubber, deterioration of vulcanized, RP464 163
hydrogen sulphide from vulcanized, RP464 163
Russell, Henry Norris, and William F. Meggers, An analysis of lanthanum spectra (La I, La II, La III), RP497 635

S

Self-inductance formula, RP479 419
Sensitization, color, RP488 529
nuclear, RP488 529
Sheet steel, cellular floor, tensile properties, stress-strain curves, Young's modulus of elasticity, RP463 131
Silicates, thermal expansion of some, of elements in Group II of the periodic system, RP456 35

Page

Silica, determination of, in steel, RP496 615
Silicate, detection of, in weighted silk, RP498 669
Silk, isoelectric point of, RP490 557
weighted, analysis of, RP498 669
Singer, George, C. F. Stoneburner, Lauriston S. Taylor and, Effective applied voltage as an indicator of the radiation emitted by an X-ray tube, RP491 561
Slate, physical properties and weathering characteristics of, RP477 377
physical properties of, RP477 377
physical tests on, RP477 377
roofing, RP477 377
tests of, RP477 377
weathering of, RP477 377
Sligh, W. H., D. W. Kessler and, Physical properties and weathering characteristics of slate, RP477 377
Snow, Chester, A simplified precision formula for the inductance of a helix with corrections for the lead-in wires, RP479 419
Snyder, W. F., An automatic reverberation meter for the measurement of sound absorption, RP457 47
Solenoid, inductance of, RP479 419
Sound absorption, measurement of, by automatic reverberation meter, RP457 47
Sound absorption of air, RP465 175
Spectra, analysis of lanthanum, RP497 625
infra-red arc, photographed with xenocyanine, RP473 309
infra-red, of helium, RP462 121
lanthanum, RP468 239
Spectrum, infra-red absorption, of xylenes, RP501 711
Spherical surface, attachment for turning on lathe, RP467 227
Spinks, A. W., H. B. Brooks and, A multirange potentiometer and its application to the measurement of small temperature differences, RP506 781
Spot welds, projection spot welds, shearing strength, specimen for determining shearing strength, RP463 131
Standard-sample steels, nitrogen content of, RP494 593
Stang, A. H., J. W. McBurney, D. E. Parsons and, Shear tests of reinforced brick masonry beams, RP504 749
Stang, A. H., L. R. Sweetman, and C. Gough, The areas and tensile properties of deformed concrete-reinforcement bars, RP486 509
Steel, determination of molybdenum in, RP453 1
endurance properties of, RP454 9
properties of, RP454 9
residue methods of analysis for, RP496 615
sheet, cellular floor, tensile properties, stress-strain curves. Young's modulus of elasticity, RP463 131
Steels, alloy, creep in, at elevated temperatures, RP481 441
tensile properties of, at elevated temperatures, RP474 327
chromium-vanadium, creep in, RP481 441
fatigue limits of coated, RP454 9
fatigue testing of, RP454 9
nitrogen in standard-sample, RP494 593
Stoneburner, C. F., George Singer, Lauriston S. Taylor and, Effective applied voltage as an indicator of the radiation emitted by an X-ray tube, RP491 561
——, *Lauriston S. Taylor and,* The low voltage X-ray intensities, RP505 769
Strain gages, Whittemore hand strain gage, RP463 131
Strength of columns, RP492 571
Sulphate, function in chromium plating, RP476 353
Sulphur dioxide (liquid), extraction of xylenes from petroleum with, RP501 711
Sulphur, loss of, from vulcanized rubber, RP464 163
Swanger, W. H., and R. D. France, Effect of zinc coatings on the endurance properties of steel, RP454 9

Page

Sweeny, W. T., Peter Hidnert and, Thermal expansion of lead, RP500 703
Sweetman, L. R., C. Gough, A. H. Stang and, The areas and tensile properties of deformed concrete-reinforcement bars, RP486 509
System: CaO–B_2O_3, RP510 825

T

Taylor, Lauriston S., and C. F. Stoneburner, The measurement of low voltage X-ray intensities, RP505 769
——, *George Singer, and C. F. Stoneburner,* Effective applied voltage as an indicator by the radiation emitted by an X-ray tube, RP491 561
——, *and K. L. Tucker,* The comparison of high-voltage X-ray generators, RP475 333
Temperature, effect of, on sound absorption of air, RP465 175
Temperatures, high, tensile properties of cast nickel-chromium-iron alloys and alloy steels at, RP474 327
Tensile properties of cast nickel-chromium-iron alloys and alloy steels at elevated temperatures, RP474 327
Tensile properties of reinforcement bars, RP486 509
Tests, axial loading fatigue, RP454 9
Tests on slate, RP477 377
Tests, rotating beam fatigue, RP454 9
Textiles, weighted silk, RP498 669
Thermal expansion of lead, RP500 703
Thermal expansion of some silicates of elements in Group II of the periodic system, RP456 35
Thermocouple, potentiometer used with, RP506 781
Thermodynamic data for hydrogen chloride, RP499 679
Thermometers, coiled filament resistance, RP508 807
Thompson, J. G., and J. S. Acken, Determination of alumina and silica in steel by the hydrochloric acid residue method, RP496 615
——, *and E. H. Hamilton,* Nitrogen content of some standard-sample steels, RP494 593
Thompson, M. R., A metal-connected glass electrode, RP511 833
Tube counters, RP509 815
Tungsten-filament lamps, characteristic equations of, RP502 721
Tin, detection of, in weighted silk, RP498 669
Titanium, infra-red arc spectrum of, RP473 309
Titanous chloride, separation of rhodium from iridium by, RP489 547
Trimethylpentane, 2, 2, 4-freezing point of, RP469 269
Tucker, K. L., Lauriston S. Taylor and, The comparison of high voltage X-ray generators, RP475 333
Turning, attachment for, spherical surfaces on lathe, RP467 227

U

Undecane, normal, physical constants of, RP482 457
purification of, RP482 457
synthesis of, RP482 457

V

Vacuum-tungsten lamps, equation of, RP502 721
Variation, angle, RP493 583
Violent chromium, nonexistence in chromic acid, RP476 353
Voltage dividers for cathode ray oscillographs, RP460 81
Voltage dividers, theory of, and their use with cathode ray oscillographs, RP160 81
Vulcanized rubber, deterioration of, RP464 163
effect of heat on, RP464 163
hydrogen sulphide from, RP464 163

W

Page

Washburn, Edward W., A calorimetric method for determining the intrinsic energy of a gas as a function of the pressure, RP487 521
——, A twin-bomb method for the accurate determination of pressure-volume-temperature data and a simple method for the accurate measurement of high pressures, RP470 271
Wave lengths, effective X-ray, RP475 333
Wave lengths in lanthanum spectra, RP468 239
Weathering of slate, RP477 377
Weber, C. G., and R. M. Cobb, Register studies in offset lithography, RP480 427
White, Joseph D., and F. W. Rose, jr., Isolation of the three xylenes from an Oklahoma petroleum, RP501 711
Whiteware, expansion of, RP472 291
Whittemore, H. L., J. M. Frankland and, Tests of cellular sheet steel flooring, RP463 131
Weight-length method of area determination, RP486 509

X

Xenocyanine, infra-red arc spectra photographed with, RP473 309
X-ray copper absorption coefficients {RP475 ..... 333 / RP491 561
X-ray dosage {RP475 ..... 333 / RP491 561
X-ray equipment, RP505 769
X-ray generator comparisons {RP475 ..... 333 / RP491 561
X-ray generators {RP475 ..... 333 / RP491 561
X-ray intensities, RP505 769
X-ray measurements {RP475 ..... 333 / RP491 ..... 561 / RP505 769
X-ray quality {RP475 ..... 333 / RP491 561
X-ray standardization {RP475 ..... 333 / RP491 ..... 561 / RP505 769
X-ray therapy machines {RP475 ..... 333 / RP491 561
X-rays, low voltage, RP505 769
Xylenes, absorption by, of infra-red light, RP501 711
content of, in petroleum, RP501 711
infra-red absorption spectrum of, RP501 711
isolation of, from petroleum, RP501 711
Xylenes mixture, separation of constituents of, RP501 711
Xylenes, physical properties of, RP501 711
presence of, in petroleum, RP501 711

Y

Young, J. C., A. N. Finn, F. W. Glaze and, The density of soda-lime-silica glasses as a function of the composition, RP507 799

Z

Zeeman effect in lanthanum spectra, RP468 239
Zicronium, infra-red arc spectrum of, RP473 309
Zinc coatings, effect of, on the endurance properties of steel, RP454 9
Zinc, detection of, in weighted silk, RP498 669

(Cut here)

SUPERINTENDENT OF DOCUMENTS,
Government Printing Office,
Washington, D. C.

DEAR SIR: Send me the Bureau of Standards publications marked X below. I inclose remittance [1] to cover the cost.

Mark X	Title of publication	Price		Amount inclosed
		United States, Canada, Cuba, Newfoundland, Republic of Panama	Foreign countries	
----	Commercial Standards Monthly (one year)	$1.00	$1.60	----
----	Bureau of Standards Journal of Research [2] (one year)	2.50	3.25	----
----	Blue buckram bound volumes 1 to 8 of above journal are now available--each volume	[3] 2.75	[3] 3.50	----
----	Technical News Bulletin (one year)	.50	.70	----
----	Standards Yearbook, 1932	1.00	1.20	----
	Total remittance	----	----	----

Send to ----

Number and Street ----

City and State (or County) ----

[1] Remittances should be either in the form of a post-office money order, coupons (issued for the specific purpose of purchasing Government publications), express money order, New York draft, or cash, at the sender's risk.

[2] This issue completes volume 9. Volume 10 will commence with the January (1933) issue. Your subscription should be submitted at once to insure starting with No. 1 of volume 10.

[3] These prices are for volumes 1 to 7. Commencing with volume 8 the price will be $2.50 and 3.25 (foreign).

○

BUREAU OF STANDARDS JOURNAL OF RESEARCH

CONTENTS OF RECENT NUMBERS—Continued

September, 1932 (Vol. 9, No. 3)

RP471. A new determination of the atomic weight of osmium. Raleigh Gilchrist.
RP472. "Moisture expansion" of ceramic whiteware. R. F. Geller and A. S. Creamer.
RP473. Infra-red arc spectra photographed with xenocyanine. W. F. Meggers and C. C. Kiess.
RP474. Tensile properties of cast nickel-chromium-iron alloys and of some alloy steels at elevated temperatures. William Kahlbaum and Louis Jordan.
RP475. The comparison of high voltage X-ray generators. Lauriston S. Taylor and K. L. Tucker.
RP476. The structure of the chromic acid plating bath: the theory of chromium deposition. Charles Kasper.
RP477. Physical properties and weathering characteristics of slate. D. W. Kessler and W. H. Sligh.
RP478. Radiation from cæsium and other metals bombarded by slow electrons. C. Boeckner.
RP479. A simplified precision formula for the inductance of a helix with corrections for the lead-in wires. Chester Snow.
RP480. Register studies in offset lithography. C. G. Weber and R. M. Cobb.
RP481. Creep at elevated temperatures in chromium-vanadium steels containing tungsten or molybdenum. William Kahlbaum and Louis Jordan.

October, 1932 (Vol. 9, No. 4)

RP482. The synthesis, purification, and certain physical constants of the normal hydrocarbons from pentane to dodecane, of *n*-amyl bromide and of *n*-nonyl bromide. B. J. Mair.
RP483. A study of some ceramic bodies of low absorption maturing at temperatures below 1,000° C. R. F. Geller and D. N. Evans.
RP484. The determination of magnesia in phosphate rock. James I. Hoffman.
RP485. Collisions of the first and second kind in the positive column of cæsium discharge. F. L. Mohler.
RP486. The areas and tensile properties of deformed concrete-reinforcement bars. A. H. Stang, L. R. Sweetman, and C. Gough.
RP487. A calorimetric method for determining the intrinsic energy of a gas as a function of the pressure. Edward W. Washburn.
RP488. The photographic emulsion; variables in sensitization by dyes. Burt H. Carroll and Donald Hubbard.
RP489. A method for the separation of rhodium from iridium and the gravimetric determination of these metals. Raleigh Gilchrist.
RP490. The isoelectric point of silk. Milton Harris.
RP491. Effective applied voltage as an indicator of the radiation emitted by an X-ray tube. Lauriston S. Taylor, George Singer, and C. F. Stoneburner.
RP492. Column curves and stress-strain diagrams. William R. Osgood.

November, 1932 (Vol. 9, No. 5)

RP493. The variation with angle of emission of the radiation from metals bombarded by slow electrons. C. Boeckner.
RP494. Nitrogen content of some standard sample steels. J. G. Thompson and E. H. Hamilton.
RP495. Analytical methods for the determination of levulose in crude products. R. F. Jackson, J. A. Mathews, and W. D. Chase.
RP496. Determination of alumina and silica in steel by the hydrochloric acid residue method. J. G. Thompson and J. S. Acken.
RP497. An analysis of lanthanum spectra (La I, La II, La III). Henry Norris Russell and William F. Meggers.
RP498. Analysis of weighted silk. Ralph T. Mease.
RP499. The heat of formation of hydrogen chloride and some related thermo-dynamic data. Frederick D. Rossini.
RP500. Thermal expansion of lead. Peter Hidnert and W. T. Sweeney.

Research papers, where price is given, are already available, and others will be available in the near future as separates for purchase from the Superintendent of Documents, United States Government Printing Office, Washington, D. C.

A monthly periodical of pure and applied science published by our National Government

BUREAU OF STANDARDS JOURNAL OF RESEARCH

PUBLISHED AT WASHINGTON, D. C.

¶ With the July issue, the JOURNAL begins its ninth semiannual volume. The JOURNAL contains the bureau's research papers and critical reviews in the fields of science and technology. These will be comparable in interest and importance with the bureau papers formerly issued as Scientific and Technologic Papers.

¶ Several hundred researches are always in progress at the Bureau of Standards and the outlet for the results is the "BUREAU OF STANDARDS JOURNAL OF RESEARCH."

¶ If you are interested in following the latest developments in science and technology you need the BUREAU OF STANDARDS JOURNAL OF RESEARCH. If you are a subscriber, renew your subscription promptly; if not, your subscription will be appreciated. Copies are limited and it is not always possible to supply back numbers.

PRICES

New subscription (or renewal)[1] to Journal of Research for United States, Canada, Cuba, Mexico, Newfoundland, and the Republic of Panama (vol. 8, and thereafter)		$2.50*
Blue buckram bound	Volume 1, July to December, 1928	$2.75*
	Volume 2, January to June, 1929	$2.75*
	Volume 3, July to December, 1929	$2.75*
	Volume 4, January to June, 1930	$2.75*
	Volume 5, July to December, 1930	$2.75*
	Volume 6, January to June, 1931	$2.75*
	Volume 7, July to December, 1931	$2.75*
	Volume 8, January to June, 1932	$2.50*

[1] Yearly subscription, 12 issues. * For other countries, add 75 cents.

Research papers (printed separately with durable paper cover and priced according to cost)—see list of research papers on cover pages 2 and 3 of this issue.

Address orders only to
Superintendent of Documents
Government Printing Office
Washington, D. C.

The value of prompt and adequate news of the latest research results can not be measured by ordinary standards. They are permanent gainful assets for the expert. He can not afford to be without such basic sources